UNIVERSITY OF CALGARY

Characterization of *puf-8's* role as a negative regulator of proliferation in the *C. elegans* germ line

by

Hilary Eliisa Racher

A THESIS

SUBMITTED TO THE FACULTY OF GRADUATE STUDIES

IN PARTIAL FULFILMENT OF THE REQUIREMENTS FOR THE

DEGREE OF DOCTOR OF PHILOSOPHY

DEPARTMENT OF BIOLOGICAL SCIENCES

CALGARY, ALBERTA

SEPTEMBER, 2010

UNIVERSITY OF
CALGARY

Abstract

Understanding how stem cell populations are maintained is an important biological problem. For instance, stem cells have been implicated in such events as cancer and have the potential for use in regenerative medicine. Using the germline stem cells (GSCs) and the transit-amplifying cells in the distal *C. elegans* germ line as a model, this work contributes to the understanding of stem cell maintenance by characterizing the role of an important regulator called PUF-8.

PUF-8 is a member of the conserved PUF family of RNA-binding proteins that regulate the expression of target mRNAs by binding to their 3' UTRs. PUF-8 is one of twelve *C. elegans* Pumilio homologues and has been shown to regulate spermatogenesis (Subramaniam and Seydoux, 2003), germline sex determination in hermaphrodites (Bachorik and Kimble, 2005), promoting mitotic cell cycle procession (Ariz et al., 2009; Bachorik and Kimble, 2005) and vulva development (Walser et al., 2006). In this thesis a new role for *puf-8* was identified; that of inhibiting stem cell proliferation. *puf-8* mutants do not have excess stem cell proliferation on their own, but when Notch signalling is elevated, *puf-8* strongly enhances over-proliferation, resulting in a germline tumour. Genetic analysis reveals that *puf-8* does not function in either of the *gld-1* or *gld-2* pathways to promote meiotic entry and/or inhibit proliferation, rather *puf-8* likely functions genetically upstream of *gld-1* and *gld-2* as a negative regulator of mitosis-promoting components. The tumours formed in *puf-8(0); glp-1(gf)* mutant animals are due to a failure of proliferating germ cells to enter meiotic prophase, rather than meiotic cells dedifferentiating into proliferative cells. PUF-8 works in opposition to two

other Pumilio homologues, FBF-1 and FBF-2 in controlling proliferation. The PUF-8 protein is most highly expressed in the distal germ line, in the region thought to contain transit-amplifying cells (Ariz et al., 2009). The work in this thesis identifies PUF-8 as a key regulator in controlling stem cell proliferation in the *C. elegans* germ line. Understanding PUF-8's role in this process will assist in understanding how stem cell populations are controlled in general.

Acknowledgements

I would first like to thank my supervisor, Dr. Dave Hansen. His patience, kindness and enthusiasm for science has provided me with a very positive and inspiring graduate student experience.

Thank you to my supervisory committee, Dr. Paul Mains, Dr. Doug Muench and Dr. Vanina Zaremberg, who have provided helpful suggestions, insight and words of encouragement throughout my studies. In addition, I would like to thank Dr. Savraj Grewal and Dr. Eleanor Maine for agreeing to be part of my defence committee.

I would like to thank all the past and present members of the Hansen lab for their cooperative spirits and helpful advice. Thank you to Dr. Chris Wang for his technical assistance on all things protein-related and for always being available for questions. Thank you to Dr. Laura Gauthier for sharing many interesting life experiences, for critically reviewing my thesis and for carrying on the *puf-8* story.

I would like to thank all of the Calgary *C. elegans* researchers, for allowing me to be a part of such a welcoming and supportive community. The sharing of reagents, equipment and advice has been invaluable.

Thank you to Graduate Studies at the University of Calgary and the CIHR Training Grant in genetics, child development and health for providing funding throughout my graduate degree.

Thank you to Anna Urbanska, Vishal Sharma, Taryn Brown, Vivian Fung and Helen Dick for all their research assistance.

I am very grateful for the supportive graduate community within the department of Biological Sciences. The friendships I have made will certainly last a life time.

I am also very thankful for my loving and supportive family. My parents, Patricia and William Leivo, for always encouraging me to excel. To my grandfather, Eric Kent, for stimulating my love of science. To my brother, Davin Leivo, and cousin, Michael Kent, for being good friends. And to my mother-in-law, Pamela Tourigny, for all her positive encouragement.

Finally, to my husband, Corey Racher. I would not be where I am today without his tremendous love and support. He has never stopped believing in me and for that I am forever grateful.

Dedication

To my parents,

Patricia and William

and to my husband,

Corey

Table of Contents

List of Tables

List of Figures and Illustrations

List of Symbols, Abbreviations and Nomenclature

Symbol	Definition
3’ UTR	3’ untranslated region
AC/VU	anchor cell/ventral uterine cell
BSA	bovine serum albumin
cM	centiMorgans
DABCO	1,4-diazobicyclo[2,2,2]-octane
DAPI	4′,6′-diamidino-2-phenylindole hydrochloride
DIC	differential interference contrast microscopy
DNA	deoxyribonucleic acid
DTC	distal tip cell
EMS	ethyl methane sulfonate
FBF	*fem-3* mRNA binding factor
gcd	germ cell diameter
gf	gain-of-function mutation
GFP	green fluorescent protein
Glp	abnormal germline proliferation
GSC	germline stem cell
HA	Hawaiian wild-type strain
HRP	horse radish peroxidase
kb	kilobase
kDa	kilodalton
L1	larval stage 1
LB	Laria-Bertani medium (or Lysogeny broth)
lf	loss-of-function mutation
LG	linkage group
mAb	monoclonal antibody
N2	Bristol wild-type strain
NGM	nematode growth medium
O/N	over-night
PBS	phosphate buffered saline
PCR	polymerase chain reaction
Pro	proximal proliferation tumour
PUF	Pumilio and FBF
RNA	ribonucleic acid
RNAi	RNA interference
SAP	shrimp alkaline phosphatase
SDS	sodium dodecyl sulfate
SNP	single nucleotide polymorphism
Tum	tumourous

Chapter One: **Introduction**

1.1 Stem cells

Arguably one of the most exciting topics in science today involves a very unique entity called a stem cell. Stem cells are unique in that they have the ability to both self-renew, to produce more stem cells, and undergo sequential commitment to form a variety of different cell types. One of the first documented discoveries regarding stem cells took place during the late 1800's through studies performed by a German biologist, Hans Driesch, which revealed that individual cells in an early embryo each have the ability to develop into a full individual (Lanza, 2004). In addition to the embryo, stem cells also reside within adult tissues (McKay, 1997; Pittenger et al., 1999; Spangrude et al., 1988). In many adult organisms, the ability to maintain tissue homeostasis and replace damaged cells is possible, in part, due to the presence of stem cell populations. For this reason stem cells have the potential for usage in the treatment of a variety of degenerative illnesses such as multiple sclerosis, diabetes, and Parkinson's disease (Cho et al., 2008; Fassas et al., 2000; Urban et al., 2008).

In order for a stem cell population to function appropriately, a balance must be maintained between self-renewal and differentiation. Loss of this balance can have devastating consequences. If a stem cell population undergoes excessive self-renewal, tissue formation is arrested and, in some cases, tumours can develop. In fact, many different cancers are believed to be triggered by aberrant stem cell self-renewal (Bonnet and Dick, 1997; O'Brien et al., 2007; Singh et al., 2003). Conversely, if a stem cell

population undergoes too much differentiation, the stem cell population will be lost. To regulate the balance between self-renewal and differentiation, organisms employ a variety of strategies that include both intrinsic and extrinsic modes of regulation. Much of what is currently known about these regulatory strategies have been discovered using the stem cell populations found in the germ lines of *Drosophila* (Lin and Spradling, 1993), *C. elegans* (Kimble and White, 1981) and mice (Brinster and Avarbock, 1994).

1.2 Germline Stem cells

Within the germ lines of many sexually reproducing organisms are populations of stem cells that possess the ability to both self-renew and differentiate (Brinster and Avarbock, 1994; Jones and Lin, 1993; Kimble and White, 1981; Lin and Spradling, 1993; Nishimiya-Fujisawa and Sugiyama, 1993). These stem cell populations are referred to as germline stem cells (GSC). GSCs are a unique variety of stem cell, as they are devoted, in their differentiation capacity, to the production of gametes (Lin, 1997). In order to produce gametes, GSCs must leave the mitotic cell cycle, required for self-renewal, and enter into the meiotic cell cycle. Meiosis is necessary for diploid organisms to produce haploid gametes that contain half the genetic information of the original cell. The union of two haploid gametes results in the formation of a diploid offspring. The reproductive strategies of many animals rely on the production of a large number of gametes (Weir and Rowlands, 1973). Thus, to maintain the reproductive fitness of an organism, a balance must occur between GSC self-renewal (mitosis) and differentiation (meiosis).

To illustrate this balance, three of the best-described GSC systems will be briefly introduced, which includes the *Drosophila* ovary, mouse testis and *C. elegans* germ line.

In the *Drosophila* ovary, the balance between GSC mitosis and meiosis is maintained using both intrinsic and extrinsic regulatory mechanisms. GSCs in the *Drosophila* ovary are encased within a cap-like structure that consists of cap cells and escort stem cells (ESC) (Lin and Spradling, 1993) (Figure 1.1). The cap-like structure creates a microenvironment (or niche) that provides physical protection, as well as extrinsic factors to support the undifferentiated GSC fate (Xie and Spradling, 2000). When *Drosophila* ovary GSCs divide, one cell remains in the niche and retains a GSC fate, while the other cell leaves the niche and differentiates into a cystoblast, which undergoes further divisions to form a female gamete (Brown and King, 1964; Wieschaus and Szabad, 1979). This division pattern is called asymmetric stem cell division (Lin, 2002). While *Drosophila* ovary GSCs typically undergo asymmetric cell division, they are also capable of dividing symmetrically to form two undifferentiated GSCs that both remain within the niche (Xie and Spradling, 2000). The extrinsic factors synthesized by the niche cells in the *Drosophila* ovary include the Dpp (Decapentaplegic) and Gbb (Glass bottom boat) ligands that both go on to activate the BMP (Bone Morphogenetic Protein) signalling pathway in the GSC, which is required to represses differentiation (Chen and McKearin, 2003; Song et al., 2004). In combination with the niche, intrinsic factors also affect the GSCs mitosis vs. meiosis decision. Some intrinsic factors include chromatin

remodelling factors (Xi and Xie, 2005), translational regulators (Lin and Spradling, 1997b) and cell cycle regulators (Wang and Lin, 2005).

The testes of male mice also contain a population of GSCs (also called spermatogonial stem cells) that are capable, throughout the duration of the animal's life, of self-renewing and differentiating to produce a large number of committed progenitors destined to form sperm (Brinster, 2002). Unlike the *Drosophila* ovary GSCs, mouse testis GSCs are not easily distinguished from the other more differentiated germ cells, which creates a challenge for researchers (Hofmann et al., 2005). However, like *Drosophila*, mouse testes GSCs are maintained, in part, by a niche environment (Figure 1.1). Transplantation experiments suggest that the somatic Sertoli cells, within the seminiferous tubules, are the cells that constitute the niche in mouse testes, providing extrinsic signals to promote GSC self-renewal (Brinster and Zimmermann, 1994; Shinohara et al., 2003). One identified extrinsic signal produced and released by the Sertoli cells is the GDNF (Glial cell line-Derived Neutrophic Factor) (Meng et al., 2000). Once secreted, GDNF then binds to two heterologous receptors, Ret (REarranged during Transformation) and GFR-α1 (GDNF-family Receptor α1) that are expressed in the GSCs (Meng et al., 2000; Yomogida et al., 2003), promoting GSC self-renewal. In mice defective for *gdnf*, GSCs in the testes are prematurely lost (Meng et al., 2000). Alternatively, over-expression of GDNF in mouse testes results in stimulation of GSC self-renewal and blockage of GSC differentiation (Meng et al., 2000; Yomogida et al., 2003). In addition to promoting GSC self-renewal (proliferation), Sertoli cells also send

extrinsic signals to adjacent committed spermatogonia cells to promote further differentiation (de Rooij et al., 1999; Ohta et al., 2000; Yoshinaga et al., 1991). Mouse testis GSCs are also maintained by intrinsic factors including Nos-2 (Nanos homolog 2) and Plzf (Promyelocytic Leukemia zinc-Finger) (Buaas et al., 2004; Costoya et al., 2004; Tsuda et al., 2003). A Nanos protein was also identified as an intrinsic factor important for GSC self-renewal in the *Drosophila* ovary (Wang and Lin, 2004), revealing an important commonality between *Drosophila* and mouse GSCs.

The *C. elegans* hermaphrodite gonad consists of two U shaped arms that are connected at a common uterus (see section 1.4) (Hirsh et al., 1976). In the distal most regions of both arms resides a population of GSCs, which are in direct contact with the niche cell, the somatic distal tip cell (DTC) (Kimble and White, 1981). The *C. elegans* niche uses Notch signalling to maintain undifferentiated GSCs (Figure 1.1) (discussed further in Section 1.5.1). Thus, while the three organisms discussed use a niche to maintain their undifferentiated GSCs, the specific signalling pathway used by the niche is unique for each organism (Figure 1.1). Unlike *Drosophila,* GSCs in *C. elegans* are thought to divide predominantly through a symmetric stem cell division pattern, which results in the production of GSC daughter cells with equivalent development potential (Kimble and Hirsh, 1979; Kimble and White, 1981). These cells go on to acquire distinct fates depending on the position within the niche. As the cells move proximally, towards the uterus, germ cells undergo differentiation, eventually forming male and female gametes (Hirsh et al., 1976). The focus of this thesis is to more fully understand how GSCs are

Figure 1.1. Basic comparison of GSC maintenance strategies between *Drosophila* ovary, mouse testis and *C. elegans* GSCs.

There are many other factors involved in addition to the factors shown here, for simplicity sake only a few details are shown in this figure. In each system, the niche cells (yellow) sends signals to the GSCs (green), which promote the undifferentiated state. Other intrinsic factors are expressed within the GSC (green) and differentiated cell (purple) that support the undifferentiated state and the differentiate state, respectively. Many of the proteins depicted in the illustration of the *C. elegans* germ line are expressed in both cell types; however, with respect to GSC maintenance, these proteins function primarily in only one of the two cell types.

ESC= escort stem cell, CB= cystoblast, SC= Sertoli cell, DS= differentiated spermatogonia, DTC= distal tip cell, MC= meiotic cell

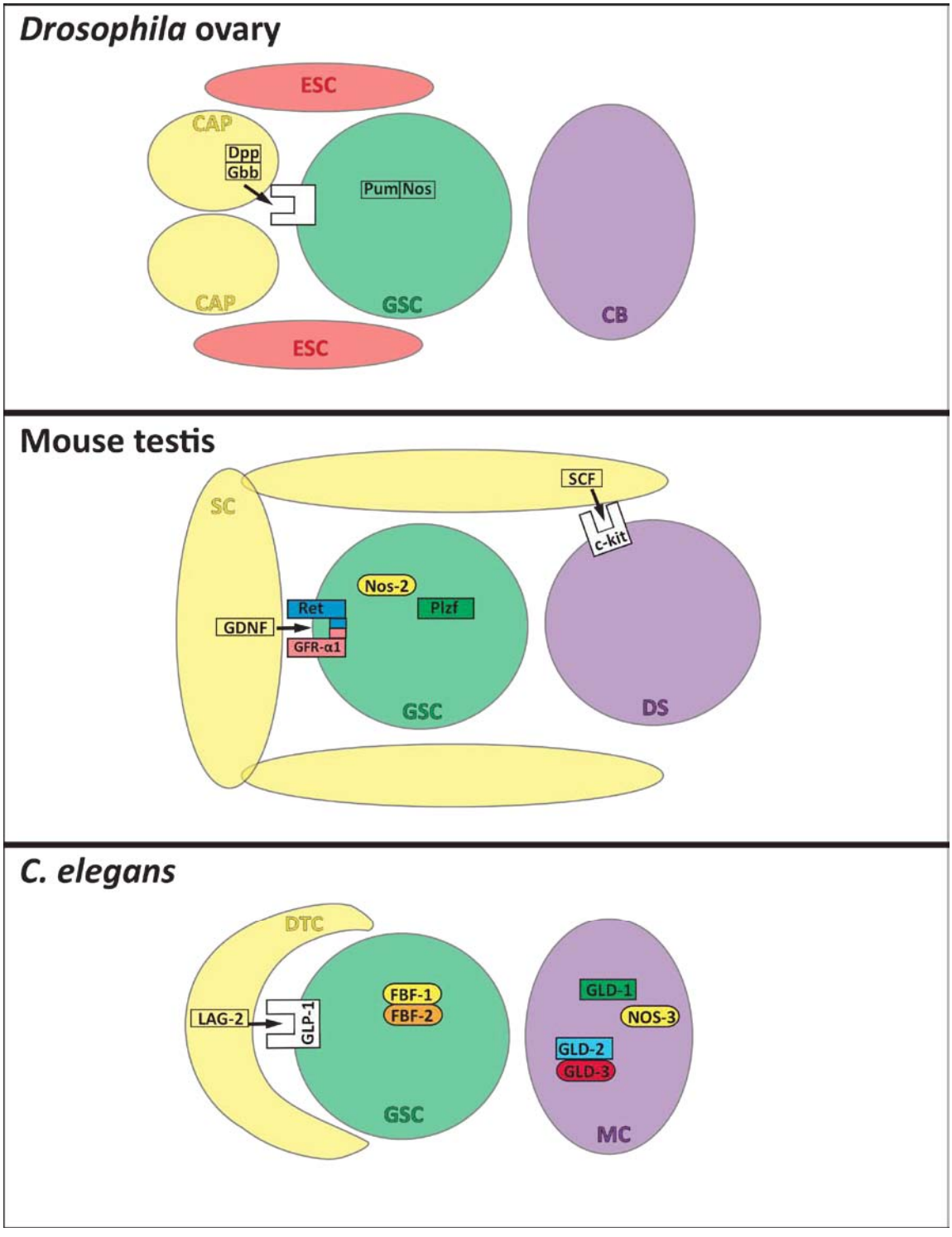
Drosophila ovary
ESC
CAP
Dpp
Gbb
Pum
Nos
CAP
GSC
CB
ESC
Mouse testis
SCF
SC
c-kit
Nos-2
Ret
Plzf
GDNF
GFR-α1
GSC
DS
C. elegans
DTC
FBF-1
FBF-2
LAG-2
GLP-1
GLD-1
NOS-3
GLD-2
GLD-3
GSC
MC

maintained in *C. elegans* by studying a specific regulator of the mitosis vs. meiosis decision. Advantages to using *C. elegans*, as well as background on the *C. elegans* germ line, will be discussed in the following sections, in order to set the stage for the work done in this thesis.

1.3 Using *C. elegans* as a Model Organism

The free-living, soil dwelling nematode *Caenorhabditis elegans* was first recognized as an excellent biological model some 60 years ago (Dougherty and Calhoun, 1948; Nigon and Dougherty, 1950). However, it was not until 1965, through the ground breaking work of Sydney Brenner, that *C. elegans* first became used as a model organism (Brenner, 1973). Brenner's initial reasons for selecting *C. elegans* was based on its suitability for genetic analysis and its relatively simple nervous system (Brenner, 1974). *C. elegans* also possess many other features that make it an useful model organism for studying germline regulation.

One beneficial attribute is the rapid life cycle of *C. elegans*. Within 3-4 days, *C. elegans* undergoes embryogenesis and four larval stages (L1-L4) to form the adult animal. This means experimental results can be produced relatively quickly. Another useful feature of *C. elegans* is the existence of both hermaphrodite and male sexes. This is highly beneficial for genetic analysis as the *C. elegans* self-fertile hermaphrodite can be used for inbreeding purposes as well as for mating crosses with males. The anatomy of *C. elegans* also provides some beneficial features such as a transparent body, which

allows for clear visualization of its internal structures without the need for dissection, especially beneficial when studying the germ line. Additionally, the cell number, lineage and spatial position of the somatic cells remain largely invariant across individuals, which makes this nematode an excellent model for developmental studies (Sulston et al., 1988).

C. elegans was the first multicellular organism to have its genome completely sequenced (Consortium, 1998). As well, the genome is highly annotated (wormbase.org). This has many great benefits for *C. elegans* researchers including ease of gene mapping and genome comparison studies. Genome sequencing also revealed that ~38% of *C. elegans* genes have homologs in humans (Lesney, 2001), illustrating that research done with *C. elegans* can be used to understand more complex eukaryotic species, such as humans.

1.4 The *C. elegans* Hermaphrodite Germ Line

The germ line is an essential tissue of all sexually reproductive organisms, as it is responsible for passing genetic information to successive generations through the efficient production of gametes. In the *C. elegans* hermaphrodite and male germ lines, gametes are continuously produced throughout their adult lives (Hirsh et al., 1976). Since this thesis deals primarily with the hermaphrodite sex, only the *C. elegans* hermaphrodite germ line will be described; however, similar developmental processes do occur within the *C. elegans* male germ line (Kimble and Hirsh, 1979).

1.4.1 Development of the Hermaphrodite Gonad

In *C. elegans*, the development of the germ line occurs in three phases: specification, growth and maintenance (Hubbard and Greenstein, 2005). In the embryo, specification of the germline precursor cells occurs early in embryogenesis and requires the expression of the PIE-1 protein (Mello et al., 1996). At the ~100 cell stage, the germline precursor cell (P4) divides to form the Z2 and Z3 primordial germ cells (Deppe et al., 1978). Shortly after division, PIE-1 levels decrease in the Z2 and Z3 cells, which lead to the expression of genes required for germline development (Mello et al., 1996).

At hatching, the Z2 and Z3 primordial germ cells are positioned next to the somatic gonad precursor cells Z1 and Z4 (Figure 1.2) (Chitwood and Chitwood, 1950). It is not until mid-L1 that the Z2 and Z3 cells begin to mitotically divide (proliferate), albeit in a variable fashion; the plane of cell division and times of division vary between individuals (Kimble and Hirsh, 1979). Alongside germline development is the development of the somatic gonad. By the end of the L1 stage, the Z1 and Z4 cells have divided to form 12 somatic gonad primordial cells (Figure 1.2) (Kimble and Hirsh, 1979). Two of these somatic cells become the distal tip cells (DTCs), which do not undergo any further divisions (Kimble and White, 1981). During the L2 stage, the 12 somatic gonad primordial cells reposition themselves to form the somatic gonad primordium, with one DTC cell capping the ends of each gonad arm (Kimble and Hirsh, 1979). At the same time, two of the somatic gonad primordial cells, Z1.ppp and Z4.aaa, undergo one of two alternate positions, forming one anchor cell and one ventral uterine precursor cell

Figure 1.2. Illustration of the post-embryonic development of the *C. elegans* hermaphrodite gonad/germ line.

In the early L1 animal, the yellow cells represent the Z2 and Z3 primordial germ cells and the white cells represent the Z1 and Z4 somatic gonad precursor cells. During the L1/L2 period, the somatic gonad precursor cells divide to form 12 somatic gonad primordial cells (10 white cells, 2 red cells) and the germ cells begin to proliferate (yellow cells). The L2/L3 phase illustrates the cell fate locations of the Z4 and Z1 cell divisions. Germ cell proliferation continues (yellow region= mitotic germ cells). Beginning in the mid-L3 stage, germ cells being to enter into meiosis (Green region). By the late L3 stage, a sharp mitosis/meiosis border develops. During this stage, the somatic DTCs lead the gonad arms to form the anterior and posterior U shape structures. By the late L4 stage, four distinct germ cell regions exist; distal mitotic zone (yellow region), transition zone/cells entering meiosis (light green region), cells undergoing the different stages of meiosis (green region) and cells undergoing spermatogenesis (blue region). By the L4 stage, the somatic gonad cells have divided to produce 143 cells; these cells include the two DTC (red), the sheath cells (light blue), the cells of the uterus walls (white central structure) and the cells of the spermatheca (grey regions on either side of uterus). In the adult, germ cells no longer differentiate to form sperm, but instead undergo female meiotic development (green region) and oogenesis (pink region), forming oocytes. Oocytes are fertilized by sperm in the spermatheca. Embryogenesis begins inside the

uterus. Later the embryos are ejected out of the hermaphrodite uterus via the vulva, an ventral opening (not shown). Adapted from (Hubbard and Greenstein, 2005).

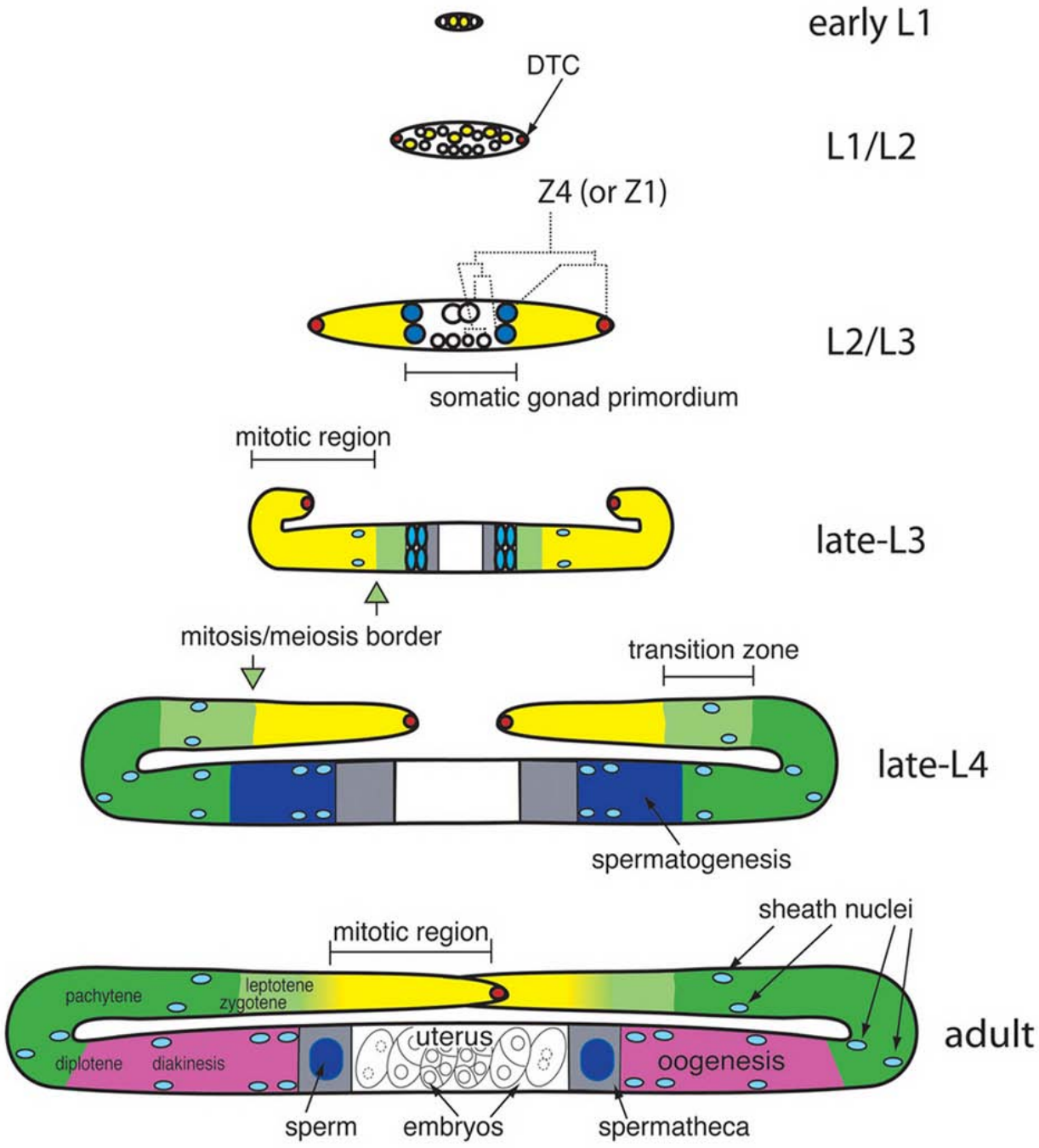
early L1
DTC
L1/L2
Z4 (or Z1)
L2/L3
somatic gonad primordium
mitotic region
late-L3
mitosis/meiosis border
transition zone
late-L4
spermatogenesis
sheath nuclei
mitotic region
pachytene
leptotene
zygotene
uterus
diplotene
diakinesis
oogenesis
adult
sperm
embryos
spermatheca

(more on this cell fate decision in chapter 5) (Greenwald et al., 1983; Kimble and Hirsh, 1979; Kimble and White, 1981). During this time, the germ cells continue to proliferate. By the early L3 stage, an increase in the proliferation of germ cells occurs due to signals from the DTCs and sheath cells (see below) (Killian and Hubbard, 2005; Kimble and White, 1981; McCarter et al., 1997). It is important to note that the germ cells are considered syncytial because their nuclei are only partially surrounded by cell membranes (Hirsh et al., 1976). For the purpose of this thesis, and in keeping with common practice in the field, each germ cell nucleus, its surrounding cytoplasm, and partially enclosed membranes will be nevertheless referred to as a ‘‘cell’’.

While germ cells continue to proliferate, somatic gonadal sheath cells undergo further divisions during the L3-L4 stages, forming a total of 143 somatic gonad cells (Kimble and Hirsh, 1979). During the L3 stage, the somatic AC initiates vulva development (Sulston and White, 1980) and the two DTCs lead each gonad arm to form the anterior and posterior U shaped structures (Hirsh et al., 1976). By L4, the somatic gonad includes the following features; the distal end of each gonad arm is capped with a somatic DTC, anterior and posterior sheath cells encapsulate the germline components of the gonad and sheath cells form the walls of the spermatheca and uterus (Figure 1.2) (Kimble and Hirsh, 1979).

During mid-L3, in addition to mitotic divisions, germ cells undergo sex determination and entry into meiosis (Austin and Kimble, 1987; Kimble and White, 1981). This marks the beginning of the mitosis vs. meiosis decision (discussed in detail

later). By late L3, two populations of germ cells exist; a distal population of germ cells undergoing mitosis and a proximal population of germ cells undergoing male meiotic development (Figure 1.2) (Kimble and Hirsh, 1979). By late L4, male meiotic development and spermatogenesis (male gametogenesis) is completed, forming a total of ~300, initially non-motile, sperm per animal (Hirsh et al., 1976). Also during the L4 stage, a sexual switch occurs in the germ line, and all subsequent germ cells that enter into meiosis undergo female meiotic development (Ahringer and Kimble, 1991). By adulthood, female meiotic development is coupled with oogenesis (female gametogenesis) (Figure 1.2). However, unlike male meiotic development, developing oocytes arrest at diakinesis of meiosis I and do not complete development until after fertilization by sperm (Hirsh et al., 1976). Fertilization occurs within the spermatheca, after which the zygote undergoes the initial stages of embryogenesis inside the uterus (Figure 1.2) (Hill et al., 1989; Ward and Carrel, 1979). Later, the developing embryo is expelled through the ventral opening of the uterus, called the vulva (Hirsh et al., 1976).

Once adulthood has begun, the germline growth phase ceases. An overview of the adult hermaphrodite germ line can be found in Figure 1.3. For the remainder of the hermaphrodite's life, in order to continuously make oocytes, the mitosis vs. meiosis decision must be maintained in the distal germ line. Many genes are known to regulate the mitosis vs. meiosis decision. This thesis identifies *puf-8* as one of the important regulators involved in the mitosis vs. meiosis decision.

Figure 1.3. The *C. elegans* hermaphrodite germ line.

(A) A wild-type (N2) *C. elegans* hermaphrodite visualized using differential interference contrast microscopy (DIC) (head is on the left). Outlined is one of two gonad arms (white dashed line). An asterisk marks the vulva, which is the opening from the uterus where the embryos are expelled from the animal (three embryos that have been expelled are shown). (B) Dissected gonad arm from a wild-type adult *C. elegans* hermaphrodite stained with the DNA marker DAPI. Starting from the left, the most distal cell is the somatic distal tip cell (DTC), followed by the mitotic region. Cells undergoing M-phase of mitosis can be distinguished by their condensed DNA (arrow heads), indicative of chromosomes aligning along the metaphase plate. As the mitotic cells move away from the DTC they begin to differentiate and enter into meiosis. The transition zone marks the region where entry into meiosis is first visible, as cells in the leptotene and zygotene stages of prophase I have crescent-shaped nuclei (Crittenden et al., 1994; Dernburg et al., 1998; Francis et al., 1995a; MacQueen and Villeneuve, 2001). Moving proximally, the cells undergo the various stages of meiosis. The first ~40 cells, in each arm, to complete meiosis form ~160 sperm, which are stored in the somatic structure called the spermatheca. All subsequent gametes formed are oocytes. Gonadal sheath cells line the exterior of the gonad arm. Scale bars = 20 mm. (C) Cartoon version of gonad arm in B. DTC (yellow, half-moon shaped cell), proliferative cells (green), cells entering into meiosis/transition zone (red, crescent shaped cells), meiotic cells (red),

cells undergoing oogenenesis (yellow, with red nuclei), sperm (blue). Adapted from (Racher and Hansen, 2010).

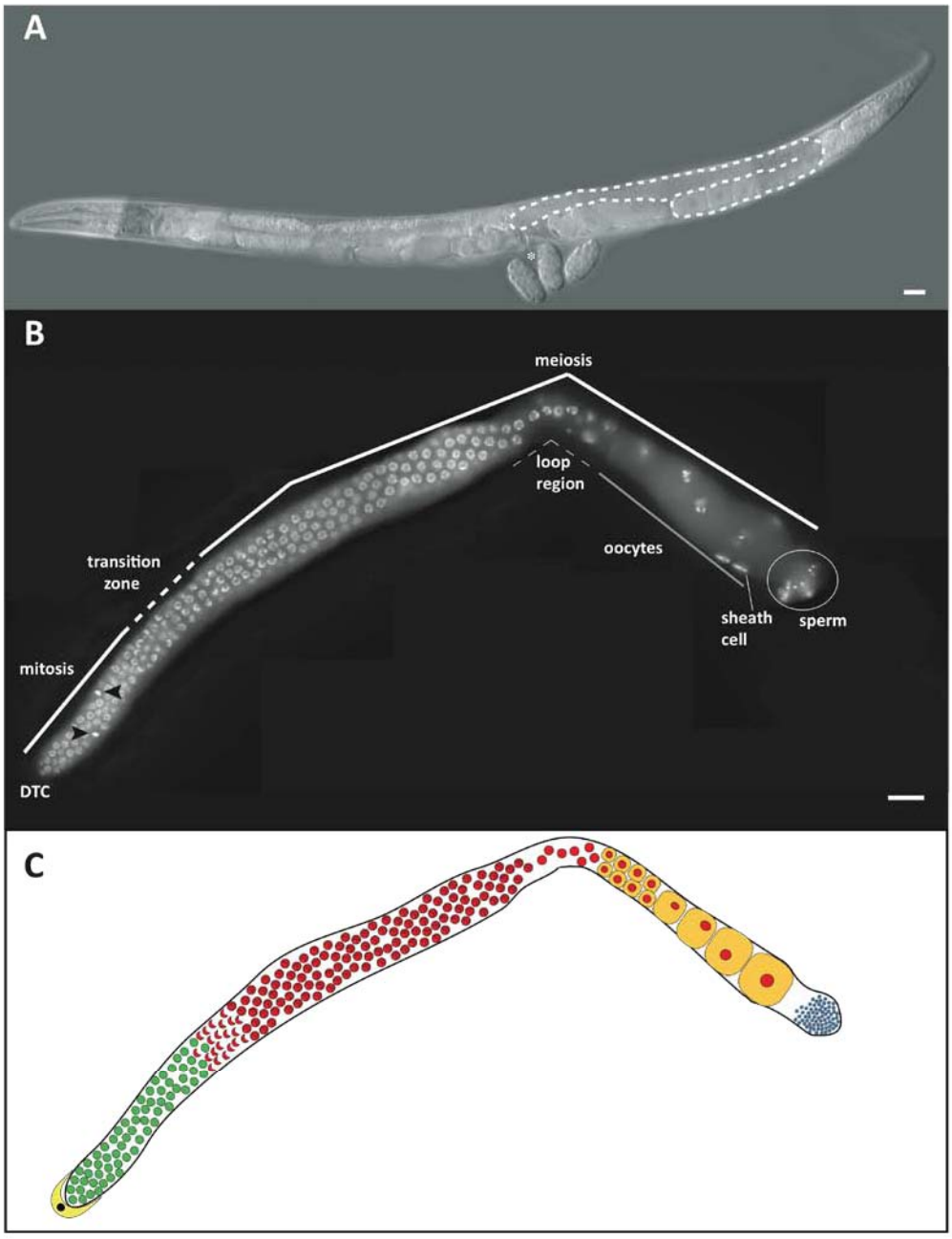
A
B
meiosis
loop
region
oocytes
transition
zone
sheath
cell
sperm
mitosis
DTC
C

1.5 Mitosis vs. Meiosis Decision

C. elegans hermaphrodites are able to produce thousands of gametes throughout their lives (Schedl, 1997; Sulston and Horvitz, 1977). To maintain a constant supply of gametes, the hermaphrodites maintain a balance between the proliferation and differentiation of their distal mitotic cells. This balance is often referred to as the mitosis versus meiosis decision.

In the distal end of each gonad arm, in the region farthest from the uterus, resides a population of ~200–250 mitotically dividing germ cells (Killian and Hubbard, 2005; Lamont et al., 2004). This population of mitotic cells can be defined further into two sub-populations; the first (most distal) ~30-70 cells are thought to represent the undifferentiated GSCs, while the remaining mitotic cells are hypothesized to consist of a distal to proximal maturation gradient of transit-amplifying cells (Cinquin et al., 2010). Transit-amplifying cells are distinct from stem cells in that they are more restricted in their developmental potential (Jones and Watt, 1993). As the transit-amplifying cells move out of the mitotic zone, they enter into meiotic prophase. The region of the germ line where cells enter into the meiotic cell cycle is referred to as the transition zone (Crittenden et al., 1994). Using DAPI staining, cells in the transition zone can be distinguished by their crescent-shaped nuclear morphology, representative of cells entering the leptotene and zygotene stages of prophase I (Crittenden et al., 1994; Dernburg et al., 1998; Francis et al., 1995a; MacQueen and Villeneuve, 2001). The transition zone is quite small during L3-early L4 larval development (Figure 1.2) (Kimble

and White, 1981). In late larva and adult germ lines, the transition zone boundary is no longer sharp; the border of the transition zone contains interspersed mitotic and meiotic cells (Figure 1.2) (Hansen et al., 2004a). In order to more clearly analyze the transition between mitosis and meiosis, antibodies against REC-8 and HIM-3 can be used (Hansen et al., 2004a). REC-8 is part of the sister-chromatid cohesion protein family that is found in the nucleoplasm and on the DNA of cells in both the proliferative and meiotic prophase regions (Pasierbek et al., 2001). However, when germ lines are analyzed under mild fixation techniques, antibodies against REC-8 recognize only proliferative cells and, thus, serves as an excellent marker for cells in the mitotic zone, including both the GSCs and transit-amplifying cells (Figure 1.4) (Hansen et al., 2004a). HIM-3 is a component of the proteinaceous core synaptonemal complex that forms between replicated sister chromatids during meiotic prophase I (Zetka et al., 1999) and as such, antibodies against HIM-3 are useful for identifying cells that have entered into meiosis (Figure 1.4) (Hansen et al., 2004a; MacQueen and Villeneuve, 2001). As the cells, which have entered into meiosis, travel proximally, they progress through meiosis, ultimately forming gametes.

Disruptions in the mitosis vs. meiosis decision produce recognizable germline phenotypes. When mitosis is disrupted, all germ cells prematurely enter into meiosis. This produces a germline phenotype referred to as Glp (abnormal GermLine Proliferation) (Austin and Kimble, 1987). The severity of the Glp phenotype varies depending on the point in germline development when mitosis is disrupted. The most

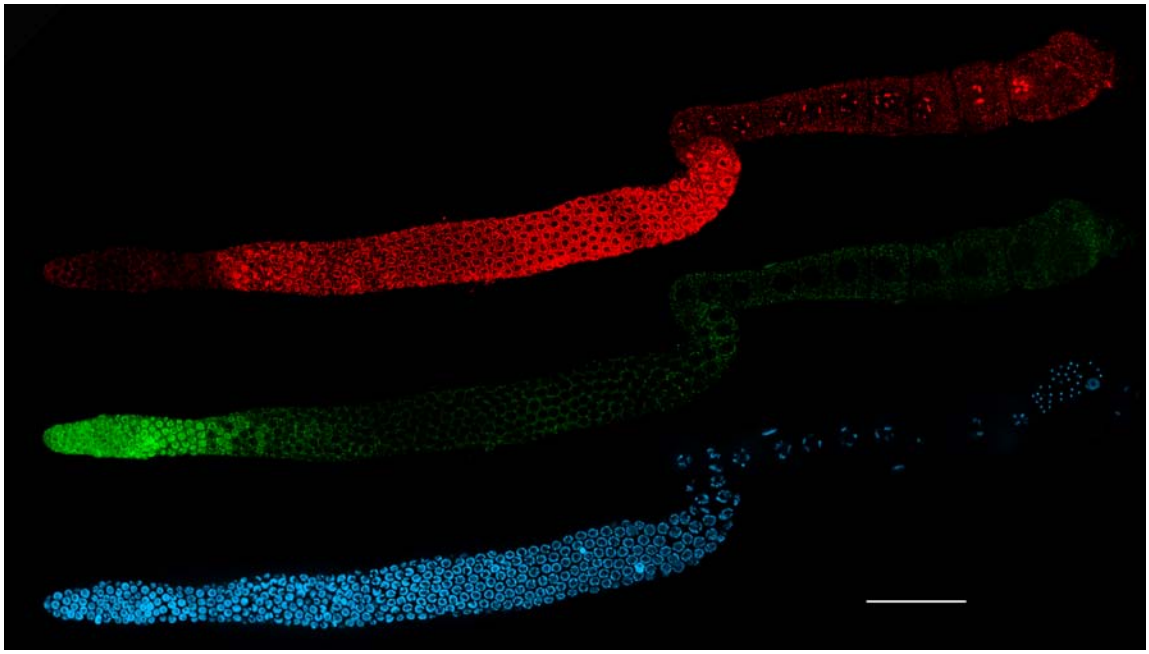

Figure 1.4. N2 animal probed with αREC-8 and αHIM-3.

Wild-type (N2) dissected gonad arm stained with DAPI (blue), probed with anti-REC-8 (αREC-8) (green) and αHIM-3 (red) antibodies. Scale bar = 50 μM

severe Glp phenotype consists of gonads containing only ~16 sperm per animal and no other germ cells (Austin and Kimble, 1987). Alternatively, when entry into meiosis is disrupted, a germline tumour is formed that consists of ectopic, mitotically dividing germ cells (Berry et al., 1997; Kadyk and Kimble, 1998).

Three broad categories of germline tumours exist: complete, proximal proliferation and late-onset germline tumours (Figure 1.5) (Wilson-Berry, 1998). Complete germline tumours arise from the failure of germ cells to enter into meiosis (Berry et al., 1997). Using the germ cell markers discussed above to analyze these tumours, all cells in complete germline tumours are REC-8 positive and HIM-3 negative (Hansen et al., 2004a). A proximal proliferation (Pro) germline tumour arises when proximal germ cells fail to enter into meiosis and, instead, undergo ectopic proliferation in the proximal germ line, in the region closest to the uterus (Pepper et al., 2003; Seydoux et al., 1990). In Pro germline tumours, some germ cells do enter into meiosis. Thus, a germ line that contains a Pro tumour has REC-8 positive cells in both the distal and proximal ends of the germ line, while the middle portion has HIM-3 positive cells and, potentially, gametes. Finally, in late-onset germline tumours the distal mitotic region is expanded in adults due to a failure of germ cells to exit the mitotic cell cycle (Berry et al., 1997). However, since the mitosis vs. meiosis decision occurs relatively normally during the larval stages, normal germline polarity is established. In late-onset tumours, more REC-8 positive cells are found in the distal region of the gonad than in wild-type animals. In gonads with late-onset tumours, germ cells enter meiosis

Figure 1.5. Cartoon of a wild-type gonad and three types of germline tumours.

(A) Wild-type hermaphrodite germ line (top illustration) has proliferative/mitotic germ cells (green) only in the distal most region of the germ line. (B) Late-onset germline tumours have more proliferative germ cells in the distal region. (C) Pro germline tumours are characterized by the presence of proliferative cells in the proximal region of the germ line. (D) Complete germline tumours contain only proliferative germ cells.

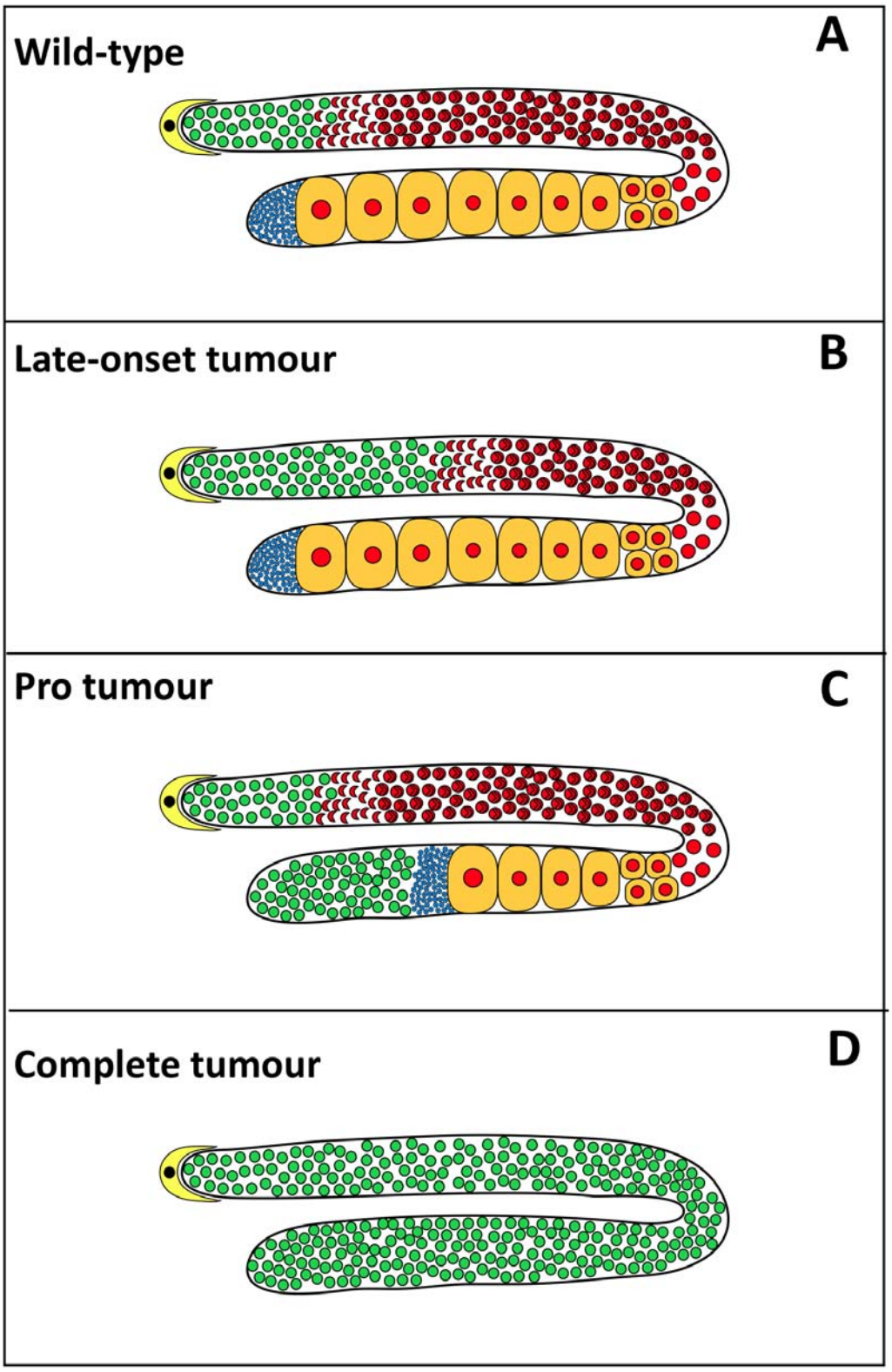
Wild-type
A
Late-onset tumour
B
Pro tumour
C
Complete tumour
D

relatively normally; HIM-3 positive cells are present following the REC-8 positive cells and more proximal regions often contain functional gametes. However, as an animal with a late-onset tumour ages, distal proliferation continues to expand and eventually the tumour can occupy the entire germ line; thus, late-onset tumours can eventually become complete tumours, filled with REC-8 positive cells (Berry et al., 1997; Pepper et al., 2003). These phenotypic designations will be used throughout this thesis to describe the phenotypes of a variety of mutations in genes that affect the mitosis vs. meiosis decision.

1.5.1 Mitosis-Promoting Components

The distal population of mitotic cells, from early larval development through to germ cell maintenance in adults, are maintained by way of the canonical GLP-1/Notch signalling pathway (Figure 1.6). Signalling occurs between the germ line and the surrounding somatic cells to activate this signalling cascade. Specifically, interactions between the somatic DTC, which caps and extends projections along the distal gonad arm (Kimble and White, 1981), and the distal most germ cells, are crucial for the maintenance of the distal proliferative zone. When the DTC is removed, through laser ablation, mitotic germ cells are not maintained; instead a Glp germ line is formed, which contains only ~16 sperm (Kimble and White, 1981). As well, when the DTC is repositioned to another location within the germ line, the DTC is capable of causing

Figure 1.6. Mitosis versus meiosis decision.

The distal end of the germ line is the region that contains mitotic/proliferative germ cells (green cells), at least some of which are GSCs. The Notch signalling pathway (A) is responsible for maintaining mitosis in the distal end. The mitosis-promoting components are shown in green, while the meiosis-promoting components are shown in red. Arrows represents positive interactions and negative interactions are represented with T-bars. The Notch ligand, LAG-2, resides on the surface of the DTC (yellow tentacle cell in (B)), which caps and extends projections along the distal end of each gonad arm (Henderson et al., 1994; Kimble and White, 1981; Tax et al., 1994). Expressed on the surface of the mitotic germ cells is the Notch receptor, GLP-1 (Crittenden et al., 1994). When LAG-2 interacts with GLP-1, a cleavage event occurs, releasing the intracellular portion of the GLP-1 receptor, called GLP-1(INTRA) (Mumm and Kopan, 2000). GLP-1(INTRA) translocates into the nucleus of the cell, where it complexes with the transcription factor LAG-1, and transcriptional co-activator LAG-3/SEL-8 (Christensen et al., 1996; Nam et al., 2006; Petcherski and Kimble, 2000; Wilson and Kovall, 2006). This nuclear complex likely activates the transcription of genes required to promote mitosis. Notch signalling activates fbf-1, fbf-2, fog-1 and lst-1, which in turn inhibits *gld-1* and *gld-3*, components of the meiosis-promoting pathways (Lamont et al., 2004). As cells move away from the DTC, Notch signalling gradually decreases, allowing GLD-1 levels to gradually increase (Hansen et al., 2004b; Jones et al., 1996). When GLD-1 levels reach a threshold (vertical dashed line), cells enter into meiosis. NOS-3 and GLD-2/GLD-3 are

also important for entry into meiosis and for positively regulating *gld-1* (Eckmann et al., 2002; Hansen et al., 2004b; Kadyk and Kimble, 1998). In addition to the GLD-1 and GLD-2 pathways, a third pathway is believed to also function to promote entry into meiosis (Hansen et al., 2004a). Currently, the components of this third pathway are unknown. This third pathway may also be negatively regulated by FBF-1, FBF-2, FOG-1, and/or LST-1. The first clear signs of entry into meiosis occur within the transition zone, where cells undergoing the leptotene and zygotene stages of prophase I have a crescent-shaped nuclear morphology (red crescent cells). Figure adapted from Hansen and Schedl (2006).

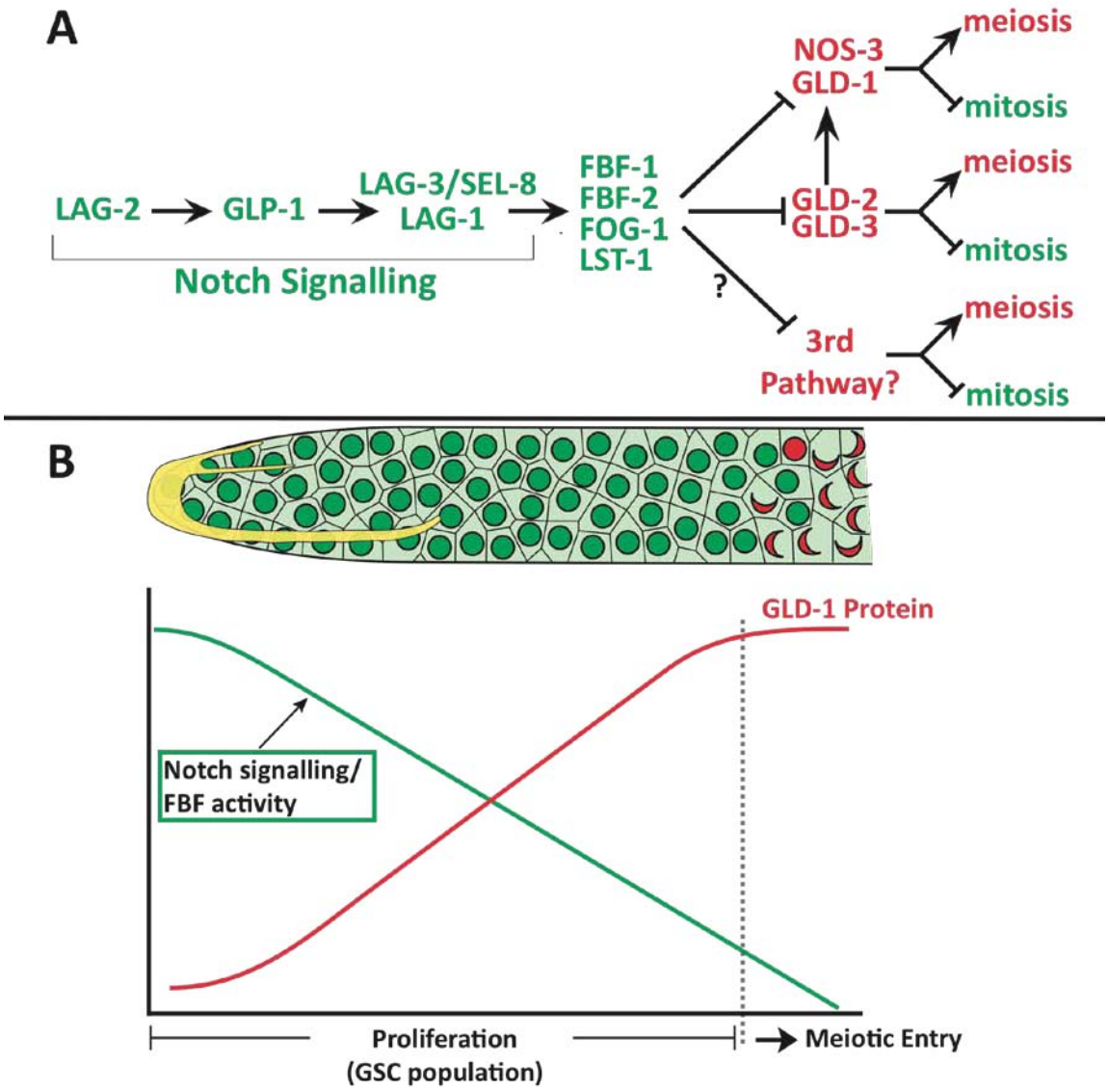
A
LAG-2
GLP-1
LAG-3/SEL-8
LAG-1
Notch Signalling
FBF-1
FBF-2
FOG-1
LST-1
NOS-3
GLD-1
GLD-2
GLD-3
?
3rd
Pathway?
meiosis
mitosis
meiosis
mitosis
meiosis
mitosis
B
GLD-1 Protein
Notch signalling/
FBF activity
Proliferation
(GSC population)
Meiotic Entry

ectopic germ cell proliferation at the new location (Henderson et al., 1994; Kimble and White, 1981). These experiments revealed that the DTC creates a niche environment that is both necessary and sufficient to promote germ cell proliferation. Through genetic and molecular analysis, it was later discovered that the DTC expresses the transmembrane LAG-2 (Lin-12 And Glp-1 phenotype) protein, a conserved DSL Notch ligand (Delta-Serate-LAG-2) (Henderson et al., 1994; Tax et al., 1994). The LAG-2 ligand signals to the germ cells by interacting with the GLP-1 (abnormal GermLine Proliferation)/Notch receptor, located on the surface of the germ cells (Crittenden et al., 1994). This interaction is thought to cause proteolytic cleavage of the GLP-1/Notch receptor, which results in the entry of the intracellular cleaved portion of GLP-1 (called GLP-1(INTRA)) into the germ cell nucleus (Mumm and Kopan, 2000). Within the nucleus, GLP-1(INTRA) complexes with the LAG-1 CSL (CBF-1/RBPJκ-Su(H)-LAG-1) transcription factor and the SEL-8/LAG-3 MAML (MAsterMind-LAG-3) transcriptional coactivator, after which this ternary complex activates the transcription of downstream target genes, thereby promoting proliferation of distal mitotic germ cells (Christensen et al., 1996; Nam et al., 2006; Petcherski and Kimble, 2000; Wilson and Kovall, 2006). Loss of any component of the ternary complex results in phenotypes similar to loss of the DTC (Austin and Kimble, 1987; Christensen et al., 1996; Doyle et al., 2000; Henderson et al., 1994; Lambie and Kimble, 1991; Petcherski and Kimble, 2000; Tax et al., 1994). Alternatively, gain-of-function (gf) mutations in *glp-1*, in which GLP-1(INTRA) is produced in a ligand independent fashion, result in animals with excessive germ cell

over-proliferation (germline tumours) (Berry et al., 1997; Kerins et al., 2010; Pepper et al., 2003). Thus, the current model is that germ cells close to the DTC have active GLP-1/Notch signalling (Hansen and Schedl, 2006; Kimble and Crittenden, 2007). As the germ cells move proximally, the *LAG-2* ligand is no longer in contact with the GLP-1 receptor, thus, no GLP-1(INTRA) is produced, resulting in no ternary complex. Without active GLP-1/Notch signalling, germ cells cease proliferation and instead enter into meiosis.

In addition to maintaining GSCs in *C. elegans*, Notch signalling has also been implicated in promoting stem cell proliferation in other systems. In mammals, proliferation of hematopoietic stem cells (HSC) is controlled, in part, by Notch signalling (Stier et al., 2002; Varnum-Finney et al., 2000). Osteoblast cells, which surround HSC populations, make up the stem cell niche by expressing the Notch ligand, Jag1 (Jagged 1) (Calvi et al., 2003), which goes on to interact with the Notch receptor, Notch1, in the HSC, promoting self-renewal (Stier et al., 2002). Notch signalling is also important for neural stem cell maintenance (Kageyama et al., 2008; Kopan and Ilagan, 2009). In telencephalic neural stem cells, Notch signalling is required for self-renewal; in knock-out mice that lack the intracellular CSL transcription factor, *Rbpj*, neural stem cells are completely lost (Imayoshi et al., 2010). Thus, Notch signalling appears to be a conserved mechanism used to maintain proliferative stem cell populations.

In the *C. elegans* gonad, other somatic cells, the gonadal sheath cells, are also required to promote robust proliferation, in addition to the DTCs (McCarter et al., 1997).

Specifically, the distal-most pair of sheath cells (Sh1) are important for distal germ cell proliferation, as laser ablation of these cells result in reduced germ cell proliferation (Killian and Hubbard, 2005). Additionally, proximal sheath cells (Sh2-5/Spth) are also capable of inducing proliferation; when the Sh2-5/Spth cells are laser ablated in a Pro mutant background, the incidence of Pro tumours is reduced or completely abrogated (Killian and Hubbard, 2005). While the mechanism used by sheath cells to promote proliferation is still unknown, it has been suggested that Notch signalling may be involved (Killian and Hubbard, 2005).

In the distal germ line, one target of GLP-1/Notch signalling that promotes proliferation and/or inhibits entry into meiosis is the gene *fbf-2* (Figure 1.6) (Fem-3 Binding Factor) (Lamont et al., 2004). *fbf-2* is presumed to be a direct target of Notch signalling based, in part, on the presence of four LAG-1 binding sites in its 5' promoter sequence (Lamont et al., 2004). While *fbf-2* appears to be a direct target of GLP-1/Notch signalling, genetic analysis indicates that other genes also function redundantly with *fbf-2,* downstream of GLP-1/Notch signalling, to promote germ cell proliferation and/or inhibit entry into meiosis (Figure 1.6) (Crittenden et al., 2002; Thompson et al., 2005). One gene is *fbf-1*, which is 93% identical in nucleotide sequence to *fbf-2* (Zhang et al., 1997). In *fbf-1* and *fbf-2* single mutants, relatively wild-type germ lines are formed (Crittenden et al., 2002). In *fbf-1 fbf-2* double mutants, germ cell proliferation is normal during early larval development; however, by the L4 stage, all germ cells leave the mitotic cell cycle and enter into meiosis, eventually forming Glp germ lines that

contain ~400 sperm per animal (Crittenden et al., 2002). *fbf-1* and *fbf-2* also have redundant roles during the sperm to oocyte switch (Zhang et al., 1997). Collectively, *fbf-1* and *fbf-2* are referred to as the *fbf* genes.

The *fbf* genes are not the only components that function downstream of GLP-1/Notch signalling to promote proliferation and/or inhibit entry into meiosis (Figure 1.6). Since *fbf-1 fbf-2* double mutants undergo substantially more proliferation than *glp-1/*Notch null mutants before the mitotic cells are depleted (Crittenden et al., 2002), another factor(s) must function with FBF, downstream of Notch signalling, to promote proliferation. Interestingly, a protein originally identified for its role in the specification of sperm, FOG-1 (Feminization Of the Germline) (Barton and Kimble, 1990; Schedl and Kimble, 1988), appears to function with FBF to promote proliferation of GSCs (Thompson et al., 2005). For instance, *fog-1; fbf-1 fbf-2* triple mutants make only approximately 10 germ cells per gonad arm (similar to the number of germ cells in animals lacking GLP-1/Notch signalling) (Austin and Kimble, 1987; Thompson et al., 2005). FOG-1 is a CPEB (Cytoplasmic Polyadenylation Element-Binding)-related protein that contains RRM and ZnF domains; therefore, FOG-1 likely functions as an RNA-binding protein (Luitjens et al., 2000). Only at low levels is FOG-1 believed to promote proliferation (Thompson et al., 2005). To maintain low levels of FOG-1 in the distal region of the germ line, post-transcriptional repression via FBF has been suggested, as FBF binds to FBF-binding elements (FBE) in the *fog-1* 3' UTR (Thompson et al., 2005). FOG-1 is believed to promote germ cell proliferation by positively regulating mitosis-

promoting mRNAs; however, no FOG-1 mRNA targets have yet been identified (Thompson et al. 2005). Mechanistically, it has been hypothesized that FOG-1 may function, like other CPEB proteins, in a regulatory complex to control polyadenylation of mRNA targets (Jin et al., 2001). In addition to *fog-1*, other genes have been proposed to function redundantly with the *fbfs* to promote proliferation and/or inhibit entry into meiosis and include *fem-3*, *fog-3* (Thompson et al., 2005) and *lst-1* (personal communication); however, the specific roles of these genes (*fem-3, fog-1* and *lst-1*) have not yet been determined.

One way in which the *fbfs* promote proliferation is by negatively regulating the *gld-1* and *gld-2* meiosis promoting pathways (see section 1.5.2). The FBFs belong to the PUF (PUmilio and FBF) family of RNA-binding proteins (Zhang et al., 1997). PUF proteins bind regulatory elements in the 3' untranslated regions (UTRs) of target mRNAs, which often leads to repression of the target mRNAs (Wickens et al., 2002). Specifically, FBF binds to 3'UTR sites called FBE (FBF-Binding Elements) (Crittenden et al., 2002; Eckmann et al., 2004; Lamont et al., 2004; Thompson et al., 2005; Zhang et al., 1997). To promote germ cell mitosis, the FBFs bind to the FBE sites in the 3'UTRs of *gld-1* and *gld-3* (Crittenden et al., 2002; Eckmann et al., 2004). Based on studies in yeast, PUF proteins are thought to bind specific targets and promote mRNA degradation by stimulating deadenylation (Goldstrohm et al., 2007). Recently, it has been hypothesized that the FBFs repress *gld-1* mRNA by recruiting the CCR-4/NOT deadenylase complex, as removal of this complex stabilizes *gld-1* mRNA levels (Schmid et al., 2009). In yeast, CCr4 forms a

heterodimer with Pop2, another type of deadenylase (Denis and Chen, 2003). FBF also interacts with CCF-1, the Pop2 homologue in *C. elegans*, and stimulates deadenylation of *gld-1 in vitro* (Suh et al., 2009). Whether *fog-1, lst-1, fem-3* and/or *fog-3* use similar mechanisms to promote proliferation as the *fbfs* awaits further research.

1.5.2 Meiosis-Promoting Components

As cells move proximally, away from the DTC, Notch signalling levels are thought to decrease, which in turn decreases FBF activity. This decrease in FBF activity allows genes in the *gld-1* and *gld-2* pathways to become active and inhibit proliferation and/or promote meiotic entry, resulting in germ cell entry into meiotic prophase (Figure 1.6). When the activity of only one of the two pathways (*gld-1* or *gld-2*) is removed through genetic mutation, the mitosis versus meiosis decision occurs similarly to wild-type (Francis et al., 1995b; Kadyk and Kimble, 1998). However, when the activities of both pathways are removed, very little entry into meiosis occurs and a germline tumour results (often referred to as a 'synthetic germline tumour) (Eckmann et al., 2004; Hansen et al., 2004b; Kadyk and Kimble, 1998). A small proportion of germ cells in these double mutants still enter into meiosis (unlike strong *glp-1(gf)* mutants in which no cells appear to enter meiosis); therefore, a third uncharacterized pathway may also exist parallel to the *gld-1* and *gld-2* pathways to promote entry into meiosis (Figure 1.6) (Hansen et al., 2004a).

The *gld-1* pathway contains the *gld-1* and *nos-3* genes. GLD-1 belongs to the STAR/KH family of RNA-binding proteins (Jones and Schedl, 1995). In addition to GLD-1's role during the mitosis vs. meiosis decision, GLD-1 also promotes the male sexual fate in hermaphrodites and is needed for meiotic prophase progression in female germ cells (Francis et al., 1995a; Francis et al., 1995b). In *gld-1* null mutants, a normal mitosis vs. meiosis decision is made in the distal germ line; however, female germ cells are unable to progress past the pachytene stage of meiosis I and instead exit the meiotic cell cycle and return to mitosis (Francis et al., 1995a). How GLD-1 is able to drive germ cells from mitosis into meiosis is presumed to involve repression of mitosis-promoting mRNAs (Hansen and Schedl, 2006; Kimble and Crittenden, 2007). NOS-3 is the second component of the *gld-1* pathway. NOS-3 belongs to the Nanos family of zinc finger proteins, which in *Drosophila*, are known to function as translational regulators (Kraemer et al., 1999). Through genetic analysis, *nos-3* was determined to function with *gld-1* to promote entry into meiosis (Hansen et al., 2004b). In *gld-2; nos-3* double mutants, a synthetic germline tumour is formed that is epistatic to a *glp-1(0)* mutant (Hansen et al., 2004a). As well, *gld-1; nos-3* double mutants do not form a synthetic tumour, suggesting that *nos-3* functions in the *gld-1* pathway to promote entry into meiosis and/or inhibit proliferation (Hansen et al., 2004a). Mechanistically, NOS-3 is believed to control meiotic entry, in part, by promoting the accumulation of GLD-1 protein (Hansen et al., 2004a).

Contained within the second meiosis-promoting pathway are the *gld-2* and *gld-3* genes. The GLD-2 protein is the catalytic portion of a cytoplasmic poly(A) polymerase (Wang et al., 2002). In *gld-2* loss-of-function (lf) mutants, meiotic entry occurs normally; however, gametogenesis for both male and female germ cells is defective (Kadyk and Kimble, 1998). In *gld-2(lf) gld-1(0)* double mutants, synthetic tumours are formed, which are epistatic to *glp-1(0)* mutants (Kadyk and Kimble, 1998). This suggests that *gld-1* and *gld-2* function redundantly to promote meiotic development. Mechanistically, while GLD-2 possesses the catalytic capacity to promote translation, intrinsically it does not appear to have the ability to bind to RNA; thus, GLD-2 complexes with GLD-3, a KH-domain-containing RNA-binding protein, which is thought to provide the mRNA binding function (Eckmann et al. 2002; Wang et al. 2002). Support for *gld-3* functioning in the same pathway as *gld-2* was the observation that *gld-1; gld-3* double mutants are synthetically tumourous (Eckmann et al., 2004). One way in which the GLD-2/GLD-3 poly(A) polymerase complex promotes meiotic entry is by positively regulating GLD-1 protein accumulation, through lengthening of the *gld-1* mRNA poly(A) tail (Hansen et al., 2004b; Suh et al., 2006). However, *gld-1* cannot be the only target of GLD-2 activity in controlling the switch from mitosis to meiosis; otherwise, the *gld-1* single mutant would have the same phenotype as the *gld-2 gld-1* double mutant.

1.6 Additional Regulators of the Mitosis vs. Meiosis Decision

In addition to the regulators described above, other genes, not included in Figure 1.6, have been identified as additional regulators/modulators of the mitosis vs. meiosis decision. Some of these other regulators likely do not function within the core mitosis vs. meiosis pathway, but rather in a parallel pathway. The purpose of this section is not meant to be a comprehensive list of all identified regulators that affect the mitosis vs. meiosis decision but rather to demonstrate the further intricacies involved in the mitosis vs. meiosis decision, not illustrated in Figure 1.6. Due to the large number of additional regulators, only a few examples will be discussed.

Many regulators were identified that suppress and/or enhance *glp-1*/Notch signalling. Five genes that enhance a weak *glp-1* lf temperature sensitive allele include *ego-1* to *-5* (Enhancer of *Glp-One*) (Qiao et al., 1995). Specifically, EGO-1 functions as an RNA-directed RNA polymerase, which links RNA interference (RNAi) and potentially microRNA (miRNA) regulation to germline proliferation (Smardon et al., 2000). Several other uncharacterized genes were found to suppress lf alleles of *glp-1* include *sog-1* to *-6* (Maine and Kimble, 1993) and sog-*10* (Suppressors Of *Glp-1*) (Maine and Kimble, 1993). There are also numerous *sel* (Suppressor and Enhancer of *Lin-12*) genes that both suppress and enhance *glp-1* alleles including *sel-1, -5, -7, -9, -10* and *-12* (Chen et al., 2004; Fares and Greenwald, 1999; Grant and Greenwald, 1996; Hubbard et al., 1997; Levitan and Greenwald, 1995; Sundaram and Greenwald, 1993; Wen and Greenwald,

1999). Some of the *sel* genes have been postulated to modulate Notch signalling via proteolysis (*sel-10*) and intracellular trafficking (*sel-9*).

Other regulators that function in more broad biological roles also show specific roles in the mitosis vs. meiosis decision. For instance, mutations in many splicing factors affect the mitosis vs. meiosis decision, such as *teg-4* (Tumourous Enhancer of *Glp-1*) (Mantina et al., 2009), *prp-17* (yeast PRP (splicing factor) related) (Kerins et al., 2010) and *mog-1, -4* and *-5* (Masculinization Of the Germ line) (Belfiore et al., 2002; Puoti and Kimble, 1999, 2000). As well, mutations in *pas-5* (Proteasome Alpha Subunit), a component of the proteasome, or general knock-down (RNAi) of the proteasome also affect the balance between mitosis and meiosis (Macdonald et al., 2008). As would be anticipated, cell cycle regulators are also involved in controlling the mitosis vs. meiosis decision. Examples include *cdk-1* (Cyclin-Dependent Kinase family) (Boxem et al., 1999), *cye-1* (CYclin E) (Fay and Han, 2000), *kin-10* (protein KINase) (X. Wang and D. Hansen, unpublished data) and *cdc-25.1* (Cell Division Cycle related) (Ashcroft and Golden, 2002), just to name a few.

Since the mitosis vs. meiosis decision is essential for the reproductive success of *C. elegans*, it is not surprising that many different forms of regulation are employed. Future studies will no doubt reveal even more regulators of this decision.

1.7 Translational Regulation in the Germ Line via RNA-Binding Proteins

In order for a eukaryote to accomplish complex events like growth and differentiation, the expression of multiple genes must be coordinated. Proteins that regulate gene expression are broadly referred to as regulatory proteins. The way in which regulatory proteins control gene expression involves many different mechanisms. Transcriptional regulatory proteins control gene expression at the level of transcription. They often achieve this by binding to regulatory sequences within the gene's promoter; thereby, positively or negatively affecting transcription (Carlson, 1997). Transcriptional regulators are often referred to as DNA-binding proteins. Other regulatory proteins affect gene expression at the mRNA level and, as such, are called post-transcriptional or translational regulators. Many post-transcriptional/translational regulators are also RNA-binding proteins (Siomi and Dreyfuss, 1997). Post-transcriptional regulation is a broad term used to define regulatory events that affect gene expression after RNA polymerase has completed transcription (McCarthy, 1998). There are many levels in which regulation could occur post-transcriptionally, such as regulation of mRNA splicing, mRNA nuclear export, mRNA localization, translation, as well as post-translational events such as protein modification or protein degradation (Curtis et al., 1995; St Johnston, 1995). Proteins defined as translational regulators only control cytoplasmic events that affect translation, such as mRNA stability and mRNA localization (Mendez and Richter, 2001; Suzuki et al., 2009). Finally, some regulatory proteins control just

post-translational events, such as protein modifications (Chew et al., 2009; Janke et al., 2008).

The study of germline gene activity in many organisms, including *C. elegans*, has demonstrated that the regulation of the activity of many germline-expressed genes relies on sequences found within their mRNAs (Hagele et al., 2009; Mendez and Richter, 2001; Rangan et al., 2009; Zhang and Sheets, 2009). In *C. elegans*, the temporal and spatial expression of many germline-expressed proteins is controlled primarily by sequences in the 3' untranslated regions (UTRs) of the corresponding mRNAs (Merritt et al., 2008). In addition, cytoplasmic RNA-binding proteins are more highly expressed in the *C. elegans* germ line than in the soma (Wang et al., 2009a), suggesting that the control of RNA metabolism and/or translational control is likely utilized more in the germ line than the soma to control gene expression. RNA-binding proteins also show important post-transcriptional/translational roles in the germ lines of other organisms, including male mice (Bettegowda and Wilkinson, 2010) and *Xenopus* females (Radford et al., 2008).

Many of the components that make up the current mitosis vs. meiosis decision pathway are predicted to function as RNA-binding proteins/translational regulators. This includes the FBFs, FOG-1, GLD-1, NOS-3 and the GLD-2/GLD-3 complex. Each of these RNA-binding proteins are thought to function as translational regulators by binding mRNA through one of more RNA-binding domains. FOG-1 contains two RRM (RNA-Recognition Motif) domains followed by a zinc finger C/H domain (Luitjens et al.,

2000). GLD-1 contains a STAR (Signal Transduction Activators of RNA) domain that is composed of one KH (K-Homology) domain (Jones and Schedl, 1995) and two flanking domains called QUA1 and QUA2 (Lehmann-Blount and Williamson, 2005). NOS-3 contains a Nanos RNA binding domain that consists of CCHC zinc fingers (Kraemer et al., 1999). GLD-3 contains five KH-like domains (Eckmann et al., 2002). Finally, FBF contains the PUM-HD (Pumilio homology domain), or PUF domain, that consists of eight tandem copies of an imperfect, 36 amino acid sequence motif, called the PUF (or PUM) repeats (Zamore et al., 1997; Zhang et al., 1997). This thesis focuses on the role of another PUF protein family member, PUF-8, in the mitosis vs. meiosis decision. Thus, further details on this RNA-binding protein family will be discussed.

1.7.1 PUF Proteins

The PUF domain crystal structure, bound to its cognate mRNA, has been solved for *Drosophila* PUM (Edwards et al., 2001), Human PUM1 (Wang et al., 2001) and *C. elegans* FBF (Wang et al., 2009b). The overall structures of the PUF domains are quite similar among the three different organisms and consist of a curved structure reminiscent of a half doughnut (Figure 1.7) (Edwards et al., 2001; Wang et al., 2001; Wang et al., 2009b). The inner concave surface of the domain contacts the RNA molecule (Figure 1.7) (Edwards et al., 2001; Wang et al., 2001). Specifically, each PUF repeat, consisting of three α-helices, contacts one base of the mRNA target (Figure 1.7). Within the second α-helix of the repeat, three conserved amino acids interact with a

single RNA base; two amino acid residues contact the edge of the base through hydrogen bonding or van de Waals interactions, while the third residue typically provides stacking interactions by sandwiching itself between the two RNA bases (Figure 1.7) (Cheong and Hall, 2006; Wang et al., 2001).

All PUF proteins, analyzed thus far, bind invariably to mRNA 3'UTR sequences, which generally harbour a $UGUN_{3-5}AU$ sequence, where N is any nucleotide (Chritton and Wickens, 2010). Recently, 3000 mRNA targets were identified for Human Pum2, of which 93% contained PUF binding sites in the 3'UTRs (Hafner et al., 2010). In some cases, the specificity of an interaction between a PUF protein and an mRNA molecule involves additional RNA-binding proteins (Wickens et al., 2002). RNA-binding proteins known to interact with PUF proteins include Nanos proteins (Curtis et al., 1995; Kraemer et al., 1999; Nakahata et al., 2001; Sonoda and Wharton, 1999), CPEB (Cytoplasmic Polyadenylation Element-Binding) proteins (Luitjens et al., 2000; Richter, 2000) and Brat proteins (Frank and Roth, 1998; Slack and Ruvkun, 1998; Sonoda and Wharton, 2001). Upon binding to an mRNA 3'UTR, PUF proteins typical cause repression of the target (Wickens et al., 2002). In yeast, PUF proteins repress specific mRNAs by recruiting deadenylase complexes to the 3'UTR, which can cause mRNA destabilization and/or translational repression (Goldstrohm et al., 2006). FBF is believed to also use a similar strategy to stimulate the deadenylation of *gld-1* (Suh et al., 2009). *Drosophila* Pum uses a different strategy to repress *hunchback (hb)* mRNA: when DmPum binds to 3'UTR sites in *hb* mRNA, it recruits the protein Brat, which, in turn, binds the protein d4EHP, which

Figure 1.7. All PUF proteins share a similar functional domain.

(A) PUF domain derived from the Human Pum-RNA co-crystallization structure (Wang et al., 2001). The PUF domain consists of eight PUF repeats. The bound RNA molecule (yellow) interacts with the inner, concave surface of the PUF domain (purple ribbon structure). Three conserved amino acids residues (red, green and purple), within each of the eight repeats, directly interact with the RNA molecule. Image adapted from (Stumpf et al., 2008). (B) One individual PUF repeat consists of three α-helices. Image adapted from (Wang et al., 2001).

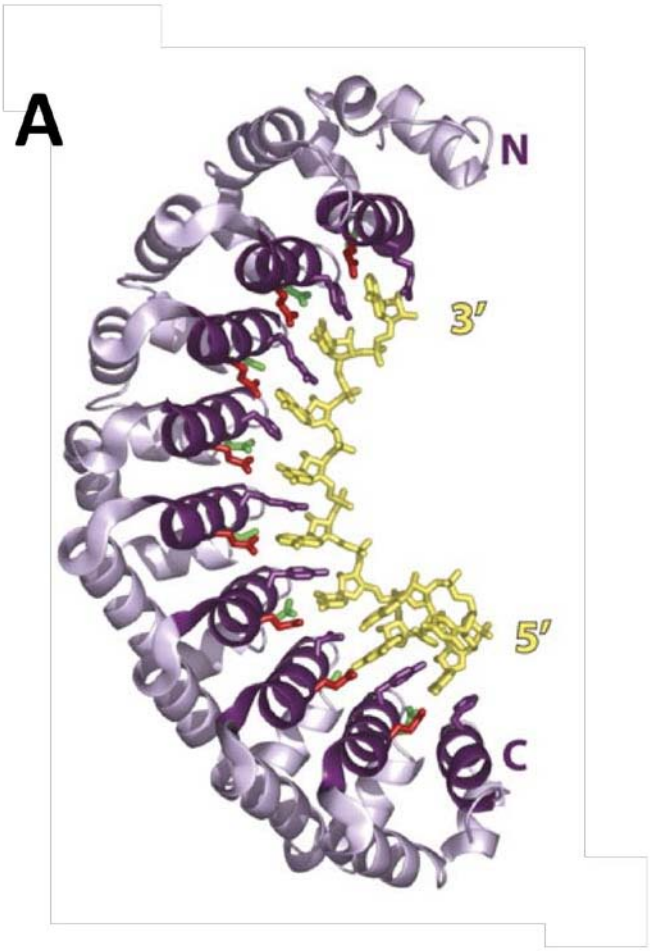
A
N
3′
5′
C

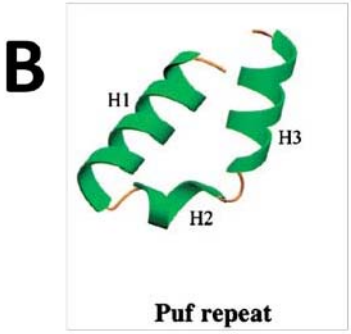
B
H1
H3
H2
Puf repeat

then binds the 5' (m7GpppG) cap, thereby inhibiting translation by blocking translation initiation (Cho et al., 2006). In some rare cases, binding of PUF proteins has also led to target activation (Kaye et al., 2009; Pique et al., 2008; Suh et al., 2009).

The *C. elegans* genome encodes 12 PUF proteins: FBF-1, FBF-2, PUF-3 to -12. The majority of the *C. elegans* PUF proteins can be clustered into four groups based on amino acid sequence similarities; group one includes PUF-8 and PUF-9, group two includes FBF-1 and FBF-2, group three includes PUF-5, -6 and -7 and group four includes PUF-3 and PUF-11 (Figure 1.8) (Stumpf et al., 2008). Alignment of the PUF repeats among all known PUF proteins revealed that PUF-8 and PUF-9 are the most similar to *Drosophila* PUM, mouse (PUM1 & PUM2) and Human (PUM1 & PUM2) (Wickens et al., 2002). The PUF-8 protein is expressed primarily in the germ line (see below), while the PUF-9 protein is expressed primarily in the soma (Subramaniam and Seydoux, 1999). The FBFs are essential for GSC self-renewal (Crittenden et al., 2002), the sperm to oocyte switch in hermaphrodites (Zhang et al., 1997) and act in neurons to modulate olfactory adaptation (Kaye et al., 2009). The third group includes PUF-5, -6 and -7, which function redundantly to regulate maternal mRNAs in the developing oocytes (Lublin and Evans, 2007). One of the maternal mRNAs targeted by PUF-5, -6 and -7 in the oocytes is *glp-1* (Lublin and Evans, 2007). The fourth and final group of PUF proteins includes PUF-3 and PUF-11. Little is known about PUF-3 and PUF-11; however, RNAi against each gene, individually, causes severe early embryonic defects (Sonnichsen et al., 2005). Additionally, binding assays reveal that PUF-11 binds mRNA using multiple

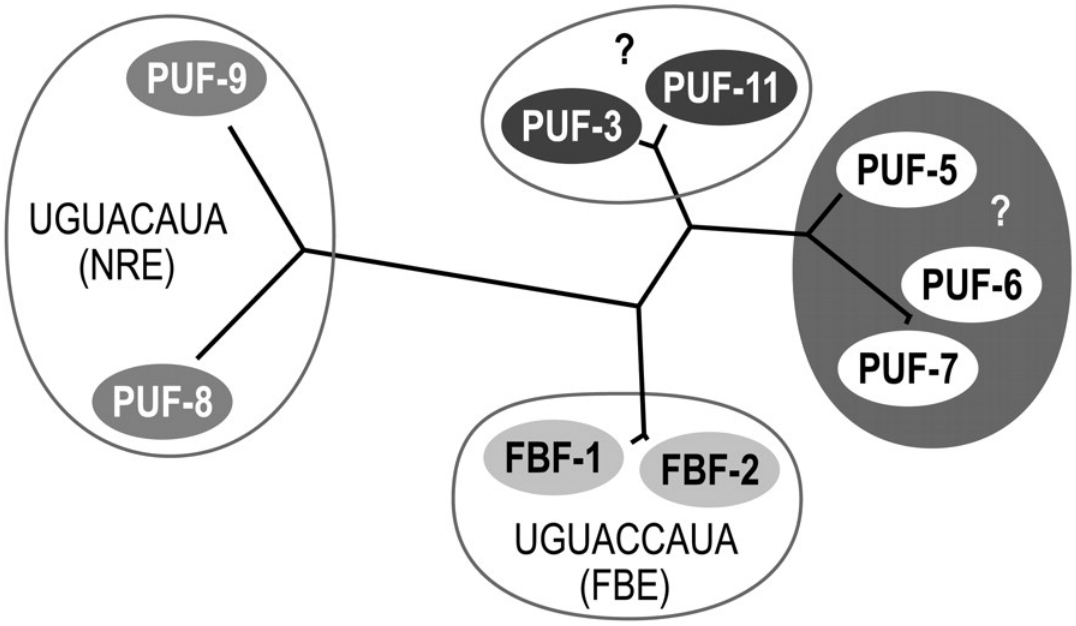

Figure 1.8. Four groups of *C. elegans* PUF proteins

The *C. elegans* PUF proteins can be clustered into four groups based on the similarities in amino acid sequence. Figure adapted from (Stumpf et al., 2008)

modes, which may potentially reveal alternative ways in which PUF proteins regulate mRNA targets (Koh et al., 2009). The remaining *C. elegans* PUF proteins that do not fall with in one of the four groups described above include PUF-4, -10 and -12. PUF-12 is a recently identified PUF protein; its homologs include PUF-A in humans and PENGUIN in *Drosophila* (Kuo et al., 2009). PUF-4 and PUF-10 are potentially pseudogenes, as no ESTs have been reported (wormbase.org).

1.8 PUF-8's Role in the Germ Line

PUF-8 is the germline-expressed PUF protein most similar to PUF proteins in higher eukaryotes (Wickens et al., 2002). In the germ line, PUF-8 has many important roles. During male meiotic development, PUF-8 is required to maintain meiosis and prevent re-entry into mitosis (Subramaniam and Seydoux, 2003). In a proportion of animals deficient for *puf-8,* grown at restrictive temperatures (25°C), primary spermatocytes do not complete meiosis, but instead dedifferentiate into mitotic germ cells (Subramaniam and Seydoux, 2003). PUF-8 is also important in hermaphrodites for the sperm to oocyte switch (Bachorik, 2005). In 3% of *puf-8* null mutants, excessive sperm are produced and animals fail to switch to oogenesis (Bachorik, 2005). This phenotype is exacerbated upon the removal of *fbf-1*; thus, PUF-8 and FBF-1 function redundantly to control the sperm to oocyte switch in *C. elegans* hermaphrodites (Bachorik, 2005). PUF-8 also functions in the distal germ line to promote proliferation of mitotic germ cells (Ariz et al., 2009). Loss of *puf-8* results in a decrease in the number of

mitotic germ cells (Ariz et al., 2009; Bachorik, 2005). In *puf-8; mex-3* double mutants, the number of mitotic germ cells is further reduced in comparison to either single mutant or wild-type animals (Ariz et al., 2009). Further genetic analysis revealed that PUF-8 and MEX-3 contribute to GSC maintenance by promoting mitotic proliferation, as opposed to blocking meiotic entry (Ariz et al., 2009). Finally, PUF-8 also has a function outside of the germ line in the development of the vulva (Walser et al., 2006). Specifically, PUF-8 restricts the temporal competency of vulval cells by promoting the fusion of the uninduced 3° cells with hyp7 (see Chapter 5) (Walser et al., 2006).

In this thesis, a new role for PUF-8 is described; PUF-8 functions in the mitosis vs. meiosis decision as a negative regulator of germ cell proliferation. Thus, the focus of this thesis is to characterize PUF-8's role in the mitosis vs. meiosis decision. This role implicates PUF-8 as an important regulator of proliferative germ cells and may offer new insights into the regulatory mechanisms controlling GSCs in higher eukaryotes. In other organisms, PUF proteins are also involved in GSC maintenance, such as *Drosophila* Pum (Forbes and Lehmann, 1998) and Pum2 in mice (Moore et al., 2003; Xu et al., 2007). PUF-8's role in the mitosis vs. meiosis decision was first identified in an enhancer screen to isolate mutations that enhance the over-proliferation phenotype of a weak gf allele of the *glp-1/*Notch receptor (see below, section 1.9). However, it was not known at the time that the isolated mutation was in the *puf-8* gene.

1.9 Screen to Identify Additional Regulators of the Mitosis vs. Meiosis Decision

The maintenance of the mitosis vs. meiosis decision is essential for preserving the reproductive fitness of *C. elegans*. The currently described pathway controlling the mitosis vs. meiosis decision includes the mitosis-promoting components (GLP-1/Notch signalling pathway and the FBFs) and the downstream meiosis-promoting components (GLD-1/NOS-3 and GLD-2/GLD-3). In order to better understand this important cell fate decision, identification of additional regulators is of great benefit. Since *C. elegans* shares a high degree of homology with other eukaryotic species (Consortium, 1998), knowledge gained from the mitosis vs. meiosis decision in *C. elegans* may be applicable to similar processes in other organisms.

One classic approach to identify regulators of the mitosis vs. meiosis decision is to screen for sterile mutants that disrupt this decision; this type of genetic approach identified *lag-1*, *lag-2* and *glp-1* as important components of the mitosis vs. meiosis decision (Austin and Kimble, 1987; Lambie and Kimble, 1991). This same approach was used to screen for additional genes that function in the mitosis vs. meiosis decision; however, after little success, it was hypothesized that other regulators in this pathway may have redundant functions and, thus, when mutated, may not have an obvious phenotype in a wild-type background (Maine and Kimble, 1993; Qiao et al., 1995). Based on this hypothesis, researchers have turned to using genetic enhancer and suppressor screens, mostly with alleles of *glp-1,* in order to identify additional genes that function in the mitosis vs. meiosis decision (Kerins et al., 2010; Maine and Kimble,

1993; Mantina et al., 2009; Qiao et al., 1995; Wilson-Berry, 1998). The theory behind *glp-1* enhancer and suppressor screens is that by using a sensitized *glp-1* mutant background, small changes will be amplified that either increase or decrease the activity or signalling, producing visible phenotypic changes to the germ line. For example, in a screen to identify enhancers of a weak *glp-1* lf mutation, *glp-1(bn18)*, five new genes were identified, *ego-1* to *-5* (Enhancer of *Glp-One*) (Qiao et al., 1995). Other sensitized backgrounds have also been used to identify additional factors that function in the mitosis vs. meiosis decision, including a *gld-2* synthetic tumour screen (Hansen et al., 2004a; Macdonald et al., 2008) and a *gld-3* synthetic tumour screen (X. Wang and D. Hansen, unpublished data).

The *glp-1* enhancer screen that identified *puf-8* (formally known as *teg-2)* as a regulator of the mitosis vs. meiosis decision was performed by Dr. Laura Wilson-Berry (Wilson-Berry, 1998). The sensitized background used for this screen was the *glp-1(oz112oz120)* mutant. The *glp-1(oz112)* allele is a strong gf mutation that causes complete germ line tumours at 25°C. In a screen to look for revertants of the *glp-1(oz112)* phenotype, the *glp-1(oz120)* intragenic mutant was discovered. In combination, *glp-1(oz112oz120)* functions as a temperature-sensitive allele (Berry et al., 1997). At higher temperatures (25°C), *glp-1(oz112oz120)* functions as a strong lf allele, forming Glp germ lines (Wilson-Berry, 1998). However, at 15°C, *glp-1(oz112oz120)* functions as a weak gf allele due to retention of residual *glp-1(oz112)* gf activity: 99.95% of the animals have germ lines that show wild-type levels of distal proliferation, while

the remaining 0.05% have late-onset over-proliferation defects (Wilson-Berry, 1998). The retention of weak gf activity makes *glp-1(oz112oz120)* an excellent sensitized background. Mutations that enhance the *glp-1(oz112oz120)* over-proliferative phenotype represent genes that function either as negative regulators of proliferation (mitosis) or positive regulators of entry into meiosis. From 8200 haploid genomes screened, Wilson-Berry identified seven alleles that enhanced the *glp-1(oz112oz120)* over-proliferative phenotype. These seven alleles occupy four separate complementation groups, referred to as *teg-1* to *-4* (Tumourous Enhancement of weak *Glp-1(gf)*) (Wilson-Berry, 1998). This thesis focuses specifically on *teg-2(oz192)*. Characterization of *teg-4* has been published (Mantina et al., 2009) and work on the *teg-1* gene is currently underway (C. Wang and D. Hansen, personal communication).

Prior to initiation of this thesis project, *teg-2(oz192)* had been partially characterized (Wilson-Berry, 1998). To provide sufficient background of *teg-2(oz192)*, a summary of Laura Wilson-Berry's results are included below.

1.10 Initial Characterization of *teg-2* Performed by Laura Wilson-Berry

1.10.1 Characterization of teg-2's *enhancement of* glp-1(oz112oz120)

Four mutations in *teg-2(oz192, oz194, oz216* and *oz218*) were isolated in the Teg screen; however, three of the mutations were lost shortly after isolation. All four mutations in *teg-2* enhanced the late-onset over-proliferation phenotype of *glp-1(oz112oz120)* and also induced the formation of a Pro tumour. Further

characterization was done using only the *teg-2(oz192)* allele. Separating the late-onset and Pro tumours, *teg-2(oz192); glp-1(oz112oz120)* mutants have a small region of meiotic entry that contains normal germline polarity of cells undergoing the various stages of male meiosis. Furthermore, Pro tumours were also observed in *teg-2; glp-1(oz112oz120)/+* heterozygotes. Wilson-Berry hypothesized that mutations in *teg-2* restore the genetic dominance of the *glp-1(oz112)* gf allele. This phenomenon will be discussed again (see Chapter 4, section 4.1.3) with reference to other strains made during this thesis project.

1.10.2 Characterization of the teg-2 *Single Mutant Phenotype*

In a *glp-1(+)* background at permissive temperatures (15-20°C), *teg-2* single mutants have reduced proliferation in the distal germ line. Wilson-Berry observed that *teg-2(oz192)* mutants have a mitotic zone length of ~10 germ cell diameters (gcd) to the transition zone, while mitotic zones in N2 (wild-type) animals are ~20 gcd to the transition zone. While the *teg-2(oz192)* distal mitotic zones are reduced in size compared to wild-type, the rest of the *teg-2(oz192)* germ line undergoes normal germ cell progression and form functional gametes. Comparing early larval staged germ lines from *teg-2* mutants with N2, Wilson-Berry observed that the number of germ cells in *teg-2(oz192)* animals was less than in wild-type, suggesting that *teg-2* functions early in larval development to promote robust germline proliferation. When *teg-2(oz192)* animals were shifted to higher temperatures, more dramatic phenotypes were

observed. At 25°C, two types of phenotypes arose; the most predominant was a much smaller than wild-type germ line with normal germ cell polarity, while the remaining 20% showed proximal proliferation (Pro tumours). These temperature sensitive defects were also observed in *teg-2* males. Other *teg-2* phenotypes at 25°C include a "jackpot" male phenotype, in which the amount of male progeny varied from plate to plate. This phenotype has been observed in mutations of genes involved in chromosome segregation during mitosis (Riddle et al., 1997). Wilson-Berry also observed that *teg-2(oz192)* did not interact with a *glp-1* allele that disrupts GLP-1's role during embryogenesis; however, *teg-2(oz192)* did suppress the Glp phenotype of a *glp-1* temperature-sensitive lf allele, *glp-1(q231)*. This revealed that *teg-2* likely does not function with *glp-1* during embryogenesis and that *teg-2* can interact with other *glp-1* alleles. Finally, Wilson-Berry also observed that *teg-2(oz192)* interacted with *lin-12* during vulval development, another Notch receptor in *C. elegans*, suggesting that *teg-2* functions as a general negative regulator of Notch signalling. Genetic analysis performed by Walser et al. 2006 and analysis performed during this thesis (see Chapter 5), suggests that *teg-2 (puf-8)* is likely not a general negative regulator of Notch signalling but is either a germline-specific negative regulator of Notch or of proliferation.

1.11 Thesis Goals

The overall goal of this thesis is to characterize *teg-2's (puf-8's)* role as a negative regulator of proliferation in the *C. elegans* germ line. Ultimately, the aim is to uncover

new insights into the regulatory mechanisms controlling GSCs and transit-amplifying cells in higher eukaryotes. The specific goals of this project include:

(1) Identify the gene that is disrupted by the *teg-2(oz192)* mutation (Chapter 3).

(2) Characterize *teg-2's* (*puf-8's)* role in the mitosis vs. meiosis decision (Chapter 4).

(3) Determine if *teg-2 (puf-8)* functions in other Notch-related developmental decisions (Chapter 5).

(4) Determine the expression pattern of the TEG-2 (PUF-8) protein in the *C. elegans* germ line (Chapter 6 and Appendix A).

1.12 Contributions from Publications

Excerpts from this Chapter have been taken from Racher and Hansen (2010) Genome 53:83-102.

Chapter Two: **Materials and Methods**

2.1 General Methods

All strains were maintained using standard methods on nematode growth medium (NGM) plates seeded with *E. coli* OP50 (Brenner, 1974). Strains were grown at temperatures varying between 15-25°C, depending on the presence of a temperature-sensitive mutation. Strains were derived from the wild-type Bristol strain (N2), unless otherwise noted. Strains used for SNP mapping were derived from both N2 and Hawaiian (HA) CB4856, a wild-type strain of *C. elegans* isolated from Hawaii (Wicks et al., 2001).

2.2 Nomenclature

Mutations used in this study are listed below by linkage group (LG) (section 2.2.1). For descriptions of the different mutations, see (Hodgkin and Martinelli, 1999). The gene names are: *ain* (ALG-1 INteracting protein), *bli* (BLIster), *clr* (CLeaR)*, cup* (Coelomocyte UPtake defective), *dpy* (DumPY), *eff* (Epithelia Fusion Failure), *fbf* (*Fem-3* mRNA Binding Factor), *fem* (FEMinization of XX and XO animals)*, fog* (Feminization Of Germline), *gld* (GermLine Defective), *glp* (GermLine Proliferation defective), *lin* (abnormal cell LINeage), *lst* (Lateral Signalling Target), *puf* (PUmilio and FBF domain-containing), *rol* (ROLler), *sel* (Suppressor/Enhancer of *Lin-12*), *sma* (SMAll)*, spe*

(defective SPErmatogenesis)*, teg* (Tumourous Enhancer of *Glp-1(weak gf)*)*, unc* (UNCoordinated).

Other nomenclature rules that apply to this project include the following. Integrated transgenes are designated by italicized names consisting of the laboratory allele prefix, the two letters *Is*, and a number (ex. *arIs4251*). Integrated transgenes, using MosSCI, are designated by italicized names consisting of the laboratory allele prefix, the two letters *Si*, and a number (ex. *ugSi1*). Chromosomal aberrations are given italicized names consisting of the laboratory mutation prefix, the abbreviation of the type of aberration (deficiencies (*Df*), translocations (*T*) and chromosomal balancers of unknown structure (*C*)), a number and sometimes the affected linkage groups are provided in parentheses (ex. from each category: *mnDf30, hT2(I; III), mC6g(II)*). Laboratory-specific prefixes can be found through the *Caenorhabditis* Genetics Center (www.cbs.umn.edu/CGC).

2.2.1 Alleles, Balancers and Deficiencies Used in this Study

LGI: *gld-1(q485), gld-2(q487), ccIs4251*[*myo-3::Ngfp-lacZ; myo-3::Mtgfp*] *unc-15(e73), fog-1(e2121), unc-11(e47), ain-2(tm2432), cup-2(tm2838), hT2[dpy-18]*(I, III)

LGII: *puf-8(oz192, q725), unc-4(e120), bli-2(e768) rol-6(e187), nos-3(oz231), gld-3(q730), fbf-1(ok91), fbf-2(q704), dpy-10(e128), lin-4(e912), sma-6(e1482), unc-*

85(e1414), clr-1(e1745), eff-1(hy21), lst-1(ok814), maDf4, mDf14, mnDf30, mnDf88, mnDf96, mDf18, mC6g (also called *mIn1 [dpy-18, myo-2::gfp])*

LGIII: *glp-1(ar202, oz264, oz112oz120, bn18, q175), lin-12(n302), unc-32(e189), spe-6(hc49) unc-25(e156), hT2[dpy-18]*(I, III)

LGIV: *fem-3(e1996), unc-24(e138), dpy-20(e1282), arIs51*[*cdh-3::gfp*]*,ugSi1*[*puf-8 prom::puf-8 coding::gfp::tap::puf-8 3'UTR*]

LGV*: sel-10(bc243), fog-2(q71), unc-76(e911), rol-9(sc148)*

2.3 Isolation of the *teg* Mutations

A total of 4 *teg* genes (*teg-1* to *-4*) were identified in an enhancer screen, using *glp-1(oz112oz120gf)* animals (Wilson-Berry, 1998). The following is a brief description of the screen performed by Laura Wilson-Berry. To induce mutations, larval stage 4 (L4) *glp-1(oz112oz120)* animals were mutagenized with EMS (Ethyl Methane Sulfonate) at 20°C for 4 hr (Brenner, 1976), separated individually onto large NGM plates and stored at 15°C. One week later, L4 F1 progeny were cloned to individual plates. Then 6-10 days later, the F2 progeny were screened for over-proliferative germline phenotypes. All identified enhancer mutations were outcrossed two times.

2.4 Whole Worm Lysis for PCR

Standard procedures were used to extract DNA from worms for PCR (Hope, 1999). In brief, 2-3 animals were added to 2.5 µL of worm lysis buffer (50 mM KCL, 10 mM Tris-

HCl pH 8.2, 25 mM $MgCl_2$, 0.45% NP-40, 0.45% Tween-20, 0.01% Gelatin, 3 mL of proteinase K/mL) and freeze-cracked at -80°C for a minimum of 10 min. To lyse the worms and release the genomic DNA, each sample was heated at 65°C for 60 min, followed by 95°C for 15 min to inactivate the proteinase K.

2.5 Mapping

Previous two-factor and three-factor mapping placed *teg-2(oz192)* on linkage group (LGII) in a 425 kb region between *lin-4* and *sma-6* (Figure 2.1) (Wilson-Berry, 1998). Work done in this thesis involved further mapping in this region of LGII and found that *teg-2(oz192)* was not located between *lin-4* and *sma-6*, but 385 kb to the right between *dpy-10* and *rol-6*. The mapping procedure that was used to determine this mapping error is outlined below, as well as the mapping procedure used to identify the correct location for *teg-2(oz192)*. A description of the outcomes from these mapping strategies can be found in Chapter 3.

2.5.1 Single Nucleotide Polymorphism (SNP) Mapping

SNP mapping was performed to determine the location of the *teg-2* genetic locus (Jakubowski and Kornfeld, 1999). Appropriate SNPs were selected using the wormbase.org database. Selection priority was given to SNPs that disrupted a restriction recognition site (snip-SNP) in either the N2 or HA DNA (Wicks et al., 2001). The snip-SNPs tested are found in Figure 2.2.

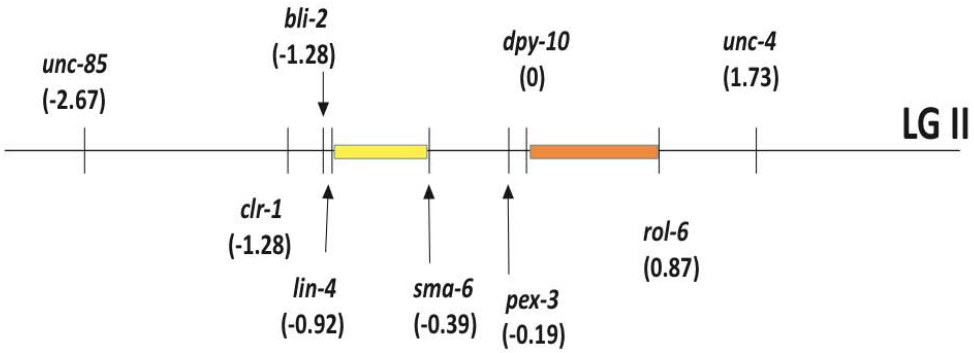

Figure 2.1. Location of the "old" and "new" *teg-2* critical regions on linkage group two (LGII).

The "old" *teg-2* region (yellow rectangle) was proposed to be located between the genes *lin-4* and *sma-6*. Through SNP and deficiency mapping, the "new" *teg-2* region (orange rectangle) was determined to be between the genes *dpy-10* and *rol-6*. The genetic positions (in centimorgans (cMs)) for each visible marker gene is shown in brackets below gene name.

Figure 2.2. The snip-SNPs tested for SNP mapping.

All snip-SNPs tested are located between the *bli-2* and *unc-4* genes on LGII. The following information is provided for each snip-SNP: snip-SNP identifier name, the physical chromosomal location (in kb), the restriction enzyme site the snip-SNP disrupts and whether the SNP change causes N2 or HA DNA to be digested (cut) by the corresponding restriction enzyme. All snip-SNPs included in this figure were tested via PCR followed by restriction digest; however not all snip-SNPs included in this figure were tested on all SNP mapping recombinant strains.

snip-SNP	location (kb)	cuts	Enzyme
pKP2147	5761	HA	ScaI
K05F1[1]	5802	HA	SspI
F55C12[1]	5865	HA	AseI
uCE2-1648	5924	HA	TaqI
uCE2-1653	6007	HA	SfaNI
uCE2-1656	6085	N2	DdeI
F13H8[2]	6256	N2	BglI
C29F5[2]	6303	N2	MnlI
K03H9[1]	6410	N2	NspI
R0569[1]	6507	N2	DdeI
C18H9[2]	6678	N2	AluI
F31E8[1]	6812	N2	EcoRI
F32A5[2]	7257	HA	DdeI
uCE2-1720	7278	N2	Taq1
uCE2-1722	7278	HA	Tsp5091
snp_C30G12[2]	7288	HA	MnlI or BfaI
uCE2-1725	7289	N2	HpyCH4IV
uCE2-1729	7295	HA	AluI
uCE2-1730	7296	N2	FatI
CE2-155	7298	HA	Tsp5091
uCE2-1731	7298	HA	BaeI
pkP2150	7314	N2	ApoI
uCE2-1732	7324	N2	CjeI
uCE2-1736	7340	HA	BciVI
snp_F21D12[1]	7341	HA	ApoI or Tsp5091
uCE2-1737	7355	N2	SfaNI
ZK1290[2]	7538	N2	NspI
uCE2-1752	7669	N2	BtgZI
C06A8[4]	7798	N2	DdeI
T05A6[1]	7812	N2	AccI
DH11[1]	7994	N2	BstXI
T05T10[1]	8061	N2	Af1III
CE2-163	8132	N2	FatI
F49E12[1]	8387	N2	Hpy188I
uCE2-1791	8410	N2	FokI
uCE2-165	8479	HA	FatI
T13H5[3]	8516	N2	HphI
pkP2109	9401	N2	EcoRI

SNP mapping between *lin-4* and *sma-6*: The physical distance between *lin-4* and *sma-6* is 425 kb and contains 91 genes. To map from the *sma-6* right border, *teg-2(oz192) unc-4(e120)/mC6g; glp-1(ar202)* animals were mated to *HA(*CB4856*); glp-1(ar202)* males. Non-GFP hermaphrodites (*teg-2(oz192) unc-4(e120)/HA; glp-1(ar202)*) were selected to individual plates and allowed to self-fertilize. From the F2 self-progeny, Unc non-Tum recombinants (*HA unc-4(e120)/ teg-2(oz192) unc-4(e120); glp-1(ar202)*) were recovered onto individual plates and allowed to self-fertilize. Homozygous *HA unc-4(e120); glp-1(ar202)* lines were selected based on 100% Unc non-Tum progeny. DNA was prepared from each recombinant homozygous line using whole worm lysis (see section 2.4). PCR amplification of snip-SNPs was performed using primers flanking each polymorphism. Resultant PCR products were tested for the presence of N2 or HA DNA at each SNP by restriction digest. To map from the *lin-4* left border, the *bli-2(e768) teg-2(oz192)/HA; glp-1(ar202)* strain was generated and recombinants were picked using the same procedure as with *teg-2 unc-4*. Based on the SNP mapping results (see Chapter 3), *teg-2* was determined not to be between *lin-4* and *sma-6*, but between *dpy-10* and *rol-6*.

SNP mapping between *dpy-10* and *rol-6*: The physical distance between *dpy-10* and *rol-6* is 2022 kb and contains approximately 463 genes. To map from the *rol-6* right border, the *teg-2(oz192) rol-6(e187)/HA; glp-1(ar202)* strain was generated, recombinants were recovered, using the logic described above, and genomic DNA was

analyzed using nearby snip-SNPs (Figure 2.2). Results from the SNP mapping strain *bli-2(e768) teg-2(oz192)/HA; glp-1(ar202)* were used to map from the left border.

2.5.2 Deficiency Mapping

In addition to SNP mapping, deficiency mapping was performed to further determine the location of the *teg-2* genetic locus (Sigurdson et al., 1984). Deficiency strains were selected using wormbase.org database.

Deficiency mapping between *lin-4* and *sma-6*: The deficiency strains that map within, or overlap with the *lin-4* to *sma-6* region, include *maDf4*, *mnDf30* and *mDf14*. *teg-2(oz192) unc-4(e120); glp-1(ar202)* males was crossed to each deficiency strain to generate *teg-2 unc-4/Df; glp-1(ar202)/+* animals, which were picked to individual plates and allowed to self. Note: homozygous deficiencies cause embryonic lethality. The progeny of *teg-2 unc-4/Df; glp-1(ar202)/+* animals were then screened for non-Unc Tum animals.

Deficiency mapping between *dpy-10* and *rol-6*: The deficiency strains that map within, or overlap with the *dpy-10* to *rol-6* region, include *mnDf88*, *mnDf96* and *mDf18*. Each deficiency strain was crossed to *teg-2(oz192) unc-4(e120); glp-1(ar202)* males to generate *teg-2 unc-4/Df; glp-1(ar202)/+* animals, which were picked to individual plates and allowed to self. The progeny was then screened for the presence of non-Unc Tum animals.

2.6 Candidate RNAi

While mapping of *teg-2* was underway, RNAi (by feeding) against the genes between *lin-4* and *sma-6* was performed to see if any gene, when knock-downed, phenocopied the *teg-2(oz192); glp-1(gf)* tumourous phenotype. Of the 91 genes between *lin-12* and *sma-6*, RNAi feeding vectors for 74 of these genes were available in the Ahringer RNAi bacterial library (Kamath and Ahringer, 2003). In brief, each RNAi bacterial colony was grown at 37°C for 16 hr in 1 mL LB with 100 μg/mL of ampicillin. 100 μL of each RNAi bacterial culture was used to seed agar plates containing NGM, 25 mg/mL of carbenicillin and 20% β-lactose. The seeded plates were grown at room-temperature for 2 days until a lawn of bacteria was formed. Plates seeded with RNAi bacteria against *gfp* or *elt-2* were used as negative and positive controls, respectively. One L4 and one adult *glp-1(ar202)* animal were added to each plate and incubated at 20°C for 4 days. F1 progeny were screened for plates that phenocopied the *teg-2(oz192); glp-1(ar202)* tumourous phenotype. To monitor the background level of tumour formation, bacteria with the empty RNAi feeding vector (pL4440) was fed to *glp-1(ar202)* animals.

2.7 Sequencing Candidate Gene

After SNP and deficiency mapping in the *dpy-10* to *rol-6* region, the potential candidate genes for *teg-2* was reduced to 18 genes. One candidate gene that was selected for sequencing was *puf-8*. Primers were designed to amplify the entire *puf-8*

gene; PUF8_PCRREV1(Q53): CCGGTATAACAACCGGATTTG and PUF8_PCRFOR1 (Q54): GGAGAAATGGGTTTCACCAC. Genomic DNA from *teg-2(oz192)* animals was prepared using whole worm lysis and PCR amplified using *puf-8* specific primers (Q54/Q53). Using sequencing primers, the *puf-8* PCR product was sequenced by the University of Calgary Core DNA Services Laboratory to identify molecular lesions. The sequencing primers include: PUF8_REV1 (Q55): GTGCTTTCCATGAGGGAATTG, PUF8_REV2 (Q56): GCTTTCTGAAGAACACGGCA, PUF8_REV3(Q57): GGCAAATTGAAACTCTGGTG, PUF8_FOR1 (Q58): CACCAAGCGCATTCTCAAAG, PUF8_FOR2(Q59): GTGTTGTCCAACGTTGTCTC, PUF8_FOR3 (Q61): CCACCGACGATCTTCTAACT. Three strains containing *teg-2(oz192)* were sequenced with *puf-8* primers.

2.8 Complementation Test

Prior to the complementation test, the *puf-8(q725); glp-1(ar202)* strain was generated and was confirmed to also produce tumours. To test if *teg-2(oz192)* was an allele of *puf-8*, a complementation test was performed at 15°C using the following steps. First N2 males were crossed to *puf-8(q725)/mC6g; glp-1(ar202)* L4 hermaphrodites. Non-green males were selected then crossed to *teg-2(oz192) rol-6(e187)/mC6g; glp-1(ar202)* L4 hermaphrodites. Non-green non-Rol L4 hermaphrodite cross-progeny were picked onto individual plates. The genotype of the resulting progeny was: *teg-2(oz192) rol-6(e187)/puf-8(q725) [or teg-2(oz192) rol-6(e187)/+]; glp-1(ar202) [*or *glp-1(ar202)/+]*. Plates containing *teg-2(oz192) rol-6(e187)/+; glp-1*(ar202) *[*or *glp-*

1(ar202)/+] animals produced both tumourous roller progeny and wild-type progeny. Plates containing *teg-2(oz192) rol-6(e187)/puf-8(q725); glp-1(ar202) [*or *glp-1(ar202)/+]* animals produce no progeny, as they are tumourous; tumours are produced in the presence of either one or two copies of *glp-1(ar202)* (see Materials and Methods section 2.13).

2.9 Gonad Dissections

Gonad dissections were performed using procedures modified from (Hansen et al., 2004a). For most experiments, 50-100 L4 staged animals were placed onto one seeded NGM plate. One day later the animals were washed off the plate using 1XPBS (Phosphate Buffered Saline; 137 mM NaCl, 2.7 mM KCl, 100 mM Na_2HPO_4, KH_2PO_4) and transferred into a microcentrifuge tube to wash off the residual bacteria. Next the animals were transferred to a watchglass using 1XPBS and 0.2 mM levamisole (Sigma) was added. After 5 mins, the gonads are dissected out of the paralyzed animals by cutting off the heads using $25G^{5/8}$ needles. Once dissected, the gonad arms were fixed for 10 min in 3% paraformaldehyde (16% paraformaldehyde (Electron Microscopy Sciences), 1 M K_2HPO_4 , 1 M KH_2PO_4, ddH_20) in the fume hood. After fixation, the gonads were washed with 1XPBT (1XPBS + 0.1% Tween 20) and permeabilized in ice-cold methanol for a minimum of 10 min at -20°C.

2.10 Antibody Staining for Immunofluorescence

Fixed and permeabilized gonads were washed with 1XPBT before blocking with 3% BSA (Bovine Serum Albumin) for 1 hr at 4°C. Primary (1°) antibodies were diluted using 3% BSA. The following 1° antibodies and dilutions were used: 1/20, αGLD-1 rabbit (Jones et al., 1996): 1/50, αREC-8 rat (Pasierbek et al., 2001): 1/150, αHIM-3 rabbit (Zetka et al., 1999): 1/500, and αGFP 3E6 mouse (Molecular Probes): 1/750. Blocked gonads were incubated with 1° antibodies over-night (O/N) at 4°C. On the same day, Secondary (2°) antibodies were diluted with 3% BSA + trace amounts of N2 worm acetone powder and incubated O/N at 4°C with end-over-end rotation. The 2° antibodies and dilutions used were as follows: Donkey αrabbit Alexa594 (Molecular Probes): 1/500, Donkey αrat Alexa488 (Molecular Probes): 1/200, Donkey αmouse Alexa488 (Molecular Probes): 1/200. The next day, excess unbound 1° antibodies were washed off the gonads using 1XPBT. The gonad arms were then incubated with the 2° antibodies for 2-4 hrs at room-temperature. Unbound excess 2° antibodies were removed by washing with 1XPBT. To visualize the nuclear DNA, the gonad arms were incubated with 100 ng/mL of 4,6-diamidino-2-phenylindole hydrochloride (DAPI) in 1XPBS for 5 mins. After incubation, DAPI was removed and -20°C DABCO (1% 1,4-diazobicyclo[2,2,2]-octane (DABCO) in 90% glycerol in PBS) was added before mounting gonads on agar-pad slides with a cover slip.

2.11 Imaging

Fluorescent images were captured with a Zeiss Imager Z1 microscope equipped with Axiocam MrM camera (Ziess). Images were viewed and analyzed using the AxioVision software. Photoshop software was used to assemble whole gonad arms from individual images.

2.12 Special Considerations for Strains Containing *glp-1(ar202)* and *glp-1(oz264)*

Both gf alleles of *glp-1* used in this thesis, *ar202* and *oz264*, are essentially wild-type at 15°C (Kerins et al., 2010; Pepper et al., 2003). However, at 25°C, both *glp-1(ar202)* and *glp-1(oz264)* display over-proliferative germline defects. Therefore, it is necessary that strains containing *glp-1(ar202)* or *glp-1(oz264)* be maintained at temperatures ranging from 15-20°C. However, in order to increase Notch signalling, *glp-1(ar202)* or *glp-1(oz264)* animals need to be shifted to 25°C. The exception to this rule is when *puf-8* mutations are present: *puf-8(q725* or *oz192); glp-1(ar202* or *oz264)* animals are tumourous at all temperatures (15-25°C).

2.13 Generating *puf-8(oz192); glp-1(ar202)/+*

To analyze *puf-8*'s interaction with *glp-1(ar202)/+* heterozygous animals, the following steps were employed. First, *puf-8(oz192)* males were crossed to *puf-8(oz192) unc-4(e120)/mC6g; glp-1(ar202)* L4 hermaphrodites. Then F1 non-green non-Unc cross-progeny L4 hermaphrodites (*puf-8(oz192) unc-4(e120)/puf-8(oz192); glp-1(ar202)/+)*

were selected and grouped onto a new seeded plate. The next day, the young adult germ lines were dissected and stained with αREC-8 and αHIM-3 antibodies.

Note: *puf-8(q725* or *oz192); glp-1(ar202* or *oz264)* animals were generated from, *puf-8(q725* or *ôz192)/mC6g; glp-1(ar202* or *oz264)* stocks.

2.14 Generating Recombinant Mutant Strains

2.14.1 Generating fbf-1 fbf-2 puf-8 *Triple Mutants*

fbf-1 fbf-2 and *puf-8* are located close to each other on chromosome II: *fbf-1* (-0.59 cM) (centiMorgans), *fbf-2* (-0.54 cM) and *puf-8* (0.5 cM). The *fbf-1 fbf-2* mutant was already constructed (strain JK3107) and obtained from the CGC (www.cbs.umn.edu/CGC). In order to generate triple mutant strains, first *fbf-1 fbf-2* and *puf-8* mutants were marked with *rol-6* and *bli-2*, respectively. The alleles used were *fbf-1(ok91), fbf-2(q704),* and *puf-8(q725)*.

To make a *fbf-1 fbf-2 rol-6* strain, *bli-2 rol-6/+* males were crossed to *fbf-1 fbf-2/mC6g* L4 hermaphrodites. Non-green L4 progeny (*bli-2 rol-6/fbf-1 fbf-2* or *+/fbf-1 fbf-2*) were picked onto individual plates and allowed to self. Those that failed to segregate *fbf-1 fbf-2* were discarded. *rol-6* is located 1.4 cM to the right of *fbf-2*. The plates that contained *bli-2 rol-6/fbf-1 fbf-2* animals were then screened for recombinants by looking for non-Bli Rol animals that segregated 1/4th Glp (i.e., *bli-2 rol-6/fbf-1 fbf-2 rol-6)*; all other non-recombinant self-progeny were either wild-type (*bli-2 rol-6/fbf-1 fbf-2*),

Bli Rol (*bli-2 rol-6/bli-2 rol-6*) or Glp (*fbf-1 fbf-2/fbf-1 fbf-2*). Recombinants were then balanced with mC6g.

To make a *bli-2 puf-8* strain, *bli-2 rol-6/+* males were crossed to *puf-8* L4 hermaphrodites. L4 progeny (*bli-2 rol-6/puf-8* or *+/puf-8*) were picked onto individual plates and allowed to self. *bli-2* is located 1.5 cM to the left of *puf-8*. Plates were then screened for *bli-2 puf-8/bli-2 rol-6* recombinants by identifying non-Rol Bli animals. All non-recombinant self-progeny were either wild-type (*bli-2 rol-6/puf-8* or *puf-8/puf-8)* or Bli Rol (*bli-2 rol-6*). The recombinant strain was maintained as *bli-2 puf-8*, as this double mutant is homozygous viable.

Next the two marked strains were crossed to each other; *bli-2 puf-8/+* males were crossed to *fbf-1 fbf-2 rol-6/mC6g* L4 hermaphrodites. Non-green L4 progeny (*fbf-1 fbf-2 rol-6/bli-2 puf-8* or *+/ fbf-1 fbf-2 rol-6*) were picked onto individual plates and allowed to self. Plates containing *fbf-1 fbf-2 rol-6/bli-2 puf-8* animals were then heat-shocked to produce males (Sulston and Hodgkin, 1988) and a *fbf-1 fbf-2 rol-6/bli-2 puf-8* males stock was generated and maintained. *fbf-2* is located 1 cM away from *puf-8*; thus, 0.5% of the gametes in the *fbf-1 fbf-2 rol-6/bli-2 puf-8* males were predicted to contain *fbf-1 fbf-2 puf-8* recombinants. In order to identify these recombinants, *fbf-1 fbf-2 rol-6/bli-2 puf-8* males were crossed to *bli-2 rol-6* L4 hermaphrodites. 4-5 days later, the plates were screened for wild-type cross-progeny, which represent the recombinant animals (*fbf-1 fbf-2 puf-8/bli-2 rol-6*). If recombination did not occur between *fbf-2* and *puf-8* in the cross to *bli-2 rol-6* hermaphrodites, then all the cross-progeny were either

Rol (*fbf-1 fbf-2 rol-6/bli-2 rol-6*) or Bli (*bli-2 rol-6/bli-2 puf-8*). Wild-type cross-progeny were selected onto individual plates and allowed to self. Recombinants were balanced with mC6g. The presence of *fbf-1, fbf-2* and *puf-8* were confirmed using PCR.

2.14.2 Generating glp-1(ar202) spe-6(hc49) *Double Mutants*

The *glp-1* and *spe-6* genes are both located on chromosome III, 10.4 cMs away from each other. To generate *glp-1(ar202) spe-6(hc49)* recombinants, *glp-1(ar202)/hT2g* males were crossed to *spe-6(hc49) unc-25(e156)* L4 hermaphrodites. This cross was performed at 18°C to prevent *glp-1(ar202)* temperature-sensitive over-proliferation phenotypes from occurring. The *spe-6 unc-25* animals (strain BA606) were provided by the CGC (www.cbs.umn.edu/CGC). *spe-6(hc49)* mutants (from a stock rescued with a duplication) do not produce functional sperm; however, they do produce functional oocytes (Varkey et al., 1993) and, thus, can be mated with males. Non-green cross-progeny (*glp-1/spe-6 unc-25*) were selected. In order to detect recombinants, *hT2g/+* males were crossed to *glp-1/spe-6 unc-25* L4 hermaphrodites. Green L4 hermaphrodite progeny were placed onto individual plates and shifted to 25°C, to induce the temperature-sensitive *glp-1(ar202)* over-proliferation defect. Such plates were rescreened to find plates that had 1/4th Tum Unc recombinant animals (*glp-1 spe-6 unc-25*). Plates containing non-recombinant animals showed either 1/4th Tum or 1/4th Unc Spe animals. Recombinant animals were maintained as *glp-1 spe-6 unc-25/hT2g*.

This recombinant strain was used to generate *puf-8; glp-1 spe-6 unc-25*, discussed in Chapter 4 (section 4.3).

2.15 *puf-8::gfp* Construct for Biolistic Transformation

The pGB2 [*puf-8 promoter::puf-8 genomic::gfp::unc-54 3'UTR]* construct, made by the Hajnal lab (Walser et al., 2006), was used as the backbone to generate a *puf-8::gfp* construct for biolistic transformation (see below). Biolistic transformation involves bombarding *unc-119(ed3)* animals with rescuing constructs to generate low-copy integrants (Praitis et al., 2001). Thus, to make a low-copy *puf-8::gfp* integrant, *unc-119(+)* must be included in the biolistic transformation plasmid. In addition to the inclusion of *unc-119(+)*, two other modifications were also made to the pGB2 plasmid; one involved replacing the *unc-54 3'UTR* with the *puf-8 3'UTR* (in an effort to better recapitulate the endogenous expression pattern) and the second involved adding an additional epitope tag (TAP tag).

2.15.1 Adding unc-119(+) *to pGB2*

To incorporate the *unc-119(+)* gene sequence into pGB2, the following steps were performed. First pGB2 and MM016 (*unc-119(+)*-containing plasmid) (Maduro and Pilgrim, 1995) were digested with the restriction enzyme ApaI at 25°C for 4 hr. Then ApaI was heat inactivated at 65°C for 20 min. Next the ApaI-cut pGB2 and MM016 linearized plasmids were digested with SpeI and XbaI, respectively, O/N at 37°C. SpeI

and XbaI produce compatible cohesive overhangs. pGB2 was treated with 1 unit/µL of SAP (Shrimp Alkaline Phosphatase) at 37°C for 1 hr to prevent self-ligation.

Next, the *unc-119(+)* fragment (5.7 kb) from the MM016 plasmid was ligated into pGB2 using T4 ligase O/N 18°C (Roche). The plasmid DNA (presumably pGB2 + *unc-119(+)*) was analyzed through restriction enzyme digestion with SacI and EagI and compared to pGB2 vector only control. When the digested plasmid DNA was run on an agarose gel, the band patterns did not appear correct for either the pGB2 vector or our intended cloned produce. Based on this result, pGB2 was sequenced (primers Q56: GCTTTCTGAAGAACACGGCA, R3: GGAAACAGCTATGACCATG, R33: GATCTGGGTATCTCGAGAAG, R34: GGTGCTGAAGTCAAGTTTG). The sequencing results revealed that the GFP portion of the plasmid was in the opposite orientation from *puf-8* and thus, did not code for the proper fusion protein. The Hajnal lab was contacted, after which they sent a new sample of pGB2 that had GFP in the correct orientation. This new pGB2 vector was verified by digesting the DNA with EagI and the appropriate bands were observed. Following verification, the *unc-119(+)* (using the steps outlined above), was ligated into pGB2 (cut with ApaI/SpeI). The resulting plasmid containing pGB2 + *unc-119(+)* and was given the name pDH134 (Table 2.1).

2.15.2 Replacing the unc-54 *3'UTR with* puf-8 *3'UTR*

SOEing (Splicing by Overlap Extension) PCR was used to replace the *unc-54* 3'UTR with the *puf-8* 3'UTR (Figure 2.3). The SOEing PCR strategy involves engineering primers

Plasmid Name	Description
pGB2[a]	*puf-8* promoter + *puf-8* coding + *gfp* + *unc-54* 3'UTR
MM016[b]	contains *unc-119(+)*
pDH134	pGB2 plasmid + *unc-119(+)*
pDH141	pCRII plasmid + SOEing PCR product #1 (*gfp* coding sequence + *puf-8* 3'UTR)
pDH142	pGB2 plasmid + *unc-119(+)* + *puf-8* 3'UTR
pDH143	pCRII plasmid + SOEing PCR product #2 (contains the fixed 'G')
pDH144	pGB2 plasmid + unc-119(+) + added 'G' + puf-8 3'UTR
pDH122[c]	pCRII + TAP + *teg-1*
pDH147	pGB2 plasmid + unc-119(+) + added 'G' + TAP + puf-8 3'UTR
pCFJI78[d]	MosSCI plasmid
pDH173	pCFJI78 + *unc-119(+)* + *puf-8* promoter + *puf-8* coding + gfp + added 'G' + TAP + *puf-8* 3'UTR

Table 2.1. A list of the different plasmids used/generated and their corresponding inserts.

[a] made by (Walser et al., 2006)

[b] made by (Maduro and Pilgrim, 1995)

[c] made by (Chris Wang, unpublished data)

[d] made by (Frokjaer-Jensen et al., 2008)

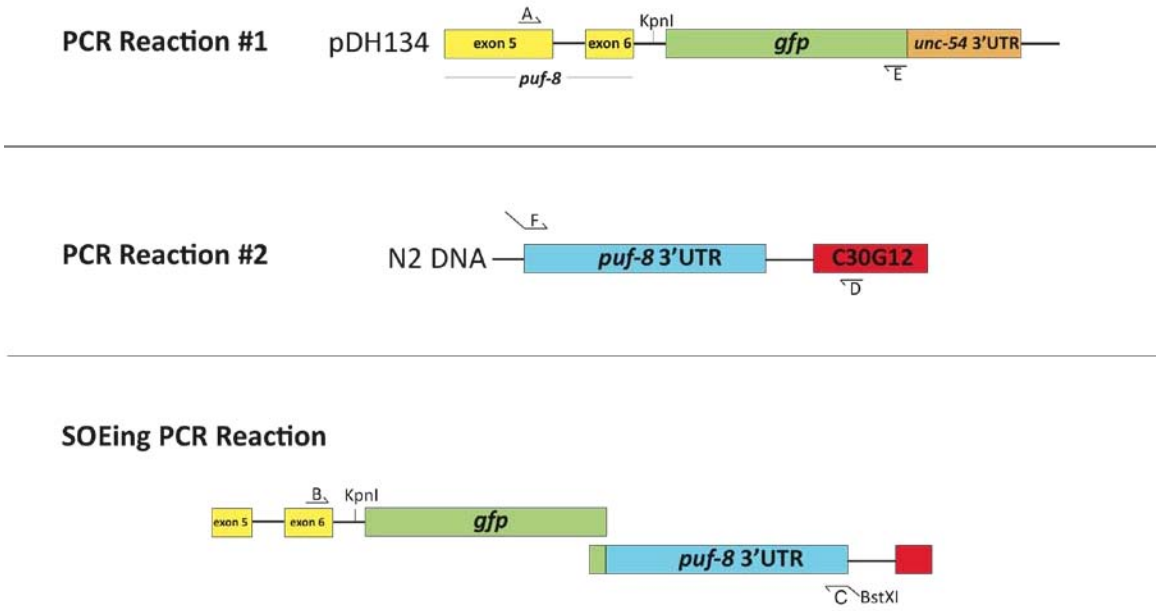

Figure 2.3. Illustration representing the three PCR reactions required for SOEing PCR to replace the *unc-54 3'UTR* with the *puf-8 3'UTR*.

Primer F includes sequence from the 3' end of the *gfp* gene and as a result, the PCR products from reaction #1 and reaction #2 overlap with each other. This overlapping region is crucial for the SOEing PCR reaction. To incorporate a unique restriction enzyme site at the end of the *puf-8* 3'UTR, the BstXI site was incorporated into the Primer C sequence.

that create PCR products which themselves can be used to prime DNA synthesis during overlap-extension reactions (Horton, 1995). The primers used for SOEing PCR included: two 5' nested primers (Primer A(S53): CCCGTTTTGAGACAATTCCC & Primer B(S54): CCATACCAAGATATGCAGGG), one primer at the end of pDH134 *gfp* coding site (Primer E(S57): TTTGTATAGTTCATCCATGC), one SOEing primer designed with additional sequence complementary to primer E + restriction enzyme sites for TAP tag cloning (SacII & SpeI) + stop codon + 5'end of *puf-8 3'UTR* Primer F(S59): ACATGGCATGGATGAACTATACAAACCGCGGtttACTAGTTAACCCAATCAGTTTTGTACTATTCCCA) and two 3'nested primers (Primer C(S55): TTTCCATTTGAATGGCCGAGATGATCACCAGACTC [includes a BstXI site for cloning) and Primer D(S56): CATCGTTATCCTCTTCTACC).

First, using pDH134 plasmid DNA, primers A and E were used to amplify a portion of *puf-8* plus the *gfp* coding sequence (1135 bp) (Figure 2.3). Note the KpnI site upstream of the *gfp* coding sequence was also amplified in this PCR reaction (Figure 2.3). Standard PCR ingredients and conditions were used. Standard PCR ingredients for a 25 μL reaction include: 2.5 μL of template DNA (if using 2-3 lysed worms/tube) or 1 μL of purified genomic DNA (100 ng/μL), 1 μL of each Primer (10 pmol/μL), 1 μl of $MgCl_2$ (25 mM), 0.5 μL of dNTPs mix (25 mM of each), 2.5 μL of 10X PCR buffer (100 mM Tris-HCl pH 8.3, 500 mM KCl, 1.5 mM $MgCl_2$), 0.5 μL of *Taq* DNA polymerase (5 Units/μL) and brought up to a 25 μL volume with autoclaved dd$H_2$0. Standard PCR conditions include: an initial denaturation cycle of 95°C for 5 min, followed by 30 cycles of denaturation

(95°C for 30 sec), annealing (50-65°C for 30 sec) and extension (72°C for 1 min, based on 1 min/kb), and ends with a final extension cycle of 72°C for 5-10 min. The predicted ideal annealing temperature for PCR reaction #1 was 65°C. At the same time, the *puf-8 3'UTR* sequence was amplified from diluted N2 genomic DNA using primers F and D (produce size= 349 bp)(PCR reaction #2, Figure 2.3). Standard PCR ingredients and conditions (annealing temperature = 52°C) were used for PCR reaction #2. The PCR products from reaction #1 and #2 were run on a 1% agarose gel, extracted and gel purified. Next, the two PCR products were mixed together and SOEing PCR was performed using primers B and C, Figure 2.3). Standard PCR ingredients and conditions (annealing temperature = 59°C) were used. The final SOEing PCR product (called SOEing PCR product #1) (1400 bp) was run on a 1% agarose gel, extracted and gel purified. Next the SOEing PCR product was TOPO cloned into the pCRII vector (Invitrogen TOPO cloning kit). The resulting pCRII + SOEing PCR plasmid was named pDH141 (Table 2.1).

Next, both the pDH134 and pDH141 (Table 2.1) were digested with KpnI and BstXI for 4 hr at 37°C. Both digests were run on 1% low molecular weight agarose gel, appropriate bands were extracted and gel purified. Then the SOEing PCR insert was ligated into the digested vector. Potential positives were selected and sequenced. The resulting plasmid that contained the SOEing PCR product #1 and thus had the *unc-54* 3'UTR replaced with the *puf-8* 3'UTR was named pDH142. Unfortunately, sequencing results also revealed another issue with the Hajnal lab pGB2 plasmid, outside of the

SOEing PCR site; at the end of *puf-8* exon 6 there was a missing 'G', which resulted in the downstream *gfp* coding sequence to be out of frame.

2.15.3 Fixing the Reading Frame: Adding the Missing 'G'

SOEing PCR was employed to add a 'G' to the sequence directly following the *puf-8* exon 6 coding sequence. The missing 'G' caused a frame shift; therefore, all sequence downstream of this missing 'G' would not be correctly transcribed including *gfp,* the stop codon and the *puf-8* 3'UTR. Using the same strategy as the SOEing PCR performed in section 2.15.2, six primers were used: two 5' nested primers positioned in *puf-8* exon 4 (S66: ACAATCTATTCGAGTTTGCC & S67: GTACTCGTCGAACGTTATCG), one SOEing primer positioned at the end of *puf-8* exon 6 that includes the missing 'G' plus a AvrII site plus complementary sequence with S68 (S69: CTTTGGCCAATCCCGGGGATCCcCTAGGTGAGATCCCTGCATATCTTGGTATGG), one primer located after exon 6 that contained the missing 'G' (S68: GGATCCCCGGGATTGGCCAAAG) and two 3'nested primers located in the *gfp* coding sequence (R33: GATCTGGGTATCTCGAGAAG and S70: TGCCCATTAACATCACCATC).

First, two PCR products were generated from pDH142 (Table 2.1); one amplified using the primers S66 and S69 and the other amplified using the primers S63 and R33. Standard PCR ingredients and conditions were used. Next, the two PCR products were mixed together and SOEing PCR was performed using the primers S67 and S70. The correct 603 bp SOEing PCR fragment was amplified and tested via restriction digest, as

the PCR product contains an AvrII site. The correct SOEing PCR fragment was TOPO cloned into pCRII and verified with appropriate restriction digests. Potential positives were selected and sequenced. The resulting pCRII + SOEing PCR product (called SOEing PCR produce #2) was given the name pDH143 (Table 2.1).

Next both pDH143 and pDH142 (Table 2.1) were digested first with KpnI for 4 hr at 37°C. Since the restriction enzymes used in this digest require different buffers, the digested DNA was isolated using a PCR clean-up kit (Promega). Then both digested plasmids were cut with BglII O/N at 37°C. Potential positives were selected and sequenced. The resulting plasmid (pDH142 with added 'G') was given the name pDH144 (Table 2.1).

2.15.4 Adding TAP tag to pDH144

As an alternative protein purification motif, a TAP tag was inserted after the *gfp* coding sequence, upstream of the *puf-8* 3'UTR in the pDH144 plasmid (Table 2.1). The TAP tag includes the HA epitope, 8X His tag and a Myc tag (Polanowska et al., 2004). First the TAP tag was PCR amplified from pDH122 [Chris Wang's TOPO::TAP::*teg-1*] using the primers S60(TTTTCCGCGGTACCCATACGATGTCCCAG), which contains a SacII site, and S61(ACTAGTGCTAGCCAAATCCTCCTCGCTGATC), which contains an NheI site (creates compatible cohesive ends with SpeI). Standard PCR ingredients and conditions (annealing temperature = 56°C) were used. The PCR product was run on a gel, extracted and gel purified. Next the TAP tag PCR product was digested with SacII and NheI for 3 hr

at 37°C. At the same time, the plasmid pDH144 was digested with SacII and SpeI for 3 hr at 37°C. Potential positives were selected and sequenced. The resulting plasmid (pDH144 + TAP tag) was named pDH147 (Table 2.1).

NOTE: pDH147 was used for biolistic transformation; however, no positive integrants were recovered. In the meantime, a new integration strategy was published that was much less labour intensive. So pDH147 was modified yet again to accommodate this new procedure (below, section 2.16).

2.16 *puf-8::gfp::tap* Construct for Mos1 Mediated Single-Copy Insertion (MosSCI)

To make the targeting plasmid for MosSCI, first the plasmid pDH147 was digested with the restriction enzyme SbfI at 37°C for 4 hr. Since the second restriction enzyme required a different buffer, SbfI was heat inactivated at 65°C for 20 min. Then the linearized pDH147 plasmid was digested with BspEI at 37°C for 4 hr. Note BspEI creates compatible cohesive overhanging ends with XmaI. BspEI cuts pDH147 in two locations, thereby producing three fragments (7120 bp, 1665 bp and 4014 bp). The digested pDH147 was run on a 1% agarose gel to separate the three fragments and the 7120 bp fragment was excised and gel purified. At the same time, the MosSCI plasmid, pCFJI78 (Frokjaer-Jensen et al., 2008), was digested with SbfI and XmaI at 37°C for 4 hr. Following digestion, the linearized pCFJ178 plasmid was SAP treated at 37°C for 1 hr.

To ligate the 7120 bp insert into the SbfI/XmaI digested pCF178 (7204 bp), the TAKARA DNA ligation Kit ver. 2.1 was used (TAKARA Bio Inc). The ligation reaction, using

the optimized T4 TAKARA ligase, was performed at 15°C for 1 hr. After ligation, solution III (transformation enhancer) was added before transformation into XL1-Blue chemically competent cells and grown on LB + ampicillin plates at 37°C for 16 hr. A sample of each plasmid was run on a 1% agarose gel to verify the size and correctly sized plasmids were sequenced. A correct plasmid was obtained and was given the name pDH173 (Table 2.1).

2.17 Injection of pDH173 MosSCI Construct

The MosSCI targeting plasmid, pDH173, was injected into young adult EG5003 [*unc-119(ed3) III; cxTi10882 IV*] animals using the 'direct method' outlined in (Frokjaer-Jensen et al., 2008). The injection mix was as follows: 50 ng/µl pDH173, 50 ng/µl Mos1 transposase (pJL43.1(*Pglh-2::transposase*)), 5 ng/µl pGH8 (*Prab-3::mCherry*), and 2.5 ng/µl pCFJ90 (*Pmyo-2::mCherry*). After injection, the animals were given time to recover at room-temperature for 4 hr. After the recovery period, each animal was selected to an individually seeded plate and incubated at 15°C for 2-3 days. Next, the F1 progeny were screened for successful transformation by selecting plates with non-Unc animals. Plates showing successful transformation of the transgene (pDH173) were transferred to 20°C. Once starved, the plates were chunked to new seeded plates and starved again. Since *unc-119(ed3)* animals are not capable of entering dauer, all non-transformed animals should be dead after this second starvation. The remaining animals were screened under fluorescence to select for integrants (i.e., non-Unc, non-

red). In contrast, extrachromosomal arrays will contain the marker plasmids and, thus, will be red. Ten integrants were selected from each positive plate and moved individually to new seeded plates. Homozygous animals were selected and maintained.

2.18 Verification of Integration

If proper integration of the targeting plasmid (pDH173) occurred, then the Mos1 element, present in the *cxTi10882* site of LGIV, would be replaced with the pDH173 insert. Using internal primers for the Mos1 element (Primers oJL102: CAACCTTGACTGTCGAACCACCATAG/ oJL103: TCTGCGAGTTGTTTTTGCGTTTGAG) PCR was performed using DNA from the integrant homozygous line and DNA from EG5003 animals (the original Mos-1 line). Additional PCR analysis was performed to verify that (1) the integrant contained the appropriate insert (Primers Q59:GTGTTGTCCAACGTTGTCTC/R33: GATCTGGGTATCTCGAGAAG & Q59/Q53: CCGGTATAACAACCGGATTTG), (2) that the integrant was properly positioned in the *cxTi10882* site of chromosome IV (Primers U60: GCAAGGACCAAAGGGACCAA /U40: CAATTCATCCCGGTTTCTGT) and (3) that the integrant was homozygous (Primers U60/V3: CCTTTATGGCCCTCTATGC) (Figure 2.4). Once verified, the homozygous integrant line was given the named ugSi1.

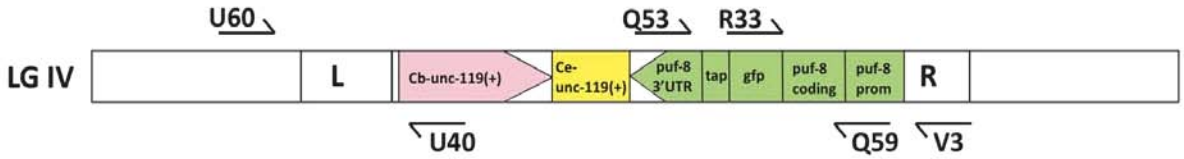

Figure 2.4. Primers used for verification of the *ugSi1* integrant on LGIV.

The direction of each primer is represented by the direction of the corresponding arrow. L represents the Left recombination region and R represents the right recombination region. Both the L and R sites are also present in the pDH173 targeting plasmid, which allows for homologous recombination after excision of the Mos1 element.

2.19 Quantitative Analysis of PUF-8::GFP Expression

To quantify the expression of PUF-8::GFP, gonad arms were dissected from identically staged 1 day past L4 *puf-8(q725); ugSi1* and N2 animals. Both sets of dissected gonads were fix and permeabilized using the same conditions outlined in section 2.9. In order to distinguish *puf-8(q725); ugSi1* from N2, the N2 gonad arms were pre-treated with αHIM-3 antibodies. After appropriate washes, the gonad arms from *puf-8(q725); ugSi1* and N2 were mixed together and incubated with αGFP antibodies, followed by secondary antibody detection with both Donkey αrabbit Alexa594 and Donkey αmouse Alexa488 (using standard protocol, section 2.9). PUF-8::GFP expression levels were quantified based on pixel intensity generated using the ImageJ program. First the rectangular selection tool was used to capture the same distal germline region within ten *puf-8(q725); UgSi(puf-8::gfp::tap)* and ten control (N2) gonad arms. The selected region was analyzed using the 'Plot Profile' function, which plots the pixel intensity against the pixel distance. Average values for pixel intensity amongst the different samples were used to construct a graph for the PUF-8::GFP expression in the distal germ line (see Chapter 6). To determine the background expression level of the αGFP and secondary antibodies in non-GFP expressing animals, data from the N2 control gonad arms were used.

Chapter Three: **Cloning of *teg-2(oz192)* and the discovery that *teg-2* is allelic to *puf-8***

This chapter outlines the mapping strategies that were used to determine that *teg-2* is allelic to *puf-8*. This chapter also describes the initial challenges that were faced upon initiation of *teg-2* cloning.

3.1 Discovery of the *teg-2* Mapping Error

Upon initiation of this project, *teg-2(oz192)* had been roughly mapped to a 425 kb region of LGII, between the genes *lin-4* and *sma-6* (Wilson-Berry, 1998). This region contains 91 genes. In order to identify which of these genes carried the *oz192* mutation, RNAi, SNP mapping and deficiency mapping was performed.

3.1.1 RNAi of Candidate Genes between lin-4 *and* sma-6

Using the *teg-2(oz192)* enhancement of the *glp-1(gf)* over-proliferative germline phenotype as a guide (see chapter 4), a number of approaches were undertaken at the same time. Recall, that *teg-2(oz192)* was isolated as an enhancer of *glp-1(oz112oz120)* (Wilson-Berry, 1998). One approach was to use RNAi by feeding to systematically knock-down the expression of each gene found between *lin-4* and *sma-6* using *glp-1(ar202gf)* animals. RNAi knock-down of the gene containing the *teg-2* mutation in *glp-1(ar202)* animals should phenocopy the *teg-2(oz192); glp-1(ar202)* double mutant phenotype, assuming *teg-2(oz192)* is a lf allele. RNAi feeding vectors are commercially available for 74 of the 91 potential *teg-2* genes in this region (Kamath and Ahringer,

2003). To monitor the efficiency of the RNAi, appropriate controls were included. RNAi against the *elt-2* gene was used as a positive control as knock-down of *elt-2* reproducibly results in larval lethality (Fukushige et al., 1998). For a negative control, RNAi against the *gfp* gene was used, which should have no effect, as the *gfp* gene is not naturally present in the *C. elegans* genome. Since the RNAi experiment was conducted at 20°C, it was also necessary to monitor the background level of tumours formed in *glp-1(ar202)* single mutants; *ar202* is a temperature sensitive allele of *glp-1* known to produce Pro tumours at higher temperatures (Pepper et al., 2003). The background level of tumours was monitored by feeding *glp-1(ar202)* animals bacteria containing the empty RNAi feeding vector (i.e., no gene knock-down, second negative control). Note RNAi against *gfp* could have also been used to monitor for background tumours. From this control, the background level of tumours produced by *glp-1(ar202)* alone at 20°C was determined to be 3%. Therefore, to be significantly above background, tumours produced by RNAi knock-down of the tested genes needed to occur in more than 3% of the resulting progeny. Of the 74 genes available in the Ahringer RNAi library, 67 were tested at least once; the bacteria for the remaining 7 RNAi vectors did not grow under standard conditions and, therefore, were not tested. The first round of RNAi (trial 1) was conducted with the assistance from two undergraduate Honours Project students, Anna Urbanska and Vishal Sharma. Results from trial 1 showed 8 genes that, when knocked-down in the *glp-1(ar202)* background, produced germline tumours at levels greater than background (Table 3.1, highlighted results). However, additional trials

Table 3.1. RNAi against some of the 92 genes between *lin-4* and *sma-6*.

Trial 1 was conducted by two undergraduate honours project students, Anna Urbanska and Vishal Sharma. Highlighted in yellow are the RNAi results that showed tumourous germline phenotypes. However, none of the tested genes completely phenocopied *teg-2(oz192); glp-1(ar202)* double mutants.

	Gene Name	Sequence Name	Library location	Trial 1	Trial 2
	lin-4	F59G1.6			
1	tsp-18	F59G1.2	15 -H11	average progeny, 10% tumourous	embryonic lethal
2		F59G1.8	N/A	-	
3	vps-35	F59G1.3	15 -H12	average progeny, 10% tumourous	
4	cgt-3	F59G1.1	15 -H10	WT	
5	frh-1	F59G1.7	16 -A03	many worms move slowly	
6	ptp-2	F59G1.5	16 -A02	WT	
7	tag-223	F28B12.3	16 -A06	WT	
8	egl-44	F28B12.2	16 -A05	most look WT, some sick looking	
9		F28B12.1	16 -A04	WT	
10		B0034.2	16 -A08	some tumour-like appearences	low % tumourous
11	cdh-11	B0034.3	16 -A09	WT	
12		B0034.4	N/A	-	
13	mir-261	B0034.6	N/A	-	
14		B0034.1	16 -A07	WT	
15		B0034.5	16 -A11	WT	
16	ins-2	ZK75.2	N/A	-	
17	ins-3	ZK75.3	N/A	-	
18	ins-4	ZK75.1	N/A	-	
19	ins-5	ZK84.3	16 -B02	WT	
20	ins-6	ZK84.6	16 -B05	WT	
21	ins-20	ZK84.7	N/A	-	
22		ZK84.2	16 -B01	WT	
23		ZK84.5	16 -B04	higher prog, WT	
24		ZK84.1	16 -A12	WT	
25		R12C12.9	16 -C02	WT, maybe slow growth	
26		R12C12.3	N/A	-	
27		R12C12.4	16 -B09	WT	
28		R12C12.5	16 -B10	WT, slight tum	
29		R12C12.6	16 -B11	WT	
30	ran-5	R12C12.2	16 -B07	very low prog, not many eggs, possibly unc	
31		R12C12.1	16 -B06	WT	
32		R12C12.7	16 -B12	few prog, WT	10% tumourous
33		R12C12.8	16 -C01	lower prog, some unc	fertile, avg progeny, background level of tumours
34		H12I13.1	16 -C06	WT	
35		H12I13.2	16 -C05	WT, background tum	
36		H12I13.3	16 -C04	WT	
37		H12I13.5	N/A	-	
38		H12I13.6	N/A	-	
39	fbf-1	H12I13.4	16 -C03	low prog, no tum	5-10% tum (prox tum),
40		F21H12.3	16 -C10	high prog, 60% tum	4% tumourous(prox tum, often in just one arm), most healthy, one protruding vulva
41	ptc-2	F21H12.4	16 -C11	low prog, no tum	some tum (some full tum, some prox), smaller size
42		F21H12.2	N/A	-	
43	fbf-2	F21H12.5	16 -C12	avg prog, 40% tum	9% tumourous
44		F21H12.6	16 -D01	WT, some background	
45		F21H12.1	16 -C08	WT	
46	rgs-3	C29H12.3	16 -D04	WT	
47		C29H12.5	16 -D05	low prog, not many eggs, WT	
48		C29H12.6	16 -D06	lower prog, WT with some background	
49	**OPERON**	**CE0P2236**	N/A		
50		C29H12.2	16 -D03	WT	
51	rrt-2	C29H12.1	16 -D02	lower prog, WT	4% tum (prox tum), lots of prog
52	abts-3	F57F10.1	16 -D07	WT	
53	exp-1	H35N03.1	16 -D08	~1/5 possible tum	
54	hst-3	F40H3.5	16 -E01	low prog, only 2 adults, very tum	very low prog, possibly larval lethal
55		F40H3.3	16 -D11	low prog, 1/3 tum	3.3% tum (prox tum, 2/10 tum both arms prox)
56		F40H3.2	16 -D10	WT	
57		F40H3.1	16 -D09	some background (~5)	1.6% Pro tum, slower and slightly less prog
58		F40H3.6	N/A	-	3% tum (mainly prox tum with interspersed differeniated cells)
59	fkh-8	F40H3.4	16 -D12	WT	
60	cpb-2	C30B5.3	16 -E04	slightly tum, few oocytes visible	
61		C30B5.4	16 -E05	WT, some slight tum	
62		C30B5.2	16 -E03	WT, some slightly tum	
63		C30B5.1	16 -E02	WT	
64		C30B5.5	N/A	-	
65		C30B5.6	16 -E07	adult:WT, L4: lethal, possibly L1/L2 arrest	
66		C30B5.7	16 -E08	WT	
67	tat-4	T24H7.5	16 -F01	slightly sick	
68		T24H7.4	16 -E12	WT	
69		T24H7.3	16 -E11	WT	
70		T24H7.2	16 -E10		
71	phb-2	T24H7.1	16 -E09	WT	
73		F13H8.11	16 -F06	WT	
74		F13H8.4	N/A	-	
75		F13H8.12	N/A	-	
76		F13H8.3	16 -F04	WT	
77		F13H8.8	16 -F09	tum	
78		F13H8.2	16 -F03	slightly tum	
79	bpl-1	F13H8.10	N/A	-	
80		F13H8.9	16 -F10		
81		F13H8.1	16 -F02	WT	
82		F13H8.6	16 -F07	WT	
83		F13H8.7	16 -F08	WT	
84		C29F5.3	16 -G01	WT	
85	mps-1	C29F5.4	16 -G02	WT	
86		C29F5.5	16 -G03	WT	
87		C29F5.2	16 -F12		
88		C29F5.6	16 -G04	WT	
89		C29F5.1	16 -F11		
90		C29F5.7	16 -G05		
91		C32D5.3	16 -G08		
92		C32D5.4	16 -G09		
	sma-6	C32D5.2			

proved that these results were not reproducible and lower levels (closer to background levels) of germline tumours were observed for each of these genes (Table 3.1). The fact that none of the 67 genes tested strongly phenocopied *teg-2(oz192); glp-1(ar202)*, was initially troubling; however, while the RNAi experiment was being conducted, results from SNP and deficiency mapping determined that *teg-2(oz192)* was not located between *lin-4* and *sma-6* (see below). Thus, these negative results did contribute to the cloning of *teg-2*, as they provided a third line of evidence that *teg-2(oz192)* was not located between *lin-4* and *sma-6*. Had this region not been excluded, the next step would have been to construct RNAi feeding vectors for the 18 genes not present in the Ahringer library.

3.1.2 SNP Mapping Within the lin-4 *to* sma-6 *Region*

In parallel with the RNAi of candidate genes experiment, mapping using single nucleotide polymorphisms (SNPs) was performed as an additional strategy to determine the location of *teg-2(oz192)*. Genomic DNA comparisons between two geographically isolated wild-type strains, Hawaiian (HA) and Bristol (N2), revealed a high density of SNPs (Wicks et al., 2001). Using these differences between wild-type strains, SNP mapping in *C. elegans* is performed by generating animals heterozygous for DNA from both HA and N2 animals (Fay, 2006). In addition to sequence differences, many of these SNPs also disrupt restriction enzyme recognition sites and, as such, are referred to as snip-SNPs (Wicks et al., 2001). If a snip-SNP disrupts a restriction enzyme recognition

site in one of the two strains (either HA or N2), this provides a convenient physical marker for positional cloning.

To map into the *lin-4* to *sma-6* region from the right (*sma-6*) side, recombinants were obtained from the strain *teg-2(oz192) unc-4(e120)/HA; glp-1(ar202)*. A total of 80 Unc non-Tum recombinants (*HA unc-4(e120); glp-1(ar202)*) were isolated (see section 2.5.1 for strain construction details). In these recombinants, the N2 DNA, which contained the *teg-2(oz192)* mutant, has been replaced with HA DNA through a chromosomal cross-over event. Using snip-SNPs between *lin-4* and *unc-4*, the location of the cross-over event was approximated based on whether N2 or HA DNA was present. Surprisingly, the furthest *HA unc-4(e120); glp-1(ar202)* recombinants tested underwent a cross-over event between the snip-SNPs F32A5[2] and T05A6[1]; at F32A5[2] the recombinant's DNA was determined to be HA, whereas at T05A6[1], the DNA was identified as N2 (Figure 3.1). The snip-SNP F32A5[2] is over 900 kb to the right of the *sma-6* gene. This suggests that *teg-2(oz192)* is not located between *lin-4* and *sma-6,* but somewhere between the snip-SNPs F32A5[2] and T05A6[1].

To map from the *lin-4* side, recombinants were recovered from *bli-2(e768) teg-2(oz192)/HA; glp-1(ar202)* animals. A total of 34 Bli non-Tum recombinants (*bli-2(e768) HA; glp-1(ar202))* were identified. Again, the results from SNP mapping were not consistent with *teg-2(oz192)* being located between *lin-4* and *sma-6*. The furthest *bli-2(e768) HA; glp-1(ar202)* recombinant underwent a cross-over event between the snip-

Figure 3.1. Analysis of SNP mapping recombinants *HA unc-4; glp-1(ar202)*.

A total of 80 *HA unc-4; glp-1(ar202)* recombinants were isolated (box in column on the right). To identify the location of the cross-over event, five snip-SNPs were used (listed in a row at the top of the figure). Above each snip-SNP is the physical chromosomal location in kb. At the top of the figure is the approximate location of each marker gene in relation to each snip-SNP. The recombinants were tested from right to left. The restriction enzyme details for each snip-SNP can be found in the Materials and Methods Section Figure 2.2. The yellow cells represent DNA that was tested and found to be from N2. When the DNA tested was found to be from HA, cells were labelled 'HA'. The most informative recombinants (i.e., the recombinants that had a cross-over event furthest to the left, towards *sma-6*) were #3, 4, 6, 9, 10, 12 and 15. All 80 recombinants were tested and found to contain HA DNA at snip-SNP F32A5[2]. This observation assisted in the discovery that *teg-2(oz192)* was not between the genes *lin-4* and *sma-6*, but to the right of the snip-SNP F32A5[2].

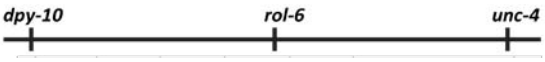

6812 F31E8[2]	7257 F32A5[2]	7812 T05A6[1]	8516 T13H5[3]	9401 pKP2109	*HA unc-4 ; glp-1(ar202)* recombinants
HA	HA	HA	HA		1
HA	HA	HA			2
HA	HA				3
HA	HA				4
HA	HA	HA	HA		5
HA	HA				6
HA	HA	HA	HA		7
HA	HA	HA	HA		8
HA	HA				9
HA	HA				10
HA	HA	HA	HA		11
HA	HA				12
HA	HA	HA	HA		13
HA	HA	HA	HA		14
HA	HA				15
HA	HA				16
	HA				17
	HA				18
HA	HA				19
	HA				20
	HA				21
	HA				22
	HA				23
	HA				24
	HA				25
	HA				26
	HA				27
	HA				28
	HA				29
	HA				30
	HA				31
	HA				32
	HA				33
	HA				34
	HA				35
	HA				36
	HA				37
	HA				38
	HA				39
	HA				40
	HA				41
	HA				42
	HA				43
	HA				44
	HA				45
HA	HA				46
	HA				47
HA	HA				48
	HA				49
	HA				50
	HA				51
	HA				52
	HA				53
	HA				54
	HA				55
	HA				56
	HA				57
	HA				58
	HA				59
	HA				60
	HA				61
	HA				62
	HA				63
	HA				64
	HA				65
HA	HA				66
	HA				67
	HA				68
HA	HA				69
	HA				70
	HA				71
	HA				72
HA	HA				73
HA	HA				74
	HA				75
HA	HA				76
HA	HA				77
HA	HA				78
HA	HA				79
	HA				80

Figure 3.2. Analysis of SNP mapping recombinants *bli-2 HA; glp-1(ar202)* and *HA rol-6; glp-1(ar202)*.

A total of 34 *bli-2 HA; glp-1(ar202)* recombinants were isolated (left most column) and a total of 24 *HA rol-6; glp-1(ar202)* recombinants were isolated (right most column). To identify the locations of the cross-over events, nine snip-SNPs were used (listed in a row at the top of the figure). Above each snip-SNP is the physical chromosomal location in kb. The approximate location of each marker gene in relation to each SNP is shown above. The restriction enzyme details for each snip-SNP can be found in the Materials and Methods Section Figure 2.2. The *bli-2 HA; glp-1(ar202)* recombinants were tested from left to right; from snip-SNP uCE2-1656 to uCE2-1725. The black cells for *bli-2 HA; glp-1(ar202)* recombinants represent N2 DNA at the designated snip-SNP. Where the DNA from a *bli-2 HA; glp-1(ar202)* recombinant changes from N2 (black cell) to HA, this represents the location of a cross-over event. The most informative *bli-2 HA; glp-1(ar202)* recombinants were #3, 7, 8, and 10. For *HA rol-6; glp-1(ar202)*, the recombinants were tested from the right to left; from snip-SNP T05T10[1] to pKP2150. The red cells represent N2 DNA in *HA rol-6; glp-1(ar202)* recombinants. The distance between a red cell and the first 'HA' cells, represents the location of cross-over for each recombinant. The most informative *HA rol-6; glp-1(ar202)* recombinants was #1. Recombinants that do not have any information listed were not analyzed, as the identity of *teg-2(oz192)* was determined during the process of SNP mapping. The results of

these SNP mapping experiments narrowed the critical region containing *teg-2* to a 98 kb region between the snip-SNPs F32A5[2] and uCE2-1737.

bli-2 HA; glp-1(ar202) recombinants	6085 uCE2-1656	6812 F31E8[1]	7257 F32A5[2]	7289 uCE2-1725	7314 pkP2150	7355 uCE2-1737	7798 C06A8[4]	7812 T05A6[1]	8061 T05T10[1]	*HA rol-6; glp-1(ar202)* recombinants
1		HA	HA		HA					1
2			HA					HA		2
3				HA		HA			HA	3
4			HA					HA		4
5			HA					HA		5
6			HA			HA				6
7				HA		HA				7
8						HA				8
9			HA			HA				9
10				HA		HA				10
11		HA				HA				11
12		HA				HA				12
13	HA					HA				13
14		HA								14
15										15
16		HA								16
17										17
18				HA						18
19				HA						19
20				HA						20
21										21
22										22
23										23
24										24
25										
26										
27										
28										
29										
30										
31										
32										
33										
34										

SNPs F32A5[2] and uCE2-1725, a region 900 kb to the right of the *sma-6* gene (Figure 3.2).

Results from both the right and left SNP mapping strains suggested that *teg-2* was not located between *lin-4* and *sma-6*. Using the results from the most informative recombinants, the new *teg-2* region was determined to be located between the snip-SNPs F32A5[2] and T05A6[1]. This 550 kb region is flanked by the visible marker genes dpy-10 and rol-6 (Figure 3.2).

3.1.3 Deficiency Mapping within the lin-4 *to* sma-6 *Region*

In addition to SNP mapping, deficiency strains were also used to help determine the physical location of the *teg-2(oz192)* gene. Most chromosomal deficiencies are formed from large deletions, which remove numerous genes (Hodgkin, 2005). If the end-points of these deletions are known, strains containing these chromosomal deficiencies can be used for mapping by performing a complementation test with a mutant presumed to be located near or within the deficiency (Sigurdson et al., 1984). The deficiency strains known to delete chromosomal regions at or near the *lin-4* to *sma-6* region include *maDf4*, *mnDf30* and *mDf14* (Figure 3.3). Complementation tests were conducted, generating *teg-2(oz192)/Df; glp-1(ar202)* heterozygous strains. All three deficiencies complemented *teg-2(oz192)*, producing viable heterozygotes. This suggests that *teg-2(oz192)* was not present in the region covered by these deficiencies. This

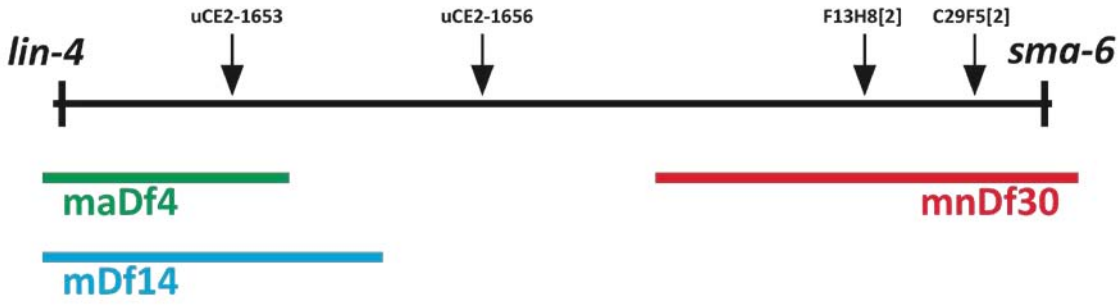

Figure 3.3. Deficiencies located between *lin-4* and *sma-6*.

maDf4 and *mDf14* overlap with each other. All three deficiencies complement *teg-2(oz192)*, suggesting that *teg-2(oz192)* is not located within any of these deficiencies.

result was consistent with the SNP mapping results, again suggesting that *teg-2* was not located within the *lin-4* to *sma-6* region.

3.1.4 SNP Mapping within the dpy-10 *to* rol-6 *Region*

Using the results from the SNP strains *teg-2(oz192) unc-4(e120)/HA; glp-1(ar202)* and *bli-2(e768) teg-2(oz192)/HA; glp-1(ar202)*, the new *teg-2(oz192)* region was assigned to a 550 kb region between the snip-SNPs F32A5[2] and T05A6[1], which resides between the visible marker genes *dpy-10* and *rol-6*. To narrow this region further, an additional SNP mapping strain, *teg-2(oz192) rol-6(e187)/HA; glp-1(ar202),* was generated. While it would have also been possible to select for more recombinants from the *teg-2(oz192) unc-4(e120)/HA; glp-1(ar202)* strain*, rol-6* is much closer to the right border of the new *teg-2(oz192)* region (Figure 3.1). Therefore, the recombinants recovered from the *teg-2(oz192) rol-6(e187)/HA; glp-1(ar202)* strain are more likely to be informative; however, because *rol-6* is closer to the *teg-2* region, a smaller proportion of recombinants will be produce as compared to the *teg-2(oz192) unc-4(e120)/HA; glp-1(ar202)* strain. A total of 24 Rol non-Tum recombinants were isolated (Figure 3.2). The most informative recombinant (i.e., recombination event furthest from *rol-6*) underwent a cross-over event between the snip-SNPs pkP2150 and uCE2-1737. This SNP mapping result reduced the *teg-2(oz192)* region to 98 kb between the snip-SNPs F32A5[2] and uCE2-1737. This 98 kb region contains 18 genes (Figure 3.4).

Figure 3.4. Overall illustration of mapping results between the genes *dpy-10* and *rol-6*. (A) visible marker genes located on linkage group II (LGII). Below each gene name is the genetic position in cM. (B) magnified region between the gene *dpy-10* and *rol-6* showing the locations of some important snip-SNPs used during SNP mapping. The arrows on either side represent the SNP mapping direction for left and right SNP mapping recombinants. (C) magnified region between the snip-SNP F32A5[2] and uCE2-1737. This region contains 18 genes, one of which is *puf-8* (shown in grey). (D) Gene model of the *puf-8* gene. The locations of the *puf-8* deletion alleles (*ok302* and *q725*) are represented as lines under the *puf-8* genomic region. The locations of the three *puf-8* point mutation alleles (*oz192, zh17* and *ga145*) are represented with asterisks (*). All of which function as strong lf or null alleles of *puf-8* (Walser et al., 2006) (this work). The *puf-8* gene contains eight PUF repeats (purple boxes) and six exons (green boxes). Introns (black lines) connect each exon. The 5'UTR (small black box) is located on the far right, as part of exon 1. The 3'UTR (black arrow box) is located on the far left, as part of exon 6. Downstream of *puf-8* (on the left) is the gene C30G12.6 (blue box). (E) snap-shot of the sequencing read illustrating the single base pair mutation in *puf-8(oz192)* (highlighted in blue), which consists of a G937T transversion.

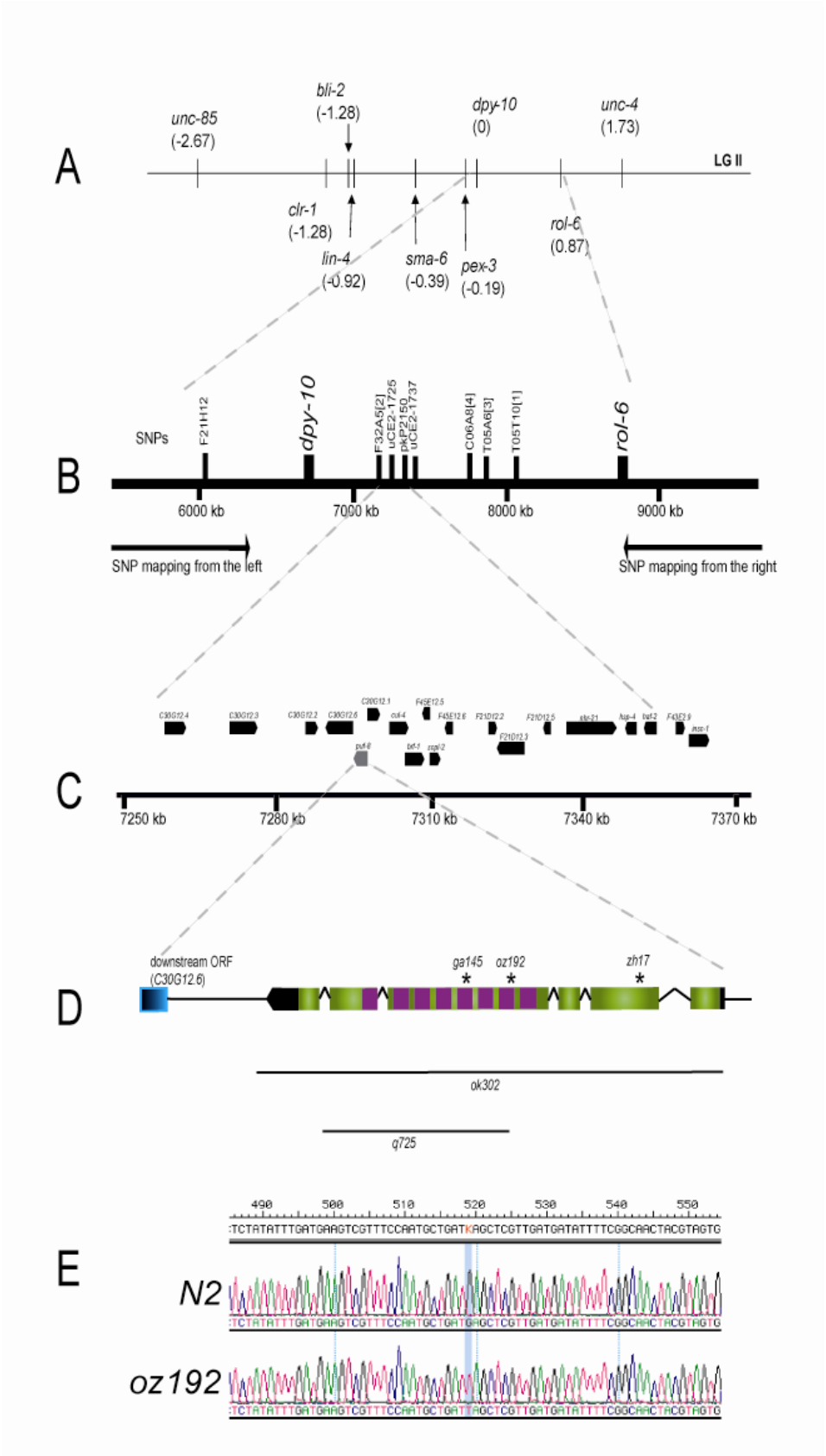
A
unc-85
(-2.67)
bli-2
(-1.28)
dpy-10
(0)
unc-4
(1.73)
LG II
clr-1
(-1.28)
lin-4
(-0.92)
sma-6
(-0.39)
pex-3
(-0.19)
rol-6
(0.87)
B
SNPs
F21H12
dpy-10
F32A5[2]
uCE2-17725
pkP2150
uCE2-17737
C06A8[4]
T05A6[3]
T05T10[1]
rol-6
6000 kb
7000 kb
8000 kb
9000 kb
SNP mapping from the left
SNP mapping from the right
C
7250 kb
7280 kb
7310 kb
7340 kb
7370 kb
D
downstream ORF
(C30G12.6)
ga145
oz192
zh17
ok302
q725
E
490
500
510
520
530
540
550
N2
oz192

3.1.5 Deficiency Mapping in the dpy-10 *to* rol-6 *Region*

The deficiencies within or overlapping with *dpy-10* and *rol-6* include *mnDf88*, *mnDf96* and *mDf18* (Figure 3.5). Complementation tests were performed with each of these deficiencies by crossing into *teg-2(oz192); glp-1(ar202)* males. When *teg-2(oz192)* was crossed to the deficiency strain *mnDf88* (*teg-2(oz192) rol-6(e187)/mnDf88 unc-4; glp-1(ar202)*), the resulting phenotype phenocopied *teg-2(oz192); glp-1(ar202)*. In other words, *mnDf88* failed to complement *teg-2(oz192)*, thereby suggesting that the genomic region occupied by *teg-2(oz192)* is within the *mnDf88* deficiency. The other two deficiencies complemented *teg-2(oz192)* and, therefore, do not contain the *teg-2(oz192)* locus. The end-points of the *mnDf88* deficiency extend roughly from the gene *spon-1* to the gene *let-237*, a region which spans ~2200 kb. While the *mnDf88* deficiency results did not help to reduce the 98 kb *teg-2* region, it did provide two important pieces of information. First, the *mnDf88* deficiency result supports the SNP mapping results suggesting that *teg-2(oz192)* is located between the snip-SNPs F32A5[2] and uCE2-1737, which are both deleted by *mnDf88*. Second, deficiencies can be used for more than just mapping; deficiencies can also help to define an allele type (Sigurdson et al., 1984). For example, a heterozygote with a null mutation opposite a deficiency should phenocopy a null homozygote (Sigurdson et al., 1984). Since *teg-2(oz192)/mnDf88; glp-1(ar202)* phenotype phenocopied *teg-2(oz192); glp-1(ar202),* this indicates that the *oz192* allele is likely a strong lf or null allele.

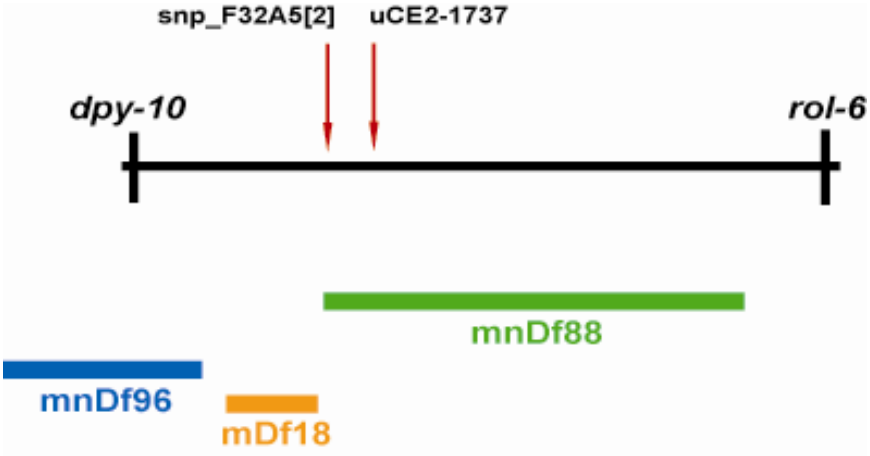

Figure 3.5. Deficiencies located between *dpy-10* and *rol-6*.

The three deficiency strains do not overlap with each other. Only *mnDf88* deletes the region between the snip-SNPs F32A5[2] and uCE2-1737. *mnDf88* deficiency spans from the gene *spon-1* to *let-237*. *mDf18* deficiency spans from the gene *tra-2* to *unc-104*. *mnDf96* spans from the gene *exp-1* to *snt-1*. Of the three deficiencies, only *mnDf88* fails to complement *puf-8(oz192)*.

3.2 Identifying *teg-2(oz192)* as an Allele of *puf-8*

3.2.1 Annotation Comparison and Sequencing

Since the new *teg-2* minimal region contained only 18 genes, before starting a time consuming RNAi screen to identify a *teg-2* candidate, the annotation data for each of the genes (using wormbase.org) was first analyzed to see if any genes in the region have known lf phenotypes that resembled *teg-2(oz192)*. The phenotypes of a *teg-2(oz192)* single mutant include low brood size, small distal mitotic zone and germline defects at 25°C (Table 3.2, 3.3 & 3.4). One gene, when mutated, shared all three features with *teg-2* was *puf-8* (Table 3.2, 3.3 & 3.4) (Bachorik and Kimble, 2005; Subramaniam and Seydoux, 2003). Sequencing of the *puf-8* gene in three strains containing *teg-2(oz192)* revealed a single point mutation at the 937th nucleotide in the *puf-8* genomic sequence (starting at the A in the ATG start codon). This molecular lesion caused a guanine to thymine (G to T) transversion (Figure 3.4). Transversion mutations (purine to pyrimidine change) are not typically induced by EMS, the mutagen used to induce the *teg-2(oz192)* mutation: 92% of EMS induced mutations are transition mutations (purine to purine or pyrimidine to pyrimidine) (Anderson, 1995). Regardless, this G to T transversion mutation is predicted to be detrimental to the PUF-8 protein as it is predicted to convert a glutamate (GAG) to an amber stop codon (UAG). This stop codon truncates the protein within the second PUF repeat (Figure 3.4) and since it has

Table 3.2. Brood sizes of three *puf-8* mutants

Age	**N2**	***puf-8(oz192)***
L4-1d	60	13
1d-2d	175	80
2d-3d	16	30
3d-4d	4	8
4d-5d	2	0
5d-6d	2	0
Total overall progeny =	260	131
Totals from *puf-8(ok302)* =*	240	150 (*ok302)*
Totals from *puf-8(q725)^ =*	320	198 (*q725)*

Comparing the brood size (progeny number) of *puf-8(oz192)* to wild-type (N2) during specific one day developmental windows (e.g. Larval stage 4 (L4) to 1 day old adult). The numbers are averaged from 10 plates containing one animal each. Each day the adult was removed from the plate and put onto a new seeded plate. The progeny on each plate were counted one day after hatching. The plates were stored at 20°C. After 6 days the total overall number of progeny was added. For comparison, highlighted in grey are the total brood sizes for N2, *puf-8(ok302)* *(Subramaniam and Seydoux, 2003) and *puf-8(q725)* ^(Bachorik and Kimble, 2005)

Table 3.3. Distal mitotic zone size of three *puf-8* mutants

Genotype	Temperature (C)	Germ cell diameter	n
N2	20	20	31
puf-8(oz192)	15	13	10
puf-8(oz192)	18	12	14
puf-8(oz192)	20	13	47
puf-8(oz192)	25	14	13
puf-8(q725)	20	13	11
puf-8(ok302)	N/A	small germ line^	N/A

Analysis of the size of the mitotic zones in different *puf-8* mutants compared to wild-type (N2). Gonads were dissected and stained with DAPI, αREC-8 antibodies and αHIM-3 antibodies. The size of the mitotic zone was determined by counting the number of germ cell diameters from the DTC cell to the first HIM-3 positive meiotic cell (designated the start of the transition zone). Four different temperatures were tested with *puf-8(oz192)*.

^small germ line observed; however, the GSC diameters were not recorded

(Subramaniam and Seydoux, 2003)

N/A = not available

Table 3.4. Overall phenotypic comparison between three alleles of *puf-8*

Allele	**20°C**	**25°C**
N2	healthy and viable (n=31)	mostly healthy and viable, 0.12% males (n=808)
*puf-8(ok302)**	subfertile: 53% dead embryos and 11% males	100% sterile (n=82): 56% small germ line and 44% Pro tumours
*puf-8(q725)^*	most self-fertile, 3% Mog (n=1952)	83% Pro tumours (n=64)
puf-8(oz192)	fertile, low level of males (0.6%, n=640)	25% Pro tumours, 4% males (n=689), most smaller than normal germ lines, progeny levels lower (subfertile)

* all data on *ok302* from (Subramaniam and Seydoux, 2003)

^ all data on *q725* from (Bachorik and Kimble, 2005)

Mog = Masculinization Of the Germline

Pro = PROximal proliferation tumour

been shown that all eight PUF repeats are required for RNA binding (Zhang et al., 1997), this would suggest that the truncated PUF-8 protein, if it is produced at all, is likely non-functional. Consistent with the *mnDf88* deficiency result, the consequence of this molecular lesion in *puf-8* also suggests that *oz192* functions as a strong lf or null allele.

3.2.2 Complementation Test

To further validate that *teg-2(oz192)* is allelic to *puf-8*, a complementation test was conducted using the *puf-8(q725)* deletion allele (Bachorik and Kimble, 2005). A complementation test is a quick method to determine if two mutations are alleles of the same gene (Yook, 2005). When one copy of *teg-2(oz192)* was introduced to one copy of *puf-8(q725)* in a *glp-1(ar202)* background (*teg-2(oz192) rol-6(e187)/puf-8(q725); glp-1(ar202)*), sterile fully tumourous germ lines were formed. This phenotype was identical to the tumourous germline phenotype found in *teg-2(oz192) rol-6(e187); glp-1(ar202)* and *puf-8(q725); glp-1(ar202)* animals. Since *teg-2(oz192)* failed to complement *puf-8(q725)*, *oz192* is an allele of *puf-8*. Additionally, the complementation test results reinforced that the deletion allele, *q725*, and the point mutation allele, *oz192,* both function similarly to enhance the *glp-1(ar202)* over-proliferation phenotype (further discussion of this observation found in Chapter 4).

3.2.3 puf-8 *RNAi*

To further confirm that a reduction/loss of *puf-8* activity is sufficient to produce tumourous germ lines in a *glp-1(gf)* background, RNAi against *puf-8* in *glp-1(ar202)* animals was performed. When bacteria expressing *puf-8(RNAi)* was fed to *glp-1(ar202)* L4 animals, all resulting progeny had germline tumours (n=24). This result further supports that *teg-2(oz192)* is an allele of *puf-8*, as *puf-8(RNAi) glp-1(ar202)* animals are identical to *teg-2(oz192); glp-1(ar202)* animals. In addition, the *puf-8* RNAi result also reveals that *puf-8* is a strong enhancer of *glp-1(ar202*), as even knock-down (via RNAi) is sufficient to induce the formation complete germline tumours.

Summary

In summary, using SNP and deficiency mapping, the location of *teg-2(oz192)* was determined to not be between *lin-4* and *sma-6*, a location that was previous assigned to *teg-2(oz192)* (Wilson-Berry, 1998). Using SNP and deficiency mapping, *teg-2(oz192)* was assigned to a new 98 kb location between the snip-SNPs F32A5[2] and uCE2-1737. To determine which of the 18 genes, within this region, was *teg-2(oz192)*, information on each gene was analyzed to look for similarities to the *teg-2(oz192)* phenotype. Of the 18 genes, *puf-8* was the strongest candidate for *teg-2(oz192)*. A complementation test demonstrated that *teg-2(oz192)* failed to complement a deletion allele of *puf-8* for the enhancement of *glp-1(gf)*, strongly suggesting that *oz192* is an allele of *puf-8*. Results from RNAi against *puf-8* in a *glp-1(ar202)* background further confirmed that *puf-8* and

teg-2 are the same gene. From this point onward, *teg-2(oz192)* will be referred to as *puf-8(oz192)*.

Chapter Four: ***puf-8's* Involvement in the Mitosis vs. Meiosis Decision**

Since *puf-8(oz192)* (formerly *teg-2*) is able to enhance the over-proliferative phenotype of *glp-1(oz112oz120)*, indicates an involvement for *puf-8* in the mitosis vs. meiosis decision. First, to determine if *puf-8's* interaction with *glp-1* is allele specific, mutations in *puf-8* were combined individually with both gf and lf alleles of *glp-1*. Next, since *puf-8* is known to be involved during different aspects of germline development, the *puf-8(0); glp-1(gf)* germline phenotype was analyzed in different mutant backgrounds to determine if the tumourous phenotype was due to issues with the mitosis vs. meiosis decision or due to other *puf-8* germline roles. Finally, to explore where *puf-8* genetically functions within the mitosis vs. meiosis decision, numerous genetic strains were constructed using the known mitosis- and meiosis-promoting genes.

4.1 *puf-8's* Interaction With *glp-1* Gain-of-Function Alleles

puf-8(oz192) enhances the over-proliferative phenotype of the weak gf allele, *glp-1(oz112oz120)* (Wilson-Berry, 1998). Since the identification of the *oz192* allele in the Teg enhancer screen, numerous other gf alleles of *glp-1* have been isolated (Kerins, 2006; Pepper et al., 2003). It is possible that the *puf-8(oz192)* enhancement of *glp-1(oz112oz120)* could be a *glp-1(oz112oz120)* allele specific interaction. If this is the case, *puf-8(oz192)* would not be able to enhance the over-proliferative phenotypes of other *glp-1(gf)* alleles.

Two *glp-1(gf)* alleles were selected for interaction studies with *puf-8(oz192)*. Both alleles are temperature-sensitive; at permissive temperatures they appear wild-type, but at non-permissive temperatures, their germ lines show over-proliferative defects (Pepper et al., 2003). The first *glp-1(gf)* allele tested was *ar202*; at 25°C, *glp-1(ar202)* animals have both ectopic proliferation in the proximal germ line (Pro tumour) and have an extended distal proliferative zone (late-onset tumour) (Pepper et al., 2003). The molecular lesion associated with *glp-1(ar202)* causes a single amino acid change in a conserved residue in the extracellular portion of the GLP-1 protein that is thought to negatively regulate receptor activity in the absence of ligand binding (Pepper et al., 2003). The second *glp-1(gf)* allele tested was *oz264*, the molecular lesion of which is adjacent to the *glp-1(ar202)* lesion, in the extracellular portion of the GLP-1 receptor (Kerins, 2006; Kerins et al., 2010). The temperature-sensitive over-proliferation phenotype of *glp-1(oz264)* at 25°C is similar to *glp-1(ar202),* showing both late-onset tumours and Pro tumours; however, the majority (67%) of the *glp-1(oz264)* animals are wild-type at 25°C (Kerins, 2006; Kerins et al., 2010), suggesting that the *glp-1(oz264)* allele is a weaker gf allele than *glp-1(ar202)*.

To determine if *puf-8(oz192)* enhances the over-proliferation phenotype of other *glp-1(gf)* alleles, *puf-8(oz192); glp-1(ar202)* and *puf-8(oz192); glp-1(oz264)* double mutants were constructed. In both strains, completely tumourous germ lines were formed at 15°C (Figure 4.1, Table 4.1). This phenotype was much more over-proliferative than that which was observed for *puf-8(oz192); glp-1(oz112oz120)* in the

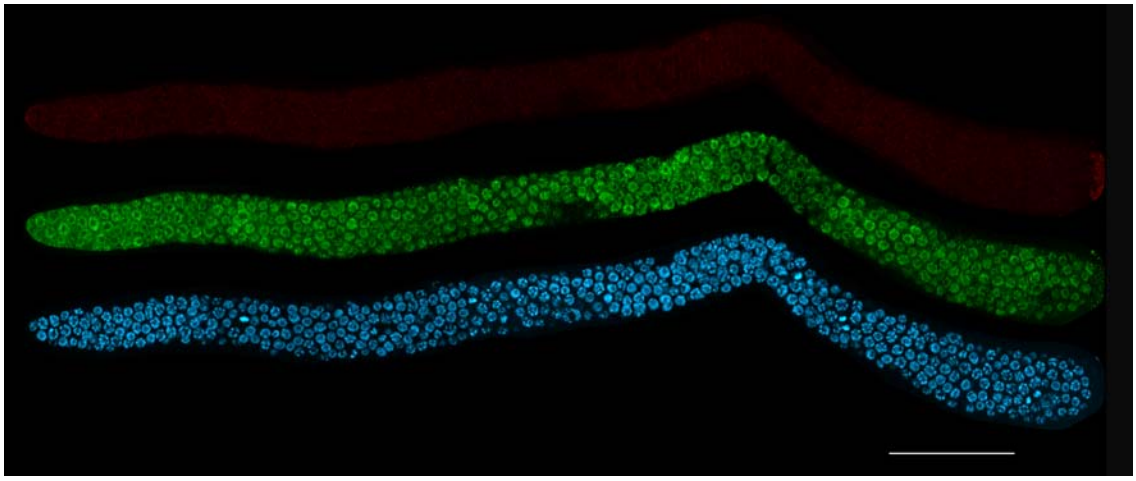

Figure 4.1. *puf-8; glp-1(gf)* tumourous germ line.

Dissected gonads stained with DAPI (blue) and probed with αREC-8 (green) and αHIM-3 (red) antibodies. The distal end of the germ line is on the left. These complete germline tumours contain only REC-8 positive cells. DAPI staining reveals M-phase nuclei throughout the germ line. Scale bar = 50 μM.

Table 4.1 *puf-8* enhances three *glp-1(gf)* alleles

Genotype	Phenotype[a]	N[e]
glp-1(ar202)	Wild-type	10
puf-8(oz192); glp-1(ar202)	Completely tumourous	35
puf-8(q725); glp-1(ar202)	Completely tumourous	35
puf-8(oz192); glp-1(ar202)/+[b]	74% completely tumourous, 26% tumourous with small patches of differentiated cells	27
glp-1(oz264)	Wild-type	9
puf-8(oz192); glp-1(oz264)	Completely tumourous	23
puf-8(q725); glp-1(oz264)	98% completely tumourous , 2% have small central regions of sperm	54
glp-1(oz112oz120)[c]	99.95% WT, 0.05% late-onset tumour	N/A
puf-8(oz192); glp-1(oz112oz120)[d]	Late-onset tumour, male meiotic development, Pro tumour	N/A

[a] Animals were maintained at 15°C. To analyze each animal's germ line, gonads were dissected and stained with DAPI, αREC-8 antibodies and αHIM-3 antibodies.

[b] Actual genotype= *puf-8(oz192) unc-4(e120)/puf-8(oz192); glp-1(ar202)/+.*

[c] Actual genotype= *unc-36(e252) glp-1(oz112oz120)*. Made and analyzed by (Wilson-Berry, 1998)

[d] Actual genotype= *puf-8(oz192) unc-4(e120); unc-36(e252) glp-1(oz112oz120)*. Made and analyzed by (Wilson-Berry, 1998)

[e] number of gonads analyzed

N/A= data Not Available

original *teg* screen. In *puf-8(oz192); glp-1(oz112oz120)* germ lines, meiotic cells are present; between the late-onset and Pro tumours are cells that have entered into meiosis, cells which are progressing through meiosis and cells that have completed spermatogenesis (Wilson-Berry, 1998). In *puf-8(oz192); glp-1(ar202)* and *puf-8(oz192); glp-1(oz264)* animals, all cells within the germ lines are mitotic at temperatures ranging from 15-25°C (Figure 4.1, Table 4.1). To analyze the germ lines of *puf-8(oz192); glp-1(ar202* or *oz264)* animals, dissected gonad arms were analyzed using three markers; DAPI, for nuclear morphology, as well as αREC-8 and αHIM-3 antibodies, for mitotic and meiotic cells, respectively (Hansen et al., 2004a). DAPI staining revealed the presence of metaphase plate nuclei, indicative of cells undergoing mitosis, throughout both the distal and proximal germ lines (Figure 4.1). Consistent with the DAPI staining, all *puf-8(oz192); glp-1(ar202* or *oz264)* germ line cells were REC-8 positive and HIM-3 negative (Figure 4.1). Thus, at the resolution of the markers used, the germ lines of *puf-8(oz192); glp-1(ar202* or *oz264)* animals appear to contain only mitotically dividing cells.

4.1.1 puf-8(q725) *Also Enhances the* glp-1(gf) *Over-Proliferative Phenotype*

Based on the associated molecular lesion, the *puf-8(oz192)* allele likely functions as a molecular null. However, it is also possible that *puf-8(oz192)* has some gf or neomophic functions that may be causing the over-proliferation enhancement. To differentiate between these possibilities, the *puf-8(q725)* deletion allele was tested for its ability to enhance the over-proliferative defect of *glp-1(gf)* alleles. The *puf-8(q725)*

deletion removes seven of the eight PUF repeats and since all eight PUF repeats are required for PUF protein function (Zhang et al., 1997), *puf-8(q725)* is most likely a null allele of *puf-8* (Bachorik and Kimble, 2005). In *puf-8(q725); glp-1(ar202* or *oz264)* animals, complete germline tumours are also formed, except for 2% of *puf-8(q725); glp-1(oz264);* these animals have tumourous germ lines that contain a small central patch of mature sperm (Table 4.1). The presence of sperm is likely due to the fact that *puf-8(q725)* animals have a low penetrant Mog (Masculinization Of the Germ line) phenotype; while most *puf-8(q725)* animals are self-fertile, 3% produce only sperm (Bachorik and Kimble, 2005). Why sperm was only observed in *puf-8(q725); glp-1(oz264)* animals and not in *puf-8(q725); glp-1(ar202)*, might be due to the differences in strength of the two *glp-1(gf)* alleles. *oz264* is a weaker *glp-1(gf)* allele that shows lower levels of over-proliferation in comparison to *ar202.* The *glp-1(oz264)* weaker gf phenotype may have permitted the *puf-8* single mutant phenotype to penetrate. Also, why sperm was not observed in *puf-8(oz192); glp-1(ar202* or *oz264)* animals is currently unknown, but may suggest that the genetic backgrounds are slightly different between the two alleles, or that *puf-8(oz192)* may have some dominant-negative effects.

4.1.2 Of the Four teg *Genes,* puf-8 *(formerly* teg-2*) More Strongly Enhances the* glp-1(gf) *Over-Proliferative Phenotype*

Of the four *teg* genes identified (Wilson-Berry, 1998), *puf-8* (*teg-2*) is the strongest enhancer of the *glp-1(gf)* over-proliferation phenotype. In *teg-4; glp-1(ar202)*

and *teg-1; glp-1(ar202)* animals, the germ lines contain late-onset and Pro tumours, which are separated by cells that have entered into meiosis (Mantina et al., 2009) (C. Wang and D. Hansen, personal communication). The strong enhancement seen with *puf-8(q725* and *oz192)* alleles could imply that *puf-8* plays a more central role in the mitosis vs. meiosis decision in comparison to *teg-4* and *teg-1*.

4.1.3 puf-8(oz192); glp-1(ar202)/+ *is Tumourous*

Interestingly, *puf-8(oz192)* enhances the over-proliferative defect in *glp-1(ar202)/+* heterozygotes. In *puf-8(oz192); glp-1(ar202)/+,* the majority of the animals form completely tumourous germ lines, characterized by gonads containing only REC-8 positive/HIM-3 negative proliferative mitotic cells (Table 4.1). The other fraction (26%) of *puf-8(oz192); glp-1(ar202gf)/+* animals are also tumourous but, in addition to the tumour, have small isolated patches of HIM-3 positive meiotic cells (only one patch per gonad arm) (Table 4.1). The HIM-3 positive cells appear to be undergoing the initial stages of meiosis and no mature gametes were ever observed.

Over-proliferative defects were also observed in *puf-8(oz192); glp-1(oz112oz120)/+* animals (Wilson-Berry, 1998). Since these animals contain the semi-dominant gf allele, *glp-1(oz112)*, it was suggested that two copies of *puf-8(oz192)* restores the dominance of *oz112* (Wilson-Berry, 1998). In *glp-1(ar202)* single mutants, 56% of *ar202/+* heterozygotes from *ar202* homozygous mothers have over-proliferative

defects in their germ lines. Potentially, two copies of *puf-8(oz192)* are also capable of enhancing the *glp-1(ar202)/+* heterozygote phenotype.

4.2 *puf-8(0)* Alleles Suppress the *glp-1* Loss-of-Function Glp Phenotype

Thus far, mutations in *puf-8* has been shown to enhance three different *glp-1(gf)* alleles. If *puf-8(0)* is also able to suppress *glp-1* loss-of-function (lf) alleles, this would provide further support that the *puf-8 glp-1* interaction is not allele specific and this would imply that *puf-8(+)* is a negative regulator of *glp-1(+)*. When *glp-1* function is reduced in lf alleles, germ cells prematurely enter into meiosis, a phenotype that is referred to as Glp (abnormal GermLine Proliferation) (Austin and Kimble, 1987). The lf allele tested in this project was *glp-1(bn18)*. *glp-1(bn18)* is a temperature-sensitive lf allele; at 15°C, *glp-1(bn18)* animals are virtually wild-type, but when the animals are raised at 25°C, sterile Glp germ lines are formed (Kodoyianni et al., 1992). The molecular lesion in *glp-1(bn18)* causes a single amino acid change in the highly conserved intracellular ankyrin repeat domain (repeat #4) (Kodoyianni et al., 1992). The ankyrin repeat domain is the site in GLP-1 that interacts (directly or indirectly) with the LAG-1 transcription factor (Roehl et al., 1996).

In *puf-8(oz192* or *q725); glp-1(bn18)* animals, suppression of the *glp-1(bn18)* 25°C Glp phenotype is observed in a low percentage of animals (Table 4.2). Suppression of the Glp phenotype was also tested at a reduced temperature of 22°C; at this temperature, 20% of *glp-1(bn18)* animals are Glp. Almost complete suppression of the

Table 4.2. *puf-8* suppresses three *glp-1(lf)* alleles

Animals were maintained at permissive temperatures (15°C).

[a] To perform analysis, individual L4 hermaphrodites were allowed to self at restrictive temperatures (22 and 25°C). After 3 days, the progeny were analyzed for suppression. Glp= abnormal GermLine Proliferation; germ lines contain only sperm.

[b] Actual genotype: *unc-32(e189) glp-1(q231)*, made and analyzed by (Wilson-Berry, 1998)

[c] Actual genotype: *puf-8(oz192) unc-4(e120); unc-32(e189) glp-1(q231),* made and analyzed by (Wilson-Berry, 1998)

[d] While *puf-8(oz192) unc-4(e120); unc-32(e189) glp-1(q231)* mutant animals show suppression of the Glp phenotype, animals are Mel (Maternal-effect Embryonic Lethal) (Wilson-Berry, 1998)

[e] Actual genotype: *unc-36(e252) glp-1(oz112oz120)*. At 25°C, these mutants are Glp and Mel (Wilson-Berry, 1998).

[f] Actual genotype: *puf-8(oz192) unc-4(e120); unc-36(e252) glp-1(oz112oz120)*. *puf-8* mutants suppress the Glp phenotype but not the Mel phenotype of *glp-1(oz112oz120)*. Animals are fertile but all progeny die during embryogenesis (Wilson-Berry, 1998).

N/A= Not Available (data not provided in (Wilson-Berry, 1998))

[g] number of gonads analyzed

Genotype	**Temp (°C)**	**% Glp[a]**	**N[g]**
glp-1(bn18)	22	20%	45
glp-1(bn18)	25	100%	15
puf-8(oz192); glp-1(bn18)	22	3%	141
puf-8(oz192); glp-1(bn18)	25	96%	17
puf-8(q725); glp-1(bn18)	22	0.4%	488
puf-8(q725); glp-1(bn18)	25	70%	110
glp-1(q231)[b]	25	100%	10
puf-8(oz192); glp-1(q231)[c]	25	0%[d]	8
glp-1(oz112oz120)[e]	25	100%	N/A
puf-8(oz192); glp-1(oz112oz120)[f]	25	0%	N/A

20% Glp phenotype was observed in *puf-8(oz192* or *q725); glp-1(bn18)* animals. In addition to the suppression seen in *puf-8(oz192* or *q725); glp-1(bn18)* animals, *puf-8(oz192)* also suppresses the 25°C Glp phenotype of *glp-1(q231lf)* and *glp-1(oz112oz120lf)* animals (Wilson-Berry, 1998). Combining the results from the studies with gf and lf *glp-1* alleles reveals that *puf-8*'s interaction with *glp-1* is not allele specific.

4.3 *puf-8(0); glp-1(gf)* Tumours are Not Due to the Dedifferentiation of Male Germ Cells

At restrictive temperatures (25°C), a proportion of *puf-8* single mutant animals have spermatocytes that exit meiosis and dedifferentiate back into mitotic cells (Subramaniam and Seydoux, 2003). Thus, *puf-8* is required, in male germ cells, to promote meiotic divisions and to prevent primary spermatocytes from re-entering mitosis (Subramaniam and Seydoux, 2003). Based on this *puf-8* role, it is possible that the tumourous germ lines in *puf-8(0); glp-1(gf)* animals could be formed due to the dedifferentiation of male germ cells and not due to misregulation of the mitosis vs. meiosis decision.

To explore if *puf-8(0); glp-1(gf)* tumours arise through the dedifferentiation of male germ cells, two approaches were taken. First *puf-8(0); glp-1(gf)* animals were introduced into a feminized background, using *fem-3(e1996)* mutants. *fem-3* is required for the specification of the male fate and as such, loss of *fem-3* results in feminized germ lines (Hodgkin, 1986). If tumours were no longer formed in *puf-8(0); glp-1(gf)* feminized

animals, this would suggest that the completely tumourous germline phenotype requires the dedifferentiation of male germ cells to develop. To maintain *fem-3(e1996)* animals, the mutant is balanced over *unc-24(e138) dpy-20(e1282)*. To determine the *puf-8(0); glp-1(gf); fem-3(0)* phenotype, non-green and non-Unc Dpy animals were selected from *puf-8(0)/mC6g; glp-1(gf); fem-3/unc-24 dpy-20*. Using Nomarski optics, all non-green non-Unc Dpy animals (n=33) were completely tumourous (Table 4.3). Since it is not possible to differentiate between *fem-3* and *fem-3/unc-24 dpy-20* animals in a *puf-8(0); glp-1(gf)* background, both were present in this population. However, based on Mendelian ratios, 1/3 should have been *fem-3/fem-3*. All the germ cells in *puf-8(0); glp-1(gf); fem-3* or *puf-8(0); glp-1(gf); fem-3/unc-24 dpy-20* animals were REC-8 positive and HIM-3 negative. As well, DAPI revealed that M-phase nuclei were distributed throughout the gonad arm. Since complete germline tumours were formed in the absence of male germ cells and in *fem-3/unc-24 dpy-20* heterozygous animals, *puf-8(0); glp-1(gf)* tumours are likely due to a defect in the mitosis vs. meiosis decision and not due to dedifferentiation of male germ cells.

For further validation that the tumour in *puf-8(0); glp-1(gf)* animals is not due to the dedifferentiation of male germ cells, *puf-8(0); glp-1(gf)* animals were placed in a spermatogenesis defective *spe-6(hc49)* mutant background, in which male germ cells are unable to complete spermatogenesis and arrest at diakinesis of prophase I (Varkey et al., 1993). Dedifferentiation of primary spermatocytes in *puf-8* mutants, at 25°C, occurs after diakinesis of prophase I and no dedifferentiation occurs in *puf-8; spe-6*

Table 4.3. *puf-8(0); glp-1(ar202)* tumours are not due to dedifferentiation of male meiotic cells

[a] Strains with *glp-1(ar202)* were grown at 18°C, all other strains were grown at 20°C.

[b] Dissected gonads of each genotype were analyzed using DAPI, αREC-8 antibodies and αHIM-3 antibodies. Complete tumours contain only REC-8 positive cells. Fem = FEMinization of the germ line. Spe= defective SPErmatogenesis. Pro= PROximal proliferation

[c] *fem-3(e1996)* hermaphrodites contain only oocytes. *spe-6(hc49)* primary spermatocytes are blocked at diakinesis of meiosis I.

[d] Actual genotype: *puf-8(q725); glp-1(ar202); fem-3(e1996)* or *puf-8(q725); glp-1(ar202); fem-3(e1996)/unc-24(e138) dpy-20(e1282)*

[e] Actual genotype: *puf-8(q725); fem-3(e1996)*

[f] Actual genotype: *glp-1(ar202); fem-3(e1996)*

[g] Actual genotype: *puf-8(q725); glp-1(ar202) spe-6(hc49) unc-25(e156)*

[h] Actual genotype: *puf-8(q725); spe-6(hc49) unc-25(e156)*

[I] Actual genotype: *glp-1(ar202) spe-6(hc49) unc-25(e156)*

[j] Actual genotype: *puf-8(q725); glp-1(ar202) unc-25(e156)*

[k] Actual genotype: *glp-1(ar202) unc-25(e156)*

[l] number of gonad arms analyzed

Genotype[a, c]	**Phenotype**[b]	**N**[l]
(1/3) *puf-8; glp-1(gf); fem-3*[d] (2/3) *puf-8; glp-1(gf); fem-3/unc-24 dpy-20*[d]	Complete tumour	33
puf-8; fem-3[e]	Fem	18
glp-1(gf); fem-3[f]	50% Fem, 50% Fem+Pro	11
puf-8; glp-1(gf) spe-6[g]	Complete tumour	8
puf-8; spe-6[h]	Spe	6
glp-1(gf) spe-6[i]	Spe	7
puf-8; glp-1(gf)[j]	Complete tumour	5
glp-1(gf)[k]	WT	11

mutants (Subramaniam and Seydoux, 2003). Thus if *puf-8(0); glp-1(gf)* tumours are due to dedifferentiation of primary spermatocytes, then in a *spe-6* mutant background, these tumours will not be able to form. In *puf-8(q725); glp-1(ar202) spe-6(hc49)* animals, all germ lines are completely tumourous, showing only REC-8 positive/HIM-3 negative cells (Figure 4.2, Table 4.3).

Using two genetic backgrounds to prevent dedifferentiation of male germ cells, it was observed that *puf-8(0); glp-1(gf)* tumours are not formed through the dedifferentiation of primary spermatocytes. Instead, the tumours formed in *puf-8; glp-1(gf)* animals are likely due to an absence of entry into meiosis (i.e., misregulation of the mitosis vs. meiosis decision). Additionally, these results reveal that the *puf-8(0); glp-1(gf)* phenotype is distinct from *puf-8's* role during male germ cell meiosis.

4.3.1 puf-8(0); glp-1(gf) Germ Cells Never Enter Into Meiosis

To further explore if germ cells within *puf-8(0); glp-1(gf)* animals ever enter into meiosis, and possibly re-enter mitosis after entering briefly into meiosis, early larval staged animals were analyzed. For example, in *gld-1(0)* hermaphrodite mutants, early larval germline proliferation is similar to wild-type; however, later in development *gld-1(0)* meiotic cells exit meiotic prophase and return to the mitosis, forming tumourous germ lines (Francis et al., 1995a). Thus, it is possible that *puf-8(0); glp-1(gf)* tumours are the result of meiotic cells re-entering mitosis.

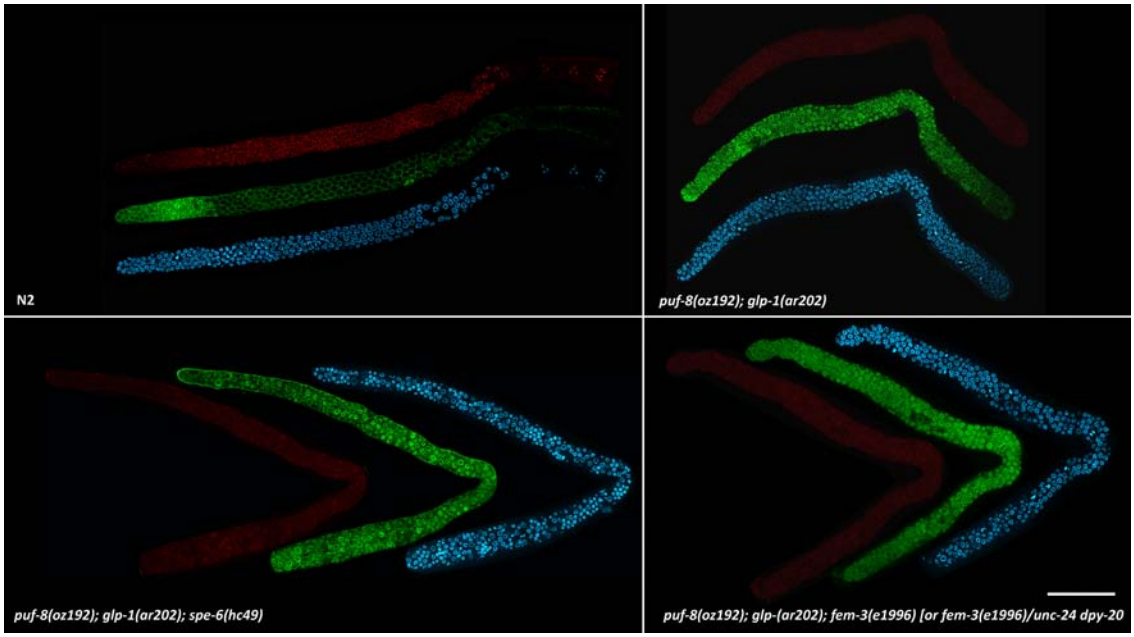

Figure 4.2. *puf-8(0); glp-1(gf)* complete germline tumours are not due to the dedifferentiation of male meiotic cells, but rather due to the absence of meiotic entry. *puf-8(oz192); glp-1(ar202)* double mutants tumours are indistinguishable from *puf-8(oz192); glp-1(ar202); spe-6(hc49)* and *puf-8(oz192); glp-1(ar202); fem-3(e1996) [or fem-3(e1996)/unc-24 dpy-20]* triple mutants. Antibodies against REC-8 (green) and against HIM-3 (red). DAPI staining (blue). Scale bar = 50 μM

In wild-type germ lines, from larval stage 2 (L2) to young L3, only mitotic undifferentiated germ cells are present (Figure 1.2). During late L3, a small proximal population of germ cells begins to enter into meiosis. To determine if the mitotic cells in *puf-8(0); glp-1(gf)* animals ever enter into meiosis, gonads from L2-late L3 staged animals were dissected and analyzed with αREC-8 and αHIM-3 antibodies. All germ lines from L2 to late L3 animals showed only REC-8 positive/HIM-3 negative cells, indicative of mitotic cells (Figure 4.3, Table 4.4). Since larval *puf-8(0); glp-1(gf)* germ lines never show signs of meiotic entry, *puf-8* likely has an early larval role in the mitosis vs. meiosis decision and also suggests that the mitotic cells in *puf-8(0); glp-1(gf)* tumours are not due to meiotic cells re-entering into mitosis.

4.4 *puf-8's* Interaction With the Mitosis/Meiosis Pathway Genes

Mutations in *puf-8* enhance the *glp-1(gf)* germline over-proliferation phenotype. This implies that *puf-8* functions either as a negative regulator of mitosis or a positive regulator of entry into meiosis. To explore which of these two hypotheses is most likely for *puf-8*, a genetic approach was used. *puf-8* mutants were combined with mutations in a number of genes involved in regulating the mitosis vs. meiosis decision. The resulting phenotypic outcomes were determined to clarify *puf-8's* functional location in the genetic pathway regulating the mitosis vs. meiosis decision.

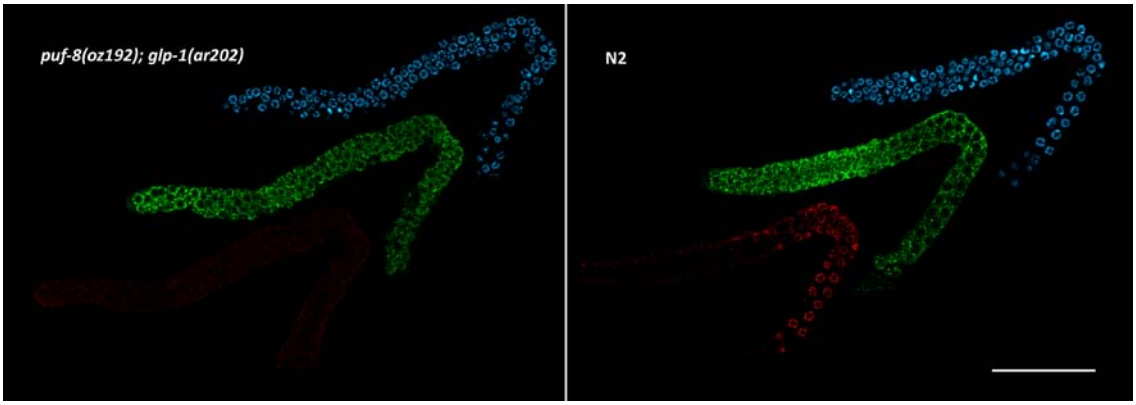

Figure 4.3. *puf-8; glp-1(gf)* animals never enter into meiosis.

Comparison between *puf-8(oz192); glp-1(ar202)* vs. N2 L3 staged animals. *puf-8; glp-1(gf)* animals only have REC-8 positive cells. In N2 animals of the same age, the proximal region contains HIM-3 positive cells. Distal end of the germ line on the left. DAPI staining (Blue), αREC-8 (Green) and αHIM-3 (Red). Scale bar = 50 μM.

Table 4.4. *puf-8(0); glp-1(ar202)* early larval stages are devoid of meiotic cells

% animals with meiotic cells[a]			
Genotype	**L2**	**Late L3**	**N[b]**
N2	0%	100%	7
puf-8(oz192); glp-1(ar202)	0%	0%	25
puf-8(q725); glp-1(ar202)	0%	0%	12

All strains were maintained at 20°C

[a] Gonads from L2-late L3 staged animals were dissected and stained with DAPI, αREC-8 and αHIM-3 antibodies.

[b] the N value for each strain represents ~50% L2 and ~50% L3 dissected gonads analyzed

4.4.1 puf-8's *Interaction With Meiosis Promoting Genes*

One possible reason for why *puf-8* mutants are able to enhance *glp-1(gf)* over-proliferation could be that *puf-8* functions downstream of Notch signalling, in one of the meiosis promoting pathways, to positively regulate germ cell entry into meiosis and/or negatively regulate proliferation. Downstream of Notch signalling are two redundant pathways that promote meiotic differentiation. One pathway includes the genes *gld-1* and *nos-3*, while the second pathway includes the genes *gld-2* and *gld-3*. When the activity of only one of the two pathways (*gld-1* or *gld-2*) is removed through genetic mutation, the mitosis vs. meiosis decision occurs similarly to wild type (Francis et al., 1995b; Kadyk and Kimble, 1998). However, when the activities of both pathways are removed, very little entry into meiosis occurs and a germline tumour results (Eckmann et al., 2004; Hansen et al., 2004b; Kadyk and Kimble, 1998). Importantly, mutations in genes in the *gld-1* and *gld-2* pathways singly enhance the over-proliferative phenotype of *glp-1* gf alleles (Kadyk and Kimble, 1998), so *puf-8* could function in one or the other pathways. If *puf-8* functions in one of the two meiosis promoting pathways, then removal of *puf-8* and removal of a component from the redundant pathway would result in the formation of a germline tumour. No germline tumours were observed in any of the double mutant strains (*gld-1; puf-8, gld-2; puf-8, gld-3 puf-8,* or *puf-8 nos-3)* (Table 4.5). However, there were some other interesting phenotypes that will be discussed later in this thesis (Appendix B). The lack of tumour formation suggests that

Table 4.5. *puf-8's* interaction with meiosis promoting genes

All strains maintained at 20°C

[a] When *puf-8* mutants are combined with mutations in any of the four meiosis promoting genes, no germline tumours are formed. To analyze each animal's germ line, gonads were dissected and stained with DAPI, αREC-8 antibodies and αHIM-3 antibodies.

[b] Unmarked *puf-8(oz192)* was used in the construction of each strain; therefore, sequencing was required to verify the presence of the *oz192* allele.

While no synthetic tumours were formed, some other interesting phenotypes were present:

[c] *gld-3(q730) puf-8(oz192)* animals show a delay in development. 1 day past L4 50% are Mog and 50% produce sperm, oocytes and embryos. 2 days past L4 all have sperm, oocytes and embryos. *gld-3(q730) puf-8(oz192)* embryos undergo embryogenesis to various stages then arrest; only a very low percentage hatch and mature to adults. In contrast, *gld-3(q730)* single mutant embryos arrest at the 2 cell stage (Eckmann et al 2002).

[d] *puf-8(oz192) nos-3(oz231)* animals are mainly wild-type; however, some show a mild Egl (EGg-Laying defective) phenotype or a Mog (Masculinization Of the Germ line) phenotype that may also be due to a slight delay in development.

[e] *gld-2(q497); puf-8(oz192)* animals look much like *gld-2(q487)* single mutant; *gld-2(q497)* have defective spermatocytes and oocytes (Kaydk and Kimble 1998).

[f] *gld-1(q485); puf-8(oz192)* animals have normal distal proliferation and wild-type numbers of sperm. In 76% of the animals, Pro tumours are formed (discussed further in Appendix B). In contrast, *gld-1(q485)* have germ cells that enter into meiosis, fail in pachytene, re-enter mitosis and form large Pro tumours. *gld-1(q485)* animals never form sperm (Francis et al 1995).

[g] number of gonads analyzed

Genotype[b]	**Tumour?**[a]	**N**[g]
gld-3(q730) puf-8(oz192)[c]	No	60
puf-8(oz192) nos-3(oz231)[d]	No	36
gld-2(q497); puf-8(oz192)[e]	No	21
gld-1(q485); puf-8(oz192)[f]	No	35

puf-8 does not function in either of the two redundant pathways to promote entry into meiosis.

4.4.2 puf-8's *Interaction With the Mitosis Promoting Genes Downstream of Notch*

puf-8 functions either as a negative regulator of mitosis or a positive regulator of entry into meiosis. Results from section 4.4.1 suggest that it is unlikely that *puf-8* functions in either of the *gld-1* or *gld-2* pathways to promote entry into meiosis. To test if *puf-8* may function instead to negatively regulate mitosis, upstream of the *gld-1* and *gld-2* pathways, *puf-8* mutants were combined with mutations in the mitosis promoting genes found downstream of Notch signalling, but upstream of the *gld* pathways. These genes include *fbf-1, fbf-2, fog-1* and *lst-1* (Figure 1.6) (Lamont et al., 2004; Thompson et al., 2005) (A. Kershner, personal communication).

First, interactions between *puf-8* and the *fbfs* were tested. FBF-1 and FBF-2 promote proliferation of GSCs by negatively regulating downstream meiosis-promoting pathways (Eckmann et al., 2004; Zhang et al., 1997). While FBF-1 and FBF-2 belong to the same protein family as PUF-8, their functions in the mitosis vs. meiosis decision are opposite, as *puf-8* appears to inhibit proliferation. This suggests that *puf-8's* function is distinct from the *fbfs* in the mitosis vs. meiosis decision. In order to better understand the potential regulatory relationships between *puf-8* and the *fbfs*, *fbf-1 fbf-2 puf-8* triple mutants were generated. In an *fbf-1 fbf-2* double mutant, germ cells prematurely enter

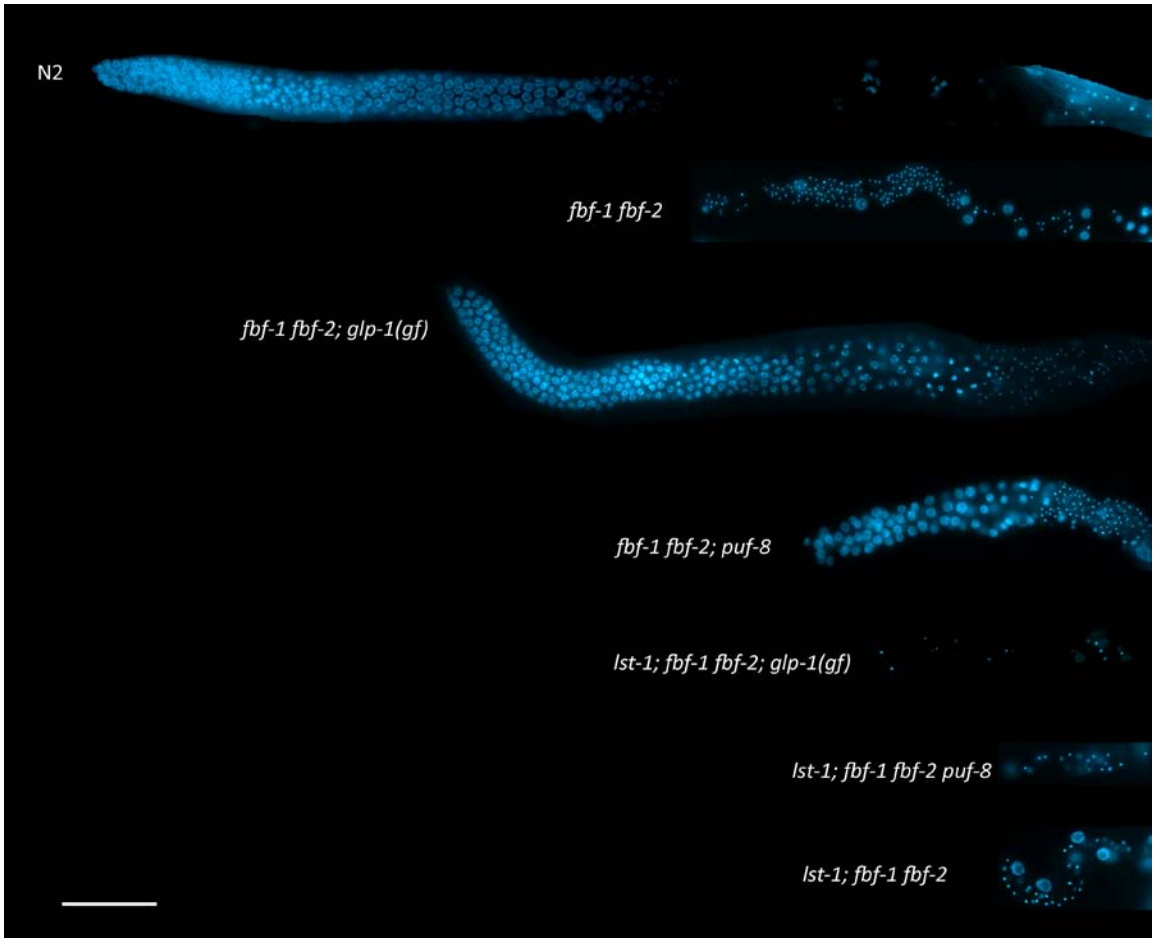

Figure 4.4. Comparison of mutant germ lines.

Dissected gonads stained with DAPI. Distal end of each gonad arm is on the left. Wild-type (N2) germ line at top. *fbf-1 fbf-2* germ lines are Glp; contain only sperm (large, round cell are sheath cells). However, when Notch signalling is increased (*fbf-1 fbf-1; glp-1(gf)* or when *puf-8* is removed in an *fbf-1 fbf-2* background, mitotic cells are present in the distal region. The mitotic cells are no longer present in when *lst-1* is mutated: *lst-1; fbf-1 fbf-2; glp-1(gf), lst-1; fbf-1 fbf-2 puf-8* and *lst-1; fbf-1 fbf-2* animals are all Glp. Scale bar = 50 μM.

Table 4.6. *puf-8* and *glp-1(gf)'s* interaction with *fbf-1, fbf-2, fog-1* and *lst-1*

[a] The alleles used for each gene are as follows: *puf-8(q725), fbf-1(ok91), fbf-2(q704), fog-1(e2121), lst-1(ok814), unc-11(e47)* and *glp-1(ar202).* To increase Notch signalling in *glp-1* strains that did not contain *puf-8*, strains were shifted to 25°C. Otherwise, all strains were analyzed at 18°C.

[b] Young animals (1 day past L4) of each genotype were analyzed using DIC microscopy. In some cases, gonad arms were dissected and stained with DAPI, αREC-8 antibodies and αHIM-3 antibodies. Germ lines were characterized based on whether they contained tumours (includes complete, late-onset and/or Pro germline tumours), contained only meiotic cells (Glp) or had a functional mitosis vs. meiosis decision. It is possible for a mutant strain to have both a Pro tumour and a functional mitosis vs. meiosis decision; however, if a strain is Glp, no functional mitosis vs. meiosis decision is possible.

[c] number of gonad arms analyzed

See Appendix C for phenotypic descriptions of each strain.

Phenotype[b]				
Genotype[a]	**Tumourous**	**Glp**	**Mitosis/Meiosis**	**N[c]**
glp-1	X		X	11
puf-8			X	11
puf-8; glp-1	X			35
fbf-1 fbf-2		X		11
fbf-1 fbf-2; glp-1			X	14
fbf-1 fbf-2 puf-8			X	26
fbf-1 fbf-2 puf-8; glp-1			X	17
fog-1 unc-11			X	7
fog-1 unc-11; glp-1	X			12
fog-1 unc-11; fbf-1 fbf-2		X		18
fog-1 unc-11; puf-8			X	15
fog-1 unc-11; fbf-1 fbf-2 puf-8			X	45
fog-1 unc-11; fbf-1 fbf-2 puf-8; glp-1			X	14
fog-1 unc-11; fbf-1 fbf-2; glp-1	X			18
fog-1 unc-11; puf-8; glp-1	X			7
unc-11; glp-1	X			17
unc-11; fbf-1 fbf-2		X		14
unc-11; fbf-1 fbf-2 puf-8			X	12
unc-11; puf-8			X	10
unc-11; fbf-1 fbf-2 puf-8; glp-1			X	40
unc-11; fbf-1 fbf-2; glp-1	X			8
unc-11; puf-8; glp-1	X			14
lst-1			X	26
lst-1; puf-8			X	15
lst-1; fbf-1 fbf-2		X		19
lst-1; fbf-1 fbf-2 puf-8		X		35
lst-1; glp-1	X		X	18
lst-1; puf-8; glp-1	X			9
lst-1; fbf-1-2; glp-1		X		20
lst-1; fbf-1 fbf-2 puf-8; glp-1		X		9

meiosis, forming ~200 sperm per adult gonad arm (Figure 4.4, Table 4.6) (Crittenden et al., 2002). In *fbf-1 fbf-2 puf-8* animals, the premature meiotic entry defect was partially suppressed; all animals had a distal region of mitotic cells, followed by a proximal region of male meiotic development and differentiated sperm (Figure 4.4, Table 4.6). At first glance, this result may indicate that *puf-8* functions downstream of, or in parallel to, *fbf-1* and *fbf-2* to negatively regulate proliferation. However, *fbf-1* and *fbf-2* are not the only genes that function downstream of Notch signalling to promote proliferation and/or negatively regulate entry into meiosis. The premature meiotic entry defect in *fbf-1 fbf-2* double mutants is less severe than the 8 sperm/gonad arm produced in *glp-1* null mutants, demonstrating that other genes likely function in parallel to the *fbfs* to promote proliferation and/or negatively regulate entry into meiosis (Austin and Kimble, 1987; Crittenden et al., 2002). Thus, loss of the *fbfs* does not completely knock out this portion of the pathway. With this in mind, it is possible that the suppression seen in *fbf-1 fbf-2 puf-8* animals could still occur if *puf-8* functions upstream of the *fbfs*. If *puf-8* functions upstream of the *fbfs*, then removal of *puf-8* could increase the activity of the genes that function redundantly with the *fbfs*, which may be the reason why proliferation was able to occur in *fbf-1 fbf-2 puf-8* animals. If this hypothesis is correct, that a mutation in a gene that functions upstream of the *fbfs* can suppress the *fbf* premature meiotic entry defect, then *glp-1(gf)* mutants, which also function upstream of the *fbfs*, should be able to suppress the *fbf* premature meiotic entry phenotype. Indeed, increased proliferation through an increase in Notch signalling was able to

suppress the *fbf-1 fbf-2* premature meiotic entry phenotype. In *fbf-1 fbf-2; glp-1(ar202)* animals, suppression of the premature meiotic entry phenotype was observed, even though *fbf-1* and *fbf-2* function downstream of *glp-1* (Figure 4.4, Table 4.6). In light of the *fbf-1 fbf-2; glp-1(ar202)* results, it may also be possible that *puf-8* functions upstream of the *fbfs* to negatively regulate proliferation (Figure 1.6).

The results from the *fbf-1* and *fbf-2* studies leave open the possibility that *puf-8* functions either upstream or downstream of the *fbfs* to negatively regulate proliferation. To explore *puf-8's* functional location further, interactions between *puf-8* and the other genes that work in parallel to the *fbfs* were analyzed. One gene that functions in parallel to the *fbfs* is *fog-1*. FOG-1 (Feminization Of Germline) is a CPEB RNA-binding protein that is important for sperm specification (Barton and Kimble, 1990). In *fog-1; fbf-1 fbf-2* animals, a further reduction in germ cell number was observed in comparison to *fbf-1 fbf-2* animals (Thompson et al., 2005). This suggests that *fog-1* functions redundantly with the *fbfs* to promote mitosis. If *puf-8* functions upstream of the *fbfs* and *fog-1*, and presuming that no other genes, other than *fog-1,* work in parallel to the *fbfs*, then suppression of the premature entry into meiosis should be abolished in *fog-1; fbf-1 fbf-2 puf-8* animals. In *fog-1; fbf-1 fbf-2 puf-8* germ lines, suppression of the premature entry into meiosis phenotype is still present (Table 4.6, Table 4.7, Appendix C). These results suggest that *puf-8* may function downstream of *fbf-1, fbf-2* and *fog-1*. However, as stated earlier, this is only true if *fog-1; fbf-1 fbf-2* completely knock out this portion of the pathway. To test this, *fog-1; fbf-1 fbf-2; glp-*

Table 4.7. Summary of *puf-8's* interaction with *fbf-1, fbf-2, fog-1* and *lst-1*

Genotype	**Phenotype**	**N[e]**
fbf-1 fbf-2[a]	Glp; ~200 sperm	11
fbf-1 fbf-2 puf-8[b]	Distal mitotic cells, proximal sperm	26
fog-1; fbf-1 fbf-2 puf-8[c]	Distal mitotic cells, proximal meiotic cells	45
lst-1; fbf-1 fbf-2 puf-8[d]	Glp; ~27 sperm	35

[a] Actual genotype: *fbf-1(ok91) fbf-2(q704)*

[b] Actual genotype: *fbf-1(ok91) fbf-2(q704) puf-8(q725)*

[c] Actual genotype: *fog-1(e2121) unc-11(e47); fbf-1(ok91) fbf-2(q704) puf-8(q725)*

[d] Actual genotype: *lst-1(ok814); fbf-1(ok91) fbf-2(q704) puf-8(q725)*. PCR was performed to determine the presence of the *lst-1(ok814)* deletion allele.

[e] number of gonads analyzed

1(ar202) quadruple mutants were made. It was observed that *glp-1(ar202)* was able to suppress the *fog-1; fbf-1 fbf-2* premature meiotic entry phenotype (Table 4.8, Appendix C). Therefore, this suggests that *fog-1, fbf-1* and *fbf-2* are not the only factors in this section of the pathway, which leaves open the possibility that *puf-8* functions upstream of these factors.

In addition to *fog-1*, *lst-1* is another gene that has been proposed to function with the *fbfs* to promote mitosis. The *lst-1* (Lateral Signalling Target) gene is a target of LIN-12 lateral signalling during vulva development and encodes a protein that functions as a negative regulator of EGFR-MAPK (Yoo et al., 2004). *lst-1; fbf-1 fbf-2* triple mutants have fewer germ cells than *fbf-1 fbf-2* double mutants, suggesting that *lst-1* functions in parallel to the *fbfs* (A. Kershner personal communication) (Figure 4.4, Appendix C). If *puf-8* functions upstream of the *fbfs* and *lst-1* and if mutations in these genes completely block this section of the pathway, then *puf-8(0)* mutants will be unable to suppress the *lst-1; fbf-1 fbf-2* premature entry into meiosis phenotype. Analysis of *lst-1; fbf-1 fbf-2 puf-8* germ lines revealed that *puf-8(0)* mutants were unable to suppress the premature entry into meiosis defect. *lst-1; fbf-1 fbf-2 puf-8* germ lines are indistinguishable from *lst-1; fbf-1 fbf-2* (Table 4.6, Table 4.7). Both animals have Glp germ lines that contain ~27 sperm per gonad arm (Table 4.7). Also, in *lst-1; fbf-1 fbf-2; glp-1(ar202)* germ lines, no mitotic germ cells were present in the adult gonad (Table 4.6, Table 4.8). *lst-1; fbf-1 fbf-2; glp-1(ar202)* germ lines, however, are not identical to *lst-1; fbf-1 fbf-2*; instead of forming mature sperm, *lst-1; fbf-1 fbf-2; glp-1(ar202)* germ

Table 4.8. Summary of *glp-1(gf)'s* interaction with *fbf-1, fbf-2, fog-1* and *lst-1*

Genotype	Phenotype	N[e]
fbf-1 fbf-2[a]	Glp; ~200 sperm	11
fbf-1 fbf-2; glp-1[b]	Robust distal proliferation, proximal sperm	14
fog-1; fbf-1 fbf-2; glp-1[c]	Majority tumourous with patches of meiotic cells	18
lst-1; fbf-1-2; glp-1[d]	Glp; ~23 spermatocytes	20

[a] Actual genotype: *fbf-1(ok91) fbf-2(q704)*

[b] Actual genotype: *fbf-1(ok91) fbf-2(q704); glp-1(ar202)*

[c] Actual genotype: *fog-1(e2121) unc-11(e47); fbf-1(ok91) fbf-2(q704); glp-1(ar202)*

[d] Actual genotype: *lst-1(ok814); fbf-1(ok91) fbf-2(q704); glp-1(ar202)*

[e] number of gonads analyzed

lines contain an average of 23 partially developed spermatocytes (Figure 4.4, Table 4.8). The results from the *lst-1* genetic studies suggest that *puf-8* likely functions upstream of the *fbfs*; however, it is still formally possible that *puf-8* could function downstream in a redundant pathway that is not sufficient to cause suppression. It is also possible that *puf-8* functions in a parallel pathway.

4.4.3 puf-8's *Interaction with the* glp-1 *Null Allele*

puf-8 may function upstream of Notch signalling, but it is still formally possible that *puf-8* functions downstream of Notch. To help differentiate between these possibilities, *puf-8* mutants were combined with a *glp-1* null mutant. *glp-1(q175)* null mutants completely knock out the mitosis section of the pathway; *glp-1(q175)* animals are Glp, producing a total of ~16 sperm per hermaphrodite (or ~7 sperm/gonad arm) (Austin and Kimble, 1987). If *puf-8* functions upstream of Notch, *puf-8* mutants will not be able to suppress the *glp-1(q175)* phenotype. Some (but not all) genes that function downstream of Notch can partially suppress the *glp-1(q175)* phenotype. For example, *gld-1* and *gld-2* can partially suppress *glp-1(q175)*; in *gld-1(0); glp-1(q175)* ~64 sperm are formed per animal (Francis et al., 1995b) and in *gld-2(lf); glp-1(q175)* ~32 sperm are formed per animal (Kadyk and Kimble, 1998). The reason for the partial suppression is because *gld-1* and *gld-2* function in redundant pathways (Kadyk and Kimble, 1998). In *puf-8(0); glp-1(q175)* animals only ~10-12 sperm are produced per animal (or ~5-6 sperm per gonad arm) (Table 4.9). The fact that *puf-8* mutants are unable to suppress

Table 4.9. *puf-8's* interaction with *glp-1(q175)* null allele

All strains were maintained at 20°C

[a] All sperm counts were scored using dissected gonads stained with DAPI. The sperm in each gonad arm was counted 3X and then averaged.

[b] Glp= abnormal GermLine Proliferation

[c] Actual genotype: *unc-32(e189) glp-1(q175)*

[d] Actual genotype: *puf-8(oz192); unc-32(e189) glp-1(q175)*

[e] Actual genotype: *puf-8(q725); unc-32(e189) glp-1(q175)*

[f] Actual genotype: *gld-1(q485); unc-32(e189) glp-1(q175)*

[g] Actual genotype: *gld-1(q485); puf-8(q725); unc-32(e189) glp-1(q175)*

[h] Actual genotype: *gld-2(q497) gld-1(q485); unc-32(e189) glp-1(q175)*

[i] in addition to the Glp phenotype, 56% of *gld-1(q485); puf-8(q725); unc-32(e189) glp-1(q175)* animals were also Muv (MUlti-Vulva), containing 1 or 2 additional pseudovulvae.

[j] data from (Kadyk and Kimble, 1998)

[k] data from (Hansen et al., 2004a)

[l] data from (Francis et al., 1995b), N/A= data Not Available

[m] number of gonad arms analyzed

Genotype	**Phenotype**	**Avg n of sperm/gonad arm[a]**	**N[m]**
glp-1(q175)[c]	100% Glp[b]	7.5	22
puf-8(oz192); glp-1(q175)[d]	100% Glp	5	18
puf-8(q725); glp-1(q175)[e]	100% Glp	6.3	20
gld-1; glp-1(q175)[f]	100% Glp	64[l]	N/A
gld-1; puf-8(q725); glp-1(q175)[g]	100% Glp[i]	30	18
gld-2 gld-1; glp-1(q175)[h]	Tumourous[j,k]	0	72[k]

(neither partially or fully) the *glp-1(q175)* Glp phenotype further supports that *puf-8* functions upstream of Notch. However, not all downstream genes can suppress *glp-1(q175)*. For example, *nos-3* mutants do not suppress the *glp-1(q175)* phenotype, presumably due to its relatively minor role in the *gld-1* pathway (D. Hansen, personal communication). However, *puf-8(0)'s* enhancement of *glp-1(gf)* alleles is much stronger than *nos-3(0)'s* enhancement of *glp-1(gf)* alleles, suggesting a more major role for *puf-8* in comparison to *nos-3*. Therefore, the results from *puf-8(0); glp-1(q175)* double mutant analysis likely suggest that *puf-8* does not function downstream of Notch; however, the results do not provide conclusive evidence.

Further genetic analysis with the *glp-1(q175)* mutant revealed additional support that *puf-8* does not function downstream in the *gld-2* pathway. In *gld-1; puf-8; glp-1(null)* triple mutants, the germ lines are Glp (Table 4.9). However, in *gld-2 gld-1; glp-1(null)* triple mutants, the Glp phenotype is suppressed and a tumour is formed (Table 4.9) (Kadyk and Kimble, 1998). The Glp phenotype seen in *gld-1; puf-8; glp-1(null)* triple mutants suggests that loss of *puf-8* does not affect the *gld-2* pathway. In *gld-1; puf-8; glp-1(null)* triple mutants, the *gld-2* pathway is functional, allowing meiotic entry to occur.

Summary

Two different alleles of *puf-8(oz192* and *q725)* enhance and partially suppress *glp-1(gf)* and *glp-1(lf)* mutant phenotypes, respectively, suggesting that (1) both *puf-8*

alleles disrupt *puf-8* function in a similar fashion, (2) that both *puf-8* alleles likely function as strong lf or molecular nulls and (3) that *puf-8's* interaction with *glp-1* is not allele specific. The *puf-8(0); glp-1(gf)* enhancement phenotype consists of germ lines that likely only contain mitotic germ cells, which reveals that *puf-8* is a stronger enhancer of *glp-1(gf)* in comparison to other identified regulators from the *teg* screen. The complete *puf-8(0); glp-1(gf)* germline tumours are due to misregulation of the mitosis vs. meiosis decision and are not due to (1) the re-entry into mitosis of early meiotic cells or (2) the dedifferentiation of male germ cells. *puf-8(0)* mutants ability to enhance the *glp-1(gf)* over-proliferative phenotype suggests that *puf-8* likely functions either as a negative regulator of proliferation or a positive regulator of entry into meiosis. Double mutant analysis with the *gld-1* and *gld-2* pathways suggests that *puf-8* likely does not function in either of these redundant pathways to promote meiotic entry. This could suggest that *puf-8* functions upstream of *gld-1* and *gld-2* to negatively regulate proliferation. To determine where *puf-8* functions upstream, genetic analysis was performed with mitosis promoting genes. Results from over fifty different genetic crosses with mitosis promoting genes reveals that *puf-8* likely functions upstream of Notch signalling. However, no single result conclusively rules out the possibility that *puf-8* functions downstream of Notch signalling.

Chapter Five: ***puf-8's*** **Interaction with the *lin-12/*Notch Receptor**

PUF-8 functions as a negative regulator of proliferation in the *C. elegans* germ line upstream of the *gld-1* and *gld-2* pathways. Thus, one possibility is that PUF-8 may negatively regulate the canonical *glp-1/*Notch signalling pathway. In addition to GLP-1, the *C. elegans* genome also encodes another Notch receptor, LIN-12 (abnormal cell LINeage). Both Notch receptors are remarkably similar (Yochem and Greenwald, 1989). While GLP-1 and LIN-12 have functionally distinct roles throughout development (Austin and Kimble, 1987; Greenwald et al., 1983), they are also biochemically interchangeable: GLP-1 can be substituted for LIN-12-mediated events and vice versa (Fitzgerald et al., 1993). They also have some overlapping or redundant roles, as *lin-12(0) glp-1(0)* double mutants display a highly penetrant larval lethality phenotype, a different phenotype than either single mutant (Lambie and Kimble, 1991). Therefore, if PUF-8 is a general negative regulator of Notch signalling, then mutations in *puf-8* may also affect *lin-12*-mediated cell fate decisions.

5.1 AC/VU Decision

One well-studied *lin-12*-mediated event is the anchor cell (AC)/ventral uterine precursor cell (VU) decision, a developmental decision in early vulval development (Figure 5.1) (Seydoux and Greenwald, 1989). In brief, the AC/VU decision begins in two equivalent cells, Z1.ppp and Z4.aaa, with both cells expressing both LIN-12 and LAG-2

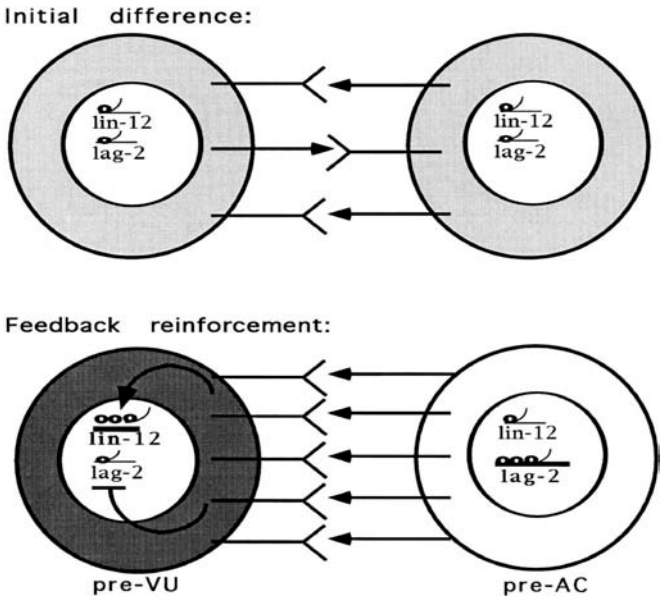

Figure 5.1. AC/VU Decision.

The AC/VU decision begins with two equivalent cells, each which has the potential of forming the AC or VU. These two cells interact with each other and eventually one cell produces a different level of LIN-12 or LAG-2. This random small difference in ligand or receptor activity is amplified by feedback mechanisms (bottom) that involve differential transcription of the genes encoding the ligand (LAG-2*)* and the receptor (LIN-12*)*. Figure adapted from (Greenwald, 1998).

(the Notch ligand). Through a feedback mechanism, one cell begins to express higher levels of LIN-12 and stops expressing LAG-2, while the other cells begins expressing more LAG-2 and stops expressing LIN-12 (Seydoux and Greenwald, 1989; Wilkinson et al., 1994). In the end, the cell expressing LIN-12 becomes the VU, whereas the cell expressing LAG-2 becomes the AC (Kimble and Hirsh, 1979). Both Z1.ppp and Z4.aaa can become the AC or VU, and it is random as to which cell adopts which fate; however, only one of the two cells will take on a given fate. The AC is a terminally differentiated cell required for various stages of vulva development, whereas the VU cell divides to form cells of the ventral uterus (Seydoux and Greenwald, 1989; Sternberg, 2005, Sulston and Horvitz, 1977).

To investigate whether PUF-8 negatively regulates Notch signalling during the AC/VU decision, a partial lf allele of *lin-12*, *ar170*, was used to construct double mutant strains with *puf-8*. The *lin-12(ar170)* mutation causes 73% of animals to produce two ACs at 20°C (Hubbard et al., 1996). In order to visualize the AC, *arIs51[cdh-3::gfp]* was included in this strain (Hubbard et al., 1996). If *puf-8* is a general negative regulator of Notch signalling, then *puf-8(0)* mutants should suppress (i.e., decrease) the proportion of *lin-12(ar170)* animals with two ACs. The number of *puf-8(oz192); lin-12(ar170); arIs51* animals with 2 AC's was not significantly different from the control strain (Table 5.1). This suggests that *puf-8* does not function as a negative regulator of *lin-12/*Notch signalling during the AC/VU decision.

Table 5.1. Mutations in *puf-8* do not affect *lin-12(ar170)* during the AC/VU decision

Genotype	**Phenotype[c]**	**N[d]**
lin-12(ar170) [b]	46% 2AC, 54% 1AC	151
puf-8; lin-12(ar170)[a]	44% 2AC, 56% 1AC	144

[a] Actual genotype: *puf-8(oz192) unc-4(e120); unc-32(e189) lin-12(ar170); arIs51*[*cdh-3::gfp*]

[b] Actual genotype: *unc-4(e120); unc-32(e189) lin-12(ar170); arIs51*[*cdh-3::gfp*]

[c] Due to the presence of *arIs51*, anchor cells (AC) expressed GFP. The number of ACs were scored in L2-L3 animals under fluorescent microscopy.

[d] number of animals analyzed

5.2 Specification of VPCs

Another developmental event requiring *lin-12* is during the specification of the vulva precursor cells (VPCs). Six VPCs are involved in the development of the *C. elegans* hermaphrodite vulva; each of the six VPCs develops one of three distinct fates (1°, 2°, or 3°) (Sternberg and Horvitz, 1986). Specifically, LIN-12 is required for the lateral signalling that specifies the 2° VPCs and inhibits the 1° VPC fates (Figure 5.2) (Sternberg and Horvitz, 1989). The 1° and 2° VPCs go on to divide and form the cells of the vulva, whereas the 3° VPC fate is to produce non-vulva epidermal cells that fuse with the large hypodermal synctium, hyp7 (Sulston and Horvitz, 1977).

In order to establish if *puf-8* negatively regulates Notch signalling during the VPC specification lateral signalling event, *puf-8(oz192); lin-12(n302)* animals were generated. The *lin-12(n302)* mutant is a vulva-less weak hypermorph: 99% of *lin-12(n302)* animals lack an anchor cell (AC) and thus cannot produce the 1° VPC necessary to form the vulva (Greenwald et al., 1981). However, a low percentage (<1%) of *lin-12(n302)* animals with an AC have a multivulva (Muv) phenotype, because the AC presence induces the 1° fate (de Souza et al., 2007). Additionally, *lin-12(n302)* animals have insufficient constitutive *lin-12* activity and, thus, cannot support the lateral signalling to promote the 2° VPC fates (Greenwald et al., 1981; Sundaram and Greenwald, 1993); however, due to the low level of constitutive Notch signalling, *lin-12(n302)* functions as a sensitized background for increases in 2° VPC formation. As a result all VPCs adopt the

Figure 5.2. The inductive and lateral signalling pathways for vulva development. The red arrows indicated the inductive EGFR/RAS/MAPK signalling pathway from the anchor cell (AC). The AC sends a signal via LIN-3, the EGF ligand, this signal is recognized by LET-23, the EGFR on the P6.p cell. This begins the signal cascade through LET-60 (RAS), MPK-1 (MAPK) and other components. In addition to determining the 1° VPC fate (P6.p), this pathway also represses the 2° VPC fate, by repressing *lin-12* expression in this cell. The blue arrows represent the LIN-12/Notch lateral signalling pathway, where the dsl (Delta/Serrate/LAG-2) Notch ligand binds to the LIN-12/Notch receptor. Components of this pathway repress the LET-23 signalling in the P5.p and P7.p, preventing the 1° VPC fate from occurring in the 2° VPCs. Figure adapted from (Yoo and Greenwald, 2005).

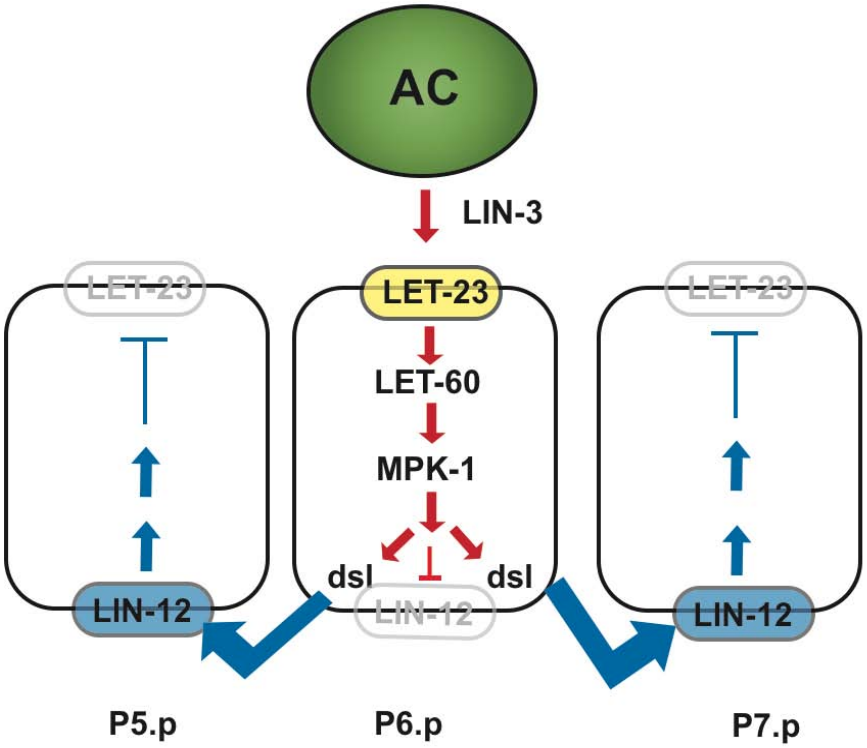
AC
LIN-3
LET-23
LET-23
LET-23
LET-60
MPK-1
dsl
dsl
LIN-12
LIN-12
LIN-12
P5.p
P6.p
P7.p

3° fate, forming hypodermal cells. Without a vulva, embryos develop inside the hermaphrodite, producing the "bag of worms" phenotype (Ferguson and Horvitz, 1985). If *puf-8* functions as a general negative regulator of Notch signalling then *puf-8(oz192); lin-12(n302)* double mutants should show increased levels of LIN-12/Notch signalling. Increased levels of LIN-12, due to loss of a negative regulator, have been shown to cause all six VPCs to adopt the 2° fate and generate multiple psuedovulvae (also called Muv) (de Souza et al., 2007; Yoo and Greenwald, 2005). In *puf-8(oz192); lin-12(n302)* animals, enhancement of the low penetrant Muv phenotype was observed (Figure 5.3, Table 5.2). Unlike the results from the AC/VU decision, this result suggests that *puf-8* may be a negative regulator of *lin-12*. However, this result is complicated by the fact that *puf-8* also has a role during vulva development (see below, section 5.3).

5.3 *puf-8's* Role During Vulva Development

In addition to *puf-8's* roles in the germ line, a role for *puf-8* in the soma has also been identified. Specifically, PUF-8 restricts the temporal competency of vulva cells by promoting the fusion of the uninduced 3° cells with hyp7 (Walser et al., 2006). This is based on the finding that *puf-8* mutants show delayed fusion of 3° VPCs (Walser et al., 2006). As well, when *puf-8* mutants were combined with mutations in *gap-1*, a negative regulator of the inductive EGFR/RAS/MAPK pathway, *puf-8; gap-1* animals produced the Muv phenotype (Walser et al., 2006), similar to the phenotype of *puf-8(oz192); lin-12(n302)* animals. The formation of Muvs was suggested to be due to the prolonged

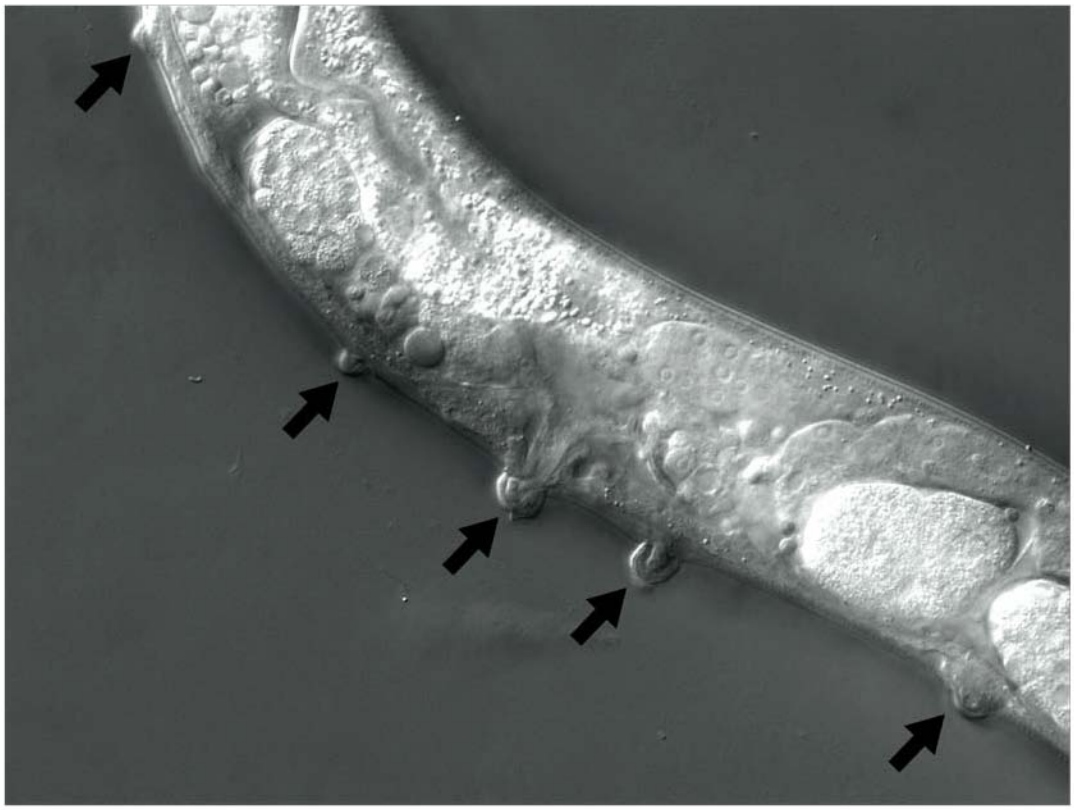

Figure 5.3. *puf-8(q725); lin-12(n302)* double mutant Muv phenotype.

This *puf-8(q725); lin-12(n302)* double mutant has five psuedovulvae (arrows); vulval-like protrusions on the ventral epithermal surface of the animal. Since this animal has multiple pseudovulvae, the phenotype of this animal is referred to as Muv. The number of pseudovulvae in a *puf-8(q725); lin-12(n302)* double mutant ranges from 1-5. DIC image.

Table 5.2. Mutations in *puf-8* enhance the *lin-12(n302)* Muv phenotype

Genotype	**Percentage of Muv[a]**	**N[e]**
lin-12(n302)[b]	2%	630
puf-8[c]	0%	75
puf-8; lin-12(n302)[d]	35%	108

All strains maintained at 20°C.

[a] Muv = Multiple-Vulva; 1 or more pseudovulva

[b] Actual genotype: *lin-12(n302)*

[c] Actual genotype: *puf-8(oz192)*

[d] Actual genotype: *puf-8(oz192); lin-12(n302)*

[e] number of animals analyzed

exposure of the 3° cells to the inductive signal as a result of the delay in cell fusion (Walser et al., 2006). These results suggest that the Muvs in *puf-8(oz192); lin-12(n302)* animals may also be due to a delay in 3° cell fusion and not due to an increase in Notch signalling, through the loss of the *puf-8* negative regulator. To determine the nature of the Muvs in *puf-8(oz192); lin-12(n302),* a cell fusion defective mutant, *eff-1(hy21),* was combined with *lin-12(n302)* animals. If defects in cell fusion, in combination with mutations in *lin-12,* are also able to produce multiple pseudovulvae, this could suggest that the Muv phenotype in *puf-8(oz192); lin-12(n302)* animals is due to the *puf-8* mutant 3° cell fusion delay and not due to increased Notch signalling through loss of a negative regulator (*puf-8)*. *eff-1(hy21)* animals are unable to undergo cell fusion; in 2% of *eff-1(hy21)* mutant hermaphrodites, multiple pseudovulva are produced (Mohler et al., 2002), showing that fusion defects do have an influence on vulva cell fates. 78% of *eff-1(hy21); lin-12(n302)* animals are Muv, characterized by 1 or more pseudovulvae, as compared to 1-2% in single mutant animals (Table 5.3). This suggests that the Muv phenotype seen in *puf-8(oz192); lin-12(n302)* animals is likely due to the 3° cells being present longer and receiving more signalling from *lin-12*. Due to PUF-8's role during vulva development, it is difficult to determine if PUF-8 functions as a negative regulator of *lin-12* during the VPC specification lateral signalling event.

Table 5.3. Cell fusion mutants also enhance the *lin-12(n302)* Muv phenotype

Genotype	**Phenotype**	**N[h]**
eff-1[c]	2% Muv[a], 1% Muv[b]	784[a], 82[b]
lin-12(n302)[d]	2% Muv[f]	630
eff-1; lin12(n302)[e]	78% Muv[g]	120

All strains maintained at 20°C.

[a] data from (Mohler et al, 2002); 2% of *eff-1(hy21)* (n= 784) single mutants form 1 to 2 psuedovulvae.

[b] Personal data. In addition to the 1% Muv phenotype, *eff-1(hy21)* (n= 82) single mutants showed the following: 26% had protruding vulva, 1% had an exploding vulva, 4% has dorsal hypodermal protrusions.

[c] Actual genotype: *eff-1(hy21)*

[d] Actual genotype: *lin12(n302)*

[e] Actual genotype: *eff-1(hy21); lin12(n302)*

[f] the number of pseudovulva produced by *lin-12(n302)* single mutants ranges from 1 to 2.

[g] The number of pseudovulva produced by *eff-1; lin-12* double mutants ranges from 1 to 5; 45% have a 1 pseudovulva, 21% have 2 pseudovulvae, 10% have 3 pseudovulvae, 0.8% have 4 pseudovulvae and 0.8% have 5 pseudovulvae.

[h] number of animals analyzed

5.4 *puf-8's* Interaction with *lin-12 glp-1* Double Mutants

The results from sections 5.1-5.3 suggest that PUF-8 likely does not negatively regulate *lin-12* during two specific *lin-12*-mediated events. As one final experiment to test if *puf-8* is a general negative regulator of Notch signalling, *puf-8* mutants were combined with mutants that have a reduction of both Notch receptors. *lin-12(q269) glp-1(q231)* double mutant animals exhibit an L1 arrest phenotype (Lambie and Kimble, 1991). If PUF-8 is a general negative regulator of Notch signalling, then *puf-8* mutants should suppress the L1 arrest *lin-12(q269) glp-1(q231)* phenotype. In *puf-8(q725); lin-12(q269) glp-1(q231)* triple mutant animals, the L1 arrest phenotype occurs similar to what is observed in the *lin-12 glp-1* double mutants (Table 5.4). In addition to L1 arrest, *puf-8(q725); lin-12(q269) glp-1(q231)/unc-32* animals also show a high percentage of embryonic lethality (Table 5.4). *puf-8; glp-1(q231)* double mutants show a Mel (Maternal-effect Embryonic Lethal) phenotype (Wilson-Berry, 1998), which may be the reason for the 19% embryonic lethality in *puf-8(q725); lin-12(q269) glp-1(q231)/unc-32*. However, the number of L1 arrest plus embryonic lethality (18%+19%= 37%) surpasses the normal expected Mendelian ratio of 25% of *puf-8(q725); lin-12(q269) glp-1(q231)/unc-32* animals, which should show such defects, suggesting that some of these defects maybe occurring in heterozygous animals. Since mutations in *puf-8* were unable to suppress the L1 arrest phenotype, PUF-8 is likely not a general negative regulator of Notch signalling. *teg-4*, identified in the same screen as *puf-8* (*teg* screen), also does not

Table 5.4. *puf-8* does not suppress the *lin-12(q269) glp-1(q231)* phenotype

Genotype	**% L1 arrest[a]**	**% Embryonic lethality[b]**	**N[c]**
lin-12(q269) glp-1(q231)/ unc-32[d]	16%	0.3%	341
puf-8; lin-12(q269) glp-1(q231)/ unc-32[e]	18%	19%	188

All strains maintained at 20°C

[a] Homozygous *lin-12 glp-1* double mutants arrest at Larval stage 1 (L1). Additionally, the heads and nose of these animals are twisted backwards.

[b] Embryonic lethality was scored by counting the number of embryos that did not hatch.

[c] the number of heterozygous animals screened

[d] Actual genotype: *lin-12(q269) glp-1(q231)/ unc-32(e189)*

[e] Actual genotype: *puf-8(q725); lin-12(q269) glp-1(q231)/ unc-32(e189)*

influence *lin-12*-mediated events (Mantina et al., 2009). Therefore, PUF-8 may negatively regulate Notch signalling only in the context of the mitosis vs. meiosis decision in germ line. Alternatively, PUF-8 may negatively regulate proliferation through a parallel pathway.

Chapter Six: **Analysis of PUF-8's Germline Expression**

6.1 PUF-8's Expression Pattern is Consistent with a Role in Regulating the Mitosis vs. Meiosis Decision

In addition to the genetic approaches, analysis of the PUF-8 protein expression pattern will greatly assist in determining how *puf-8* functions as a negative regulator of germline proliferation. Using northern analysis, Subramanium and Seydoux observed that *puf-8* mRNA is found primarily in the germ line (Subramaniam and Seydoux, 2003). Furthermore, whole mount *in situ* hybridization reveals that *puf-8* mRNA is present in the distal to loop regions of the germ line (Kohara lab NEXTDB: Nematode Expression Pattern DataBase ver. 4). Unfortunately, no antibody has been successfully raised against the PUF-8 protein (see Appendix A). Thus, an alternative strategy, using integrated transgenic arrays has been the method of choice to explore the expression pattern of the PUF-8 protein.

Recent work by Ariz *et al* 2009, showed that PUF-8::GFP is expressed highest in the distal mitotic cells and progressively less expression is observed in the more proximal cells. This *puf-8::gfp* integrant (called *kpIs*) was derived from biolistic transformation (Ariz et al., 2009), an integration procedure that has been shown to generate multiple copies of transgenes and can disrupt endogenous genes at the site of integration (Frokjaer-Jensen et al., 2008; Praitis et al., 2001). The level of expression produced from multiple copies of an integrated transgene typically results in a higher

level of expression when compared to the expression level of the endogenous gene (Frokjaer-Jensen et al., 2008).

Since it is ideal that the endogenous level of PUF-8 be determined, another *puf-8::gfp* transgenic line (called ugSi1) was constructed using the recently published Mos1-mediated Single-Copy Insertion (MosSCI) direct method protocol (see Chapter 2, sections 2.15-2.17 for construction details and below for summary of protocol) (Frokjaer-Jensen et al., 2008). The MosSCI strategy is an excellent integration protocol as transgenes are inserted into defined chromosome locations, in single copy, and the procedure is far less laborious in comparison to biolistic transformation (Frokjaer-Jensen et al., 2008). An important distinction between kpIs and ugSi1 strains is that ugSi1 also contains a TAP tag (that consists of an HA epitope, 8X His tag and a Myc tag) (Polanowska et al., 2004), which provides additional protein recognition motifs for biochemical isolation studies.

6.1.1 Summary of the Construction and Integration Strategies Used to Generate ugSi1

The foundation of the MosSCI integration technique is based on the mosTIC (MOS1 excision-induced Transgene-Instructed gene conversion) protocol (Robert and Bessereau, 2007; Robert et al., 2008), which uses the *Drosophila* Mos1 element to introduce single-copy transposon insertions into the *C. elegans* genome. The Jorgensen lab further refined this strategy by targeting transgenes to the Mos1 element positioned

in a defined chromosomal locus (strains: EG5003 and EG4322) (Frokjaer-Jensen et al., 2008).

In order to create an integrated PUF-8::GFP::TAP expressing line, a MosSCI targeting vector was first generated. This involved cloning *puf-8::gfp::tap + unc-119(+)* from the pDH147 plasmid (Table 2.1) into the pCFJ178 targeting plasmid (addgene), generating the pDH173 plasmid (Table 2.1). The pCFJ178 plasmid contains the left and right homology regions that correspond to the regions flanking the Mos1 element (*cxTi10882*) in the chromosome IV strain EG5003 (*unc-119(ed3); cxTi10882 IV*) (www.cbs.umn.edu/CGC). The pDH173 plasmid, along with selection marker plasmids and the Mos1 transposase expression plasmid, were then injected into young adult EG5003 animals. Successful injections were monitored in the progeny of the injected animals by the presence of wild-type animals (i.e., rescue of the *unc-119(ed3)* mutant). The F1 generation typically contains only extrachromosomal arrays rather than integrants. Extrachromosomal arrays can be identified based on the presence of the selection marker plasmids, which express fluorescent mCherry in specific tissues within the animal.

Integrant strains were produced when the Mos1 transposase was expressed, under the control of the germline-specific promoter *glh-2*, which results in the excision of the Mos1 element from the defined, non-coding location within chromosome IV, generating a double-strand break. The break was then repaired using the chromosome IV homology regions found within the pDH173 extrachromosomal array, thus, bringing

about the integration of the *puf-8::gfp::tap* + *unc-119(+)* fragment in place of the Mos1 element. To aid in the identification of these rare integrants, successful injection plates were starved, eliminating all *unc-119(ed3)* animals (i.e., animals that do not contain the pDH173 extrachromosomal array), as they are unable to enter dauer (Maduro and Pilgrim, 1995). Using the MosSCI procedure, successful integration typically occurs within ~19% (26/138) of the F2 or F3 rescued animals (Frokjaer-Jensen et al., 2008). However, with the pDH173 targeting plasmid, integration only occurred within ~1.4% (1/69) of the F2/F3 rescued animals. At this time, it is unclear why the integration rate of the pDH173 targeting plasmid is so low. In an attempt to produce more *puf-8::gfp::tap* lines, generation of an alternative *puf-8::gfp::tap* MosSCI targeting vector is currently underway (discussed later in this chapter). To differentiate between integrants and arrays, the animals were screened for the absence of the selection markers (i.e., presence of fluorescent mCherry). The markers are not copied into the targeted integration; thus, integrants will not express mCherry (Frokjaer-Jensen et al., 2008). Following identification of an integrant, homozygous lines were generated and PCR was performed to verify the correct genomic position of the insert (see Chapter 2, section 2.18).

6.1.2 Functional Analysis of the ugSi1(puf-8::gfp::tap) *Strain*

To establish if ugSi1(PUF-8::GFP::TAP) functions like endogenous PUF-8, rescue strains were constructed. At 25°C, *puf-8* single mutants have two main germline

defects: a proportion of the animals undergo dedifferentiation of their primary spermatocytes, while another proportion have small semi-functional germ lines (Table 3.4) (Subramaniam and Seydoux, 2003). In *puf-8(oz192* or *q725); ugSi1* animals, maintained at 25°C, wild-type germ lines are formed (Table 6.1). This result suggests that ugSi1 is able to rescue the temperature sensitive *puf-8* defect. In addition to the restrictive temperature (25°C) phenotype, *puf-8* single mutants also show a mild defect at permissive temperatures (15-20°C): *puf-8* single mutants have a shorter proliferative zone that contains fewer mitotic cells than wild-type (N2) animals (Table 3.3) (Bachorik and Kimble, 2005; Subramaniam and Seydoux, 2003). In *puf-8(oz192* or *q725); ugSi1* animals, the length and volume of the mitotic zone is only partially rescued (Table 6.2, Table 6.3). With respect to the length of the mitotic zone (gcd) between the *puf-8* single mutant and *puf-8(0); ugSi1* rescue strain, the *P* value for a two-tailed *t* test was $5.76X10^{-3}$, which suggests that the length of the mitotic zone in the rescue strain was statistically longer than the *puf-8* mutant (Figure 6.1). With respect to the volume of the mitotic zone (gcv) between the *puf-8* single mutant and the *puf-8(0); ugSi1* rescue strain, the high *P* value of 0.11 indicates that the differences between mitotic zone cell volume is not statistically significant (Figure 6.2). Since the *puf-8(0); ugSi1* rescue strain's mitotic zone is statistically longer than *puf-8* single mutants, ugSi1 may partially rescue the *puf-8* defect. However, since the *puf-8; ugSi1* rescue strain does not resemble N2, with respect to mitotic zone length and volume (Figure 6.1, Figure 6.2), *puf-8; ugSi1* does not completely rescue the *puf-8* mutant smaller mitotic zone phenotype.

Table 6.1. Rescue of the *puf-8* single mutant temperature sensitive defect at 25°C

Genotype	**Phenotype[a]**	**N[e]**
N2	Wild-type	39
puf-8[b]	25% Pro tumours, 75% smaller than normal germ lines	73
puf-8[b]*; ugSi1*[c]	Wild-type	35
puf-8[b]*; kpIs*[d]	Wild-type	29

[a] phenotypes were analyzed at 25°C

[b] *puf-8(q725)*

[c] *ugSi1* = mosSCI integrated *puf-8::gfp::tap* LGIV

[d] *kpIs* = biolistic transformation *puf-8::gfp*

[e] number of animals analyzed

Table 6.2. Rescue of the *puf-8* mutant small mitotic zone phenotype using germ cell diameter

Genotype	**Size of mitotic zone (in gcd) [a]**	**N[f]**
N2	19 ± 3.6	17
puf-8[b]	15[e], 13 ± 1.1	34[e], 11
puf-8; ugSi1[c]	16 ± 2.4	15
puf-8; kpIs[d]	17± 2.7	11

All strains maintained at 20°C

[a] The size of the mitotic zone was determined by counting the number of germ cell diameters (gcd) until the first transition zone cell. This was done using dissected gonads probed with αREC-8 and αHIM-3 antibodies. The first HIM-3 positive meiotic cell represented the beginning of the transition zone. For each genotype, the average number of gcd's and the standard deviation was determined.

[b] actual genotype: *puf-8(q725)*

[c] actual genotype: *puf-8(q725); ugSi1(puf::gfp::tap)* IV (MosSCI integration)

[d] actual genotype: *puf-8(q725); kpIs(puf::gfp)* integrated via biolistic transformation

[e] data from (Bachorik and Kimble, 2005)

[f] number of gonad arms analyzed

Table 6.3. Rescue of the *puf-8* mutant small mitotic zone phenotype using germ cell volume

Genotype	**Mitotic zone size (in gcv)[a]**	**N[d]**
N2	227 ± 26.1	10
puf-8[b]	153 ± 17.3	8
puf-8; ugSi1[c]	169 ± 22.0	11

All strains were maintained at 20°C

[a] The size of the mitotic zone was determined by counting the total number of mitotic germ cells, referred to here as the germ cell volume (gcv). This was done using dissected gonads probed with αREC-8 and αHIM-3 antibodies. The total number of REC-8 positive cells, up until the first HIM-3 positive cells, was counted using Z-stacked images. The mitotic cells in each gonad arm were counted at least two times. For each genotype, the average number of gcv's and the standard deviation was determined

[b] actual genotype: *puf-8(q725)*

[c] actual genotype: *puf-8(q725); ugSi1(puf::gfp::tap)* IV (MosSCI integration)

[d] number of gonad arms analyzed

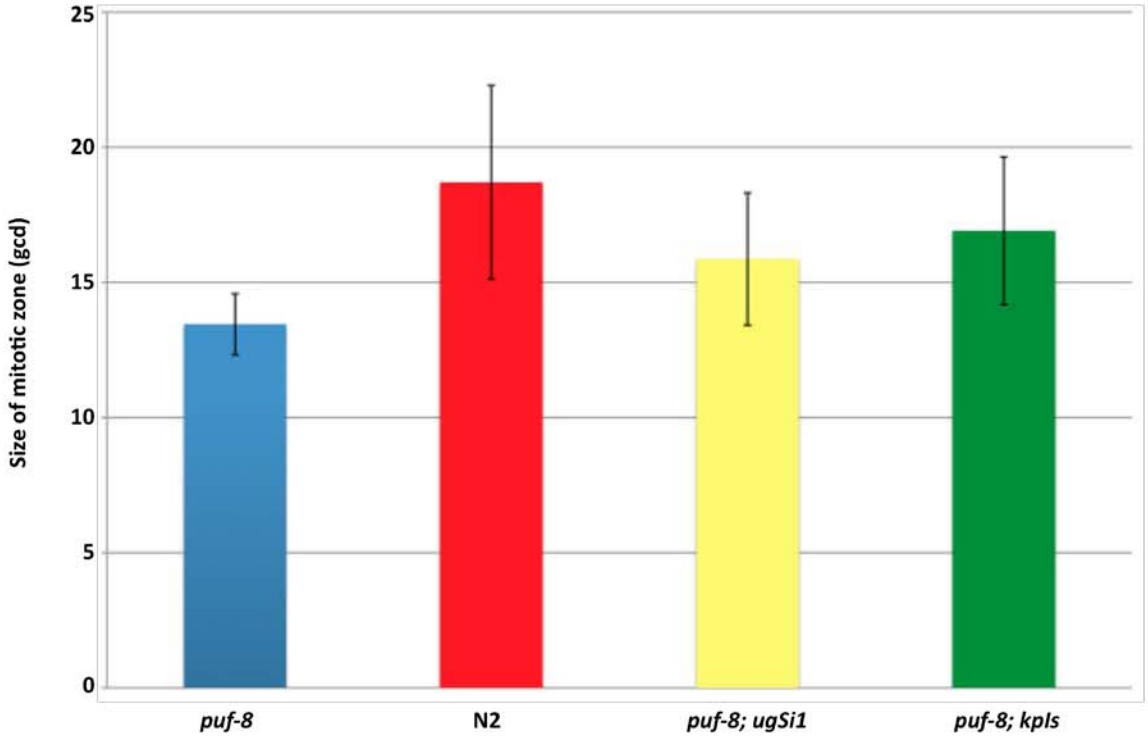

Figure 6.1. Graph of the average mitotic zone sizes, in germ cell diameter (gcd), for *puf-8* single mutants, wild-type (N2) and rescue strains.

This graph was generated from the data from Table 6.2. The *P* values for two-tailed *t* test are as follows:

puf-8 mutant vs. *puf-8; ugSi1* rescue strain $P< 5.76X10^{-3}$

puf-8 mutant vs. *puf-8; kpIs* rescue strain $P< 9.52X10^{-4}$

puf-8 mutant vs. N2, $P< 7.74X10^{-5}$

N2 vs. *puf-8; ugSi1* rescue strain, $P< 1.50X10^{-2}$

N2 vs. *puf-8; kpIs* rescue strain, $P< 0.17$

Error bars = 1 SD.

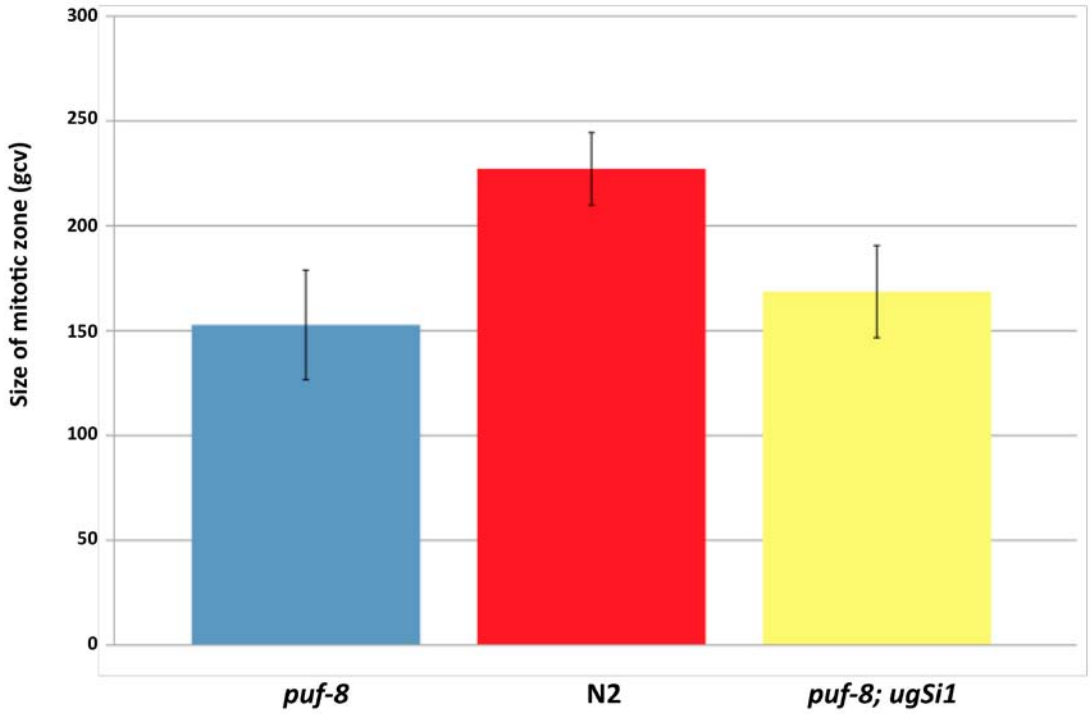

Figure 6.2. Graph of the average mitotic zone sizes, in germ cell volume (gcv), for *puf-8* single mutants, wild-type (N2) and *puf-8; ugSi1*.

This graph was generated from the data from Table 6.3. For *puf-8* mutant vs. *puf-8; ugSi1*, $P < 0.11$ two-tailed *t* test. For single mutant vs. N2, $P < 3.44 \times 10^{-6}$ two-tailed *t* test. For N2 vs. *puf-8; ugSi1*, $P < 2.21 \times 10^{-5}$ two-tailed *t* test. Error bars = 1 SD

In addition to the *puf-8* single mutant phenotype, *ugSi1* was also tested for rescue of the *puf-8(0); glp-1(gf)* tumourous phenotype. In the majority of *puf-8(oz192* or *q725); glp-1(ar202); ugSi1* animals raised at 15°C, a dramatic rescue of the tumourous phenotype was observed; the presence of ugSi1 caused 71-83% of *puf-8(oz192* or *q725); glp-1(ar202)* animals to undergo varying degrees of differentiation vs. 0% for controls (Table 6.4). Of the animals that showed germ cell differentiation, 8% of *puf-8(oz192); glp-1(ar202); ugSi1* animals were self-fertile, capable of producing sperm, oocytes and embryos at 15°C. In other words, complete rescue of the tumourous phenotype was observed in 8% of *puf-8(oz192); glp-1(ar202); ugSi1* animals.

Since ugSi1 was not able to fully rescue all *puf-8* single mutant phenotypes or the *puf-8(0); glp-1(gf)* tumourous phenotype, PUF-8::GFP::TAP protein does not completely recapitulate endogenous PUF-8 protein function. One possible reason could be due to the size and location of the attached GFP molecule. GFP is ~28kDa, which is over half the size of the total PUF-8 protein (~59kDa). As well, the GFP molecule is located at the C-terminus of the protein, close to the last PUF repeat, which may interfere with the PUF domain RNA-binding function of the protein. Alternatively, another possible reason for the reduced functionality of ugSi1 could be due to the chromosomal position of the integrant. It is possible that the integration site could be interfering with the expression of *puf-8::gfp* potentially via epigenetic regulation.

Table 6.4. Rescue of the *puf-8(0); glp-1(gf)* tumourous phenotype

All strains maintained at 15°C

[a] The percentage of gonad arms showing differentiation was determined through either DIC of whole animals or through gonad dissections. Gonad arms showing any significant population of meiotic cells was included in the count. Further characterization of the degree of differentiation is shown below for each genotype.

[b] of the 83% of *puf-8(q725); glp-1; ugSi1* animals that showed differentiation, the following distribution of differentiation was observed: 79% had just early meiotic cells, 12% had oocytes or oocyte-like cells, 5% had sperm and oocytes, 2% had just sperm and 2% were wild-type.

[c] of the 71% of *puf-8(oz192); glp-1; ugSi1* animals that showed differentiation, the following distribution of differentiation was observed: 35% had just early meiotic cells, 40% had just oocytes or oocyte-like cells, 5% had sperm and oocytes, 12% had just sperm and 8% were wild-type.

[d] all *puf-8; glp-1; kpIs* animals showed differentiation. The distribution of the differentiation included: 10% had small dysfunctional germ lines (no embryos), 22% had sperm and oocytes (but no embryos), 38% had wild-type distribution of differentiation but cells were not normal, 30% were wild-type.

[e] Actual genotype: *puf-8(q725); glp-1(ar202)*

[f] Actual genotype: *puf-8(oz192); glp-1(ar202)*

[g] Actual genotype: *puf-8(q725); glp-1(ar202); ugSi1(puf-8::gfp::tap)*

[h] Actual genotype: *puf-8(oz192); glp-1(ar202); ugSi1(puf-8::gfp::tap)*

[i] Actual genotype: *puf-8(q725); glp-1(ar202); kpIs(puf-8::gfp)*

[j] number of gonad arms analyzed

Genotype	**% of gonad arms showing differentiated cells[a]**	**N[j]**
N2	100%	19
puf-8(q725); glp-1(gf)[e]	0%	35
puf-8(oz192); glp-1(gf)[f]	0%	35
puf-8(q725); glp-1(gf); ugSi1[g]	83%[b] (2% complete rescue)	52
puf-8(oz192); glp-1(gf); ugSi1[h]	71%[c] (8% complete rescue)	87
puf-8; glp-1(gf); kpIs[i]	100%[d] (30% complete rescue)	50

To investigate the possible reasons why ugSi1 does not function identically to the endogenous PUF-8 protein, the Ariz *et al* 2009 *puf-8::gfp* C-terminus integrated transgenic line (*kpIs*), generated via biolistic transformation, was analyzed. kpIs was stated to rescue the *puf-8(zh17) unc-4(e120)* mutant phenotype (Ariz et al., 2009); however, it is unclear which of the *puf-8(zh17)* phenotypes were rescued. *puf-8(zh17)* mutants function like the *puf-8* deletion allele, *puf-8(ok302)* (Walser et al., 2006) and *puf-8(ok302)* has comparable phenotypes to *puf-8(q725)* (Bachorik and Kimble, 2005); thus, all *puf-8* mutant alleles share similar phenotypes and are thought to function as null or strong lf mutations. To investigate whether *kpIs*, which also has GFP at the C-terminus, is able to rescue the *puf-8* single mutant phenotypes and the *puf-8(0); glp-1(gf)* tumourous phenotype, rescue strains were constructed. In *puf-8(q725); kpIs* animals, the *puf-8* mutant 25°C defect is rescued (Table 6.1). As well, unlike *puf-8(q725); ugSi1*, the mitotic zones in *puf-8(q725); kpIs* animals, while smaller, are not statistically different from N2 ($P< 0.17$ two-tailed *t* test, Figure 6.1), suggesting that *kpIs* may rescue this *puf-8* single mutant phenotype. In *puf-8(0); glp-1(gf); kpIs* triple mutants, maintained at 15°C, 38% of the animals show complete rescue of the tumourous phenotype, resulting in the formation of wild-type germ lines (Table 6.4). This indicates that the kpIs(PUF-8::GFP) rescues the *puf-8* mutant phenotype slightly better than the ugSi1(PUF-8::GFP::TAP) integrant. However, both integrants are capable of partially rescuing *puf-8* mutant defects. Likely the size and location of the GFP molecule is disrupting the function of both transgenes. Based on these results, an

important future direction will be to generate a fully rescuing tagged version of PUF-8, possibly through an N-terminal FLAG tagged PUF-8 transgenic line.

6.1.3 ugSi1 Expression Pattern

Since mutations in *puf-8* enhance and suppress different *glp-1(gf)'s* and *glp-1(lf)'s* alleles, respectively, indicates that PUF-8 functions either upstream as a negative regulator of proliferation-promoting components or downstream as a positive regulator of meiotic entry (Figure 1.6). Using the expression pattern of the PUF-8::GFP integrated transgenic line should assist in determining which of these functional locations are most likely. If PUF-8 functions upstream as a negative regulator of proliferation-promoting components, then PUF-8::GFP expression should occur more predominantly within the distal proliferative/mitotic cells. While if PUF-8 functions downstream as a positive regulator of meiotic entry, then PUF-8::GFP expression should be more prevalent within the cells of the transition zone region. If this second scenario is correct, the PUF::GFP expression pattern should appear similar to the other redundant pathway proteins, such as GLD-1. GLD-1 expression is highest within the cells of the transition zone (Jones et al., 1996).

To determine the expression pattern of PUF-8, dissected gonads were screened for expression of GFP, either through direct GFP luminescence or indirectly using antibodies against GFP. Only the rescue lines were used to quantitatively establish PUF-8::GFP expression, as only the rescue lines (*puf-8(0); ugSi1)* showed consistent GFP

expression. In *ugSi1* animals alone, GFP levels were low or absent. When dissected gonads from *ugSi1* and N2 animals were compared using αGFP antibodies, the following was observed: 38% of *ugSi1* gonads had low levels of GFP expression (slightly above background), while the majority, 62% of *ugSi1* gonads had no detectable GFP expression above background. Low to absent expression was also seen with the *kpIs* integrant alone. Additionally, Ariz *et al* 2009 only used their rescue lines (*puf-8(zh17); kpIs)* to monitor expression of GFP in the *kpIs* integrant. A possible reason why only the rescue lines show consistent GFP expression could imply an auto-regulatory role for PUF-8, a role that will be explored further in the Discussion (Chapter 7) and the Future Directions chapters (Chapter 8).

Examination of young *puf-8(q725); ugSi1* adult hermaphrodites revealed that PUF-8::GFP expression was quite low at the distal end, but increased gradually up until ~12 germ cell diameters (gcd) from the DTC, at which point the protein levels gradually decreased, eventually reaching near background levels in cells that have progressed into pachytene of meiosis (~40 gcd from the DTC) (Figure 6.3). Supporting this germline immunofluorescence result was the observation that PUF-8::GFP, from whole worm extracts, can also be recognized by αGFP antibodies on Western blots (Figure 6.4). The region where PUF-8::GFP expression is highest corresponds with the part of the distal mitotic region presumed to contain transit-amplifying cells (Cinquin et al., 2010). Using genetic approaches, PUF-8 is believed to function as a negative regulator of mitosis, upstream of the *gld-1* and *gld-2* pathways; thus, the PUF-8::GFP expression pattern

coordinates well with the genetic results. The PUF-8::GFP expression pattern is consistent with PUF-8 negatively regulating proliferation in the proximal portion of the distal germ line. Potentially, high levels of PUF-8 protein in the proximal mitotic cells influence these cells in such a way that they cease proliferating and enter into meiosis. PUF-8 likely negatively regulates proliferation by repressing the translation of mRNAs that promote proliferation and/or mRNAs that inhibit meiotic entry. The identities of the mRNAs that are targeted by PUF-8 are currently unknown; however, three strategies are currently underway to identify these targets and are discussed in Chapter 8.

Figure 6.3. Quantitative analysis of PUF-8::GFP expression.

(A) Dissected *puf-8(q725); ugSi1* gonad arm stained with DAPI (blue) and probed with αGFP antibody (green). The highest level of GFP expression occurs within the distal germ line. (B) The red line on the graph illustrates the average level of expression of PUF-8::GFP found in the distal end of dissected/fixed 1 day past L4 *puf-8(q725); ugSi1* adult gonad arms incubated with αGFP antibody (n=10) (experimental details can be found: Chapter 2 section 2.18). The horizontal blue line illustrates the average background level of expression (due to non-specific antibody interactions) found in 1 day past L4 adult wild-type (N2) non-GFP expressing animals (n=10). The x-axis represents the distance from the distal end in germ cell diameters (gcd). The distal tip cell (DTC) occupies the x=0 point on the x-axis. For example, the x=20 represents 20 germ cell diameters (gcd) from the DTC. The dashed vertical line at 16 gcd is the average location of the transition zone in *puf-8(q725); ugSi1* animals, marking the point at which entry into meiosis is first observed (using DAPI nuclear morphology). Using the values determined in Cinquin *et al*. 2010, the most distal population of proliferative germ cells (up to 6-8 gcd) represent the population of true immature stem cells. The more proximal population of distal cells, up to the transition zone (dash vertical line), represent the transit-amplifying cells. Note: since *puf-8; ugSi1* animals have a slightly shorter than wild-type mitotic zone, the precise distal regions from Cinquin *et al.* 2010 may not correspond directly with this strain. (C) anti-GFP expression in the distal germ line in N2 (lower arm) vs. *puf-8(q725); ugSi1* (upper arm). Both gonad arms are from 1

day past L4 adult animals maintained at 20°C. As well, the gonads were stained in the same tube and are in the same field of view in order to visualize relative intensity (D) DAPI staining of the same gonad arms in B. In the *puf-8(q725); ugSi1* gonad arm, transition zone crescent shape nuclei can be observed (circled in white). Scale bar (for A, C and D) = 50 µM

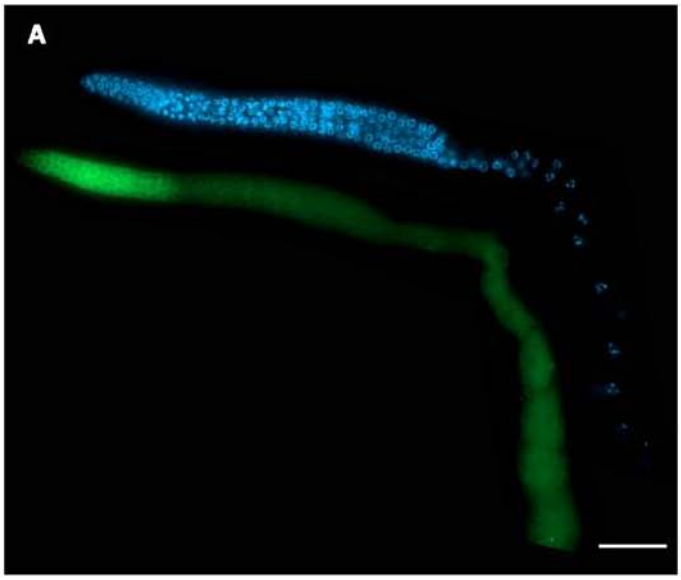
A

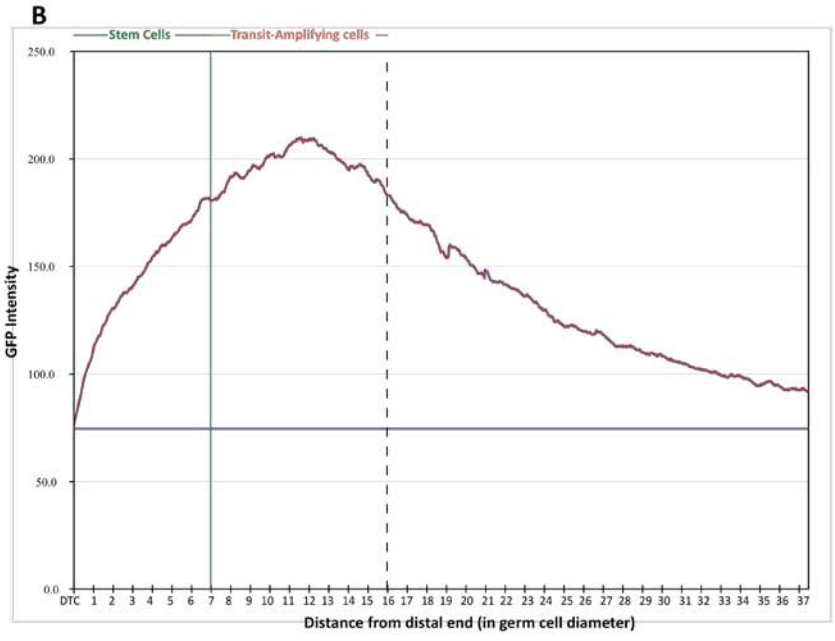
B
Stem Cells
Transit-Amplifying cells
GFP Intensity
250.0
200.0
150.0
100.0
50.0
0.0
DTC 1 2 3 4 5 6 7 8 9 10 11 12 13 14 15 16 17 18 19 20 21 22 23 24 25 26 27 28 29 30 31 32 33 34 35 36 37
Distance from distal end (in germ cell diameter)

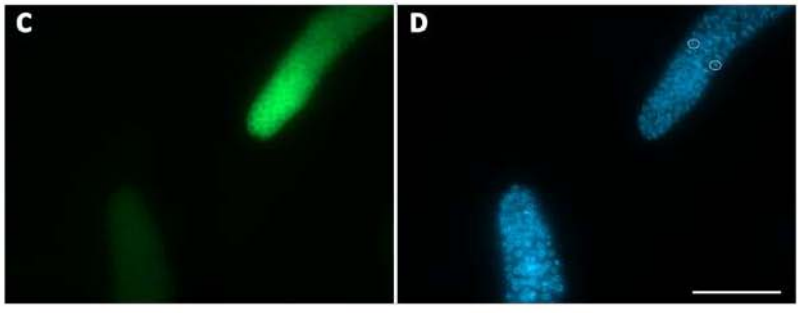
C
D

Figure 6.4. Pull-down of PUF-8::GFP protein with αGFP mAb.

PUF-8::GFP samples taken from *puf-8(q725); ugSi1(puf-8::gfp::tap)* whole worm extracts and N2 samples, from N2 whole worm extracts. First extracts were pre-cleared by incubating the samples with Protein A beads (ProtA) for 1 hr. These beads were removed and the pre-cleared extracts were then immunoprecipitated by adding 3E6 (αGFP mAb, Molecular Probes) for 2 hrs, and then incubated with fresh Protein A beads for an additional 2 hrs. The pre-cleared and IP beads were washed and then boiled for 15 min in 2X SDS sample buffer. The samples were analyzed via Western blot by probing with 1:500 goat-αGFP (Rockland), followed by secondary antibody detection with 1:100,000 α-goat HRP (Horse Radish Peroxidase, Abcam). PUF-8::GFP has a predicted molecular weight of 90.3 kDa. A band was detected at 95 kDa in the 3E6 pull-down lane with the PUF-8::GFP whole worm extracts. This band does not appear in the N2 extract or in either of the Protein A beads pre-clear lanes (ProtA lanes), suggesting that the 95 kDa band represents PUF-8::GFP. Both the heavy (55 kDa) and light (25 kDa) chain bands were also present. The ~110 kDa band represents a non-specific protein(s) bound by αGFP (Rockland) antibodies.

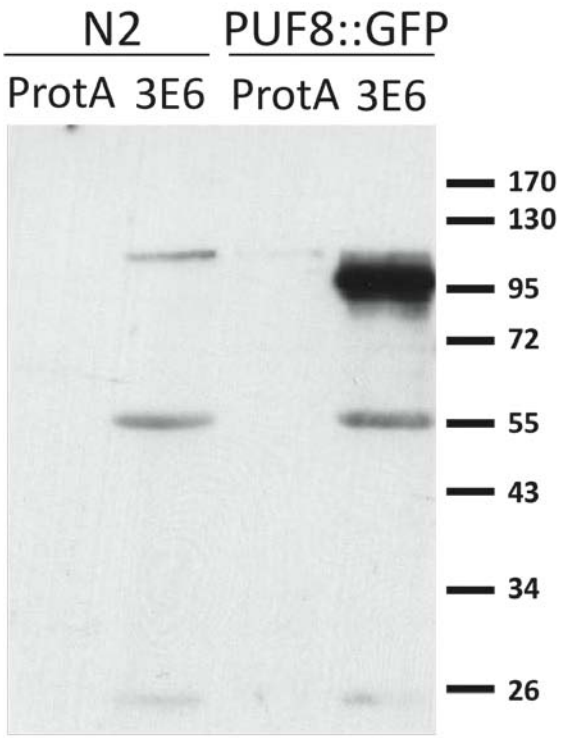
N2
PUF8::GFP
ProtA
3E6
ProtA
3E6
170
130
95
72
55
43
34
26

Chapter Seven: **Discussion and Conclusion**

Understanding the regulatory mechanisms controlling stem cell populations is an important unresolved biological problem. Using the germline stem cells (GSCs) and the transit-amplifying cells from the distal germ line of *C. elegans* as a model, this work contributes to the understanding of stem cell maintenance by characterizing the role of an important regulator called PUF-8. Through a variety of genetic approaches, PUF-8 was found to function as a negative regulator of proliferation. While PUF-8 also functions in different aspects of germline development, this work reveals that PUF-8's role as a negative regulator of proliferation is distinct from all other previously identified PUF-8 functions.

7.1 Determining the Functional Genetic Location of *puf-8* in the Mitosis vs. Meiosis Decision Pathway

Since *puf-8(0)* mutants enhance and suppress *glp-1(gf)* and *glp-1(lf)* respectively, this indicates that PUF-8 functions as either a negative regulator of proliferation or positive regulator of entry into meiosis. Using the known components of the mitosis vs. meiosis pathway as positional reference points, PUF-8 could function in one of two general regions. (1) PUF-8 could function to negatively regulate proliferation promoting components in various locations upstream of the *gld-1* and *gld-2* pathways, in the region referred to as A (Figure 7.1). (2) Alternatively, PUF-8 could function to positively regulate entry into meiosis and/or inhibit proliferation in either the *gld-1* or *gld-2*

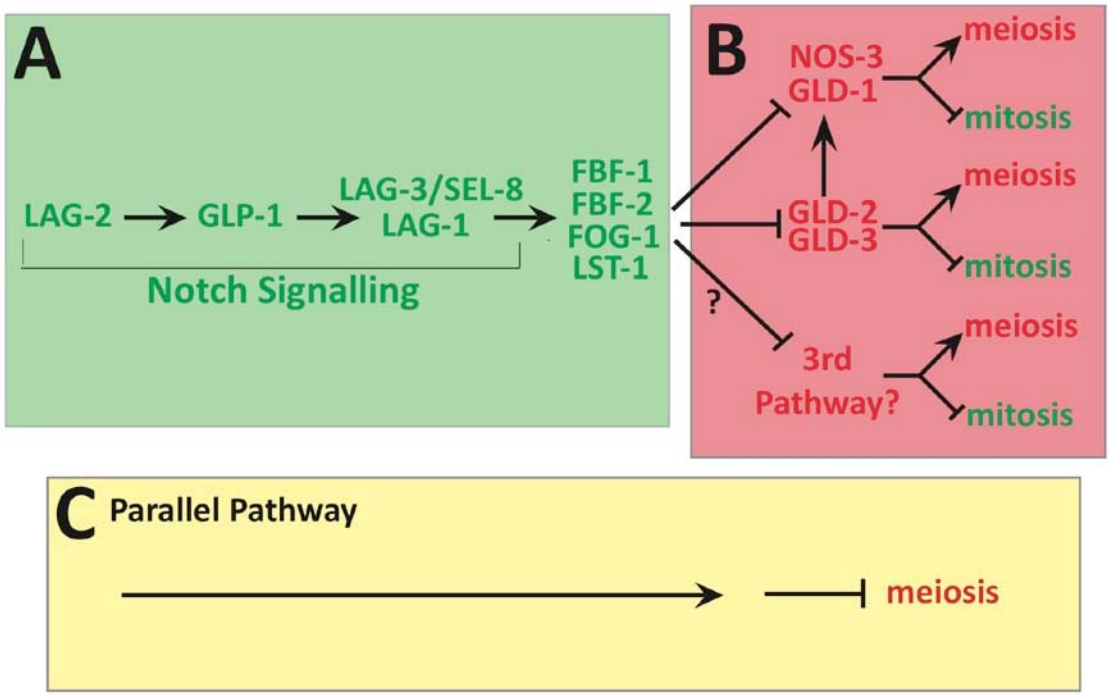

Figure 7.1. Three potential regions where PUF-8 may function.

PUF-8 may function as a negative regulator of mitosis-promoting genes (Region A). Or PUF-8 may function downstream of the FBF's (Region B); however, genetic analysis revealed that PUF-8 likely does not function in either the *gld-1* or *gld-2* pathways. A third possibility is that PUF-8 functions in a parallel pathway to the known mitosis vs. meiosis decision (Region C).

pathways, region B (Figure 7.1). In order to determine *puf-8's* functional location in the known mitosis vs. meiosis decision pathway, genetic strategies were employed.

To establish if PUF-8 functions in one of the two downstream pathways (*gld-1* or *gld-2*) to promote meiotic entry and/or inhibit proliferation, *puf-8(0)* mutants were combined individually with mutations in each of the known meiosis promoting pathway genes (*gld-1, nos-3, gld-2* and *gld-3*). Meiotic entry is controlled by two redundant pathways; one pathway includes *gld-1* and *nos-3* and the other pathway includes *gld-2* and *gld-3*. When a component in one pathway is mutated, the other pathway is sufficient to promote meiotic entry (Francis et al., 1995a; Kadyk and Kimble, 1998). However, when components from both pathways are mutated, meiotic entry is greatly affected resulting in synthetically tumourous germ lines (Kadyk and Kimble, 1998). In the germ lines of *gld-1; puf-8, puf-8 nos-3, gld-2; puf-8* or *gld-3 puf-8,* no synthetic tumours were formed (Table 4.5). This suggests that PUF-8 likely does not function in either of these downstream pathways to promote meiotic entry and/or inhibit proliferation (Region B, Figure 7.1). In comparison to the other enhancers studied in the Hansen lab, including *teg-1, teg-4* (Mantina et al., 2009)*, pas-5* (Macdonald et al., 2008) and *nos-3* (Hansen et al., 2004b), *puf-8* is the only enhancer that does not form a synthetic tumour with components from the *gld-1* and *gld-2* pathways. Thus, PUF-8 plays a unique role in the mitosis vs. meiosis decision.

Since *puf-8* does not genetically interact with either of the redundant meiosis promoting pathways, the alternative possibility is that *puf-8* functions upstream of the

gld-1 and *gld-2* pathways to negatively regulate proliferation (Region A, Figure 7.1). Germ cell proliferation is controlled predominantly by the canonical Notch signalling pathway (Figure 1.6) (Seydoux and Schedl, 2001). Downstream of Notch signalling are other proliferation promoting components that include *fbf-1, fbf-2, fog-1* and *lst-1* (Crittenden et al., 2002; Lamont et al., 2004; Thompson et al., 2005) (A. Kershner, personal communication). All four genes function redundantly to promote mitosis, at least in part, through the negative regulation of the downstream meiosis promoting pathways (this has only been conclusively shown for the *fbfs*) (Crittenden et al., 2002; Thompson et al., 2005). If PUF-8 functions as a negative regulator of proliferation then it is possible that PUF-8 negatively regulates one or more components of Notch signalling and/or the downstream proliferation promoting factors. This negative regulation could be direct or indirect.

To determine if *puf-8* functions upstream or downstream of the *fbfs*, *fbf-1 fbf-2 puf-8* triple mutants were constructed. In *fbf-1 fbf-2* double mutants, normal germline proliferation occurs during the early larval stages; however, in the adult, mitotic germ cells are not maintained and all germ cells enter into meiosis forming an average of 200 sperm per gonad arm (Glp phenotype) (Crittenden et al., 2002). In *fbf-1 fbf-2 puf-8* animals, a distal proliferation zone is present in adult germ lines followed by a proximal region filled with sperm (Figure 4.4). This result indicates that the *puf-8* mutants partially suppress the *fbf-1 fbf-2* premature entry into meiosis phenotype. The *fbf-1 fbf-2 puf-8* phenotype can be interpreted in at least two ways. One interpretation is that

since *puf-8* mutants suppress the *fbf-1 fbf-2* mutant phenotype, that *puf-8* is epistatic to the *fbfs*. In other words, *puf-8* functions downstream of *fbf-1* and *fbf-2*. However, because loss of the *fbfs* does not completely knock down germ cell proliferation (Crittenden et al., 2002), an alternative explanation for the *fbf-1 fbf-2 puf-8* phenotype is possible. A second possible interpretation is that *puf-8* functions as a negative regulator of proliferation upstream of the *fbfs*. Thus, loss of a negative regulator could increase the activity of genes that function redundantly with the *fbfs*. In the absence of the *fbfs*, *fog-1* and *lst-1* are still present to promote proliferation and could be the reason for the maintenance of proliferation zone in *fbf-1 fbf-2 puf-8* triple mutants.

If increased expression of proliferation-promoting components can cause germ cell proliferation to occur in *fbf-1 fbf-2* mutants, then increased expression of the Notch receptor (using the gf mutation, *glp-1(ar202)*) should also suppress the premature meiotic entry phenotype in *fbf-1 fbf-2* double mutants. In *fbf-1 fbf-2; glp-1(ar202)* triple mutants, proliferation is also present. This result supports the possibility that *puf-8* could function upstream of the *fbfs* as a negative regulator of proliferation. This result also confirms that increased expression of proliferation promoting components can allow proliferation to occur in the absence of the *fbfs*, supporting the observation that other components work redundantly with the *fbfs* to promote proliferation (Crittenden et al., 2002; Thompson et al., 2005).

If *puf-8* functions upstream of the *fbfs*, then loss of all genes functioning redundantly with the *fbfs* should prevent proliferation from occurring in *fbf-1 fbf-2 puf-8*

mutants. Alternatively, if *puf-8* functions downstream of the *fbfs*, then proliferation should still be possible even upon removal of the *fbfs* and associated redundant genes. Two genes that function redundantly with the *fbfs* to promote proliferation and/or inhibit meiotic entry are *fog-1* (Thompson et al., 2005) and *lst-1* (A. Kershner, personal communication). When *fog-1* was mutated in *fbf-1 fbf-2 puf-8* animals, proliferative germ cells were still present, suggesting that suppression of the meiotic entry defect still occurred. Similarly, *fog-1; fbf-1 fbf-2; glp-1(ar202)* germ lines also showed proliferation. However, when *lst-1* was mutated in *fbf-1 fbf-2 puf-8* and *fbf-1 fbf-2; glp-1(ar202)* animals, proliferation was no longer observed in adult germ lines. In *lst-1; fbf-1 fbf-2 puf-8* and *lst-1; fbf-1 fbf-2; glp-1(ar202)* adult animals, all germ cells enter into meiosis and look much like the *lst-1; fbf-1 fbf-2* triple mutants. The number of meiotic cells per gonad arm in *lst-1; fbf-1 fbf-2* (27.9 sperm/arm, n=19), *lst-1; fbf-1 fbf-2 puf-8* (28 sperm/arm, n=35) and *lst-1; fbf-1 fbf-2; glp-1(ar202)* (23 spermatocytes/arm, n=20). All three strains have meiotic germ cell numbers that are significantly less than the total number of meiotic cells in *fbf-1 fbf-2* double mutants (200 sperm/arm, n=11), suggesting that proliferation is more severely affected in the absence of both *lst-1* and the *fbfs*.

The *lst-1* results reveal some important clues about *puf-8* and the mitosis vs. meiosis decision. First, the observation that the *lst-1; fbf-1 fbf-2 puf-8* germ line is identical to the *lst-1; fbf-1 fbf-2* germ line suggests, but does not conclusively demonstrate, that *puf-8* functions upstream of *lst-1, fbf-1* and *fbf-2*. If *puf-8* functions downstream of *lst-1, fbf-1* and *fbf-2*, proliferative germ cells should have been observed

in *lst-1; fbf-1 fbf-2 puf-8* adult animals. In addition, the observation that *lst-1; fbf-1 fbf-2; glp-1(ar202)* adult animals lacked proliferative cells suggests that increases in upstream mitosis-promoting components are not sufficient to promote proliferation in the absence of *lst-1* and the *fbfs*. If *puf-8* functions upstream of the *fbf* portion of the pathway as a negative regulator of proliferation, the *lst-1; fbf-1 fbf-2; glp-1(ar202)* quadruple mutant results can explain why proliferation was not seen in *lst-1; fbf-1 fbf-2 puf-8* animals. However, it is also possible that *puf-8* may not function at all in the known mitosis vs. meiosis pathway, but rather in a putative parallel pathway to negatively regulate proliferation (Region C, Figure 7.1). One gene that has previously been proposed to function in a parallel pathway to GLP-1/Notch signalling is *atx-2* (human ATaXin related) (Maine et al., 2004). Unlike PUF-8, ATX-2 promotes proliferation. In *gld-2(0) gld-1(0); glp-1(0) atx-2(RNAi)* mutants, significantly more meiotic entry occurs in comparison to *gld-2(0) gld-1(0); glp-1(0)* triple mutants (Maine et al., 2004). Additionally, *atx-2(RNAi)* does not suppress the tumourous phenotype of a strong *glp-1(gf)* mutant, *glp-1(oz112)* (Maine et al., 2004). Together, these results suggest that ATX-2 promotes proliferation in a parallel pathway, independent of GLP-1 (Maine et al., 2004). It is possible that PUF-8 and ATX-2 may function in opposition within the same parallel pathway or may function in different parallel pathways.

7.2 *puf-8's* Role in the Mitosis vs. Meiosis Decision May Require the Presence of *glp-1(+)*

Using two different *puf-8* mutants, this work showed that *puf-8* is capable of enhancing/suppressing a variety of different *glp-1(gf)* and (*lf)* alleles. In a *glp-1(gf)* background, *puf-8* mutants enhance the over-proliferative phenotype. Alternatively, in a *glp-1(lf)* background, *puf-8* mutants partially suppress the Glp phenotype. While *puf-8* is able to enhance and suppress, gf and lf alleles of *glp-1* that still retain some *glp-1* activity, *puf-8* is not able to suppress the Glp phenotype of a *glp-1(q175)* null allele in which no functional *glp-1* is present. This may suggest that *puf-8's* role in the mitosis vs. meiosis decision relies on the presence of *glp-1(+) or* more broadly, that it relies on functional Notch signalling.

Had *puf-8* been able to suppress the *glp-1(q175)* phenotype, this would have indicated that *puf-8* was epistatic to *glp-1*. However, based on the results from other strains made with the *glp-1(null)* mutant, the lack of suppression could be interpreted in different ways. For one, mutations in *nos-3* cannot suppress the *glp-1(q175)* phenotype, even though genetic evidence favours that *nos-3* functions downstream, in the *gld-1* pathway, to promote entry into meiosis (Hansen et al., 2004b; Kraemer et al., 1999). This lack of suppression is likely due to *nos-3's* limited role, and its presence in a redundant pathway. Based on the *nos-3* findings, it is possible that *puf-8* could function downstream of *glp-1,* and that *puf-8* only has a limited or redundant role. However, the strong enhancement of *glp-1(gf)* by *puf-8(0)* makes this unlikely. Conversely, while

suppression of the premature meiotic defect was observed in *gld-1(0); glp-1(q175)*, the suppression was very weak (Francis et al., 1995b). The *gld-1(0); glp-1(q175)* result could suggest that very low levels of suppression, below the threshold of detection, may occur in *puf-8; glp-1(q175)* double mutants. Thus, the lack of suppression in *puf-8(0); glp-1(q175)* animals suggests that *puf-8* does not function downstream of *glp-1*; however, this result has caveats.

In order to determine whether *puf-8* functions upstream or downstream of *glp-1,* the integrated PUF-8::GFP transgene (ugSi1) could be used to explore the expression pattern changes in different mutant backgrounds. In *puf-8(0); glp-1(gf); ugSi1* mutants, PUF-8::GFP expression is high in proliferative germ cells and low or absent in cells undergoing meiosis (Figure 6.3). The *puf-8(0); glp-1(gf); ugSi1* expression pattern may suggest that the expression of *puf-8* is affected by the presence of GLP-1 or vice versa. To test these two scenarios, a *gld-2 gld-1* double mutant tumourous background could be used to analyze the expression pattern of PUF-8::GFP in the presence and absence of GLP-1. If PUF-8::GFP levels decrease in *gld-2(0) gld-1(0); puf-8(0); ugSi1* animals as compared to *gld-2(0) gld-1(0); puf-8(0); glp-1(0); ugSi1* animals, this could suggest that GLP-1 negatively regulates *puf-8* expression, suggesting that *puf-8* functions downstream of GLP-1 (Region A or B, Figure 7.1). However, if PUF-8::GFP expression stays the same in both mutant backgrounds, this could suggest that the expression of *puf-8* does not require the presence of GLP-1; thus, indicating that *puf-8* functions

upstream of *glp-1* (Region A, Figure 7.1) or that *puf-8* functions in a parallel pathway (Region C, Figure 7.1)

7.3 The *fog-1* and *lst-1* Results Contribute to the Overall Understanding of the Mitosis vs. Meiosis Decision

While the precise functional location of *puf-8* is still somewhat unclear, the results from the genetic analysis with *fog-1* and *lst-1* do contribute to the overall understanding of the mitosis vs. meiosis decision. The *fog-1* and *lst-1* results reveal that removal of *lst-1* more significantly affects mitosis in comparison to removal of *fog-1* in an *fbf-1 fbf-1 puf-8* or *fbf-1 fbf-2 glp-1(gf)* background. These results contradict the hypothesis that loss of *fog-1* and the *fbfs* reduce Notch signalling to the same extent as a *glp-1(null)* (Thompson et al., 2005). In *fog-1; fbf-1 fbf-2* triple mutants, only five germ cells per gonad arm are formed, which is similar to the level of proliferation in a *glp-1(null)* (Thompson et al., 2005). In *fog-1*; *fbf-1 fbf-2 puf-8* and *fog-1*; *fbf-1 fbf-2; glp-1(ar202)* animals, proliferative germ cells are still present, suggesting that loss of *fog-1* and the *fbfs* is not sufficient to prevent proliferation. Potentially, the occurrence of proliferative germ cells, in the above mutant strains, is due to the presence of wild-type *lst-1*, which due to its elevated expression level (through the loss of a negative regulator of proliferation (*puf-8)* or an increase in Notch signalling (*glp-1(gf)*) can inhibit meiotic entry and/or promote proliferation. Conversely, the presence of wild-type *fog-1*, in *lst-1; fbf-1 fbf-2 puf-8* and *lst-1; fbf-1 fbf-2*; *glp-1(ar202)* animals, is not sufficient to promote the formation of proliferative germ cells in adult germ lines. However, the

number of meiotic cells in *lst-1; fbf-1 fbf-2 puf-8* and *lst-1; fbf-1 fbf-2*; *glp-1(ar202)* is still slightly more than *glp-1(q175)* null mutants, may indicate that the presence of wild-type *fog-1* contributes to some early larval germ cell proliferation. A role for FOG-1 in the promotion of proliferation in early larvae has been suggested (Thompson et al., 2005). To test this hypothesis, it will be necessary to construct *fog-1 lst-1; fbf-1 fbf-2 puf-8* and *fog-1 lst-1; fbf-1 fbf-2; glp-1(ar202)* strains. If these quintuple mutants produce the same number of meiotic cells as *glp-1(q175)* null mutants, this would indicate that *fog-1, lst-1, fbf-1* and *fbf-2* are the only four genes that function redundantly downstream of Notch signalling to promote mitosis and/or inhibit entry into meiosis. However, if there are more cells in the quintuple mutants in comparison to *glp-1(q175)* mutants, this would suggest that additional gene(s) function redundantly with *fog-1, lst-1, fbf-1* and *fbf-2* to promote mitosis and/or inhibit entry into meiosis. Some other candidate genes include *fem-3* and *fog-3*; in *fbf-1 fbf-2; fem-3* and *fbf-1 fbf-2; fog-3* triple mutants, further enhancement of the premature entry into meiosis defect was observed (Thompson et al., 2005).

7.4 PUF-8 Regulates Germ Cell Mitosis in Two Opposing Ways

In the distal germ line, PUF-8 functions in two opposing ways to maintain the mitotic germ cell population. In this work, PUF-8 was identified as a negative regulator of proliferation; loss of *puf-8* causes increased proliferation in a *glp-1(gf)* background. Conversely, PUF-8 also promotes germ cell proliferation redundantly with MEX-3 (Ariz et

al., 2009): in *puf-8* single mutants and *puf-8; mex-3* double mutants, the size of the mitotic zone is reduced. PUF-8's ability to both promote and inhibit germ cell proliferation illustrates that PUF-8 is a key regulator in the maintenance of mitotic germ cells. However, how PUF-8 accomplishes these two opposing roles is still unknown. Other *C. elegans* PUF protein family members also have similar contrasting roles. The FBFs, in addition to their essential role in promoting germ cell proliferation, also have a nonessential role in the *gld-2/gld-3* pathway to promote entry into meiosis (Crittenden et al., 2002; Hansen and Schedl, 2006; Kimble and Crittenden, 2007). In *fbf-1 fbf-2* germ lines, GLD-1 protein levels are low, suggesting that the FBFs promote entry into meiosis by positively regulating *gld-1* expression in spermatogenic germ lines (Suh et al., 2009). Mechanistically, FBF both negatively and positively regulates *gld-1* by associating with different protein complexes that affect polyadenylation (Suh et al., 2009). It is possible that PUF-8 also accomplishes opposing roles in the distal germ line by complexing with different proteins. PUF-8's association with one complex may negatively regulate a subset of mRNAs that inhibit mitosis, while PUF-8's association with another complex may negatively regulate mitosis promoting mRNAs. Alternatively, but not necessarily mutually exclusive, PUF-8 may control mRNA targets in a concentration-dependent manner. This work shows that PUF-8's expression is low in the distal most germ cells but gradually increases and reaches highest expression in the mitotic cells ~12 germ cell diameters (gcd) from the DTC (Figure 6.3). Maybe low levels of PUF-8 are ideal to negatively regulate mRNAs that negatively regulate mitosis (i.e., PUF-8's role as a

promoter of germ cell mitosis (Ariz et al., 2009)), while high levels of PUF-8 are required to inhibit mRNAs that promote mitosis (this work). FOG-1 has been shown to have different functions based on protein concentration levels. Low levels of FOG-1 promote proliferation redundantly with the FBFs and high levels of FOG-1 direct the male fate (Thompson et al., 2005). Ultimately, in order to understand how PUF-8 functions as both a positive and negative regulator of proliferation, identification of PUF-8 mRNA targets is crucial (see Future Directions-Chapter 8).

7.5 A Conserved Role for PUF Proteins in the Maintenance of Stem Cells

Both PUF-8 and the FBFs are important regulators in the maintenance of GSCs in *C. elegans*. This PUF protein function is not restricted just to the *C. elegans* germ line. Maintenance of stem cells by PUF proteins has also been shown in a vast number of other organisms. In *Drosophila*, the absence of Pumilio causes female GSCs to prematurely differentiate as cystoblasts (Lin and Spradling, 1997a). In humans, PUM2 is expressed predominantly in human embryonic stem cells and germ cells (Moore et al., 2003). Additionally, human PUM2, in germ cells, complexes with the DAZL (Deleted in AZoospermia-Like) protein and together target mRNAs involved in growth regulation (Fox et al., 2005; Moore et al., 2003). In zebrafish, Puf-A has been implicated in the maturation of GSCs (Kuo et al., 2009). In mouse hematopoietic stem cells, both Pum1 and Pum2 are highly transcribed (Spassov and Jurecic, 2003). Mouse Pum2 is also highly expressed in male germ cells and, when mutated, *pum2(0)* animals have significantly

smaller testes (Xu et al., 2007). In the planarian species, *Dugesia japonica*, RNAi against the *DjPum* gene inhibits the formation of regenerative blastema and as a result the organism is unable to regenerate (Salvetti et al., 2005). Overwhelming evidence, from multiple organisms, supports the hypothesis that the maintenance of both somatic and GSCs is an ancestral role of PUF proteins. Therefore, the work contained in this thesis, and that which will stem from this thesis, conceive that *puf-8's* role in controlling stem cell proliferation is likely to be broadly applicable in the understanding of stem cell behaviour.

7.6 Does PUF-8 Autoregulate?

Expression studies using an integrated PUF-8::GFP transgene (*ugSi1*), revealed that GFP levels were weak or absent when *ugSi1* was analyzed in a wild-type background. However, when *ugSi1* was analyzed in a *puf-8(q725)* mutant background, consistently high GFP levels were observed in the distal germ line. One possible explanation for the observed expression pattern is that PUF-8 autoregulates. Autoregulation would allow PUF-8 the ability to control its own protein expression. In *ugSi1* animals, both PUF-8::GFP and endogenous PUF-8 will contribute to the overall expression of both proteins. In *puf-8(q725); ugSi1*, only PUF-8::GFP contributes to the level of expression; thus, higher levels of GFP were observed because only PUF-8::GFP can be detected.

Autoregulation has also been proposed for FOG-1. FOG-1 binds to specific sites, called CPEs (Cytoplasmic Polyadenylation Elements), in the 3'UTRs of target mRNAs (Jin et al., 2001). Analysis of the *fog-1* 3'UTR revealed the presence of one perfect CPE site and, through *in vitro* strategies, FOG-1 was found to bind specifically to this site (Jin et al., 2001). PUF-8 is also thought to bind to specific sites in the 3'UTR of target mRNAs (Opperman et al., 2005). To determine the mRNA sequence to which PUF-8 binds, Opperman et al. 2005 used the yeast three-hybrid system. A putative PUF-8 binding site was determined and was given the name NRE (Nanos Response Element) (Opperman et al., 2005). To investigate whether PUF-8 is capable of autoregulation, the 3'UTR of *puf-8* mRNA was analyzed for the presence of NRE's. A total of eight imperfect NRE sites were found (Figure 7.2). Experiments are currently underway to determine if autoregulation occurs with PUF-8 and descriptions of these experiments can be found in the future directions chapter.

What advantage would autoregulation provide PUF-8? Based on the PUF-8::GFP expression profile, PUF-8 is not a very highly expressed germline protein. However, based on genetic analysis, it is obvious that PUF-8 is an important protein involved in many aspects of germline development. Thus, it is possible that in order for PUF-8 to function properly in the germ line, it must be present at low levels. If this is the case, PUF-8's ability to autoregulate may be a useful strategy to keep PUF-8 protein levels low.

(A)

(B)

cccaaucaguuuuguacuauucccaacacucaacuccucacaaauguaccuuuaguuaucucaaauccgguuguu
auaccgguucuuuuuguuauucccugugcauuucuguagacagcuuaucguaauuuguaauguuacucguuuu
guaauuuuuuccuaaucuuauuuuagcauaaaaauu

(C)

uguacuauu

uguaccuuu

uguuauacc

uguuauucc

ugugcauuu

uguagacag

uguaauguu

uguaauuuu

Figure 7.2. *puf-8* 3'UTR and putative PUF-8 binding sites.

(A) a weight matrix of the PUF-8 consensus binding site from (Opperman et al., 2005). (B) the *puf-8* 3'UTR sequence. Highlighted in yellow are the eight putative PUF-8 binding sites. (C) alignment of the eight putative PUF-8 binding sites. Highlighted in green are the nucleotides that match the PUF-8 consensus sequence. Note, none of the eight sites directly match the consensus.

7.7 Conclusion

PUF-8 is an important translational regulator in the *C. elegans* germ line. In this thesis, a new role for PUF-8 was identified: PUF-8 negatively regulates proliferation in the distal germ line. Four alleles of *puf-8* (formerly *teg-2*) were identified in an enhancer screen for mutations that enhance the over-proliferative phenotype of a *glp-1* weak gf mutant (Wilson-Berry, 1998). SNP mapping, deficiency mapping, complementation, RNAi and sequencing revealed that *teg-2* was allelic to *puf-8*. The interaction that *puf-8* mutants have with *glp-1* is not allele specific: *puf-8(oz192* and *q725*) both enhance and suppress *glp-1* gf and lf alleles, respectively. *puf-8(0); glp-1(gf)* germ lines are completely tumourous and show no signs of meiotic entry during larval development. The germline tumours in *puf-8(0); glp-1(gf)* double mutants are derived from problems during the mitosis vs. meiosis decision and are not derived through the dedifferentiation of male meiotic cells or the re-entry of meiotic cells back into mitotic cells. In the mitosis vs. meiosis decision, *puf-8* does not function in either the *gld-1* or *gld-2* pathways to promote meiotic entry and/or inhibit proliferation. *puf-8* likely functions upstream of the *gld-1* and *gld-2* pathways to negatively regulate proliferation. It is also possible, but less likely, that *puf-8* may function as a negative regulator of proliferation in a parallel pathway to the known mitosis vs. meiosis pathway. *puf-8's* interaction with Notch signalling is likely to be germ line specific, as *puf-8* mutants do not influence *lin-12*-mediated events. Finally, PUF-8 is most highly expressed in the mitotic cells that are

destined for differentiation (i.e., the transit-amplifying cells), which corresponds well with PUF-8's role as a negative regulator of proliferation.

Chapter Eight: **Future Directions**

8.1 Strategies to Identify mRNA Targets of PUF-8

PUF proteins are RNA-binding proteins that bind specific sites in the 3'UTRs of mRNAs (Wickens et al., 2002). In order to better understand how PUF-8 functions as a negative regulator of proliferation upstream of the *gld-1* and *gld-2* pathways, it will be essential to identify the mRNAs that PUF-8 binds. The outcome of PUF protein binding often results in translational repression or degradation of the target mRNA (Wickens et al., 2002). Thus, when PUF-8 binds to specific mRNA targets, the hypothesis is that translation of the targets will be repressed, which will then allow germ cells to enter into meiosis. Based on this model, the potential PUF-8 targets may consist of genes that function to promote proliferation and/or genes that function to inhibit meiosis. Currently, three strategies are underway in the Hansen lab to identify PUF-8 mRNA targets.

8.1.1 A Directed RNAi Screen to Identify Potential PUF-8 Targets Genes

The first strategy to identify potential PUF-8 target genes involves screening using RNA interference (RNAi). The focus of this RNAi screen is to identify PUF-8 mRNA targets that influence the mitosis vs. meiosis decision, thus all screening is performed in *puf-8(0); glp-1(gf)* background. Using the hypothesis that PUF-8 functions as a negative regulator of proliferation upstream of *gld-1* and *gld-2*, if expression of a PUF-8 mRNA target is knocked-down, via RNAi, suppression of the *puf-8(0); glp-1(gf)* tumour and/or

the induction of meiotic entry may occur in *puf-8(0); glp-1(gf)* animals. In other words, the model is that in a *puf-8* mutant, a target gene(s) is being misexpressed, allowing for cells to remain proliferative. Knocking down the function of this gene by RNAi should suppress the tumourous phenotype of *puf-8(0); glp-1(gf)* double mutants, which may manifest phenotypically as a reduction in tumour size or may stimulate meiotic entry. To limit the effects of RNAi to the germ line and to prevent detrimental somatic phenotypes (such as larval lethality), an *rrf-1* mutant background was also included; RRF-1 is an RNA-directed RNA polymerase (Smardon et al., 2000) required for RNAi in the soma, but not in the germ line (Sijen et al., 2001). Instead of performing a genome wide RNAi screen, potential PUF-8 targets were pre-selected based on the presence of a putative PUF-8 binding site (UGU[AC][CUA][AG][UAG][AU][UGAC]) (Opperman et al., 2005) in their 3'UTRs. The 3'UTRs were analyzed and selected using the 3'UTRome database (UTRome.org). It is important to note that not all 3'UTRs of *C. elegans* mRNAs had been identified at the time of this search; thus, some potential candidates may have been missed. In total, 2068 genes were selected based on the presence of the putative PUF-8 binding site in their 3'UTR. Thus far, this screen has identified two strong candidates, *ain-2* (ALG-1 INteracting protein) and *cup-2* (Coelomocyte UPtake defective), out of the 221 genes tested so far. Work is currently underway to validate these candidates.

There are some limitations to this RNAi screen. For one, the genes were selected based on the putative PUF-8 binding site (Opperman et al., 2005) and since no bona fide

PUF-8 mRNA targets have been experimentally identified, this site may not accurately represent PUF-8's binding capacity. Additionally, there was a bias in the identification of the putative PUF-8 binding site by Opperman et al 2005, as only variations of the fly Pumilio binding site were tested. Another limitation to the gene selection strategy is the assumption that the PUF-8 protein binds only to 3'UTRs. While only 3'UTR binding has been shown for PUF proteins, other RNA-binding proteins in the *C. elegans* germ line, such as GLD-1, are also capable of binding mRNA in the 5'UTR and sites within the open reading frame (ORF), in addition to the 3'UTR (Lee and Schedl, 2001, 2004). An additional limitation to this screen is that RNAi against one target may not be sufficient to show suppression of the *puf-8(0); glp-1(gf)* tumourous germ line if multiple targets are involved.

8.1.2 RNA Co-Immunoprecipitation Strategies to Identify PUF-8 mRNA Targets

A second strategy to identify PUF-8 targets involved in the mitosis vs. meiosis decision overcomes some of the limitations found in the RNAi screen. This strategy involves identifying *in vivo* PUF-8 mRNA targets in whole worm extracts using co-immunoprecipitation (Co-IP) techniques followed by RNA isolation.

The first step in this strategy requires PUF-8 to be immunoprecipitated. Since there are currently no antibodies against PUF-8 (See Appendix A), PUF-8::GFP animals and antibodies against GFP are being used. Already, optimized conditions have been determined; *ugSi1* [PUF-8::GFP] (in a *puf-8(q725)* background) can be IP'd from whole

worm extracts and identified via Western blot using antibodies against GFP (work done by Laura Gauthier, Figure 6.4). For the RNA Co-IP experiments, non-PUF-8::GFP expressing, wild-type (N2) animals will be used as a negative control. Animals expressing GLD-1::GFP will be used as a positive control to validate the procedures as numerous mRNA targets of GLD-1 are known (Lee and Schedl, 2001, 2004).

The first strategy that will be employed involves treating PUF-8::GFP IPs with TRIzol (Invitrogen) to isolate the associated RNAs. The isolated RNAs can then be reverse transcribed and analyzed directly via PCR or on gene-chip arrays. This is a commonly used method with a strong potential to identify associated RNAs. However, this *in vitro* method has some weaknesses. For instance, if the protein-RNA interaction is not very strong, the wash conditions may disrupt the interaction (Jedamzik and Eckmann, 2009). It is also possible that since the natural cell structure has been disrupted during this procedure that some protein-RNA interactions may occur that do not normal form within an intact cell.

In addition to the more standard Co-IP, a new RNA Co-IP procedure called CLIP (UV CrossLinking and ImmunoPrecipitation) (Wang et al., 2009c) will be used to isolate mRNA bound to PUF-8::GFP. The main advantages obtained using CLIP RNA Co-IP over traditional methods are that legitimate *in vivo* mRNA targets can be identified as well as the approximate nucleic acid sequence bound by the RNA-binding protein. In brief, the CLIP procedure involves first exposing tissues (in this case, whole worms) to UV light, which results in covalent cross-linking between nucleic acids (RNA) bound to proteins.

Exposed ends of the bound RNA molecules are then digested with RNAse, leaving the RNA sequence, bound by the RNA-binding protein, protected and intact. The mRNA-protein complex is then purified via immunoprecipitation. In order to visualize the RNA, the 5' end of the bound RNA molecule is radioactively labeled and ligated to a 5' adapter. Next the RNA-protein complex is run on an SDS-PAGE gel, followed by transfer to a nitrocellulose membrane and exposure to X-ray film. Based on autoradiography and Western Blots, an RNA-binding protein bound to an RNA sequence should increase in molecular weight as well as be radioactive due to previous modification to the RNA. The region of the membrane containing the RNA-protein complex is then excised and the protein is digested away by proteinase K. The remaining, now free RNA is ligated to a 3' adapter and gel purified. Primers complementary to the adapter sequences are then used to amplify the RNA by RT-PCR, after which hybridization to an Illumina Genome Analyzer Flowcell will provide sequencing reads of each RNA molecule, which can then be compared to the *C. elegans* genome for identification. All procedural details were derived from (Wang et al., 2009c). Currently, Laura Gauthier (Hansen lab member) is testing the CLIP procedure using the GLD-1 protein control.

As detailed earlier, one of the main advantages of using the CLIP procedure is that the site where PUF-8 binds to the mRNA target can be easily identified. Identification of the *in vivo* PUF-8 binding site(s) in the mRNA targets will confirm whether all sites reside within the 3'UTRs or include other regions of binding outside of the 3'UTRs. If new PUF-8 binding sites are identified, this information could be used to

search the *C. elegans* genome for new potential PUF-8 target genes, which could then be tested using RNAi (as in section 8.1.1).

This biochemical approach has the potential to identify all PUF-8 targets, which provides an additional challenge as PUF-8 is involved in many different aspects of germline development including positive regulation of germ cell mitosis (Ariz et al., 2009), maintenance of male germ cell meiosis (Subramaniam and Seydoux, 2003), sex determination (Bachorik, 2005), and vulva development (Walser et al., 2006). Thus, in order to identify specific PUF-8 targets related to PUF-8's role as a negative regulator of proliferation upstream of *gld-1* and *gld-2,* rather than the other processes, it will be essential to validate the targets using the following approaches. Ideally, the best form of validation would be if the targets identified in the directed RNAi screen (section 8.1.1), were also identified via Co-IPs. Beyond the target overlap between strategies, another approach that will be used involves comparing the identified mRNAs with known or related components of the mitosis vs. meiosis decision and to the germline SAGE list (Wang et al., 2009a). Once a priority list has been constructed, each target will be tested for its role in the mitosis vs. meiosis decision using RNAi-mediated knock-down in the same sensitized background used in section 8.1.1.

8.1.3 A cup-2*-related RNAi Screen to Identify PUF-8 mRNA targets*

The third strategy that will be used to identify PUF-8 mRNA targets is derived from the *cup-2* RNAi result. *cup-2*, also referred to as *derlin-1* (DER1-LIke proteiN),

encodes a protein that is homologous to Der1 (Degradation in the Endoplasmic Reticulum) in yeast, an ER associated protein (Ye et al., 2004). When *cup-2* is knocked down in *rrf-1(0); puf-8(0); glp-1(gf)* triple mutants, otherwise tumourous germ lines are suppressed and form essentially wild-type germ lines, capable of producing viable sperm, oocytes and embryos (Figure 8.1). From the list of 2068 potential PUF-8 mRNA targets, 30 genes were identified that may have related functions to *cup-2*. To investigate whether the putative *cup-2*-related genes can also suppress the tumourous phenotype of *rrf-1(0); puf-8(0); glp-1(gf)* triple mutants, RNAi will be performed against each of the 30 genes. If *cup-2*-related genes also suppress the tumourous *rrf-1; puf-8(0); glp-1(gf)* phenotype, this may help identify a mechanism for how *puf-8* negatively regulates proliferation in the germ line.

8.2 Determining if PUF-8 is Capable of Autoregulation

While analyzing the expression pattern in the PUF-8::GFP integrated strain (*ugSi1*), it was observed that in a wild-type background, GFP levels were weak or absent, but when *ugSi1* was analyzed in a *puf-8(q725)* mutant background, consistently high GFP levels were observed in the distal germ line. Based on the expression pattern differences, one hypothesis is that PUF-8 autoregulates, thereby reducing its own expression. Ideally, if PUF-8 is capable of binding to its own mRNA, then *puf-8* mRNA should be identified in the PUF-8 Co-IP experiments described above (section 8.1.2). Presumably, if PUF-8 is able to autoregulate, it would do so by binding to the *puf-8*

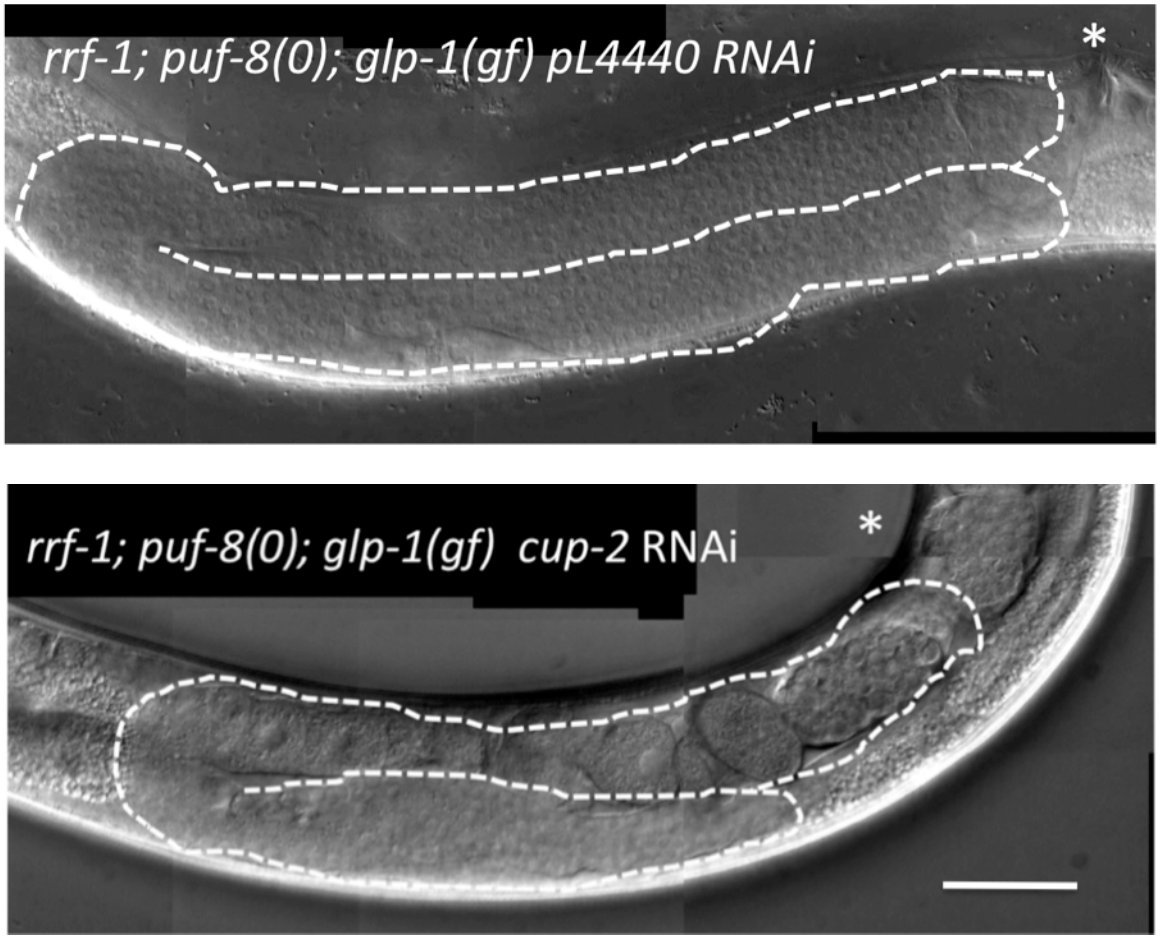

Figure 8.1. *cup-2* RNAi.

DIC image comparison of an *rrf-1; puf-8(0); glp-1(gf)* germ line vs. an *rrf-1; puf-8(0); glp-1(gf) cup-2 RNAi* germ line. In *rrf-1; puf-8(0); glp-1(gf)* animals, fed empty vector (pL4440 RNAi), the germ lines contain only proliferative germ cells. In contrast, when *cup-2* is knocked-down in *rrf-1; puf-8(0); glp-1(gf)* mutants, essentially wild-type germ lines are formed. *rrf-1; puf-8(0); glp-1(gf) cup-2 RNAi* germ lines contain viable sperm, oocytes and embryos. White dashed line outlines one gonad arm in each animal. Asterisk marks the vulva opening. Scale bar = 50 μM.

3'UTR. Autoregulation through the 3'UTR is the strategy employed by another germline expressed RNA-binding protein, FOG-1 (Jin et al., 2001). This work identified eight imperfect putative PUF-8 binding sites in the *puf-8* 3'UTR (Figure 7.2). However, the *puf-8* gene was not one of the 2068 genes identified as a potential PUF-8 mRNA targets (see section 8.1.1). This is because none of the eight sites completely match the PUF-8 binding motif identified by Opperman et al. 2005 (Figure 7.2). Thus, it is currently unknown whether any of these sites represent functional PUF-8 binding sites.

Before testing whether these putative PUF-8 binding sites in the *puf-8* 3'UTR are capable of binding PUF-8, the first test will be to establish if the *puf-8* 3'UTR is the region of the *puf-8* mRNA molecule that influences the expression pattern differences seen between *ugSi1* in a *puf-8(+)* or *puf-8(0)* background. To test the functionality of the *puf-8* 3'UTR, another MosSCI targeting vector was constructed, this time using Gateway cloning technology (Invitrogen, Gateway Cloning) and the MosSCI Destination vector (pDESTttTi5605) (Frokjaer-Jensen et al., 2008). The final targeting vector (pDH215) contains the *puf-8* promoter::*gfp* coding sequence::*puf-8* 3'UTR (i.e., no *puf-8* coding sequence) and is designed to integrate into the Mos1 site on chromosome II. This integration site is not ideal as *puf-8* is also located on chromosome II, 0.3 cM from the ttTi5605 Mos1 integration site. Once pDH215 has been incorporated into the Mos1 chromosome II site, the integrated strain will be analyzed in both *puf-8(+)* and *puf-8(0)* backgrounds. If the expression pattern matches the expression pattern observed for *ugSi1*, this could suggest that the *puf-8* 3'UTR is the site in the mRNA molecular that is

responsible for the expression pattern difference. However, this construct also includes the *puf-8* promoter sequence, therefore, it could be that the promoter, through transcriptional regulation, controls this pattern. Regulation by PUF-8 through the *puf-8* promoter is unlikely, as all mRNA targets of PUF proteins, identified thus far, only show binding through the 3'UTR (Chen et al., 2008; Crittenden et al., 2002; Hook et al., 2007). To exclude the *puf-8* promoter as a site responsible for the expression pattern differences, it will also be necessary to generate additional constructs that use different promoters, such as the *pie-1* promoter, which permits expression in all germ cell types (D'Agostino et al., 2006). If the *puf-8* promoter::*gfp* coding*::puf-8* 3'UTR integrants expression pattern does not match the *ugSi1* expression pattern, this could indicate that sites within the *puf-8* coding sequence influence the expression pattern differences. Difference in expression could also suggest that the chromosome II integration site influences the expression of the integrated transgene.

Assuming PUF-8 is capable of autoregulation, the next step will be to investigate the functionality of the putative PUF-8 binding sites in the *puf-8* 3'UTR. To test the functionality of the sites, a third MosSCI targeting vector will be generated that has alterations in all eight putative PUF-8 binding sites. If these sites are required for PUF-8 autoregulation, then loss of these sites in a *puf-8(+)* background may result in increased expression of GFP. It is also possible that modification of all eight putative PUF-8 binding sites may be too severe of an alteration to permit the PUF-8 expression pattern, thus, it may be necessary to sequentially alter each site individually.

If the results from the integrated transgene reporter approaches strongly favour the hypothesis that PUF-8 is capable of autoregulation, then it will be necessary to perform additional binding assays such as EMSA (Electrophoretic Mobility Shift Assays) and/or yeast three-hybrid assays. Positive results from these methods will be used to validate the results from the integrated transgene reporter approaches. To perform an EMSA, the *puf-8* 3'UTR sequence, as well as a PUF-8 binding site mutated version of the *puf-8* 3'UTR, will be labeled using either a radioactive, fluorescent or biotin tag (Li et al., 2004; Sully et al., 2004). The PUF-8::GFP protein will then be incubated separately with the wild-type and mutated *puf-8* 3'UTR sequences. Immediately after incubation each sample will be resolved on a native polyacrylamide gel. RNA run alone will migrate through the gel quickly. However, if the PUF-8::GFP protein binds to the labeled RNA molecule, then a large shift in mobility will be observed. Conversely, no shift in mobility should occur when the mutated *puf-8* 3'UTR is incubated with PUF-8::GFP. Additionally, an EMSA can also be used to identify the binding affinity of PUF-8 for the *puf-8* 3'UTR (Sully et al., 2004). This can be done by exposing the *puf-8* 3'UTR to different concentrations of competitor sequence (ex. unlabeled *puf-8* 3'UTR) in the presence of the PUF::GFP protein. If the competitor is capable of sequestering the *puf-8* 3'UTR sequence, then a band shift will no longer occur even in the presence of the PUF-8::GFP protein. The concentration of competitor at which the band shift is no longer observed can be used to establish the binding affinity of PUF-8::GFP for the *puf-8* 3'UTR.

Alternatively, or in addition to the EMSA, a yeast three-hybrid experiment will be performed to validate the integrated transgene reporter results. The yeast three-hybrid system has become a common strategy to analyze RNA-protein interactions (Bernstein et al., 2002; SenGupta et al., 1996). The general principle of the yeast three-hybrid system is the activation of a reporter gene through the binding of an RNA sequencing to an RNA-binding protein. To perform a yeast three-hybrid experiment to test the interaction between PUF-8 and *puf-8* 3'UTR, two constructs need to be generated and introduced into yeast cells. The first construct will contain the PUF homology domain from the PUF-8 protein fused to the Gal4 (GALatose metabolism) transcriptional activation domain (AD, Figure 8.2). The second construct, which will generate the 'hybrid RNA', will contain the *puf-8* 3'UTR sequence linked to two MS2 coat protein binding sites (from MS2 bacteriophage). To tether the RNA molecule to the promoter of the reporter gene, a fusion protein that consists of a LexA/MS2 coat protein will also be expressed. If the PUF-8 protein binds to the *puf-8* 3'UTR sequence, the associated Gal4 activation domain is brought in contact with the promoter of the LexA-regulated genes and, thus, leads to transcriptional activation of the reporter genes (Figure 8.2). If the yeast strain YBZ-1 is used, then the reporter genes under the control of the LexA operator include LacZ and *HIS3* (Bernstein et al., 2002). Thus, activation of the reporter can be monitored using B-galactosidase activity (for LacZ) and growth phenotype (for *HIS3*). As a negative control, *puf-8* 3'UTR sequence with mutated PUF-8 binding site(s) will also be tested.

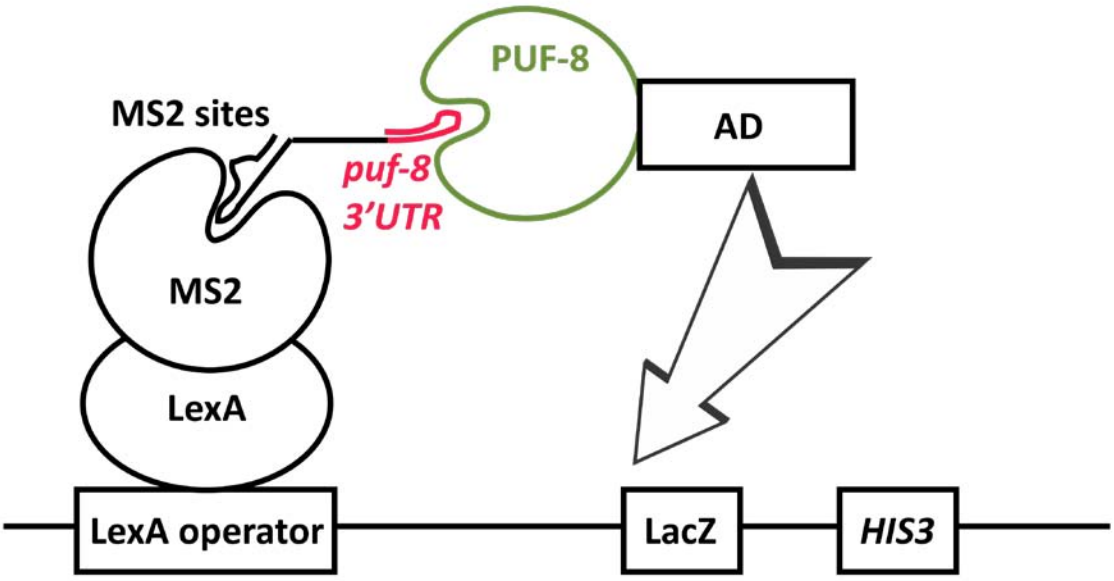

Figure 8.2. Overview of the yeast three-hybrid approach to identify if the PUF-8 protein can bind to the *puf-8* 3'UTR.

The hybrid RNA molecule that contains the *puf-8* 3'UTR and two MS2 coat protein binding sites is tethered to the yeast LexA promoter/operator region via a hybrid protein that contains a DNA-binding domain (LexA) and a RNA-binding domain (MS2 coat protein). A second hybrid protein containing the PUF homology domain from the PUF-8 protein fused to the transcriptional activation domain (AD) from Gal4 is also expressed in these yeast cells. If binding occurs between the *puf-8* 3'UTR RNA sequence and the PUF-8 protein, the AD will be brought within close proximity to the promoter and transcriptional activation of the downstream reporter genes (LacZ and *HIS3*) will take place. The yeast strain YBZ-1 has both the LacZ and *HIS3* genes under the control of the LexA operator. Adapted from (Hook et al., 2005).

8.3 PUF-8 Genetic Enhancer Screen

Genetic evidence suggests that PUF-8 likely functions most likely as a negative regulator of proliferation upstream of the *gld-1* and *gld-2* pathways (or in a novel parallel pathway to Notch signalling and FBFs). In comparison to the other enhancers studied in the Hansen lab, including: *teg-1, teg-4* (Mantina et al., 2009)*, pas-5* (Macdonald et al., 2008) and *nos-3* (Hansen et al., 2004b), *puf-8* is the only enhancer that does not form a synthetic tumour with components from the *gld-1* and *gld-2* pathways. Thus, PUF-8 plays a unique role in the mitosis vs. meiosis decision. In order to understand and characterize this unique role for *puf-8*, it will be useful to identify other genes that function with *puf-8*. Since *puf-8* appears to function in a unique position in the mitosis vs. meiosis pathway, using *puf-8(0)* as a genetic background may help to identify additional players that were not identified in other backgrounds. To perform a *puf-8* genetic enhancer screen, *puf-8* homozygous mutant animals will be mutagenized and the resulting F1 progeny will be isolated onto individual plates (Figure 8.3). Then the F2 progeny will be screened for plates that show 25% tumourous animals, which represent the homozygous double mutants. The mutation will then be isolated from heterozygous siblings, since the homozygous animals are tumourous (i.e., sterile). The mutation causing a tumourous phenotype in a *puf-8* mutant background will be cloned to identify the corresponding gene.

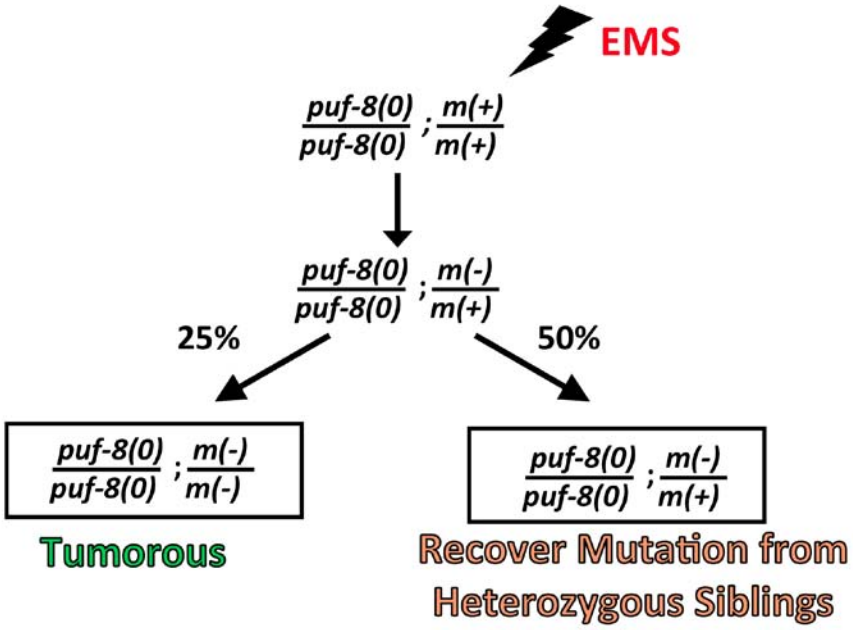

Figure 8.3. PUF-8 genetic enhancer screen.

puf-8(0) homozygous mutants will be mutagenized with EMS (Ethyl Methane sulfonate)The F1 progeny will then be separated onto individual plates and allowed to self. The self-progeny on each plate will be screened to identify plates that contain 25% tumourous animals (*puf-8(0); m(-)*). To propagate the mutation (*m(-)*) that enhances *puf-8(0)*, the mutation will be recovered from heterozygous siblings. This illustration makes the assumption that the mutation will not be located on the same chromosome as *puf-8* or that the mutation will located far from the *puf-8* locus on the same chromosome.

While cloning is underway, each promising mutation will be characterized to establish the potential role it may play in the mitosis vs. meiosis decision. Presumably, genes acting with *puf-8* will show similar interactions, thus each mutation will be tested for its ability to enhance and suppress *glp-1(gf)* and *glp-1(lf)* mutants, respectively. Using the same genetic strategies as those used to functionally map *puf-8*, each mutation's interaction will be tested with each of the known mitosis vs. meiosis components. The outcome of the genetic interaction studies may assist in characterizing the putative parallel pathway.

8.4 Contributions

I would like to acknowledge the work of Vivian Fung and Helen Dick for performing much of the genetic screening described in section 8.1.1. My involvement with this section included generation of the potential *puf-8* target list, initiation of the screen, training and overseeing the screening, and validation of the positive interactions. As well, I would like to acknowledge the work of Dr. Laura Gauthier and James Lai, whom are currently working on the strategies outlined in section 8.1.2 and section 8.1.3, respectively. My involvement with section 8.1.2 was the generation of the PUF-8::GFP::TAP strain (ugSi1). My involvement with section 8.1.3 included the initial design of the *cup-2* screening strategy.

APPENDIX A: GENERATION OF A PUF-8 SPECIFIC ANTIBODY

Introduction

Genetic analysis suggests that PUF-8 functions in the distal germ line as a negative regulator of proliferation. One way to determine where in the distal germ line PUF-8 plays such a role is to use a biochemical approach. One biochemical approach is to use antibodies against PUF-8 to specifically detect the PUF-8 protein in the germ line. A PUF-8 antibody would not only assist in identifying the expression pattern of PUF-8, but would also be beneficial for other biochemical experiments, such as co-immunoprecipitations to identify PUF-8 mRNA targets.

At this time, no antibodies against the PUF-8 protein have been generated. Throughout this project, numerous antigen strategies have been tested. These include four different peptide antigens (in 4 different regions of the PUF-8 protein) coupled to Bovine Serum Albumin (BSA) or Keyhole Limpet Hemocyanin (KLH) and one truncated N-terminus PUF-8 bacterial expressed protein. As well, a variety of animal species have been used including mice, guinea pigs and rabbits. In addition to personal attempts, the company OpenBiosystems was also employed. Thus far, none of the serums tested have been able to recognize the endogenous PUF-8 protein in whole worm extracts. Some of the serums have been able to recognize the truncated PUF-8 bacterial expressed protein, but only at very high protein concentrations (5-0.5 μg/μL) (Figure A1). Personal discussions at the last International *C. elegans* conference (Los Angeles, 2009) revealed that many labs have been unsuccessful in generating PUF-8 antibodies.

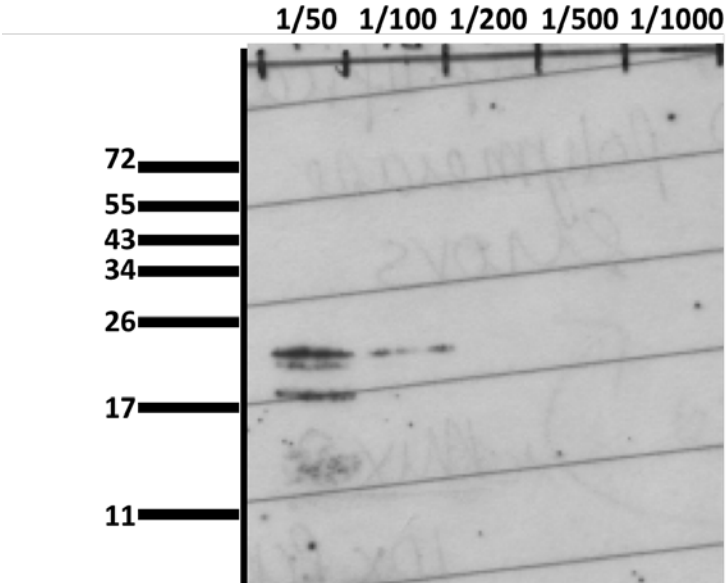

Figure A1: PUF-8 antibody, raised against peptide #1, can recognize bacterial expressed PUF-8 C-terminus protein, but only at high concentrations.

Nitrocellulose blot contains serial dilutions (labelled on top of blot) of 50 μg/μL of bacterially expressed PUF-8 C-terminus His-tag purified protein (20 kDa). The blot was incubated with affinity purified serum from rabbits injected with peptide #1, then exposed to αrabbit secondary antibody-HRP. Only a faint 20 kDa band is seen in the 1/100 dilution lane, suggesting that the antibodies that are present in the rabbit serum, can only recognize the PUF-8 C-terminus protein at high concentrations (i.e. not very specific).

This appendix chapter outlines the strategies that were used in an attempt to generate a PUF-8-specific antibody.

Challenges to Selection of an Antigenic Sequence in the PUF-8 Protein

When selecting an antigen for the generation of an antibody, it is important that the site be specific. PUF-8 is one of twelve PUF proteins in *C. elegans.* Blast alignment of the PUF-8 protein reveals that the top hits include the eleven other PUF proteins ranging in E-values from $4e^{-93}$ for PUF-9 to $9e^{-4}$ for PUF-12. The similarity between all PUF proteins makes it difficult to find unique sequence ideal for use as an antigen. Without a unique sequence, any antibodies generated may also detect other PUF proteins. Only a few regions in the N-terminus and the very last 10-15 amino acids in the C-terminus are unique to PUF-8.

Peptide strategies

Four different peptide sequences were used as antigens to generate PUF-8 specific antibodies. Peptide #1 was generated by the Peptide Synthesis Core Facility at the University of Calgary. After synthesis, peptide #1 was conjugated to two different carrier proteins, BSA and KLH, individually (work done during this project). The following are the peptides sequences and the corresponding animal species that each peptide was injected into:

Peptide #1: DSVCGSPIRSYGRH (injected into 2 rabbits)

Peptide #2: DPSASPIESLGRSIGAQK (injected into 2 guinea pigs and 2 rabbits)

Peptide #3: KIVDSVCGSPIRSYGR (co-injected with #4 into 2 rabbits)

Peptide #4: KPAVMSYPYQDMQGSH (co-injected with #4 into 2 rabbits)

Note: Peptides #2-4 were generated by OpenBiosystems. Figure A2 shows the location of each peptide in the PUF-8 protein.

A typical injection schedule for a rabbit:

Day 1: bled for pre-immune sera

1 week later: bled for second pre-immune sera and primary injection (plus complete adjuvant)

2 weeks later: Booster #1 (plus incomplete adjuvant)

2 weeks later: collect bleed #1, then booster #2 (plus incomplete adjuvant)

2 weeks later: collect bleed #2, then booster #3 (plus incomplete adjuvant)

2 weeks later: take final bleed

Bacterially expressed truncated PUF-8 N-terminus protein

The first 150 amino acids from the N-terminus of PUF-8 were used to generate a bacterially expressed PUF-8 truncated protein. To do so, the first 450 nucleotides from the N-terminus of *puf-8* was amplified from cDNA using primers that contained restriction enzyme recognition sites:

MSRPISIGNTCTFDPSASPIESLGRSIGAQKIVDSVCGSPIRSYGRHISTNPKNERLPDTPEFQFATYMH
QGGKVIGQNTLHMFGTPPSCYCAQENIPISSNVGHVLSTINNNYMNHQYNGSNMFSNQMTQMQ
AQAYNDLQMHQAHSQSIRVPVQPSATGIFSNPYREPTTTDDLLTRYRANPAMMKNLKLSDIRGALL
KFAKDQVGSRFIQQELASSKDRFEKDSIFDEVVSNADELVDDIFGNYVVQKFFEYGEERHWARLVDA
IIDRVPEYAFQMYACRVLQKALEKINEPLQIKILSQIRHVIHRCMKDQNGNHVVQKAIEKVSPQYVQF
IVDTLLESSNTIYEMSVDPYGCRVVQRCLEHCSPSQTKPVIGQIHKRFDEIANNQYGNYVVQHVIEHG
SEEDRMVIVTRVSNNLFEFATHKYSSNVIEKCLEQGAVYHKSMIVGAACHHQEGSVPIVVQMMKQ
YANYVVQKMFDQVTSEQRRELILTVRPHIPVLRQFPHGKHILAKLEKYFQKPAVMSYPYQDMQGSH

Figure A2: Location of each peptide sequence within the PUF-8 protein.

Peptide #1 (highlighted in yellow), peptide #2 (highlighted in green), peptide #3 (underlined) and peptide #4 (highlighted in blue). Peptides #2-4 were generated by OpenBiosystems and peptides #3-4 were co-injected together.

REV_puf-8Nterm: ttttGAATTCactttgagaatgcgcttgg (EcoRI site)

FOR_puf-8Nterm: ttttAAGCTTatgagtcgtccgatttcaa (HindIII site)

Next the PCR product was cloned into pET29a (Novagen), creating the pDH132 plasmid and transformed into *E. coli* expression cells (BL21(DE3)). pET29a incorporates a 6XHIS tag onto the C-terminus of the protein. To express the PUF-8 N-terminus, the *E. coli* cells were grown in LB media at 37°C O/N with agitation. To isolate soluble PUF-8 N-terminus protein, *E. coli* cells were French pressed, resuspended in urea buffer, then concentrated and buffer exchanged using 10,000 MW Amicon Ultra centrifugal filter columns (Milipore).

Purified PUF-8 N-terminus protein was injected into five BalC female mice (25 μg/mouse) with complete Freund's adjuvant at the University of Calgary Animal Care facility. A pre-immune serum was taken before the first antigen injection. Five booster injections were given every two weeks before the final bleed.

Testing the Serum for PUF-8 Antibodies

Upon receiving each test bleed, the crude serum was analyzed for the presence of αPUF-8 antibodies. One quick experiment that was done to test for the presence of antibodies against the peptide sequence or bacterially expressed protein was to perform a dot blot. The dot blot was performed by spotting a serial dilution of the purified peptide or bacterially expressed protein onto a nitrocellulose membrane. The nitrocellulose was then exposed to the crude serum, followed by incubation in the

corresponding secondary antibody, then exposure to chemiluminescence to visualize the interaction. This test only identifies antibodies that can detect the antigen; this experiment does not determine if the antibody is specific to PUF-8. A dot blot of the rabbit crude serum injected with Peptide #1 revealed that antibodies within the crude serum were able to detect the peptide #1.

Instead of using dot blots, OpenBiosystems tested the specificity of each crude serum using an ELISA (Enzyme-Linked ImmunoSorbent Assay). An ELISA is performed by first immobilizing an unknown amount of antigen to a solid surface (e.g. 96 well plate), followed by the addition of the crude serum. Antibodies that can detect the antigen will bind to the surface, and then secondary antibodies are added, which are linked to an enzyme that permits detection of the antibody-antigen interaction.

To determine if the crude serum contains antibodies that can detect the PUF-8 protein, Western blots were performed. Whole worm lysates from N2, *puf-8* mutants (*puf-8(oz192)* and *puf-8(q725)*) and *kpIs(puf-8::gfp)* were tested. Presumably, if a PUF-8 specific antibody was present in the serum, N2 animals should show a 59 kDa band, the 59 kDa band should be absent in *puf-8* mutants and *puf-8::gfp* animals should show an ~90 kDa band. In most cases, multiple bands were observed when crude serum was used on whole worm extracts (especially rabbit crude serum). This suggests that the crude serum likely contains antibodies against other *C. elegans* proteins. In order to isolate only the PUF-8 specific antibodies, purification strategies were employed.

Affinity Purification of PUF-8-specific Antibodies

To purify αPUF-8 specific antibodies away from non-specific antibodies in the crude serum, a variety of affinity purification techniques were used. Antibodies raised against the peptide #1 sequence were purified from the crude serum using the AminoLink kit (Pierce). To purify antibodies against the bacterially expressed PUF-8 N-terminus His-tag protein, a second PUF-8 N-terminus bacterial expressed protein was generated with an alternative tag (pDH148). It is possible that some of the antibodies, in the crude serum, may have been raised against the His tag, thus, by using an alternatively tagged protein, permits the purification of just PUF-8 N-terminus specific antibodies. To do this, a GST tag PUF-8 N-terminus protein was generated and coupled to glutathione-agarose beads. Then the serum was run through the coupled agarose beads.

To purify PUF-8 specific antibodies from the OpenBiosystem's crude serum, a PUF-8 C-terminus His-tagged bacterial expressed protein was generated (using identical methods as PUF-8 N-terminus His-tagged protein above). PUF-8 C-terminus His-tagged protein was coupled to a Ni-NTA-agarose column (Qiagen). In addition to the C-terminus peptide sequence (peptide #4, Figure A2), OpenBiosystem's also co-injected an N-terminus peptide sequence (peptide #3, Figure A2). To purify the antibodies against the N-terminus peptide sequence, the serum was run through the GST-PUF-8 N-terminus protein coupled to Glutathione-agarose beads column (mentioned above).

Unfortunately, purification of each crude serum tested did not result in the isolation of sufficient αPUF-8 specific antibodies, as revealed via Western blots.

Another Strategy to Reduce Non-Specific Antibody Interactions

In addition to the affinity purification techniques, another strategy that was performed to reduce the amount of non-specific antibody interactions, was to expose the crude serum and purified serum to *puf-8* worm acetone powder. Worm acetone powder was made using the following protocol (Crittenden and Kimble, 2009). Ideally, by pre-absorbing the serum against total protein from *puf-8* mutants, all antibodies that bind non-specifically will be sequestered, while antibodies against the PUF-8 protein will remain. Like with the affinity purification, worm acetone powder did not assist in isolating αPUF-8-specific antibodies.

Conclusions

It is difficult to say whether the problem is that no PUF-8-specific antibodies were generated or that the problem lies in the detection of the PUF-8 protein. The fact that the antibodies from three sets of serum were only able to detect antigenic sequences at high concentrations (ex Figure A1) suggests that there are antibodies that recognize sites within the PUF-8 protein sequence but that the antibodies have a low affinity. However, in whole worm extracts, no antibodies, in any of the serum tested, were able to recognize the endogenous PUF-8 protein. One possibility is that the

endogenous PUF-8 protein undergoes modifications or conformational changes that make it impossible for the antibodies (raised against peptides and truncated proteins) to detect the protein. One way to test this theory would be to raise antibodies against the whole PUF-8 protein; however, since PUF-8 is very similar to other PUF proteins, this would likely lead to the creation of a non-specific PUF protein antibody. Another reason for why endogenous PUF-8 was not detected may be because PUF-8 is expressed at very low levels, and thus, is difficult to detect on westerns. In order to detect low level of PUF-8 protein, it will likely be necessary to enrich using immunoprecipitations, followed by detection with a more powerful chemiluminescence solution, such as Amersham ECL Advance Western blotting kit (GE Healthcare).

Presuming no PUF-8 antibody (specific or non-specific) was raised, could suggest that the sequences tested so far do not invoke a strong immune response in the host animal. This may be because the animal has previously suffered a nematode infection (however, multiple individuals and species used) and, thus, may already produce low levels of antibodies against PUF-8.

APPENDIX B: CHARACTERIZATION OF THE *gld-1; puf-8* DOUBLE MUTANT

Introduction

While investigating whether *puf-8* functions in the mitosis vs. meiosis decision downstream of Notch signalling in the *gld-2* pathway, *gld-1; puf-8* double mutants were constructed (Chapter 4, section 4.4.1). If a synthetic germline tumour was formed in *gld-1; puf-8* double mutant animals, this would have suggested that *puf-8* functions in the *gld-2* pathway to promote meiotic entry and/or inhibit proliferation. Analyzing for a germline tumour using the *gld-1(q485)* mutant is challenging because these animals are tumourous on their own. In *gld-1(q485)* single mutant hermaphrodites, female germ cells enter normally into meiosis; however, female germ cells are unable to progress past the pachytene stage of meiosis and, instead, re-enter into mitosis forming large proximal germline tumours (Francis et al., 1995a). Thus, GLD-1 is required for meiotic progression in female germ cells (Francis et al., 1995a). As well, unmarked *gld-1(q485)* hermaphrodites do not produce sperm (Francis et al., 1995a). Feminization in *gld-1(q485)* hermaphrodites is due to a disruption in the processes required for germ cells to adopt the male fate; specifically GLD-1 and FOG-2 negatively regulate *tra-2* (TRAnsformer), and in the absence of *gld-1*, TRA-2 promotes the female fate (Figure B1) (Jan et al., 1999). In order to determine if loss of *puf-8* and *gld-1* resulted in the formation of a synthetic germline tumour, the distal mitotic zone was analyzed for extended proliferation. The distal mitotic zone in *gld-1; puf-8* double mutants was

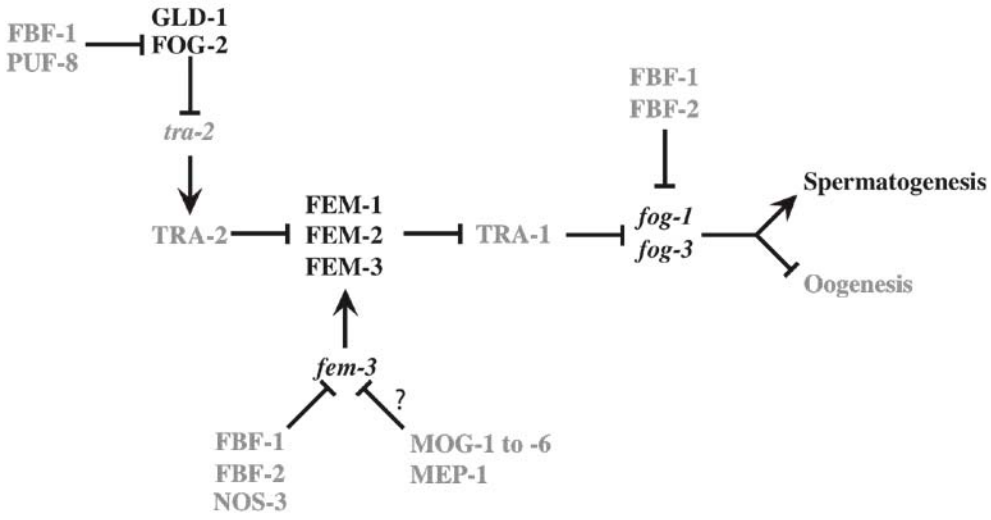

Figure B1. Sex determination in the *C. elegans* hermaphrodite germ line. This genetic pathway outlines the major factors that regulate sex determination in *C. elegans* hermaphrodites. Components in black type promote the male fate, while components in grey type promote the female fate. Proteins are shown in uppercase and genes in lowercase italics. Figure adapted from (Racher and Hansen, 2010).

roughly the same size as *puf-8* single mutants; thus, the mitotic zone was not enlarged. This suggests that *puf-8* does not function in the *gld-2* pathway to promote meiotic entry and/or inhibit proliferation, as discussed in section 4.4.1. However, other interesting phenotypes were observed; 100% of *gld-1; puf-8* double mutants produce sperm and 76% of these animals form Pro tumours (compared to 0% and 100% for *gld-1(0)* alone) (Figure B2, Table B1). This appendix chapter outlines the approaches that have been taken to characterize the *gld-1; puf-8* mutant phenotype.

Analysis of the sperm in *gld-1; puf-8* double mutants

Since unmarked *gld-1(q485)* hermaphrodites never produce sperm (Francis et al., 1995a), it is interesting that 100% of *gld-1; puf-8* double mutant hermaphrodites produce sperm. Furthermore, the number of sperm in *gld-1; puf-8* mutants was found to be similar to (in some cases higher than) wild-type (Table B2). In the sex determination pathway (Figure B1), GLD-1 promotes the male fate, redundantly with FOG-2, by negatively regulating *tra-2* (Jan et al., 1999). Conversely, PUF-8 promotes the female fate, redundantly with FBF-1, by potentially negatively regulating *fog*-2 (Bachorik and Kimble, 2005). Based on the rules of epistasis, since *gld-1's* function is opposite and downstream of *puf-8's* function in the sex determination pathway, *gld-1* should be epistatic to *puf-8*; thus, *gld-1(q485); puf-8(oz192)* animals should look like *gld-1(q485)* single mutants. The fact that *gld-1; puf-8* animals are not feminized, but instead have sperm may suggest that *gld-1* and/or *puf-8* have additional roles in the sex

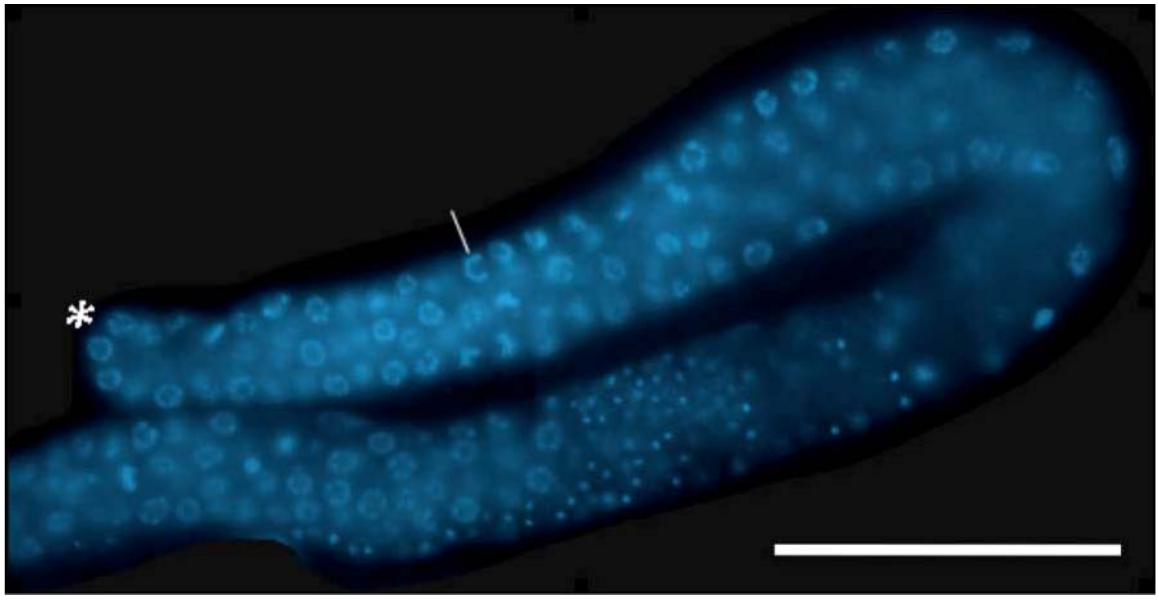

Figure B2. *gld-1(q485); puf-8(q725)* double mutant hermaphrodites, which contains a Pro tumour. To visualize the germ line, gonads were dissected and stained with DAPI. The asterisk marks the distal end of the gonad. Distal proliferation zone is small (due to *puf-8* mutant). Cells enter into meiosis normally; vertical line marks a crescent-shape nucleus indicative of a cell undergoing leptotene/zygotene stage of meiosis. Sperm are present in the proximal arm (small button nuclei), followed by proximal proliferation (Pro tumour). Note that M-phase nuclei (flatten condensed nuclei) are present in both the distal and proximal ends, indicative of cells undergoing mitosis. Scale bar = 50 μM.

Table B1. Further characterization of *gld-1; puf-8* double mutants

Genotype	Gametes			Pro	N
	Sp	Oo	both		
puf-8(q725)			X		11
gld-1(q485)				X	9, 150[a]
gld-1(q485); puf-8(q725)	X			X (76%)	34
(1/3) *gld-1(q485); puf-8(q725); fem-3(e1996)* (2/3) *gld-1(q485); puf-8(q725); fem-3(e1996)/unc-24 dpy-20*[d]				X	14
puf-8(q725); fem-3(e1996)		X			18
(1/3) *gld-1(q485); fem-3(e1996)* (2/3) *gld-1(q485); fem-3(e1996)/unc-24 dpy-20*[e]				X	12
(1/3) *gld-1(q485); puf-8(q725); fog-2(q71)* (2/3) *gld-1(q485); puf-8(q725); fog-2(q71)/unc-76 rol-9*[f]				X	5
puf-8(q725); fog-2(q71)		X[b]			37
(1/3) *gld-1(q485); fog-2(q71)* (2/3) *gld-1(q485); fog-2(q71)/unc-76 rol-9*[g]				X[c]	24

All strains analyzed at 20°C

[a] number of *gld-1(q485)* animals tested by (Francis et al., 1995a)

[b] some *puf-8(q725); fog-2(q71)* animals have atypical nuclei (maybe endoreduplication?) in the most proximal oocytes.

[c] The tumourous *gld-1(q485); fog-2(q71)* phenotype was also observed in (Francis et al., 1995b)

[d] actual genotype = *gld-1(q485); puf-8(q725); fem-3(e1996)/unc-24(e138) dpy-20(e1282)*

[e] actual genotype = *gld-1(q485); fem-3(e1996)/unc-24(e138) dpy-20(e1282)*

[f] actual genotype = *gld-1(q485); puf-8(q725); fog-2(q71)/unc-76(e911) rol-6(sc149)*

[g] actual genotype = *gld-1(q485); fog-2(q71)/unc-76(e911) rol-9(sc149)*

Sp= sperm, Oo= oocytes, both= sperm and oocytes

Table B2. Number of sperm in gld-1(q485); puf-8(q725) hermaphrodites

Genotype	**# sperm/gonad arm[a]**	**N**
N2	144	10
gld-1(q485)	0[b]	N/A
puf-8(q725)	155[c]	10
gld-1(q485); puf-8(q725) w/Pro[d]	134	6
gld-1(q485); puf-8(q725) no Pro[e]	181	3

Animals maintained at 20°C

[a] To count sperm, DAPI stained dissected gonads were examined under Nomarski fluorescence using Z-stacks. The z-stacks were then compiled into one image using ImageJ plugin 3D viewer and the sperm were counted.

[b] data from (Francis et al, 1995), N/A = not applicable

[c] data from (Bachorik and Kimble, 2005)

[d] counted the number of sperm in the 76% of *gld-1(q485); puf-8(q725)* hermaphrodites that have a Pro tumour

[e] counted the number of sperm in the 24% of *gld-1(q485); puf-8(q725)* hermaphrodites that do not have a Pro tumour

determination pathway, either as positive regulators of oogenesis or negative regulators of spermatogenesis.

In order to determine if *gld-1* and/or *puf-8* function in additional locations within the sex determination pathway, epistasis experiments were conducted. First epistasis analysis was performed with the *fem-3(e1996)* mutant in a *gld-1(q485); puf-8(oz192)* mutant background. *fem-3* functions downstream of *puf-8* and *gld-1* in the sex determination pathway to promote spermatogenesis (Figure B1), thus, *fem-3(e1996)* mutants only produce oocytes. If the triple mutant phenotype resembled *fem-3(e1996)* mutants, this could suggest that the *gld-1* and/or *puf-8* role occurs upstream of *fem-3*. Conversely, if the triple phenotype resembled *gld-1(q485); puf-8(oz192)* double mutants, then this may suggest that *gld-1* and/or *puf-8* has a role downstream of *fem-3*. In *gld-1(q485); puf-8(q725); fem-3(e1996)* triple mutants, the phenotype resembled a *fem-3* mutant; however, because *gld-1* was absent, oocytes do not form but instead female germ cells re-enter into mitosis forming a Pro tumour (Table B1) (Francis et al., 1995a). This result suggests that *gld-1* and/or *puf-8* may have an additional sex determination role upstream of *fem-3*. To test further upstream, epistasis with *fog-2* was conducted. In *gld-1(q485); puf-8(q725); fog-2(q71)* animals, the resulting phenotype resembled *fog-2(q71)* (Table B1), placing the *gld-1* and/or *puf-8's* additional sex determination role upstream of *fog-2*. Since it is already known that *puf-8* functions upstream of *fog-2*, it is unclear whether these epistasis experiments provide any new information. It is possible that the sex determination pathway includes many more

genes upstream of *fog-2*. Perhaps *gld-1* and/or *puf-8* have additional functions upstream of the known components.

Characterization of the Pro tumour

In 76% of *gld-1; puf-8* double mutants hermaphrodites, Pro tumours are formed (Table B1). The germ lines of *gld-1; puf-8* mutants have smaller than wild-type distal proliferation (due to the presence of the *puf-8* mutant), followed by normal entry into meiosis, then a wild-type number of sperm are formed, followed by proximal proliferation in 76% of the animals (Figure B2). Furthermore, 60% of *gld-1; puf-8* double mutant males also form Pro tumours (Table B3). Note that *gld-1(q485)* single mutant males do not display the return to mitosis tumourous phenotype that *gld-1(q485)* hermaphrodites show. *gld-1(q485)* males are virtually wild-type. Only female germ cells are unable to complete meiosis in *gld-1(q485)* animals. Therefore, since *gld-1(q485); puf-8(0)* male and hermaphrodite animals produce sperm it is unclear as to whether the Pro tumour is due to a return to meiosis. There are at least three different theories for why Pro tumours form in these animals; (1) the lack of *gld-1* could cause female germ cells to re-enter mitosis, (2) lack of *puf-8* could cause dedifferentiation of primary spermatocytes back into mitotic cells, or (3) early in development, mitotic cells may have been misplaced into the proximal end, where they divided to form a proximal tumour. Exploration of each theory is outlined below.

Table B3. *gld-1(q485); puf-8(q725)* male phenotype

Male genotype	Temp (°C)	Sperm[a]	Pro[a]	N
gld-1(q485)	20	X		32
puf-8(q725)	20	X		21
puf-8(q725)	**25**	X	X (83%)[b]	64[b]
gld-1(q485); puf-8(q725)	20	X	X (60%)	20
gld-1(q485); puf-8(q725); spe-6(hc49)[c, d]	20	Spe[g]	X (58%)	28
gld-1(q485); spe-6(hc49)[e]	20	Spe		13
puf-8(q725); spe-6(hc49)[f]	20	Spe		10

The mitosis vs. meiosis decision occurs normally within each strain.

[a] Animals analyzed via DIC for the presence of sperm and proximal proliferation (Pro tumour).

[b] data from (Bachorik and Kimble, 2005).

[c] *spe-6(hc49)* primary spermatocytes are blocked during diakinesis of meiosis I.

[d] actual genotype: *gld-1(q485); puf-8(q725); spe-6(hc49) unc-25(e156)*

[e] actual genotype: *gld-1(q485) spe-6(hc49) unc-25(e156)*

[f] actual genotype: *puf-8(q725); spe-6(hc49) unc-25(e156)*

[g] Spe = defective SPErmatogenesis

Theory 1: One possibility is that the Pro tumours, formed in *gld-1; puf-8* double mutants, are due to *gld-1* mutation causing female germ cells to re-enter into meiosis. If this is the case, the normal sequence of first male then female gametes being formed would appear to be backwards in *gld-1; puf-8* mutant animals, as sperm are present more distal to the Pro tumour. In wild-type *C. elegans* hermaphrodites, sperm is formed first and stored in the proximal region of the gonad, then oocytes are formed distal to the sperm (Hirsh et al., 1976). One observation that argues against theory #1 is that proximal proliferation occurred in 60% of the *gld-1; puf-8* males analyzed (Table B3), suggesting that the proximal proliferation phenotype can occur in the absence of female germ cells. Since the percentage of proximal proliferation in *gld-1; puf-8* males is similar to *gld-1; puf-8* hermaphrodites, whatever is causing the Pro tumours is similar between the sexes. Thus, it is unlikely that the Pro tumours are caused by the re-entry into mitosis of female meiotic cells.

Theory #2: Another reason for the proximal proliferation could be due to lack of *puf-8*, which is known to cause dedifferentiation of primary spermatocytes back into mitotic cells (Subramaniam and Seydoux, 2003). If this is the case, sperm should be present at reduced numbers, as compared to *puf-8* single mutants at 25°C (Subramaniam and Seydoux, 2003). However, wild-type levels (more in some animals) of sperm were formed in *gld-1; puf-8* double mutants hermaphrodites (Table B2). Furthermore, to test if the proximal proliferation was due to dedifferentiation of primary spermatocytes back

into mitotic cells, spermatogenic defective mutants were combined with *gld-1; puf-8* mutant males. The spermatogenic mutant used was *spe-6(hc49)*. *spe-6(hc49)* was shown previously to suppress the *puf-8* dedifferentiation phenotype (Subramaniam and Seydoux, 2003). If the proximal proliferation was due to dedifferentiation of primary spermatocytes, then the 60% of *gld-1; puf-8* males with proximal proliferation should no longer have proximal proliferation in a *spe-6* background. It was observed that ~58% of the *gld-1; puf-8* males analyzed still had proximal proliferation in a *spe-6* background (Table B3). This result suggests that the proximal proliferation was not due to dedifferentiation of male germ cells.

Theory #3: A final possibility for the existence of proximal proliferation in *gld-1; puf-8* hermaphrodites and males is that some mitotic cells were displaced proximally during early germline development and that, over time, the mitotic cells divided to form a Pro tumour. To determine if mitotic cells were present in the proximal regions of larval germ lines, gonads were dissected from late L3 *gld-1; puf-8* double mutant animals and probed with αREC-8 and αHIM-3 antibodies. It was discovered that 4/15 late L3 *gld-1; puf-8* hermaphrodite animals have REC-8 positive cells in the proximal most region of the germ line, while the remaining 11/15 did not. Similar results were seen in *gld-1; puf-8* male L3 germ lines. Since both sexes were affected similarly, this suggests that theory #3 is the most likely reason for why Pro tumours form in *gld-1; puf-8* double mutant animals.

However, why these mitotic cells are misguided is still an important unanswered question. Perhaps GLD-1 and PUF-8 redundantly function to promote meiotic entry during a specific stage in larval development. Stage specific control of meiotic entry has been proposed before (Hansen et al., 2004a; Pepper et al., 2003). In the absence of both *gld-1* and *puf-8*, some mitotic cells may become misplaced/misregulated in the proximal germ line. Sheath cells in the proximal germ line can stimulate proliferation in these misplaced mitotic cells (Killian and Hubbard, 2005), which could then lead the formation of Pro tumours. Certainly, further exploration into the *gld-1 puf-8* interaction will yield interesting information about these important germ line regulators.

APPENDIX C: ADDITIONAL TABLES

Table C1. Additional Phenotypes

Genotype	Temp (°C)	Phenotype	n
glp-1(ar202)	18	WT	10
glp-1(ar202)	25	late onset and Pro tumours	11
puf-8(q725)	18	small germ line	11
puf-8(q725); glp-1(ar202)	18	fully tumourous	35
fbf-1(ok91) fbf-1(q704)	18	Glp, 200 sperm/arm	11
fbf-1(ok91) fbf-1(q704); glp-1(ar202)	18	Glp	10
fbf-1(ok91) fbf-1(q704); glp-1(ar202)	25	robust proliferation, followed by spermatogenesis	14
fbf-1(ok91) fbf-1(q704) puf-8(q725)	18, 20	proliferative zone and sperm	26
fbf-1(ok91) fbf-1(q704) puf-8(q725); glp-1(ar202)	18	no sperm, early meiotic cells, not a very obvious proliferative zone	17
fog-1(e2121)	18	only produces oocytes	7
fog-1(e2121) unc-11(e49); glp-1(ar202)	18	looks like *fog-1(e2121)*	27
fog-1(e2121) unc-11(e49); glp-1(ar202)	25	Tumourous with rare spots of differentiation	12
fog-1(e2121) unc-11(e49); fbf-1(ok91) fbf-1(q704)	18	~10 oocyte-like germ cells, no sperm	18
fog-1(e2121) unc-11(e49); puf-8(q725)	18	looks like *fog-1(e2121)*	15
fog-1(e2121) unc-11(e49); fbf-1(ok91) fbf-1(q704) puf-8(q725)	18	not glp, some semi-differentiated cells present, still has proliferative zone	45
fog-1(e2121) unc-11(e49); fbf-1(ok91) fbf-1(q704) puf-8(q725); glp-1(ar202)	18	enlarged cells, more cells then *fog-1(e2121); fbfs,* still has proliferative zone	14
fog-1(e2121) unc-11(e49); fbf-1(ok91) fbf-1(q704); glp-1(ar202)	18	enlarged cells	7
fog-1(e2121) unc-11(e49); fbf-1(ok91) fbf-1(q704); glp-1(ar202)	25	Variable phenotypes: majority (50%) look mainly tumourous with some spots of differentiation	18

fog-1(e2121) unc-11(e49); puf-8(q725); glp-1(ar202)	18	most are completely tumourous, 1 had sperm	7
unc-11(e49); glp-1(ar202)	18	not very health, see: tum, prox tum, junky sterile, Muv, but some are normal	19
unc-11(e49); glp-1(ar202)	25	Tumourous with rare spots of differentiation	17
unc-11(e49); fbf-1(ok91) fbf-1(q704)	18	Glp, older animals quite degraded	14
unc-11(e49); fbf-1(ok91) fbf-1(q704) puf-8(q725)	18	looks similar to *fbf-1(ok91) fbf-1(q704) puf-8(q725),* distal zone and sperm	12
unc-11(e49); puf-8(q725)	18	relatively WT, potentially a delay in development, see some young adults without oocytes just sperm	10
unc-11(e49); fbf-1(ok91) fbf-1(q704) puf-8(q725); glp-1(ar202)	18	look similar to *fbf puf-8(q725); ar202*, however unc makes gonads smaller, grow slower	40
unc-11(e49); fbf-1(ok91) fbf-1(q704); glp-1(ar202)	18	most have prolif zone-entry into meiosis	20
unc-11(e49); fbf-1(ok91) fbf-1(q704); glp-1(ar202)	25	completely tumourous (100%)	8
unc-11(e49); puf-8(q725); glp-1(ar202)	18	completely tumourous	14
lst-1(ok814)	20	WT	26
lst-1(ok814)	25	WT, ~20% have smaller germ lines	26
lst-1(ok814); puf-8(q725)	20	WT	15
lst-1(ok814); fbf-1(ok91) fbf-1(q704)	20	Glp, 27.5 sperm/arm	19
lst-1(ok814); fbf-1(ok91) fbf-1(q704) puf-8(q725)	20	Glp, 28 sperm/arm	35
lst-1(ok814); glp-1(ar202)	25	mainly they looked like ar202 at restrictive temperatures, but also showed other phenotypes, most striking was a two distal end phenotype (4/18)	18
lst-1(ok814); puf-8(q725); glp-1(ar202)	18	completely tumourous	9
lst-1(ok814); fbf-1(ok91)-2; glp-1(ar202)	25	Sperm-like cells (later stages) and low % mature sperm, some gonads look devoid of cells	20
lst-1(ok814); fbf-1(ok91) fbf-1(q704) puf-8(q725); glp-1(ar202)	18	Sperm-like cells (earlier stages), no mature sperm, some gonads look devoid of cells	9

Further description of each strain listed in Table 4.6, Chapter 4.

Table C2. Strains constructed for use in this study

	Strain Name	Genotype
1	XB133	*gld-2(q497)/ccIs4251 unc-15(e73);unc-4(e120) puf-8(oz192)/mC6g*
2	XB134	*puf-8(oz192) unc-4(e120/mC6g; glp-1(ar202)*
3	XB135	*HA8; glp-1(ar202)*
4	XB138	*puf-8(oz192) unc-4(e120)/mC6g*
5	XB143	*unc-4(e120)/mC6g; unc-32(e189) lin-12(ar170)/hT2; arIs51[cdh-3::GFP; dpy-20(+)]*
6	XB144	*puf-8(oz192) unc-4(e120)/mC6g; unc-32(e189) lin-12(ar170)/hT2; arIs51[cdh-3::GF*
7	XB145	*puf-8(oz192) unc-4(e120)*
8	XB146	*gld-3(q730)/ dpy-10(e128) unc-4(e120)*
9	XB147	*unc-4(e120)/mC6g; unc-32(e189) lin-12(ar170); arIs51[cdh-3::GFP; dpy-20(+)]*
10	XB148	*puf-8(oz192) unc-4(e120)/mC6g; unc-32(e189) lin-12(ar170); arIs51[cdh-3::GFP; dp*
11	XB154	*puf-8(oz192) nos-3(oz231)/ dpy-10(e128) unc-4(e120)*
12	XB159	*unc-85(e1414) clr-1(e1745); glp-1(ar202)*
13	XB160	*puf-8(oz192)/unc-85(e1414) clr-1(e1745); glp-1(ar202)*
14	XB161	*puf-8(oz192)/bli-2(e768) sma-6(e1482); glp-1(ar202)*
15	XB162	*bli-2(e768) sma-6(e1482); glp-1(ar202)*
16	XB163	*puf-8(oz192) nos-3(oz231)/mC6g*
17	XB164	*dpy-10(e128) gld-3(q730)/dpy-10(e128) unc-4(e120); him-5(e1490)*
18	XB167	*dpy-10(e128) gld-3(q730)/ puf-8(oz192) unc-4(e120); him-5(e1490)*
19	XB183	*bli-2(e768) puf-8(oz192)/mC6g; glp-1(ar202)*
20	XB186	*puf-8(oz192)*
21	XB187	*puf-8(oz192)/mC6g*
22	XB202	*gld-1(q485)/hT2; puf-8(oz192) unc-4(e120)/mC6g*
23	XB214	*puf-8(oz192) unc-4(e120)/mC6g; glp-1(oz264gf)*
24	XB213	*pex-3(dx41) dpy-10(e128)/puf-8(oz192) unc-4(e120)*
25	XB212	*puf-8(oz192) unc-4(e120); hT2*
26	XB237	*puf-8(oz192) unc-4(e120); lin-12(n302gf)*
27	XB238	*unc-4(e120); lin-12(n302gf)*
28	XB232	*puf-8(oz192) rol-6(e187)/mC6g; glp-1(ar202gf)*
29	XB239	*puf-8(oz192) unc-4(e120)/bli-2(e768) rol-6(e187); glp-1(ar202)*
30	XB227	*puf-8(oz192) unc-4(e120)/maDf4; glp-1(ar202gf)*
31	XB226	*puf-8(oz192) unc-4(e120)/mDf14; unc-32(e189) glp-1(ar202gf)/hT2*
32	XB225	*puf-8(oz192) unc-4(e120); qIs19(lag-2::GFP)*
33	XB216	*puf-8(oz192) unc-4(e120)/mnDf30; glp-1(ar202gf)*
34	XB218	*puf-8(oz192) rol-6(e187)/ bli-2(e768) rol-6(e187); glp-1(ar202gf)*
35	XB249	*bli-2 (e768) puf-8 (oz192)/HA; glp-1(ar202)*
36	XB248	*puf-8(oz192) rol-6(e187)/HA; glp-1(ar202gf)*
37	XB278	*puf-8(oz192)/mC6g; unc-32(e189) glp-1(ar202)/hT2*

38	XB269	*puf-8(q725)/mC6g; unc-32(e189) glp-1(ar202)/hT2*
39	XB270	*eff-1(hy21); lin-12(n302)*
40	XB265	*puf-8(q725)/mC6g; glp-1(ar202); fem-3(e1996)/unc-24(e138) dpy-20 (e1282)*
41	XB257	*puf-8(oz192)/mC6g; glp-1(ar202)/hT2 ; fem-3(e1996)/unc-24(e138) dpy-20(e1282)*
42	XB259	*puf-8(oz192)/mC6g; glp-1(ar202) ; fem-3(e1996)/unc-24(e138) dpy-20(e1282)*
43	XB285	*daf-16(mu86); puf-8(q725)/mC6g; glp-1(ar202gf)*
44	XB303	*puf-8(q725); fem-3(e1996)/unc-24(e138) dpy-20(e1282)*
45	XB304	*fbf-1(ok91) fbf-2(q704) puf-8(q725)/mC6g*
46	XB305	*fbf-1(ok91) fbf-2(q704) puf-8(q725)/bli-2(e768) rol-6(e187)*
47	XB306	*puf-8(q725)/mC6g; glp-1(oz264)*
48	XB297	*puf-8(oz192)/mC6g; glp-1(bn18)*
49	XB295	*ugEx9[puf-8::gfp, rol-6gf]*
50	XB296	*ugEx8[puf-8::gfp, rol-6gf]*
51	XB288	*rol-6(e187) fbf-1(ok91) fbf-2(q704)/mC6g*
52	XB287	*puf-8(q725)/bli-2(e768) rol-6(e187)*
53	XB289	*bli-2(e768) puf-8(q725)*
54	XB286	*fbf-1(ok91) fbf-2(q704)/bli-2(e768) rol-6(e187)*
55	XB283	*puf-8(q725); glp-1(bn18)*
56	XB315	*fbf-1(ok91) fbf-2(q704) puf-8(q725)/mC6g; glp-1(ar202)*
57	XB316	*puf-8(q725); unc-32(e189) glp-1(oz112oz120)*
58	XB317	*puf-8(oz192)/mC6g; sel-10(bc243)*
59	XB318	*unc-11(e47); fbf-1(ok91) fbf-2(q704) puf-8(q725)/mC6g*
60	XB319	*puf-8(oz192)/mC6g; unc-32(e189) glp-1(q175)/hT2*
61	XB321	*puf-8(q725)/mC6g; fem-3(e1996)/unc-24(e138) dpy-20 (e1282)*
62	XB322	*puf-8(q725)/mC6g; unc-32(e189) glp-1(q175)/hT2*
63	XB323	*puf-8(q725); lin-12(n302)*
64	XB344	*fog-1(e2121) unc-11(e47)/hT2; fbf-1(ok91) fbf-2(q704)/ mC6g*
65	XB345	*fog-1(e2121) unc-11(e47)/hT2; puf-8(q725)/ mC6g*
66	XB346	*fog-1(e2121) unc-11(e47)/hT2; fbf-1(ok91) fbf-2(q704) puf-8(q725)/ mC6g*
67	XB350	*unc-11(e47)/hT2; puf-8(q725)/mC6g*
68	XB351	*unc-11(e47)/hT2; fbf-1(ok91) fbf-2(q704)/mC6g*
69	XB352	*fog-1(e2121) unc-11(e47)/hT2; glp-1(ar202)/hT2*
70	XB348	*fog-1(e2121) unc-11(e47)/hT2; puf-8(q725)/mC6g; glp-1(ar202)/hT2*
71	XB353	*unc-11(e47)/hT2; glp-1(ar202)/hT2*
72	XB347	*fog-1(e2121) unc-11(e47)/hT2; fbf-1(ok91) fbf-2(q704) puf-8(q725)/mC6g; glp-1(ar*
73	XB366	*glp-1(ar202)/spe-6(hc49) unc-25(e156)*
74	XB364	*puf-8(q725)/mC6g; glp-1(ar202) spe-6(hc49) unc-25(e156)/hT2*
75	XB365	*glp-1(ar202) spe-6(hc49) unc-25(e156)/hT2g*
76	XB362	*lst-1(ok814); puf-8(q725)*
77	XB360	*lst-1(ok814); fbf-1(ok91) fbf-2(q704) puf-8(q725)/mC6g; glp-1(ar202)*
78	XB363	*lst-1(ok814); fbf-1(ok91) fbf-2(q704) puf-8(q725)/mC6g*

79	XB358	*unc-11(e47)/hT2; fbf-1(ok91) fbf-2(q704) puf-8(q725)/mC6g; glp-1(ar202)/hT2*
80	XB359	*unc-11(e47)/hT2; puf-8(q725)/mC6g; glp-1(ar202)/hT2*
81	XB357	*unc-11(e47)/hT2; fbf-1(ok91) fbf-2(q704)/mC6g; glp-1(ar202)/hT2*
82	XB361	*lst-1(ok814); fbf-1(ok91) fbf-2(q704)/mC6g*
83	XB371	*dpy-10(e128) puf-8(oz192)*
84	XB373	*gld-3(q730) unc-4(e120)/mC6g*
85	XB372	*gld-3(q730) unc-4(e120)/dpy-10(e128) unc-4(e120)*
86	XB374	*unc-11(e47)/hT2g; glp-1(ar202)/hT2g*
87	XB375	*gld-1(q485)/ccIs4251unc-13; puf-8(q725)/mC6g; fem-3(e1996)/unc-24(e138) dpy-2*
88	XB381	*puf-8(q725)/mC6g; lin-12(q269) glp-1(q231)/hT2*
89	XB382	*gld-3(q730) puf-8(oz192)/dpy-10(e128) unc-4(e120)*
90	XB383	*gld-1(q485)/hT2; puf-8(q725); spe-6(hc49) unc-25(e156)/hT2*
91	XB384	*gld-1(q485)/ccIs4251unc-13; puf-8(q725)*
92	XB349	*fog-1(e2121) unc-11(e47)/hT2; fbf-1(ok91) fbf-2(q704)/mC6g; glp-1(ar202)/hT2*
93	XB391	*gld-3(q730) puf-8(oz192)/mC6g*
94	XB390	*rrf-1(pk1417); puf-8(q725)/mC6g; glp-1(ar202)*
95	XB389	*puf-8(q725)/mC6g; spe-6(hc49) unc-25(e156)/hT2*
96	XB388	*gld-1(q485)/hT2; spe-6(hc49) unc-25(e156)/hT2*
97	XB392	*glp-1(ar202); fem-3(e1996)/unc-24(e138) dpy-20(e1282)*
98	XB393	*lst-1(ok814)/hT2; glp-1(ar202)/hT2*
99	XB394	*lst-1(ok814); puf-8(q725)/mC6g; glp-1(ar202)*
100	XB395	*lst-1(ok814); fbf-1(ok91) fbf-2(q704)/mC6g; glp-1(ar202)*
101	XB396	*gld-1(q485)/hT2; puf-8(q725); unc-32(e189) glp-1(q175)/hT2*
102	XB397	*gld-3(q730)/mC6g*
103	XB405	*gld-1(q485)/ccIs4251unc-13; puf-8(q725)/mC6g; fog-2(q71)/unc-76(e911) rol-9(sc1*
104	XB399	*gld-1(q485)/ccIs4251unc-13; fog-2(q71)/unc-76(e911) rol-9(sc148)*
105	XB398	*puf-8(q725)/mC6g; fog-2(q71)/unc-76(e911) rol-9(sc148)*
106	XB401	*ugSi1 (puf-8(+)::gfp::tap #1)*
107	XB403	*puf-8(q725); ugSi1(puf-8(+)::gfp::tap #1)*
108	XB404	*puf-8(q725); glp-1(ar202); ugSi1(puf-8(+)::gfp::tap #1)*
109	XB400	*ccIs4251unc-13/+; mC6g; unc-76(e911) rol-9(sc148)/SC4*
110	XB406	*gld-2(q497)/ ccIs4251 unc-15(e73); puf-8(oz192)/ mC6g*
111	XB426	*puf-8(oz192)/mC6g; glp-1(ar202); ugSi1*
112	XB427	*puf-8(oz192)/mC6g; glp-1(ar202)/hT2; ugSi1*
113	XB428	*glp-1(ar202); ugSi1*
114	XB432	*puf-8(q725)/mC6g; glp-1(oz264); ugSi1*
115	XB433	*glp-1(oz264); ugSi1*
116	XB449	*ain-2(tm2432); glp-1(oz264)*
117	XB448	*ain-2(tm2432); puf-8(q725)*
118	XB450	*puf-8(q725)/mC6g; glp-1(ar202)/hT2; sel-10(bc243)*

List of the strains generated throughout this thesis.

References

Ahringer, J., and Kimble, J. (1991). Control of the sperm-oocyte switch in *Caenorhabditis elegans* hermaphrodites by the *fem-3* 3' untranslated region. Nature *349*, 346-348.

Anderson, P. (1995). Mutagenesis. Methods Cell Biol *48*, 31-58.

Ariz, M., Mainpal, R., and Subramaniam, K. (2009). *C. elegans* RNA-binding proteins PUF-8 and MEX-3 function redundantly to promote germline stem cell mitosis. Developmental Biology *326*, 295-304.

Ashcroft, N., and Golden, A. (2002). CDC-25.1 regulates germline proliferation in *Caenorhabditis elegans*. Genesis *33*, 1-7.

Austin, J., and Kimble, J. (1987). *glp-1* is required in the germ line for regulation of the decision between mitosis and meiosis in *C. elegans*. Cell *51*, 589-599.

Bachorik, J.L. (2005). A genetic and molecular analysis of *Caenorhabditis elegans puf-8* and *fbf-1* in germline sex determination and proliferation (Madison, The University of Wisconsin).

Bachorik, J.L., and Kimble, J. (2005). Redundant control of the *Caenorhabditis elegans* sperm/oocyte switch by PUF-8 and FBF-1, two distinct PUF RNA-binding proteins. Proc Natl Acad Sci U S A *102*, 10893-10897.

Barton, M.K., and Kimble, J. (1990). *fog-1*, a regulatory gene required for specification of spermatogenesis in the germ line of *Caenorhabditis elegans*. Genetics *125*, 29-39.

Belfiore, M., Mathies, L.D., Pugnale, P., Moulder, G., Barstead, R., Kimble, J., and Puoti, A. (2002). The MEP-1 zinc-finger protein acts with MOG DEAH box proteins to control gene expression via the *fem-3* 3' untranslated region in *Caenorhabditis elegans*. RNA (New York, NY *8*, 725-739.

Bernstein, D.S., Buter, N., Stumpf, C., and Wickens, M. (2002). Analyzing mRNA-protein complexes using a yeast three-hybrid system. Methods (San Diego, Calif *26*, 123-141.

Berry, L.W., Westlund, B., and Schedl, T. (1997). Germ-line tumor formation caused by activation of *glp-1*, a *Caenorhabditis elegans* member of the Notch family of receptors. Development *124*, 925-936.

Bettegowda, A., and Wilkinson, M.F. (2010). Transcription and post-transcriptional regulation of spermatogenesis. Philos Trans R Soc Lond B Biol Sci *365*, 1637-1651.

Bonnet, D., and Dick, J.E. (1997). Human acute myeloid leukemia is organized as a hierarchy that originates from a primitive hematopoietic cell. Nat Med *3*, 730-737.

Boxem, M., Srinivasan, D.G., and van den Heuvel, S. (1999). The *Caenorhabditis elegans* gene *ncc-1* encodes a cdc2-related kinase required for M phase in meiotic and mitotic cell divisions, but not for S phase. Development *126*, 2227-2239.

Brenner, S. (1973). The genetics of behaviour. Br Med Bull *29*, 269-271.

Brenner, S. (1974). The genetics of *Caenorhabditis elegans*. Genetics *77*, 71-94.

Brinster, R.L. (2002). Germline stem cell transplantation and transgenesis. Science *296*, 2174-2176.

Brinster, R.L., and Avarbock, M.R. (1994). Germline transmission of donor haplotype following spermatogonial transplantation. Proc Natl Acad Sci U S A *91*, 11303-11307.

Brinster, R.L., and Zimmermann, J.W. (1994). Spermatogenesis following male germ-cell transplantation. Proc Natl Acad Sci U S A *91*, 11298-11302.

Brown, E.H., and King, R.C. (1964). Studies on the Events Resulting in the Formation of an Egg Chamber in Drosophila Melanogaster. Growth *28*, 41-81.

Buaas, F.W., Kirsh, A.L., Sharma, M., McLean, D.J., Morris, J.L., Griswold, M.D., de Rooij, D.G., and Braun, R.E. (2004). Plzf is required in adult male germ cells for stem cell self-renewal. Nature genetics *36*, 647-652.

Calvi, L.M., Adams, G.B., Weibrecht, K.W., Weber, J.M., Olson, D.P., Knight, M.C., Martin, R.P., Schipani, E., Divieti, P., Bringhurst, F.R.*, et al.* (2003). Osteoblastic cells regulate the haematopoietic stem cell niche. Nature *425*, 841-846.

Carlson, M. (1997). Genetics of transcriptional regulation in yeast: connections to the RNA polymerase II CTD. Annual review of cell and developmental biology *13*, 1-23.

Chen, D., and McKearin, D. (2003). Dpp signaling silences bam transcription directly to establish asymmetric divisions of germline stem cells. Curr Biol *13*, 1786-1791.

Chen, G., Li, W., Zhang, Q.S., Regulski, M., Sinha, N., Barditch, J., Tully, T., Krainer, A.R., Zhang, M.Q., and Dubnau, J. (2008). Identification of synaptic targets of Drosophila pumilio. PLoS computational biology *4*, e1000026.

Chen, J., Li, X., and Greenwald, I. (2004). *sel-7*, a positive regulator of *lin-12* activity, encodes a novel nuclear protein in *Caenorhabditis elegans*. Genetics *166*, 151-160.

Cheong, C.G., and Hall, T.M. (2006). Engineering RNA sequence specificity of Pumilio repeats. Proc Natl Acad Sci U S A *103*, 13635-13639.

Chew, J., Biswas, S., Shreeram, S., Humaidi, M., Wong, E.T., Dhillion, M.K., Teo, H., Hazra, A., Fang, C.C., Lopez-Collazo, E.*, et al.* (2009). WIP1 phosphatase is a negative regulator of NF-kappaB signalling. Nat Cell Biol *11*, 659-666.

Chitwood, B.G., and Chitwood, M.B. (1950). An introduction to nematology (Baltimore, University Park Press).

Cho, M.S., Lee, Y.E., Kim, J.Y., Chung, S., Cho, Y.H., Kim, D.S., Kang, S.M., Lee, H., Kim, M.H., Kim, J.H.*, et al.* (2008). Highly efficient and large-scale generation of functional dopamine neurons from human embryonic stem cells. Proc Natl Acad Sci U S A *105*, 3392-3397.

Cho, P.F., Gamberi, C., Cho-Park, Y.A., Cho-Park, I.B., Lasko, P., and Sonenberg, N. (2006). Cap-dependent translational inhibition establishes two opposing morphogen gradients in Drosophila embryos. Curr Biol *16*, 2035-2041.

Christensen, S., Kodoyianni, V., Bosenberg, M., Friedman, L., and Kimble, J. (1996). lag-1, a gene required for *lin-12* and *glp-1* signaling in *Caenorhabditis elegans*, is homologous to human CBF1 and Drosophila Su(H). Development *122*, 1373-1383.

Chritton, J.J., and Wickens, M. (2010). Translational repression by PUF proteins in vitro. RNA (New York, NY *16*, 1217-1225.

Cinquin, O., Crittenden, S.L., Morgan, D.E., and Kimble, J. (2010). Progression from a stem cell-like state to early differentiation in the *C. elegans* germ line. Proceedings of the National Academy of Sciences of the United States of America *107*, 2048-2053.

Consortium, C.e.S. (1998). Genome sequence of the nematode *C. elegans*: a platform for investigating biology. Science *282*, 2012-2018.

Costoya, J.A., Hobbs, R.M., Barna, M., Cattoretti, G., Manova, K., Sukhwani, M., Orwig, K.E., Wolgemuth, D.J., and Pandolfi, P.P. (2004). Essential role of Plzf in maintenance of spermatogonial stem cells. Nature genetics *36*, 653-659.

Crittenden, S., and Kimble, J. (2009). Preparation and immunolabeling of *Caenorhabditis elegans*. Cold Spring Harb Protoc *2009*, pdb prot5216.

Crittenden, S.L., Bernstein, D.S., Bachorik, J.L., Thompson, B.E., and Gallegos, M. (2002). A conserved RNA-binding protein controls germline stem cells in *Caenorhabditis elegans*. Nature *417*, 660.

Crittenden, S.L., Troemel, E.R., Evans, T.C., and Kimble, J. (1994). GLP-1 is localized to the mitotic region of the *C. elegans* germ line. Development *120*, 2901.

Curtis, D., Lehmann, R., and Zamore, P.D. (1995). Translational regulation in development. Cell *81*, 171-178.

D'Agostino, I., Merritt, C., Chen, P.L., Seydoux, G., and Subramaniam, K. (2006). Translational repression restricts expression of the *C. elegans* Nanos homolog NOS-2 to the embryonic germline. Dev Biol *292*, 244-252.

de Rooij, D.G., Okabe, M., and Nishimune, Y. (1999). Arrest of spermatogonial differentiation in jsd/jsd, Sl17H/Sl17H, and cryptorchid mice. Biol Reprod *61*, 842-847.

de Souza, N., Vallier, L.G., Fares, H., and Greenwald, I. (2007). SEL-2, the *C. elegans* neurobeachin/LRBA homolog, is a negative regulator of *lin-12*/Notch activity and affects endosomal traffic in polarized epithelial cells. Development *134*, 691-702.

Denis, C.L., and Chen, J. (2003). The CCR4-NOT complex plays diverse roles in mRNA metabolism. Progress in nucleic acid research and molecular biology *73*, 221-250.

Deppe, U., Schierenberg, E., Cole, T., Krieg, C., Schmitt, D., Yoder, B., and von Ehrenstein, G. (1978). Cell lineages of the embryo of the nematode *Caenorhabditis elegans*. Proc Natl Acad Sci U S A *75*, 376-380.

Dernburg, A.F., McDonald, K., Moulder, G., Barstead, R., Dresser, M., and Villeneuve, A.M. (1998). Meiotic recombination in *C. elegans* initiates by a conserved mechanism and is dispensable for homologous chromosome synapsis. Cell *94*, 387-398.

Dougherty, E.C., and Calhoun, H.G. (1948). Possible significance of free-living nematodes in genetic research. Nature *161*, 29.

Doyle, T.G., Wen, C., and Greenwald, I. (2000). SEL-8, a nuclear protein required for LIN-12 and GLP-1 signaling in *Caenorhabditis elegans*. Proc Natl Acad Sci U S A *97*, 7877-7881.

Eckmann, C., Crittenden, S.L., Suh, N., and Kimble, J. (2004). GLD-3 and control of the mitosis/meiosis decision in the germline of *Caenorhabditis elegans*. Genetics *168*, 147.

Eckmann, C.R., Kraemer, B., Wickens, M., and Kimble, J. (2002). GLD-3, a bicaudal-C homolog that inhibits FBF to control germline sex determination in *C. elegans*. Dev Cell *3*, 697-710.

Edwards, T.A., Pyle, S.E., Wharton, R.P., and Aggarwal, A.K. (2001). Structure of Pumilio reveals similarity between RNA and peptide binding motifs. Cell *105*, 281-289.

Fares, H., and Greenwald, I. (1999). SEL-5, a serine/threonine kinase that facilitates *lin-12* activity in *Caenorhabditis elegans*. Genetics *153*, 1641-1654.

Fassas, A., Anagnostopoulos, A., Kazis, A., Kapinas, K., Sakellari, I., Kimiskidis, V., Smias, C., Eleftheriadis, N., and Tsimourtou, V. (2000). Autologous stem cell transplantation in progressive multiple sclerosis--an interim analysis of efficacy. J Clin Immunol *20*, 24-30.

Fay, D. (2006). Genetic mapping and manipulation: chapter 5--SNPs: three-point mapping. WormBook, 1-4.

Fay, D.S., and Han, M. (2000). Mutations in *cye-1*, a *Caenorhabditis elegans* cyclin E homolog, reveal coordination between cell-cycle control and vulval development. Development *127*, 4049-4060.

Ferguson, E.L., and Horvitz, H.R. (1985). Identification and characterization of 22 genes that affect the vulval cell lineages of the nematode *Caenorhabditis elegans*. Genetics *110*, 17-72.

Fitzgerald, K., Wilkinson, H.A., and Greenwald, I. (1993). *glp-1* can substitute for *lin-12* in specifying cell fate decisions in *Caenorhabditis elegans*. Development *119*, 1019-1027.

Forbes, A., and Lehmann, R. (1998). Nanos and Pumilio have critical roles in the development and function of Drosophila germline stem cells. Development *125*, 679-690.

Fox, M., Urano, J., and Reijo Pera, R.A. (2005). Identification and characterization of RNA sequences to which human PUMILIO-2 (PUM2) and deleted in Azoospermia-like (DAZL) bind. Genomics *85*, 92-105.

Francis, R., Barton, M.K., Kimble, J., and Schedl, T. (1995a). *gld-1*, a tumor suppressor gene required for oocyte development in *Caenorhabditis elegans*. Genetics *139*, 579-606.

Francis, R., Maine, E., and Schedl, T. (1995b). Analysis of the multiple roles of *gld-1* in germline development: interactions with the sex determination cascade and the *glp-1* signaling pathway. Genetics *139*, 607-630.

Frank, D.J., and Roth, M.B. (1998). *ncl-1* is required for the regulation of cell size and ribosomal RNA synthesis in *Caenorhabditis elegans*. J Cell Biol *140*, 1321-1329.

Frokjaer-Jensen, C., Davis, M.W., Hopkins, C.E., Newman, B.J., Thummel, J.M., Olesen, S.P., Grunnet, M., and Jorgensen, E.M. (2008). Single-copy insertion of transgenes in *Caenorhabditis elegans*. Nature genetics *40*, 1375-1383.

Fukushige, T., Hawkins, M.G., and McGhee, J.D. (1998). The GATA-factor *elt-2* is essential for formation of the *Caenorhabditis elegans* intestine. Dev Biol *198*, 286-302.

Goldstrohm, A.C., Hook, B.A., Seay, D.J., and Wickens, M. (2006). PUF proteins bind Pop2p to regulate messenger RNAs. Nat Struct Mol Biol *13*, 533-539.

Goldstrohm, A.C., Seay, D.J., Hook, B.A., and Wickens, M. (2007). PUF protein-mediated deadenylation is catalyzed by Ccr4p. The Journal of biological chemistry *282*, 109-114.

Grant, B., and Greenwald, I. (1996). The *Caenorhabditis elegans sel-1* gene, a negative regulator of *lin-12* and *glp-1*, encodes a predicted extracellular protein. Genetics *143*, 237-247.

Greenwald, I. (1998). LIN-12/Notch signaling: lessons from worms and flies. Genes Dev *12*, 1751-1762.

Greenwald, I.S., Ferguson, E.L., Tsung, N., and Horvitz, H.R. (1981). A complex locus affecting vulva development in *C. elegans*. Worm Breeder's Gazette *6*.

Greenwald, I.S., Sternberg, P.W., and Horvitz, H.R. (1983). The *lin-12* locus specifies cell fates in *Caenorhabditis elegans*. Cell *34*, 435-444.

Hafner, M., Landthaler, M., Burger, L., Khorshid, M., Hausser, J., Berninger, P., Rothballer, A., Ascano, M., Jr., Jungkamp, A.C., Munschauer, M.*, et al.* (2010). Transcriptome-wide identification of RNA-binding protein and microRNA target sites by PAR-CLIP. Cell *141*, 129-141.

Hagele, S., Kuhn, U., Boning, M., and Katschinski, D.M. (2009). Cytoplasmic polyadenylation-element-binding protein (CPEB)1 and 2 bind to the HIF-1alpha mRNA 3'-UTR and modulate HIF-1alpha protein expression. Biochem J *417*, 235-246.

Hansen, D., Hubbard, E.J., and Schedl, T. (2004a). Multi-pathway control of the proliferation versus meiotic development decision in the *Caenorhabditis elegans* germline. Dev Biol *268*, 342.

Hansen, D., and Schedl, T. (2006). The regulatory network controlling the proliferation-meiotic entry decision in the *Caenorhabditis elegans* germ line. Current topics in developmental biology *76*, 185-215.

Hansen, D., Wilson-Berry, L., Dang, T., and Schedl, T. (2004b). Control of the proliferation versus meiotic development decision in the *C. elegans* germline through regulation of GLD-1 protein accumulation. Development *131*, 93-104.

Henderson, S.T., Gao, D., Lambie, E.J., and Kimble, J. (1994). *lag-2* may encode a signaling ligand for the GLP-1 and LIN-12 receptors of *C. elegans*. Development *120*, 2913-2924.

Hill, D.P., Shakes, D.C., Ward, S., and Strome, S. (1989). A sperm-supplied product essential for initiation of normal embryogenesis in *Caenorhabditis elegans* is encoded by the paternal-effect embryonic-lethal gene, spe-11. Dev Biol *136*, 154-166.

Hirsh, D., Oppenheim, D., and Klass, M. (1976). Development of the reproductive system of *Caenorhabditis elegans*. Dev Biol *49*, 200-219.

Hodgkin, J. (1986). Sex determination in the nematode *C. elegans*: analysis of *tra-3* suppressors and characterization of fem genes. Genetics *114*, 15-52.

Hodgkin, J. (2005). Karyotype, ploidy, and gene dosage. WormBook, 1-9.

Hodgkin, J., and Martinelli, S. (1999). 1999 Genetic Map of *Caenorhabditis elegans* (St. Paul, MN, *Caenorhabditis elegans* Genetics Center).

Hofmann, M.C., Braydich-Stolle, L., and Dym, M. (2005). Isolation of male germ-line stem cells; influence of GDNF. Dev Biol *279*, 114-124.

Hook, B., Bernstein, D., Zhang, B., and Wickens, M. (2005). RNA-protein interactions in the yeast three-hybrid system: affinity, sensitivity, and enhanced library screening. RNA (New York, NY *11*, 227-233.

Hook, B.A., Goldstrohm, A.C., Seay, D.J., and Wickens, M. (2007). Two yeast PUF proteins negatively regulate a single mRNA. The Journal of biological chemistry *282*, 15430-15438.

Hope, I.A. (1999). *C. elegans*: A Practical Approach (Oxford University Press).

Horton, R.M. (1995). PCR-mediated recombination and mutagenesis. SOEing together tailor-made genes. Molecular biotechnology *3*, 93-99.

Hubbard, E.J., Dong, Q., and Greenwald, I. (1996). Evidence for physical and functional association between EMB-5 and LIN-12 in *Caenorhabditis elegans*. Science *273*, 112-115.

Hubbard, E.J., and Greenstein, D. (2005). Introduction to the germ line. WormBook, 1-4.

Hubbard, E.J., Wu, G., Kitajewski, J., and Greenwald, I. (1997). *sel-10*, a negative regulator of lin-12 activity in *Caenorhabditis elegans*, encodes a member of the CDC4 family of proteins. Genes Dev *11*, 3182-3193.

Imayoshi, I., Sakamoto, M., Yamaguchi, M., Mori, K., and Kageyama, R. (2010). Essential roles of Notch signaling in maintenance of neural stem cells in developing and adult brains. J Neurosci *30*, 3489-3498.

Jakubowski, J., and Kornfeld, K. (1999). A local, high-density, single-nucleotide polymorphism map used to clone *Caenorhabditis elegans* cdf-1. Genetics *153*, 743-752.

Jan, E., Motzny, C.K., Graves, L.E., and Goodwin, E.B. (1999). The STAR protein, GLD-1, is a translational regulator of sexual identity in *Caenorhabditis elegans*. EMBO J *18*, 258.

Janke, C., Rogowski, K., and van Dijk, J. (2008). Polyglutamylation: a fine-regulator of protein function? 'Protein Modifications: beyond the usual suspects' review series. EMBO Rep *9*, 636-641.

Jedamzik, B., and Eckmann, C.R. (2009). Analysis of RNA-protein complexes by RNA coimmunoprecipitation and RT-PCR analysis from *Caenorhabditis elegans*. Cold Spring Harb Protoc *2009*, pdb prot5300.

Jin, S.W., Arno, N., Cohen, A., Shah, A., Xu, Q., Chen, N., and Ellis, R.E. (2001). In *Caenorhabditis elegans*, the RNA-binding domains of the cytoplasmic polyadenylation element binding protein FOG-1 are needed to regulate germ cell fates. Genetics *159*, 1617-1630.

Jones, A.R., Francis, R., and Schedl, T. (1996). GLD-1, a cytoplasmic protein essential for oocyte differentiation, shows stage- and sex-specific expression during *Caenorhabditis elegans* germline development. Dev Biol *180*, 165-183.

Jones, A.R., and Schedl, T. (1995). Mutations in *gld-1*, a female germ cell-specific tumor suppressor gene in *Caenorhabditis elegans*, affect a conserved domain also found in Src-associated protein Sam68. Genes Dev *9*, 1491-1504.

Jones, P.H., and Watt, F.M. (1993). Separation of human epidermal stem cells from transit amplifying cells on the basis of differences in integrin function and expression. Cell *73*, 713-724.

Jones, R.C., and Lin, M. (1993). Spermatogenesis in birds. Oxf Rev Reprod Biol *15*, 233-264.

Kadyk, L.C., and Kimble, J. (1998). Genetic regulation of entry into meiosis in *Caenorhabditis elegans*. Development *125*, 1803-1813.

Kageyama, R., Ohtsuka, T., Shimojo, H., and Imayoshi, I. (2008). Dynamic Notch signaling in neural progenitor cells and a revised view of lateral inhibition. Nat Neurosci *11*, 1247-1251.

Kamath, R.S., and Ahringer, J. (2003). Genome-wide RNAi screening in *Caenorhabditis elegans*. Methods *30*, 313-321.

Kaye, J.A., Rose, N.C., Goldsworthy, B., Goga, A., and L'Etoile, N.D. (2009). A 3'UTR pumilio-binding element directs translational activation in olfactory sensory neurons. Neuron *61*, 57-70.

Kerins, J. (2006). PRP-17 and the premRNA splicing pathway are preferentially required for the proliferation versus meiotic development decision and germline sex determination in *Caenorhabditis elegans* (St. Louis, Washington University).

Kerins, J.A., Hanazawa, M., Dorsett, M., and Schedl, T. (2010). PRP-17 and the pre-mRNA splicing pathway are preferentially required for the proliferation versus meiotic development decision and germline sex determination in *Caenorhabditis elegans*. Dev Dyn *239*, 1555-1572.

Killian, D.J., and Hubbard, E.J. (2005). *Caenorhabditis elegans* germline patterning requires coordinated development of the somatic gonadal sheath and the germ line. Dev Biol *279*, 322-335.

Kimble, J., and Crittenden, S.L. (2007). Controls of germline stem cells, entry into meiosis, and the sperm/oocyte decision in *Caenorhabditis elegans*. Annual review of cell and developmental biology *23*, 405-433.

Kimble, J., and Hirsh, D. (1979). The postembryonic cell lineages of the hermaphrodite and male gonads in *Caenorhabditis elegans*. Dev Biol *70*, 396-417.

Kimble, J.E., and White, J.G. (1981). On the control of germ cell development in *Caenorhabditis elegans*. Dev Biol *81*, 208-219.

Kodoyianni, V., Maine, E.M., and Kimble, J. (1992). Molecular basis of loss-of-function mutations in the glp-1 gene of *Caenorhabditis elegans*. Mol Biol Cell *3*, 1199-1213.

Koh, Y.Y., Opperman, L., Stumpf, C., Mandan, A., Keles, S., and Wickens, M. (2009). A single *C. elegans* PUF protein binds RNA in multiple modes. RNA (New York, NY *15*, 1090-1099.

Kopan, R., and Ilagan, M.X. (2009). The canonical Notch signaling pathway: unfolding the activation mechanism. Cell *137*, 216-233.

Kraemer, B., Crittenden, S., Gallegos, M., Moulder, G., Barstead, R., Kimble, J., and Wickens, M. (1999). NANOS-3 and FBF proteins physically interact to control the sperm-oocyte switch in *Caenorhabditis elegans*. Curr Biol *9*, 1009-1018.

Kuo, M.W., Wang, S.H., Chang, J.C., Chang, C.H., Huang, L.J., Lin, H.H., Yu, A.L., Li, W.H., and Yu, J. (2009). A novel *puf-A* gene predicted from evolutionary analysis is involved in the development of eyes and primordial germ-cells. PLoS ONE *4*, e4980.

Lambie, E.J., and Kimble, J. (1991). Two homologous regulatory genes, *lin-12* and *glp-1*, have overlapping functions. Development *112*, 231-240.

Lamont, L.B., Crittenden, S.L., Bernstein, D., Wickens, M., and Kimble, J. (2004). FBF-1 and FBF-2 regulate the size of the mitotic region in the *C. elegans* germline. Dev Cell *7*, 697-707.

Lanza, R.P. (2004). Handbook of stem cells, Volume 1, Vol 1 (Burlington, Elsevier Academic Press).

Lee, M.H., and Schedl, T. (2001). Identification of in vivo mRNA targets of GLD-1, a maxi-KH motif containing protein required for *C. elegans* germ cell development. Genes Dev *15*, 2408-2420.

Lee, M.H., and Schedl, T. (2004). Translation repression by GLD-1 protects its mRNA targets from nonsense-mediated mRNA decay in *C. elegans*. Genes Dev *18*, 1047-1059.

Lehmann-Blount, K.A., and Williamson, J.R. (2005). Shape-specific nucleotide binding of single-stranded RNA by the GLD-1 STAR domain. J Mol Biol *346*, 91-104.

Lesney, M.S. (2001). Ecce homology: A primer on comparative genomics. Modern Drug Discovery *4*, 26-38.

Levitan, D., and Greenwald, I. (1995). Facilitation of *lin-12*-mediated signalling by *sel-12*, a *Caenorhabditis elegans* S182 Alzheimer's disease gene. Nature *377*, 351-354.

Li, Y., Jiang, Z., Chen, H., and Ma, W.J. (2004). A modified quantitative EMSA and its application in the study of RNA--protein interactions. J Biochem Biophys Methods *60*, 85-96.

Lin, H. (1997). The tao of stem cells in the germline. Annu Rev Genet *31*, 455-491.

Lin, H. (2002). The stem-cell niche theory: lessons from flies. Nat Rev Genet *3*, 931-940.

Lin, H., and Spradling, A.C. (1993). Germline stem cell division and egg chamber development in transplanted Drosophila germaria. Dev Biol *159*, 140-152.

Lin, H., and Spradling, A.C. (1997). A novel group of pumilio mutations affects the asymmetric division of germline stem cells in the Drosophila ovary. Development *124*, 2463-2476.

Lublin, A.L., and Evans, T.C. (2007). The RNA-binding proteins PUF-5, PUF-6, and PUF-7 reveal multiple systems for maternal mRNA regulation during *C. elegans* oogenesis. Dev Biol *303*, 635-649.

Luitjens, C., Gallegos, M., Kraemer, B., Kimble, J., and Wickens, M. (2000). CPEB proteins control two key steps in spermatogenesis in *C. elegans*. Genes Dev *14*, 2596-2609.

Macdonald, L.D., Knox, A., and Hansen, D. (2008). Proteasomal regulation of the proliferation vs. meiotic entry decision in the *Caenorhabditis elegans* germ line. Genetics *180*, 905-920.

MacQueen, A.J., and Villeneuve, A.M. (2001). Nuclear reorganization and homologous chromosome pairing during meiotic prophase require *C. elegans chk-2*. Genes Dev *15*, 1674-1687.

Maduro, M., and Pilgrim, D. (1995). Identification and cloning of *unc-119*, a gene expressed in the *Caenorhabditis elegans* nervous system. Genetics *141*, 977-988.

Maine, E.M., Hansen, D., Springer, D., and Vought, V.E. (2004). *Caenorhabditis elegans atx-2* promotes germline proliferation and the oocyte fate. Genetics *168*, 817-830.

Maine, E.M., and Kimble, J. (1993). Suppressors of *glp-1*, a gene required for cell communication during development in *Caenorhabditis elegans*, define a set of interacting genes. Genetics *135*, 1011-1022.

Mantina, P., MacDonald, L., Kulaga, A., Zhao, L., and Hansen, D. (2009). A mutation in *teg-4,* which encodes a protein homologous to the SAP130 pre-mRNA splicing factor, disrupts the balance between proliferation and differentiation in the *C. elegans* germ line. Mech Dev *126*, 417-429.

McCarter, J., Bartlett, B., Dang, T., and Schedl, T. (1997). Soma-germ cell interactions in *Caenorhabditis elegans*: multiple events of hermaphrodite germline development require the somatic sheath and spermathecal lineages. Dev Biol *181*, 121-143.

McCarthy, J.E. (1998). Posttranscriptional control of gene expression in yeast. Microbiol Mol Biol Rev *62*, 1492-1553.

McKay, R. (1997). Stem cells in the central nervous system. Science *276*, 66-71.

Mello, C.C., Schubert, C., Draper, B., Zhang, W., Lobel, R., and Priess, J.R. (1996). The PIE-1 protein and germline specification in *C. elegans* embryos. Nature *382*, 710-712.

Mendez, R., and Richter, J.D. (2001). Translational control by CPEB: a means to the end. Nature reviews *2*, 521-529.

Meng, X., Lindahl, M., Hyvonen, M.E., Parvinen, M., de Rooij, D.G., Hess, M.W., Raatikainen-Ahokas, A., Sainio, K., Rauvala, H., Lakso, M.*, et al.* (2000). Regulation of cell fate decision of undifferentiated spermatogonia by GDNF. Science *287*, 1489-1493.

Merritt, C., Rasoloson, D., Ko, D., and Seydoux, G. (2008). 3' UTRs Are the Primary Regulators of Gene Expression in the *C. elegans* Germline. Curr Biol.

Mohler, W.A., Shemer, G., del Campo, J.J., Valansi, C., Opoku-Serebuoh, E., Scranton, V., Assaf, N., White, J.G., and Podbilewicz, B. (2002). The type I membrane protein EFF-1 is essential for developmental cell fusion. Dev Cell *2*, 355-362.

Moore, F.L., Jaruzelska, J., Fox, M.S., Urano, J., Firpo, M.T., Turek, P.J., Dorfman, D.M., and Pera, R.A. (2003). Human Pumilio-2 is expressed in embryonic stem cells and germ cells and interacts with DAZ (Deleted in AZoospermia) and DAZ-like proteins. Proc Natl Acad Sci U S A *100*, 538-543.

Mumm, J.S., and Kopan, R. (2000). Notch signaling: from the outside in. Dev Biol *228*, 151-165.

Nakahata, S., Katsu, Y., Mita, K., Inoue, K., Nagahama, Y., and Yamashita, M. (2001). Biochemical identification of Xenopus Pumilio as a sequence-specific cyclin B1 mRNA-binding protein that physically interacts with a Nanos homolog, Xcat-2, and a cytoplasmic polyadenylation element-binding protein. The Journal of biological chemistry *276*, 20945-20953.

Nam, Y., Sliz, P., Song, L., Aster, J.C., and Blacklow, S.C. (2006). Structural basis for cooperativity in recruitment of MAML coactivators to Notch transcription complexes. Cell *124*, 973-983.

Nigon, V., and Dougherty, E.C. (1950). A dwarf mutation in a nematode; a morphological mutant of Rhabditis briggsae, a free-living soil nematode. J Hered *41*, 103-109.

Nishimiya-Fujisawa, C., and Sugiyama, T. (1993). Genetic analysis of developmental mechanisms in hydra. XX. Cloning of interstitial stem cells restricted to the sperm differentiation pathway in Hydra magnipapillata. Dev Biol *157*, 1-9.

O'Brien, C.A., Pollett, A., Gallinger, S., and Dick, J.E. (2007). A human colon cancer cell capable of initiating tumour growth in immunodeficient mice. Nature *445*, 106-110.

Ohta, H., Yomogida, K., Dohmae, K., and Nishimune, Y. (2000). Regulation of proliferation and differentiation in spermatogonial stem cells: the role of c-kit and its ligand SCF. Development *127*, 2125-2131.

Opperman, L., Hook, B., DeFino, M., Bernstein, D.S., and Wickens, M. (2005). A single spacer nucleotide determines the specificities of two mRNA regulatory proteins. Nat Struct Mol Biol *12*, 945-951.

Pasierbek, P., Jantsch, M., Melcher, M., Schleiffer, A., Schweizer, D., and Loidl, J. (2001). A *Caenorhabditis elegans* cohesion protein with functions in meiotic chromosome pairing and disjunction. Genes Dev *15*, 1349-1360.

Pepper, A.S., Killian, D.J., and Hubbard, E.J. (2003). Genetic analysis of *Caenorhabditis elegans* glp-1 mutants suggests receptor interaction or competition. Genetics *163*, 115-132.

Petcherski, A.G., and Kimble, J. (2000). LAG-3 is a putative transcriptional activator in the *C. elegans* Notch pathway. Nature *405*, 364-368.

Pique, M., Lopez, J.M., Foissac, S., Guigo, R., and Mendez, R. (2008). A combinatorial code for CPE-mediated translational control. Cell *132*, 434-448.

Pittenger, M.F., Mackay, A.M., Beck, S.C., Jaiswal, R.K., Douglas, R., Mosca, J.D., Moorman, M.A., Simonetti, D.W., Craig, S., and Marshak, D.R. (1999). Multilineage potential of adult human mesenchymal stem cells. Science *284*, 143-147.

Polanowska, J., Martin, J.S., Fisher, R., Scopa, T., Rae, I., and Boulton, S.J. (2004). Tandem immunoaffinity purification of protein complexes from *Caenorhabditis elegans*. Biotechniques *36*, 778-780, 782.

Praitis, V., Casey, E., Collar, D., and Austin, J. (2001). Creation of low-copy integrated transgenic lines in *Caenorhabditis elegans*. Genetics *157*, 1217-1226.

Puoti, A., and Kimble, J. (1999). The *Caenorhabditis elegans* sex determination gene mog-1 encodes a member of the DEAH-Box protein family. Molecular and cellular biology *19*, 2189-2197.

Puoti, A., and Kimble, J. (2000). The hermaphrodite sperm/oocyte switch requires the *Caenorhabditis elegans* homologs of PRP2 and PRP22. Proceedings of the National Academy of Sciences of the United States of America *97*, 3276-3281.

Qiao, L., Lissemore, J.L., Shu, P., Smardon, A., Gelber, M.B., and Maine, E.M. (1995). Enhancers of glp-1, a gene required for cell-signaling in *Caenorhabditis elegans*, define a set of genes required for germline development. Genetics *141*, 551-569.

Racher, H., and Hansen, D. (2010). Translational control in the *C. elegans* hermaphrodite germ line. Genome *53*, 83-102.

Radford, H.E., Meijer, H.A., and de Moor, C.H. (2008). Translational control by cytoplasmic polyadenylation in Xenopus oocytes. Biochim Biophys Acta *1779*, 217-229.

Rangan, P., DeGennaro, M., Jaime-Bustamante, K., Coux, R.X., Martinho, R.G., and Lehmann, R. (2009). Temporal and spatial control of germ-plasm RNAs. Curr Biol *19*, 72-77.

Richter, J.D. (2000). Influence of polyadenylation-induced translation on metazoan development and neuronal synaptic function. In in Translational control of gene expression, J.W.B. Hershey, M. Mathews, and N. Sonenberg, eds. (Cold Spring Harbor, NY, Cold Spring Harbor Laboratory Press), pp. 785–806.

Riddle, D.L., Blumenthal, T., Meyer, B.J., and Priess, J.R. (1997). *C. elegans* II (Cold Spring Harbor Laboratory Press).

Robert, V., and Bessereau, J.L. (2007). Targeted engineering of the *Caenorhabditis elegans* genome following Mos1-triggered chromosomal breaks. The EMBO journal *26*, 170-183.

Robert, V.J., Davis, M.W., Jorgensen, E.M., and Bessereau, J.L. (2008). Gene conversion and end-joining-repair double-strand breaks in the *Caenorhabditis elegans* germline. Genetics *180*, 673-679.

Roehl, H., Bosenberg, M., Blelloch, R., and Kimble, J. (1996). Roles of the RAM and ANK domains in signaling by the *C. elegans* GLP-1 receptor. The EMBO journal *15*, 7002-7012.

Salvetti, A., Rossi, L., Lena, A., Batistoni, R., Deri, P., Rainaldi, G., Locci, M.T., Evangelista, M., and Gremigni, V. (2005). DjPum, a homologue of Drosophila Pumilio, is essential to planarian stem cell maintenance. Development *132*, 1863-1874.

Schedl, T. (1997). Developmental Genetics of the Germ Line. In C elegans II (Plainview, Cold Spring Harbor Laboratory Press).

Schedl, T., and Kimble, J. (1988). *fog-2*, a germ-line-specific sex determination gene required for hermaphrodite spermatogenesis in *Caenorhabditis elegans*. Genetics *119*, 43-61.

Schmid, M., Kuchler, B., and Eckmann, C.R. (2009). Two conserved regulatory cytoplasmic poly(A) polymerases, GLD-4 and GLD-2, regulate meiotic progression in *C. elegans*. Genes Dev *23*, 824-836.

SenGupta, D.J., Zhang, B., Kraemer, B., Pochart, P., Fields, S., and Wickens, M. (1996). A three-hybrid system to detect RNA-protein interactions in vivo. Proc Natl Acad Sci U S A *93*, 8496-8501.

Seydoux, G., and Greenwald, I. (1989). Cell autonomy of lin-12 function in a cell fate decision in *C. elegans*. Cell *57*, 1237-1245.

Seydoux, G., and Schedl, T. (2001). The germline in *C. elegans*: origins, proliferation, and silencing. Int Rev Cytol *203*, 139-185.

Seydoux, G., Schedl, T., and Greenwald, I. (1990). Cell-cell interactions prevent a potential inductive interaction between soma and germline in *C. elegans*. Cell *61*, 939-951.

Shinohara, T., Orwig, K.E., Avarbock, M.R., and Brinster, R.L. (2003). Restoration of spermatogenesis in infertile mice by Sertoli cell transplantation. Biol Reprod *68*, 1064-1071.

Sigurdson, D.C., Spanier, G.J., and Herman, R.K. (1984). *Caenorhabditis elegans* deficiency mapping. Genetics *108*, 331-345.

Sijen, T., Fleenor, J., Simmer, F., Thijssen, K.L., Parrish, S., Timmons, L., Plasterk, R.H., and Fire, A. (2001). On the role of RNA amplification in dsRNA-triggered gene silencing. Cell *107*, 465-476.

Singh, S.K., Clarke, I.D., Terasaki, M., Bonn, V.E., Hawkins, C., Squire, J., and Dirks, P.B. (2003). Identification of a cancer stem cell in human brain tumors. Cancer Res *63*, 5821-5828.

Siomi, H., and Dreyfuss, G. (1997). RNA-binding proteins as regulators of gene expression. Curr Opin Genet Dev *7*, 345-353.

Slack, F.J., and Ruvkun, G. (1998). A novel repeat domain that is often associated with RING finger and B-box motifs. Trends Biochem Sci *23*, 474-475.

Smardon, A., Spoerke, J.M., Stacey, S.C., Klein, M.E., Mackin, N., and Maine, E.M. (2000). EGO-1 is related to RNA-directed RNA polymerase and functions in germ-line development and RNA interference in *C. elegans*. Curr Biol *10*, 169-178.

Song, X., Wong, M.D., Kawase, E., Xi, R., Ding, B.C., McCarthy, J.J., and Xie, T. (2004). Bmp signals from niche cells directly repress transcription of a differentiation-promoting gene, bag of marbles, in germline stem cells in the Drosophila ovary. Development *131*, 1353-1364.

Sonnichsen, B., Koski, L.B., Walsh, A., Marschall, P., Neumann, B., Brehm, M., Alleaume, A.M., Artelt, J., Bettencourt, P., Cassin, E.*, et al.* (2005). Full-genome RNAi profiling of early embryogenesis in *Caenorhabditis elegans*. Nature *434*, 462-469.

Sonoda, J., and Wharton, R.P. (1999). Recruitment of Nanos to hunchback mRNA by Pumilio. Genes Dev *13*, 2704-2712.

Sonoda, J., and Wharton, R.P. (2001). Drosophila Brain Tumor is a translational repressor. Genes Dev *15*, 762-773.

Spangrude, G.J., Heimfeld, S., and Weissman, I.L. (1988). Purification and characterization of mouse hematopoietic stem cells. Science *241*, 58-62.

Spassov, D.S., and Jurecic, R. (2003). Mouse Pum1 and Pum2 genes, members of the Pumilio family of RNA-binding proteins, show differential expression in fetal and adult hematopoietic stem cells and progenitors. Blood cells, molecules & diseases *30*, 55-69.

St Johnston, D. (1995). The intracellular localization of messenger RNAs. Cell *81*, 161-170.

Sternberg, P.W. (2005). Vulval development. WormBook, 1-28.

Sternberg, P.W., and Horvitz, H.R. (1986). Pattern formation during vulval development in *C. elegans*. Cell *44*, 761-772.

Sternberg, P.W., and Horvitz, H.R. (1989). The combined action of two intercellular signaling pathways specifies three cell fates during vulval induction in *C. elegans*. Cell *58*, 679-693.

Stier, S., Cheng, T., Dombkowski, D., Carlesso, N., and Scadden, D.T. (2002). Notch1 activation increases hematopoietic stem cell self-renewal in vivo and favors lymphoid over myeloid lineage outcome. Blood *99*, 2369-2378.

Stumpf, C.R., Kimble, J., and Wickens, M. (2008). A *Caenorhabditis elegans* PUF protein family with distinct RNA binding specificity. RNA (New York, NY *14*, 1550-1557.

Subramaniam, K., and Seydoux, G. (1999). *nos-1* and *nos-2*, two genes related to Drosophila nanos, regulate primordial germ cell development and survival in *Caenorhabditis elegans*. Development *126*, 4861-4871.

Subramaniam, K., and Seydoux, G. (2003). Dedifferentiation of primary spermatocytes into germ cell tumors in *C. elegans* lacking the pumilio-like protein PUF-8. Curr Biol *13*, 134-139.

Suh, N., Crittenden, S.L., Goldstrohm, A., Hook, B., Thompson, B., Wickens, M., and Kimble, J. (2009). FBF and its dual control of gld-1 expression in the *Caenorhabditis elegans* germline. Genetics *181*, 1249-1260.

Suh, N., Jedamzik, B., Eckmann, C.R., Wickens, M., and Kimble, J. (2006). The GLD-2 poly(A) polymerase activates *gld-1* mRNA in the *Caenorhabditis elegans* germ line. Proc Natl Acad Sci U S A *103*, 15108-15112.

Sully, G., Dean, J.L., Wait, R., Rawlinson, L., Santalucia, T., Saklatvala, J., and Clark, A.R. (2004). Structural and functional dissection of a conserved destabilizing element of cyclo-oxygenase-2 mRNA: evidence against the involvement of AUF-1 [AU-rich element/poly(U)-binding/degradation factor-1], AUF-2, tristetraprolin, HuR (Hu antigen R) or FBP1 (far-upstream-sequence-element-binding protein 1). Biochem J *377*, 629-639.

Sulston, J., and Hodgkin, J. (1988). Methods. In The nematode *C. elegans* (Cold Spring Harbor, New York, Cold Spring Harbor Laboratory Press).

Sulston, J., Horvitz, H.R., Kimble, J., and Wood, W.B. (1988). The nematode *Caenorhabditis elegans*. (Cold Spring Harbor, New York, Cold Spring Harbor Laboratory).

Sulston, J.E., and Horvitz, H.R. (1977). Post-embryonic cell lineages of the nematode, *Caenorhabditis elegans*. Dev Biol *56*, 110-156.

Sulston, J.E., and White, J.G. (1980). Regulation and cell autonomy during postembryonic development of *Caenorhabditis elegans*. Dev Biol *78*, 577-597.

Sundaram, M., and Greenwald, I. (1993). Suppressors of a *lin-12* hypomorph define genes that interact with both *lin-12* and *glp-1* in *Caenorhabditis elegans*. Genetics *135*, 765-783.

Suzuki, H., Tsukahara, T., and Inoue, K. (2009). Localization of c-mos mRNA around the animal pole in the zebrafish oocyte with Zor-1/Zorba. Biosci Trends *3*, 96-104.

Tax, F.E., Yeargers, J.J., and Thomas, J.H. (1994). Sequence of *C. elegans lag-2* reveals a cell-signalling domain shared with Delta and Serrate of Drosophila. Nature *368*, 150-154.

Thompson, B.E., Bernstein, D.S., Bachorik, J.L., Petcherski, A.G., Wickens, M., and Kimble, J. (2005). Dose-dependent control of proliferation and sperm specification by FOG-1/CPEB. Development *132*, 3471-3481.

Tsuda, M., Sasaoka, Y., Kiso, M., Abe, K., Haraguchi, S., Kobayashi, S., and Saga, Y. (2003). Conserved role of nanos proteins in germ cell development. Science *301*, 1239-1241.

Urban, V.S., Kiss, J., Kovacs, J., Gocza, E., Vas, V., Monostori, E., and Uher, F. (2008). Mesenchymal stem cells cooperate with bone marrow cells in therapy of diabetes. Stem Cells *26*, 244-253.

Varkey, J.P., Jansma, P.L., Minniti, A.N., and Ward, S. (1993). The *Caenorhabditis elegans spe-6* gene is required for major sperm protein assembly and shows second site non-complementation with an unlinked deficiency. Genetics *133*, 79-86.

Varnum-Finney, B., Xu, L., Brashem-Stein, C., Nourigat, C., Flowers, D., Bakkour, S., Pear, W.S., and Bernstein, I.D. (2000). Pluripotent, cytokine-dependent, hematopoietic stem cells are immortalized by constitutive Notch1 signaling. Nat Med *6*, 1278-1281.

Walser, C.B., Battu, G., Hoier, E.F., and Hajnal, A. (2006). Distinct roles of the Pumilio and FBF translational repressors during *C. elegans* vulval development. Development *133*, 3461-3471.

Wang, L., Eckmann, C.R., Kadyk, L.C., Wickens, M., and Kimble, J. (2002). A regulatory cytoplasmic poly(A) polymerase in *Caenorhabditis elegans*. Nature *419*, 312-316.

Wang, X., Zamore, P.D., and Hall, T.M. (2001). Crystal structure of a Pumilio homology domain. Mol Cell *7*, 855-865.

Wang, X., Zhao, Y., Wong, K., Ehlers, P., Kohara, Y., Jones, S.J., Marra, M.A., Holt, R.A., Moerman, D.G., and Hansen, D. (2009a). Identification of genes expressed in the hermaphrodite germ line of *C. elegans* using SAGE. BMC Genomics *10*, 213.

Wang, Y., Opperman, L., Wickens, M., and Hall, T.M. (2009b). Structural basis for specific recognition of multiple mRNA targets by a PUF regulatory protein. Proc Natl Acad Sci U S A *106*, 20186-20191.

Wang, Z., and Lin, H. (2004). Nanos maintains germline stem cell self-renewal by preventing differentiation. Science *303*, 2016-2019.

Wang, Z., and Lin, H. (2005). The division of Drosophila germline stem cells and their precursors requires a specific cyclin. Curr Biol *15*, 328-333.

Wang, Z., Tollervey, J., Briese, M., Turner, D., and Ule, J. (2009c). CLIP: construction of cDNA libraries for high-throughput sequencing from RNAs cross-linked to proteins in vivo. Methods (San Diego, Calif *48*, 287-293.

Ward, S., and Carrel, J.S. (1979). Fertilization and sperm competition in the nematode *Caenorhabditis elegans*. Dev Biol *73*, 304-321.

Weir, B.J., and Rowlands, I.W. (1973). Reproductive Strategies of Mammals. Annual Review of Ecology and Systematics *4*, 139-163.

Wen, C., and Greenwald, I. (1999). p24 proteins and quality control of LIN-12 and GLP-1 trafficking in *Caenorhabditis elegans*. J Cell Biol *145*, 1165-1175.

Wickens, M., Bernstein, D.S., Kimble, J., and Parker, R. (2002). A PUF family portrait: 3'UTR regulation as a way of life. Trends Genet *18*, 150.

Wicks, S.R., Yeh, R.T., Gish, W.R., Waterston, R.H., and Plasterk, R.H. (2001). Rapid gene mapping in *Caenorhabditis elegans* using a high density polymorphism map. Nature genetics *28*, 160-164.

Wieschaus, E., and Szabad, J. (1979). The development and function of the female germ line in Drosophila melanogaster: a cell lineage study. Dev Biol *68*, 29-46.

Wilkinson, H.A., Fitzgerald, K., and Greenwald, I. (1994). Reciprocal changes in expression of the receptor *lin-12* and its ligand *lag-2* prior to commitment in a *C. elegans* cell fate decision. Cell *79*, 1187-1198.

Wilson, J.J., and Kovall, R.A. (2006). Crystal structure of the CSL-Notch-Mastermind ternary complex bound to DNA. Cell *124*, 985-996.

Wilson-Berry, L. (1998). Regulation of the Mitotic/Meiotic Cell Fate Decision in *Caenorhabditis elegans*. In Biology and Biomedical Sciences (St. Louis, Washington Univerisity), pp. 327.

Xi, R., and Xie, T. (2005). Stem cell self-renewal controlled by chromatin remodeling factors. Science *310*, 1487-1489.

Xie, T., and Spradling, A.C. (2000). A niche maintaining germ line stem cells in the Drosophila ovary. Science *290*, 328-330.

Xu, E.Y., Chang, R., Salmon, N.A., and Reijo Pera, R.A. (2007). A gene trap mutation of a murine homolog of the Drosophila stem cell factor Pumilio results in smaller testes but does not affect litter size or fertility. Molecular reproduction and development *74*, 912-921.

Ye, Y., Shibata, Y., Yun, C., Ron, D., and Rapoport, T.A. (2004). A membrane protein complex mediates retro-translocation from the ER lumen into the cytosol. Nature *429*, 841-847.

Yochem, J., and Greenwald, I. (1989). *glp-1* and *lin-12*, genes implicated in distinct cell-cell interactions in *C. elegans*, encode similar transmembrane proteins. Cell *58*, 553-563.

Yomogida, K., Yagura, Y., Tadokoro, Y., and Nishimune, Y. (2003). Dramatic expansion of germinal stem cells by ectopically expressed human glial cell line-derived neurotrophic factor in mouse Sertoli cells. Biol Reprod *69*, 1303-1307.

Yoo, A.S., Bais, C., and Greenwald, I. (2004). Crosstalk between the EGFR and LIN-12/Notch pathways in *C. elegans* vulval development. Science *303*, 663-666.

Yoo, A.S., and Greenwald, I. (2005). LIN-12/Notch activation leads to microRNA-mediated down-regulation of Vav in *C. elegans*. Science *310*, 1330-1333.

Yook, K. (2005). Complementation. WormBook, 1-17.

Yoshinaga, K., Nishikawa, S., Ogawa, M., Hayashi, S., Kunisada, T., and Fujimoto, T. (1991). Role of c-kit in mouse spermatogenesis: identification of spermatogonia as a specific site of c-kit expression and function. Development *113*, 689-699.

Zamore, P.D., Williamson, J.R., and Lehmann, R. (1997). The Pumilio protein binds RNA through a conserved domain that defines a new class of RNA-binding proteins. RNA (New York, NY *3*, 1421-1433.

Zetka, M.C., Kawasaki, I., Strome, S., and Muller, F. (1999). Synapsis and chiasma formation in *Caenorhabditis elegans* require HIM-3, a meiotic chromosome core component that functions in chromosome segregation. Genes Dev *13*, 2258-2270.

Zhang, B., Gallegos, M., Puoti, A., Durkin, E., Fields, S., Kimble, J., and Wickens, M.P. (1997). A conserved RNA-binding protein that regulates sexual fates in the *C. elegans* hermaphrodite germ line. Nature *390*, 477-484.

Zhang, Y., and Sheets, M.D. (2009). Analyses of zebrafish and Xenopus oocyte maturation reveal conserved and diverged features of translational regulation of maternal cyclin B1 mRNA. BMC developmental biology *9*, 7.